

8-2010

## Specific, Reversible Cytostatic Protection of Normal Cells Against Negative Effects of Chemotherapy

Benjamin B. Mull

Follow this and additional works at: [https://digitalcommons.library.tmc.edu/utgsbs\\_dissertations](https://digitalcommons.library.tmc.edu/utgsbs_dissertations)



Part of the [Chemical Actions and Uses Commons](#), [Molecular Biology Commons](#), and the [Pharmacology Commons](#)

---

### Recommended Citation

Mull, Benjamin B., "Specific, Reversible Cytostatic Protection of Normal Cells Against Negative Effects of Chemotherapy" (2010). *The University of Texas MD Anderson Cancer Center UTHealth Graduate School of Biomedical Sciences Dissertations and Theses (Open Access)*. 89.  
[https://digitalcommons.library.tmc.edu/utgsbs\\_dissertations/89](https://digitalcommons.library.tmc.edu/utgsbs_dissertations/89)

This Dissertation (PhD) is brought to you for free and open access by the The University of Texas MD Anderson Cancer Center UTHealth Graduate School of Biomedical Sciences at DigitalCommons@TMC. It has been accepted for inclusion in The University of Texas MD Anderson Cancer Center UTHealth Graduate School of Biomedical Sciences Dissertations and Theses (Open Access) by an authorized administrator of DigitalCommons@TMC. For more information, please contact [digitalcommons@library.tmc.edu](mailto:digitalcommons@library.tmc.edu).

**Specific, Reversible Cytostatic Protection of Normal Cells Against Negative  
Effects of Chemotherapy**

by

Benjamin B. Mull, M.S.

APPROVED:

---

Khandan Keyomarsi, Ph.D.

---

Marvin Meistrich, Ph.D.

---

William Plunkett, Ph.D.

---

Mary Ann Smith, Ph.D.

---

Carolyn Van Pelt, D.V.M., Ph.D.

APPROVED:

---

Dean, The University of Texas  
Health Science Center at Houston  
Graduate School of Biomedical Sciences

# **Specific, Reversible Cytostatic Protection of Normal Cells Against Negative Effects of Chemotherapy**

A

THESIS

Presented to the Faculty of  
The University of Texas  
Health Science Center at Houston  
Graduate School of Biomedical Sciences  
In Partial Fulfillment  
Of the Requirements  
For the Degree of

DOCTOR OF PHILOSOPHY

By

Benjamin B. Mull, M.S.  
Houston, Texas  
May 2011

## **Acknowledgements**

I would like to thank my advisor, Dr. Khandan Keyomarsi, for her assistance and guidance throughout the duration of this work. I would also like to thank my committee members, Dr. Marvin Meistrich, Dr. William Plunkett, Dr. Mary Ann Smith, and Dr. Carolyn Van Pelt for their advice and support with this project.

I would also like to thank Dr. Nicholas Terry his training and assistance with many aspects of this project, and Nalini Patel and Tuyen Bui for their technical support as well.

I would finally like to thank my wife and my mother for their support during these years, and my father, who understood this process and strove to impress it upon me as well.



# **Specific, Reversible Cytostatic Protection of Normal Cells Against Negative Effects of Chemotherapy**

Benjamin B. Mull, M.S.

Supervisory Professor: Khandan Keyomarsi, Ph.D.

Chemotherapy is a common and effective method to treat many forms of cancer. However, treatment of cancer with chemotherapy has severe side effects which often limit the doses of therapy administered. Because some cancer chemotherapeutics target proliferating cells and tissues, all dividing cells, whether normal or tumor, are affected. Cell culture studies have demonstrated that UCN-01 is able to reversibly and selectively arrest normal dividing cells; tumor cells lines do not undergo this temporary arrest. Following UCN-01 treatment, normal cells displayed a 50-fold increase in IC<sub>50</sub> for camptothecin; tumor cells showed no such increased tolerance.

We have examined the response of the proliferating tissues of the mouse to UCN-01 treatment, using the small bowel epithelium as a model system. Our results indicate that UCN-01 treatment can cause a cell cycle arrest in the gut epithelium, beginning 24 hours following UCN-01 administration, with cell proliferation remaining suppressed for one week. Two weeks post-UCN-01 treatment the rate of proliferation returns to normal levels. 5-FU administered during this period demonstrates that UCN-01 is able to provide protection to normal cells of the mouse within a narrow window of efficacy, from three to five days post-UCN-01. UCN-01 pretreated mice displayed improved survival, weight status and blood markers following 5-FU compared to control mice, indicating that UCN-01 can protect normal dividing tissues.

The mechanism by which UCN-01 arrests normal cells *in vivo* was also examined. We have demonstrated that UCN-01 treatment in mice causes an increase in the G1 phase cell cycle proteins cdk4 and cyclin D, as well as the inhibitor p27. Phosphorylated Rb was also elevated in the arrested cells. These results are a departure from cell culture studies, in which inhibition of G1 phase cyclin dependent kinases led to

hyposphorylation of Rb. Future investigation will be required to understand the mechanism of UCN-01 action. This is important information, especially for identification of alternate compounds which could provide the protection afforded by UCN-01.

## Table of Contents

Acknowledgements.....	iii
Abstract.....	iv
Table of Contents.....	vi
List of Tables.....	vii
List of Figures.....	viii
Introduction.....	1
Results.....	87
1. Arrest and Recovery of Normal Cells Following UCN-01 Treatment.....	87
2. UCN-01 Mediated Protection of Normal Cells from 5-FU Toxicity.....	110
3. Mechanism of UCN-01 Mediated Cell Cycle Arrest <i>In Vivo</i> .....	147
Discussion.....	178
References.....	190
Vita.....	228

## LIST OF TABLES

Table 1: IC <sub>50</sub> Values of UCN-01 and Staurosporine	20
Table 2: UCN-01 and Cell Cycle Arrest in Cultured Cells	22
Table 3: UCN-01 and Apoptosis in Cultured Cells	37
Table 4A: UCN-01 and S/G2 Phase Abrogation When Combined with A Second Agent or IR	46
Table 4B: UCN-01 and Apoptosis When Combined with a Second Agent	49
Table 4C: Cell Lines Demonstrating Growth Arrest When Treated with UCN-01 and a Second Agent	51
Table 4D: Studies Demonstrating p53 Dependence/Independence for UCN-01 Activity in Combination with a Second Agent	52
Table 5: <i>In vivo</i> Studies of UCN-01 in Tumor-Bearing Animals	63
Table 6: Clinical Trials of UCN-01	69

## LIST OF FIGURES

Figure 1: Proliferative Pathways Affected by UCN-01	31
Figure 2: Apoptotic Pathways Affected by UCN-01	36
Figure 3: Pathways Implicated in the Abrogation of S/G2 Phase arrest By UCN-01	54
Figure 4: Analysis of Flow Cytometry Results in Mouse Jejunum	92
Figure 5: Flow Cytometry of Mouse Jejuna 48 Hours Following UCN-01 Treatment	93
Figure 6: Determination of Baseline $F^{ld}$ for Untreated Mice	95
Figure 7: Flow Cytometry of Mouse Jejuna at One, Two, and Four Weeks Post-UCN-01/DMSO Administration	98
Figure 8: Anti-BrdU Immunohistochemistry of Mouse Jejuna at One, Two, and Four Weeks Post-UCN-01	100
Figure 9: Quantitative Analysis of anti-BrdU IHC sections	102
Figure 10: Flow Cytometry of Mouse Jejuna 24 Hours Following UCN-01 in Citrate Buffer and Low DMSO	104
Figure 11: Anti-BrdU Immunohistochemistry of Mouse Jejuna 48 Hours Following UCN-01/PBS Administration	106
Figure 12: Flow Cytometry of UCN-01 Administered in Two Half Doses	108
Figure 13: Treatment Protocol for Serial 5-FU Injections Beginning at Day 7 Post-UCN-01	116
Figure 14: Percent Change in Weight in Mice for Serial 5-FU Injections Beginning at Day 7 Post-UCN-01	116
Figure 15: Treatment Protocol for Serial 5-FU Injections Beginning at Day 3 Post-UCN-01 Administration	119
Figure 16: Percent Change in Weight in Mice Following Serial 5-FU Injections Beginning at Day 3 Post-UCN-01	119
Figure 17A: ALT Levels in Mice Treated With Serial 5-FU Injections	

Beginning at Day 3 Post-UCN-01 Administration	120
Figure 17B: AST Levels in Mice treated With Serial 5-FU Injections Beginning at Day 3 Post-UCN-01 Administration	120
Figure 17C: Alkaline Phosphatase Levels in Mice Treated With Serial 5-FU Injections Beginning at Day 3 Post-UCN-01 Administration	121
Figure 17D: Platelet Counts in Mice Treated With Serial 5-FU Injections Beginning at Day 3 Post-UCN-01 Administration	121
Figure 17E: White Blood Cells Levels in Mice Treated With Serial 5-FU Injections Beginning at Day 3 Post-UCN-01 Administration	122
Figure 17F: Hemoglobin Levels in Mice Treated With Serial 5-FU Injections Beginning at Day 3 Post-UCN-01 Administration	122
Figure 18: Treatment Protocol for Bolus 5-FU Injection 24 Hours Post-UCN-01 Administration	125
Figure 19: Percent Change in Weight in Mice Following Bolus 5-FU Injection 24 Hours Post-UCN-01 Administration	125
Figure 20: Survival of Mice Following Bolus 5-FU Injection 24 Hours Post-UCN-01 Administration	127
Figure 21A: Weekly Platelets Counts for Mice Following Bolus 5-FU Injection 24 Hours Post-UCN-01 Administration	127
Figure 21B: Weekly White Blood Cell Counts for Mice Following Bolus 5-FU Injection 24 Hours Post-UCN-01 Administration	128
Figure 21C: Weekly Red Blood Cell Counts for Mice Following Bolus 5-FU Injection 24 Hours Post-UCN-01 Administration	128
Figure 22: Treatment Protocol for Bolus 5-FU Injection Beginning at Day 5 Post-UCN-01 Administration	130
Figure 23: Percent Change in Weight in Mice Following Bolus 5-FU Injection Day 5 Post-UCN-01 Administration	130
Figure 24: Survival of Mice Following Bolus 5-FU Injection Day 5 Post-UCN-01 Administration	131
Figure 25A: Weekly Red Blood Cell Counts for Mice Following	

Bolus 5-FU Injection Day 5 Post-UCN-01 Administration	131
Figure 25B: Weekly White Blood Cell Counts for Mice Following Bolus 5-FU Injection Day 5 Post-UCN-01 Administration	132
Figure 25C: Weekly Platelets Counts for Mice Following Bolus 5-FU Injection Day 5 Post-UCN-01 Administration	132
Figure 26: Treatment Protocol for Bolus 5-FU Injection Beginning at Day 5 Post-UCN-01 Administration Without Blood Collection	134
Figure 27: Percent Change in Weight in Mice Following Bolus 5-FU Injection Day 5 Post-UCN-01 Administration (Figure 26)	134
Figure 28: Treatment Protocol for Serial 5-FU Injections Beginning at Day 3 Post-UCN-01 Administration (40 mg/kg/day)	136
Figure 29: Percent Change in Weight in Mice Following Serial 5-FU Injections Beginning at Day 3 Post-UCN-01 Administration	136
Figure 30A: Weekly Platelets Counts in Mice Following Serial 5-FU Injections Beginning at Day 3 Post-UCN-01 Administration	138
Figure 30B: Weekly Red Blood Cell Counts for Mice Following Serial 5-FU Injections Beginning at Day 3 Post-UCN-01 Administration	138
Figure 30C: Weekly White Blood Cell Counts for Mice Following Serial 5-FU Injections Beginning at Day 3 Post-UCN-01 Administration	139
Figure 31: Treatment Protocol for Bolus 5-FU Injection Beginning at Day 5 Post-UCN-01 Administration Without Blood Collection	141
Figure 32: Percent Change in Weight in Mice Following Bolus 5-FU Injection Day 5 Post-UCN-01 Administration (Figure 31)	141
Figure 33: Survival of Mice Following Bolus 5-FU Injection Day 5 Post-UCN-01 Administration (Figure 31)	142
Figure 34: Sternum H&E sections from Mice Following Bolus 5-FU Injection Day 5 Post-UCN-01 Administration (Figure 31)	144
Figure 35: Quantification of Blood Precursor Cells in Mouse Sternums Following Bolus 5-FU Injection Day 5 Post-UCN-01 Administration	145
Figure 36: Western Analysis of PCNA in Serially Fractionated Mouse	

Small Bowel Samples	155
Figure 37: H&E Sections of Mouse Small Bowel During Serial Fractionations	156
Figure 38: Western Analysis of Cdk4 in Crypt Cells of Mice Treated with UCN-01/DMSO	158
Figure 39: Western Analysis of Cyclin D in Crypt Cells of Mice Treated with UCN-01/DMSO	159
Figure 40: Western Analysis of p21 in Crypt Cells of Mice Treated with UCN-01/DMSO	161
Figure 41: Western Analysis of p27 in Crypt Cells of Mice Treated with UCN-01/DMSO	162
Figure 42: Assay of Cyclin D-Associated Kinase Activity in Crypt Cells of Mice treated with UCN-01/DMSO	163
Figure 43: Western Analysis of Cdk2 and Cyclin E in Crypt Cells of Mice treated with UCN-01/DMSO	165
Figure 44: Assay of Cdk2 Kinase Activity in Crypt Cells of Mice Treated with UCN-01/DMSO	166
Figure 45: Western Analysis of Rb and p53 in Crypt Cells of Mice Treated with UCN-01/DMSO	168
Figure 46: ICH Analysis of Phospho-T160 Cdk2 in Crypt Cells of Mice Treated with UCN-01/DMSO	170
Figure 47A: ICH Analysis of Phospho-T160 Cdk2 in Crypt Cells of Mice Treated with UCN-01/DMSO	172
Figure 47B: Quantification of Phospho-T160 Cdk2 in Crypt Cells of Mice Treated with UCN-01/DMSO	173
Figure 48: ICH Analysis of BrdU Incorporation in Crypt Cells of Mice Treated with UCN-01/DMSO	175



## **Introduction**

The nondiscriminatory action of most chemotherapeutic agents still in use today is the major limiting factor in their successful use. Most cytotoxic agents affect cells, which are actively dividing, including both the tumor and the normal dividing cells of the body (gastro-intestinal epithelium, hematopoietic cells and hair follicles). The toxic effects on these normal tissues limit the doses of chemotherapy that can be administered, and this limitation can even lead to more resistant (multidrug resistant, MDR) tumors.

To better direct the toxicity of treatment towards the cancer and away from the host, investigators have tried one of two methods; the first is directed therapy specific for a particular neoplasm. Gleevec used in the treatment of chronic myelogenous leukemia (CML) is a successful example. CML is caused by a chromosomal translocation which gives rise to a chimeric mRNA of the breakpoint cluster region of chromosome 22 (BCR) and the c-ABL tyrosine kinase gene from chromosome 9 (de Klein *et al.*, 1982). The resulting BCR-ABL kinase has increased tyrosine kinase activity and the ability to transform cells (Konopka *et al.*, 1984; Lugo *et al.*, 1990), and has been identified as the sole leukemogenic event in animal models (Daley *et al.*, 1990; Heisterkamp *et al.*, 1990). A screen for inhibitors of this kinase identified Gleevec as the most specific, and in clinical studies it was shown to be very effective in treating CML patients (Druker *et al.*, 1996). For newly diagnosed CML patients treated with Gleevec, the overall survival at 5 years was 89% (Druker *et al.*, 2006). The specific nature of the kinase inhibition and the decreased side effects in comparison to previous standard of care (IFN- $\alpha$  treatment) demonstrates the power of targeted therapy.

An alternative method seeks not to target the tumor, but rather to deflect the toxicity of chemotherapeutic agents away from the normal cells of the host. This approach will be the focus of this study. The idea of protecting normal cells from the toxicity of anticancer chemotherapeutics appeared more than 35 years ago. The majority of the protective studies employ a two step approach: cells are reversibly arrested at one of several cell cycle checkpoints, and then are subsequently exposed to cytotoxic agents which preferentially act upon dividing cells. The temporary arrest of the pretreated cells affords a measure of protection against agents, which take advantage of the processes of cell division, largely DNA synthesis and mitosis. The arrest can be caused by a variety of actions, including inhibition of protein synthesis, growth factor deprivation, and direct or indirect inhibition of specific cell cycle enzymatic processes. Other measures use modulation of growth factors to prevent the apoptotic signaling cascade following cytotoxic treatment or to stimulate cell proliferation prior to the cytotoxic insult. The latter method increases the overall population of affected epithelial tissues to allow the host to better tolerate the loss of some of these cells when treated with a chemotherapeutic drug. The following is a chronological summary of various methods used by several different laboratories over a 40 year period, all attempting to protect normal cells against toxic affects of chemotherapy in vitro and in animal studies.

### **General Inhibition of macromolecules (i.e. DNA, RNA, protein)**

The first studies reported some success in protecting cells from cytotoxic agents by inhibiting either protein or DNA synthesis prior to treatment. One inhibitor used is

cycloheximide (CHX), a drug of bacterial origin which prevents protein synthesis by blocking the movement of transfer RNA (tRNA) molecules along the ribosome (Obrig *et al.*, 1971). Two studies in rats demonstrated that simultaneous or initial treatment with CHX protected bone marrow and intestinal crypt cells from nitrogen mustard (HN2) toxicity (Ben-Ishay and Farber, 1975; Weissberg *et al.*, 1978). The rationale behind this protection is that dividing cells require protein synthesis to proceed through the cell cycle. After treatment with CHX, the cells undergo an arrest in the G2 phase of the cell cycle (Verbin and Farber, 1967); later application of a toxic agent against either DNA synthesis or mitosis will fail if the cells are held outside of these target phases of the cell cycle. Just as important as this cell cycle effect is that a differential protecting effect must exist such that normal cells are protected and tumor cells are not. As a tumor cell by definition harbors one or more cell cycle defects, it is hoped that this difference can be exploited to better protect normal cells. Using the CHX model, it has been demonstrated that normal cells are susceptible to cell cycle arrest following the loss of protein synthesis, while transformed cells can replicate independently of protein synthesis (Campisi *et al.*, 1982; Medrano and Pardee, 1980). This differential was demonstrated as protective in human myeloid progenitor cells (Slapak *et al.*, 1985). Normal granulocyte/macrophage progenitors (CFU-GM), malignant progenitor cells from CML patients, and two leukemia cells lines HL-60 and KG-1 were pretreated with CHX and then exposed to the antimetabolite cytosine arabinoside (ara-C). The survival of normal CFU-GM cells were significantly increased by CHX pretreatment, while the malignant progenitors and cell lines were afforded no such protection. However, it appears that some malignant cells are able to take advantage of the CHX cell cycle arrest and

protection from subsequent cytotoxic insult. Studies on the human osteosarcoma cell line KSu demonstrated that CHX pretreatment afforded a degree of protection against vincristine, colchicine, and  $\Delta^{12}$ -prostaglandin J<sub>2</sub> (Sakai *et al.*, 1989). Thus it appears that CHX protection may not be specific for normal cells, and given its toxicity may not be clinically relevant.

A similar protective strategy was utilized to afford protection to baby hamster kidney cells (BHK) but not their polyoma virus-transformed (Py-BHK) variant line (Pardee and James, 1975). It had previously been shown that caffeine was able to reversibly arrest cells in G1 (Walters *et al.*, 1974). The exact nature of caffeine-mediated arrest is still unclear, but inhibition of either cyclin D/cdk4 (Hashimoto *et al.*, 2004) or cyclin E/cdk2 (Qi *et al.*, 2002) or both, leading to hypophosphorylated Rb and subsequent G1 arrest. The authors showed that the arrest due to caffeine was similar to that seen following growth factor (serum) deprivation, and that streptovitamin A (SVA) also caused a reversible G1 arrest in the untransformed BHK cells. The Py-BHK cells were not affected by any of the cell cycle arresting compounds (caffeine, SVA or serum deprivation). Treating/arresting the BHK cells with SVA or caffeine significantly increased their survival when subsequently treated with ara-C or hydroxyurea (HU). The Py-BHK cells had no such protective effect and were efficiently killed by both agents. A more recent study demonstrated this differential between the immortalized MCF-10A cells and the tumor cell line MCF-7 (Blagosklonny *et al.*, 2000a). Withdrawal of epidermal growth factor (EGF) from MCF-10A cells caused them to undergo a G1/G0 arrest; similar treatment of MCF-7 cells did not affect the cell cycle profile. Growth

arrest in the MCF-10A cells prevented subsequent toxicity from the microtubule polymerizing effects of paclitaxel, while the tumorigenic MCF-7 cells were not protected. The same results were observed when each cell line was treated with the EGF receptor inhibitor AG1478; MCF-10A cells underwent a G1/G0 arrest, while MCF-7 cells were unaffected by low the same levels of AG1478. The fungal metabolite anguidine has been shown to protect normal cells from chemotherapeutics (Teodori *et al.*, 1981). Anguidine is another inhibitor of protein synthesis, and is thought to promote the disassembly of polyribosomes (Liao *et al.*, 1976). Pretreatment of Chinese hamster ovary cells (CHO) with anguidine arrested the cells and provided protection against ara-C, adriamycin, HU and fluorouracil (5-FU). It was also demonstrated that anguidine can preferentially induce cytostasis and protection in normal but not transformed cells (Hromas *et al.*, 1983). Normal WI-38 cells treated with a low concentration of anguidine exhibited a G1 arrest, while the SV40 variant WI-38 VA13 cells were had no cell cycle perturbation. Following anguidine, the normal cells were protected against the growth inhibitory effects of ara-C and adriamycin, while the VA13 cells were potently inhibited. However, as with CHX, not all tumor cells may evade the cell cycle arresting effect of anguidine. For example, the human adenocarcinoma cell line LoVo was treated with increasing concentrations of anguidine (1 µg/ml – 50 µg/ml) and underwent an arrest in the S phase of the cell cycle at all concentrations (Dosik *et al.*, 1978). Anguidine may also not be a reversible inhibitor, further limiting any clinical utility (Liao *et al.*, 1976). In this study, treatment of HeLa cells with 1mM anguidine caused degradation of polyribosomes, preventing initiation of protein chain synthesis and cell death.

Growth arrest has been successfully used *in vivo* as a protective measure prior to high dose chemotherapy (Raffaghello *et al.*, 2008). Based on studies which showed a protective effect of serum deprivation in primary glial cells but not four glioma lines from oxidative ( $H_2O_2$ ) damage, mice were starved for 48 to 60 hours and then treated with high dose etoposide. While only 8 of the 23 mice treated with etoposide alone survived, 16 out of 17 undergoing short-term starvation (STS) survived. Unfortunately, the STS protocol seems to protect injected tumors as well. Mice inoculated with the neuroblastoma line NXS2 were treated with high dose etoposide, with one group undergoing STS prior to treatment. While the STS group initially had improved survival (7/8 alive at 36 days) compared to etoposide alone (3/6 dead by day 5), long term survival was worse for the STS group. All STS/etoposide mice succumbed to tumor burden by day 53, while the 3 remaining etoposide-only mice lived for 83, 131, and 140 days. Thus, like some other measures of protection, it appears that STS may be non-specific and protect tumors in addition to normal cells.

Cell cycle arrest as a protective measure has also been induced by inhibiting protein synthesis using the histidine analogue L-histidinol. L-Histidinol reversibly arrests the growth of cells in G0 by inhibiting both protein and ribosomal RNA synthesis (Warrington *et al.*, 1977). BALB/3T3 cells incubated with L-histidinol went into a G1/G0 arrest, and this arrest was reversible after up to 3 days of L-histidinol exposure (Warrington *et al.*, 1977). This arrest was duplicated in the normal CHO variant LR73,

while transformed TR3 line continued to proliferate (Warrington and Fang, 1982b). Subsequent treatment with ara-C had no effect on the normal arrest LR73 cells, while the TR3 line was potently growth-inhibited. A similar study using cocultivated normal human foreskin fibroblasts (HFF) and transformed HeLa cells produced in identical result (Warrington, 1978). It was demonstrated that pretreatment of HFF cells with L-histidinol and theophylline produced a G1/G0 arrest, while HeLa cells continued to grow and divide. Subsequent exposure to HU or ara-C was toxic to the dividing HeLa cells, while the HFF cells survived. HeLa cells form distinct colonies in culture and can be distinguished morphologically from HFF cells. The two lines were cultured together and the experiment repeated. L-Histidinol and theophylline followed by ara-C or HU allowed the selective eradication of HeLa cells. The protective effect of L-histidinol was also established in murine spleen cells. 1 mM L-histidinol provided a reversible G1 arrest for up to 72 hours, and upon removal the cells did not enter into S phase until 96 hours (Warrington and Fang, 1982a). While arrested, the cells were protected from the toxicity of both ara-C and 5-FU. The same group found that mice inoculated with L-1210 leukemia and then treated with L-histidinol had spared normal bone marrow cells and had enhanced antitumor effects of both ara-C and 5-FU (Warrington and Fang, 1985; Warrington *et al.*, 1984). Mice (both naïve and those with implanted L1210 tumors) were injected with 5 mg of L-histidinol (~ 167 mg/kg) or PBS control, followed by either 15 or 30 mg of 5-FU (450 or 900 mg/kg) or 25 mg (130 mg/kg) ara-C. All PBS mice receiving 5-FU died by day 13, while all mice pretreated with L-histidinol survived at least three months. In addition, clonogenic assays of bone marrow cells of mice sacrificed 24 hours after 5-FU/ara-C treatment demonstrated a protection factor of up to

21,00 for the L-histidinol pretreated mice versus PBS pretreated (ratio of relative cell survival of L-histidinol pretreated to PBS pretreated). Additionally, the combination seemed to enhance the ability of 5-FU and ara-C to kill the implanted tumor cells (by clonogenic assay), and was able to increase the survival of tumor-bearing mice by 50%. Another group was able to demonstrate protection of normal cells in mice when L-histidinol was given as a 24-hour infusion *following* 5-FU, perhaps demonstrating that the G1 arrest may not be the sole source of protection (Edelstein and Heilbrun, 1988). In these experiments, mice were treated for with a 50 mg infusion of L-histidinol (or saline control) for 24 hours prior to receiving 10 mg 5-FU. The pretreated group had a 30% survival rate versus 0% for the saline control group. However, if the same 50 mg infusion began immediately following 5-FU injection, the survival rate increased to 100% (saline controls remained at 0% survival). Because the arresting effect of L-histidinol was not present when 5-FU was administered in this experiment, it cannot completely account for the increase in survival.

Unfortunately, not all L-histidinol treatments have been effective in exploiting the differences between normal and tumor cells. A panel of murine cells including the normal A31 line and three transformed derivatives (BP-A31, M-A31 and SV-A31) exhibited the expected protective effect of L-histidinol against ara-C toxicity in the normal A31 cells (Warrington and Muzyka, 1983). A 24-hour incubation in 1-3 mM L-histidinol prior to 48 hours of 0.5 – 1.0  $\mu\text{g/ml}$  ara-C significantly improved the survival of the A31 cells. However, all three transformants were also afforded varying degrees of protection by L-histidinol pretreatment, all demonstrating improved survival to 48 hours



of ara-C alone. It was further shown in the murine breast tumor model CD8F<sub>1</sub> that L-histidinol can increase the tolerance of mice for 5-FU (Stolfi *et al.*, 1987). 7 mg of L-histidinol given prior to 130 mg/kg of 5-FU resulted in a significant increase in white blood cell (WBC) counts, body weight, and survival compared to mice receiving saline prior to 5-FU treatment. Pretreatment with 7 mg of L-histidinol also increased the LD<sub>50</sub> of a single dose of 5-FU from 283 mg/kg to 504 mg/kg. However, the tumors were also afforded a measure of resistance to 5-FU, and the therapeutic result of L-histidinol plus 5-FU were not superior to 5-FU alone at the lower, unprotected dose. First passage transplants of spontaneous CD8F<sub>1</sub> breast tumors were implanted into mice receiving either 5-FU alone or L-histidinol followed by 5-FU. The mice receiving 5-FU alone had a maximal tolerated dose of 100 mg/kg/week, while the mice pretreated with L-histidinol had an increased tolerance, up to 150 mg/kg/week. However, the weights of the implanted tumors in the 5-FU group (601 +/- 96 mg) were not significantly different from those in the 5-FU plus L-histidinol group (807 +/- 227 mg). A more encouraging study exploits the antibiotic minocycline to protect the murine small intestine from 5-FU-induced mucositis (Huang *et al.*, 2009). The mice receiving minocycline concurrently with 5-FU (30 mg/kg/day for 5 days for each drug) demonstrated decreased weight loss, lower diarrhea levels, and improved villus measurements compared to the PBS plus 5-FU (30 mg/kg/day X 5) control mice. It was demonstrated that minocycline was able to repress apoptosis in the small bowel crypts by inhibiting the upregulation of PARP-1 activity induced by 5-FU. It does not appear that minocycline is exerting protection by modulating or arresting the epithelial tissues, as villi from mice sacrificed after the 5-day course of treatment were approximately the same lengths as control mice. It was also

shown that the minocycline pretreatment did not protect implanted CT-26 colon cancer xenografts from 5-FU toxicity; by three weeks, the tumors in mice pretreated with minocycline were significantly smaller compared to the tumors in mice receiving PBS prior to 5-FU. The mechanism for the improved tumor response is currently unknown, but the differential response between normal and tumor cells to minocycline treatment is encouraging. Other studies have shown an anti-angiogenic effect of minocycline, which may explain the synergistic result seen when combined with 5-FU (Frazier *et al.*, 2003; Saikali and Singh, 2003). Similar results were observed in mice treated with the benzamidine derivative CR3294 three days prior to 5-FU treatment (Letari *et al.*, 2009). By inhibiting cytokine release in the gut epithelium, CR3294 increased by 3-fold the number of mice not experiencing diarrhea and increased the surviving crypts per cross-section by 2.8 fold compared to PBS controls. CR3294 did not affect the growth of tumor xenografts (HT29 and MDA-MB231 cells) nor the efficacy of 5-FU to treat these tumors.

### **Modulation of growth factors**

Other studies have attempted to differentiate normal cells from tumor cells to afford protection against toxicity have utilized substances that occur normally in cells. The polypeptide growth factor transforming growth factor  $\beta$  (TFG- $\beta$ ) is a potent inhibitor of epithelial cell proliferation as well as an immune suppressor and hematopoietic regulator (Massague *et al.*, 1987; Roberts *et al.*, 1985; Sing *et al.*, 1988). To evaluate the possible protective effect of TFG- $\beta$ , mice were treated with 5  $\mu$ g/day TFG- $\beta$  for 5 days and sacrificed; hematopoietic progenitor cells were decreased by more than 50% compared to

control mice, indicating an arrest in the marrow. The same course of TFG- $\beta$  was then given prior to a single injection of 150 mg/kg 5-FU. Unfortunately, hematopoietic progenitor cells were lower in the TGF- $\beta$  group at the hyperproliferative phase (9 days after 5-FU treatment) compared to 5-FU alone; by 16 days, the number of blood precursors in the two groups were not significantly different. A similar study produced a different result, demonstrating that hematologic recovery following 150 mg/kg 5-FU was accelerated in mice treated given TFG- $\beta$  (two doses of 2.5  $\mu$ g daily for days -4 to 0), peaking at day 11 as opposed to day 16 after 5-FU (Grzegorzewski *et al.*, 1994). While TFG- $\beta$  did not increase survival in mice receiving a single high dose (340 mg/kg) 5-FU, it was protective against a subsequent dose of 5-FU. For this experiment, mice were treated with 150 mg/kg at day zero. On days 9-13, mice were then treated with either twice-daily 2.5  $\mu$ g TGF- $\beta$  or saline control. A second dose of 300 mg/kg 5-FU was then given on day 13. Survival in mice given TFG- $\beta$  was 90%, while the control mice survival was less than 40%. Interestingly, mice treated with TFG- $\beta$  and doxorubicin (DXR) were also protected. As before, mice were treated from days -4 to 0 with twice-daily 2.5  $\mu$ g TGF- $\beta$  or saline control, and then given a single dose of 14 mg/kg DXR. All of the control mice had died by day 15, while 80% of the TGF- $\beta$  mice survived beyond day 30. This result was interesting, in that cell cycle arrest must not be the only protective effect of TGF- $\beta$ ; DXR can damage DNA in noncycling cells. Cell culture studies using the CCL64 cell line (non-tumorigenic mink epithelial cells) demonstrated the protective effect of TFG- $\beta$  *in vitro* against vinblastine, vincristine, etoposide, taxol, ara-C, methotrexate (MTX) and 5-FU (McCormack *et al.*, 1997). Cells were incubated with 15 pM TFG- $\beta$  or control media for 24 hours, and the cytotoxic agent was added for

an additional 48 hours. In all cases, the IC<sub>50</sub> for each drug was increased (by CFU assay) by incubation with TFG- $\beta$  versus control; the increase for each drug (in  $\mu$ g/ml) was: 0.04 to 25 for ara-C; 0.05 to 50 for MTX; 0.5 to 1.0 for 5-FU; 0.15 to 0.45 for etoposide; 0.002 to 0.1 for taxol; and 0.0002 to 0.02 for vincristine. TFG- $\beta$  was also protective in a hamster model of oral mucositis (Sonis *et al.*, 1997). Topical application of TFG- $\beta$  to the oral mucosa prior to 5-FU treatment reduced cell proliferation (measured by PCNA IHC) and reduced weight loss, incidence of oral mucositis, and increased survival. Protection was also afforded to the small intestine by TFG- $\beta$  treatment prior to irradiation (Booth *et al.*, 2000). A single dose of TFG- $\beta$  increased the surviving number of crypts by 3-4 fold, and a continuous infusion resulted in a 12-fold increase. While the results using TFG- $\beta$  are promising, it remains unclear as to what the exact mechanism of protection is. The protection against toxicity that is not cell cycle specific (IR and DXR) is difficult to explain, and the likelihood that the protection could be extended to tumors seems substantial. Growth factors have also been used to stimulate proliferation of tissues susceptible to chemotherapeutic agents to enhance recovery following treatment. Granulocyte colony stimulating factor (G-CSF) had been shown to increase the proliferative index of many blood cell lineages, including granulocytes, erythrocytes, and monocytes (Pospisil *et al.*, 1995). Rats given G-CSF 2 hours after 5-FU significantly increased the production of erythrocytes in the recovery period, indicating improved hematopoiesis in the G-CSF pretreated mice (Weiterova *et al.*, 2000).

### **Cytostatic agents**

A more cell cycle-specific protection modality employs the kinase inhibitor staurosporine. As kinases are an important factor in the regulation of the cell cycle (and one which can be lost in many tumors), modulation of kinases could result in a differential effect in the two populations of normal versus tumor cells (Hartwell and Kastan, 1994; Zhou and Elledge, 2000). Indeed, it was demonstrated that three nontransformed mammalian cells (HSF-43, HSF-55 and HFL-1) were prevented from entering S phase by very low (1 ng/ml) levels of staurosporine (Crissman *et al.*, 1991). In contrast, three transformed cell lines (FT210 mouse mammary carcinoma, tumorigenic WCHE/5 Chinese hamster cells and HL-60 human leukemia cells) were unaffected at low levels (1-10 ng/ml) of staurosporine. At high levels of staurosporine (50-75 ng/ml) the transformed cells were instead arrested at the G2 phase. Similar findings were exhibited in comparing normal human lymphocytes with the lymphocytic leukemia MOLT-4 cell line treated with staurosporine (Bruno *et al.*, 1992). Normal lymphocytes treated with low (5-10 ng/ml) staurosporine accumulated in G1; high staurosporine levels (50-100 ng/ml) resulted in both a G1 and G2 block. However, the MOLT-4 cells accumulated only at G2 for all doses of staurosporine (5-100 ng/ml). The specificity of staurosporine-mediated arrest for normal cells was also shown in a panel of breast epithelial cells (Chen *et al.*, 2000). Four breast tumor cell lines (MDA-MB436, MDA-MB157, MCF-7 and T47D), the immortalized breast epithelial MCF-10A line, and two normal breast epithelial cells (76N and 81N) were treated with staurosporine and three specific cyclin dependent kinase (cdk) inhibitors: olomoucine, roscovitine and flavopiridol. While the three cdk inhibitors caused a dose-dependent growth inhibition in all cells, staurosporine was able to distinguish the two normal cell lines from the transformed ones. At 2nM,

greater than 50% inhibition was seen in both 76N and 81N cells, while no drug-mediated effect was observed in any of the transformed lines. Further exploration with two variants of the 76N line, 76NE6 (degraded p53) and 76NE7 (degraded Rb), demonstrated a p53-independent, Rb-dependent arrest at both 0.5 and 10 nM staurosporine (see Mechanism below). Induction of G1 arrest by 0.5 nM staurosporine was protective of the 81N cells against the toxicity of doxorubicin (0.125  $\mu$ M) and camptothecin (0.5 $\mu$ M); MDA-MB157 and MDA-MD436 cells realized no protective benefit from staurosporine pretreatment. The staurosporine pretreatment increased the MTD for camptothecin in the normal cells by two orders of magnitude. This protective effect was also realized when normal proliferating lymphocytes were treated with staurosporine prior to camptothecin. While staurosporine seems to select only normal cells for arrest and subsequent protection, its additional effects on normal cells are likely to prevent it from being used clinically (Way *et al.*, 2000). Staurosporine has been shown to initiate differentiation of epidermal cells (Sako *et al.*, 1988), and may function as a tumor promoter in mouse skin (Fujiki *et al.*, 1989). Staurosporine may also prevent platelet aggregation, which could impair wound healing (Secrist *et al.*, 1990; Takano, 1994). The adverse effects of staurosporine spurred the development of analogs such as UCN-01 (see below).

### **Low dose cytotoxic agents**

An alternative to using a cytostatic drug to arrest cells as a protective measure is to actually use chemotherapeutic agents to cause an initial, low level of damage to the cells. This initial event would not be so great as to cause cell death, but instead activate a cell cycle checkpoint, thus arresting the cells while the damage is repaired. During this arrest,

a second, greater insult would theoretically not affect the arrested cells with functioning checkpoints; tumor cells with defective checkpoints should continue to grow and divide, leaving them susceptible to the second cytotoxic agent. One such study uses a low level of a DNA damaging agent to cause a cell cycle arrest in cells with functioning checkpoints; subsequent treatment with microtubule-active drugs is ineffective in these arrested cells, while checkpoint-deficient cells continue to cycle and are sensitive to the secondary treatment (Blagosklonny *et al.*, 2000b). Low doses of DXR (50-100 ng/ml) for 16 hours caused a G2 arrest in HCT116 cells with wild-type p53. Subsequent paclitaxel treatment (100 ng/ml for hours 17-48) of these cells was ineffective in causing significant cell death, unlike mock-pretreated controls. MTT assay after 48 hours demonstrated that the paclitaxel-only group had a survival rate of 30%, the cells treated with DXR prior to paclitaxel had an improved survival rate of 70%. HCT116 clones deficient in either p21 or p53 were also not protected by the low dose DXR pretreatment, suggesting that a p53-dependent induction of p21 is required to realize the G2 arrest and protection of primary DXR. Indeed, adenovirus-mediated expression of p21 in the p21 -/- cells was protective against the paclitaxel treatment, similar to DXR pretreatment.

### **Specific cytoprotective agents**

Other agents have been reported to have cytoprotective effects for patients undergoing anticancer therapy. Amifostine (WR-2721) is an organic thiophosphate which has been shown to protect against hematologic toxicity and some cumulative organ damage in patients receiving radiotherapy as well as some chemotherapeutic agents (Castiglione *et al.*, 1999; Kemp *et al.*, 1996). Amifostine has selective efficacy in normal cells versus

tumor cells due to its activation; it is converted to the active WR-1065 by membrane-bound alkaline phosphatases, which are more active in normal cells versus neoplasms (Culy and Spencer, 2001). The active metabolite then acts as a free radical scavenger and can facilitate detoxification of cytotoxic agents (Pierelli *et al.*, 1998). The clinical experience with amifostine as a protective agent provides an unclear picture of its efficacy. A small phase II trial on 10 patients with advanced esophageal cancer employed 500 mg amifostine administered subcutaneously prior to 25 fractions of 45 Gy radiation treatment, plus carboplatin and 5-FU (Jatoi *et al.*, 2004). It was unclear if amifostine was protective in this setting, as it did not allow a dose escalation and seemed to carry its own toxicities (nausea, hypotension and vomiting). However, amifostine was effective in protecting salivary glands. A meta-analysis of 14 separate trials (total 1451 patients) indicates that amifostine is protective against mucositis when combined with radiotherapy compared to radiation treatment alone (Sasse *et al.*, 2006). A phase I trial for small cell lung cancer incorporated amifostine into a regimen with etoposide, radiation and cisplatin. It was determined that the MTD of fractionated radiation in the group receiving amifostine could be increased from 45 Gy to 60 Gy (Garces *et al.*, 2007). However, the authors point out that the fractions in this group were decreased from 1.5 Gy to 1.2 Gy, which may also have improved tolerance of the higher total dose of radiation. A phase II trial for advanced esophageal cancer enrolled 54 patients to be treated with a combination of carboplatin, 5-FU, paclitaxel and radiation (Jatoi *et al.*, 2007). Amifostine was given to 19 patients to evaluate its protective ability in this setting. No significant protection was observed among patients receiving amifostine, and one patient death was attributed to amifostine administration (acute hypotension immediately



following 500 mg subcutaneous amifostine) and its use was discontinued. Overall, amifostine seems to be able to protect salivary glands and some epithelial cell populations against mucositis, and does not adversely affect the efficacy of tumor treatment. The efficacy of amifostine is still being investigated in two ongoing studies (NCT00409331 and NCT00167908).

Another protective agent used to prevent mucositis following chemotherapy is palifermin/keratinocyte growth factor (KGF). Recombinant KGF is administered to patients prior to a regimen of chemotherapy. Palifermin binds the keratinocyte growth factor receptor (KGFR); KGFR is found in the epithelial cells of the gastrointestinal tract as well as the liver, pancreas and lung (Spencer *et al.*, 2005). Pretreatment with palifermin activates the KGFR leading to differentiation and maturation of epithelial cells and subsequent thickening of epithelium of the gastrointestinal tract. This increase diminishes the DNA damage and apoptosis seen in these cells (McDonnell and Lenz, 2007). A phase III trial of non-Hodgkins lymphoma patients receiving total body irradiation utilized palifermin (or placebo control) for three days prior to radiation treatment and for three days following treatment (Spielberger *et al.*, 2004). Patients receiving palifermin had significantly reduced high grade oral mucositis, and the duration of mucositis was shortened (median day 6 versus day 9 for placebo). A phase II study in head and neck squamous cell carcinoma patients also evaluated the protective ability of palifermin in a regimen of radiation, cisplatin and 5-FU (Brizel *et al.*, 2008). The duration of high grade mucositis was shorter in the patients receiving palifermin (median 6.5 weeks versus 8.1 weeks for placebo), but the difference was not statistically

significant. A much larger phase III study evaluating palifermin protection in head and neck cancer patients (NCT00626639) is currently underway.

Unfortunately one common theme among the protective measures reported in the literature is the absence of any change in the progression of cancer or time to death of the patients receiving these measures. While the decreased side effects experienced by some patients certainly enhance quality of life during and after treatment, the lack of meaningful improvement in therapeutic outcome relegates these methods to only an adjunct role in therapy. It is hoped that our work will lead to a protective scheme that is more than simply supportive. To this end, the work described in the future chapters of this thesis demonstrates how treatment of normal cells with UCN-01 can afford protection against the toxic affects of chemotherapy. To appreciate the role of UCN-01 as protector of normal cells, it is crucial to examine the journey that UCN-01 has taken as a chemotherapeutic agent in cultured cells and in animal models to its current use in clinical trials. These studies has helped pave the way to the novel use of this agent which I have pursued in my dissertation work, namely use of UCN-01 to protect normal cells against the toxic affects of chemotherapy.

### **UCN-01**

The understanding of mechanisms of cellular proliferation, malignant transformation, differentiation and apoptosis has produced a wide array of potential targets to control these events. One such element is the serine/threonine kinase family protein kinase C (PKC), which was shown to be crucial in tumor-promoting process of plant-derived

phorbol esters (Castagna *et al.*, 1982). It has been demonstrated that in cell lines transformed with p21<sup>RAS</sup> that PKC is required for cell survival; inhibition of PKC drove transformed variants of NIH/3T3 and Balb cell lines to apoptosis, while no effect was seen in the parental lines (Xia *et al.*, 2007). The search for possible inhibitors of PKC lead to the discovery of staurosporine (ST) from the bacterium *Streptomyces* sp. (Omura *et al.*, 1977). Staurosporine was found to be a potent PKC inhibitor (IC<sub>50</sub> of 2.7 nM), and was also very toxic to HeLa cells, with an IC<sub>50</sub> of 4 pM for a 72-hour exposure (Tamaoki *et al.*, 1986). Staurosporine can drive most mammalian cells types into apoptosis via mitochondrial caspase activation, although the exact mechanism of its action is unknown (Bertrand *et al.*, 1994; Jacobson and Evan, 1994; Takahashi *et al.*, 1997). In addition to its toxicity, ST has also been noted for its promiscuity of target molecules, including protein tyrosine kinases (Meggio *et al.*, 1995; Ruegg and Burgess, 1989). The inhibitory potential of ST against some of these targets is summarized in Table 1.

UCN-01 (7-hydroxystaurosporine) is an indolocarbazole compound originally isolated from a culture broth of *Streptomyces* sp. as a selective protein kinase C (PKC) inhibitor (Takahashi *et al.*, 1987). UCN-01 was found to be more specific than staurosporine inhibition of PKC (Table 1); it was also shown to be an effective inhibitor of cAMP-dependent protein kinase (PKA) and v-src tyrosine kinase (Takahashi *et al.*, 1989; Takahashi *et al.*, 1990). These studies demonstrated that UCN-01 is a more selective inhibitor of PKC than staurosporine, affecting the  $\alpha$ ,  $\beta$ , and  $\gamma$  isozymes most potently; no effect on the atypical PKC  $\zeta$  was measured (Seynaeve *et al.*, 1994). Subsequent studies

Table 1: IC<sub>50</sub> values for UCN-01 and Staurosporine

<b>Kinase</b>	<b>UCN-01</b>	<b>Staurosporine</b>	<b>Reference</b>
PKC	4.1 nM	2.7 nM	(Tamaoki, 1991)
PKC- $\alpha$	29 nM	58 nM	(Seynaeve <i>et al.</i> , 1994)
PKC- $\beta$	34 nM	65 nM	(Seynaeve <i>et al.</i> , 1994)
PKC- $\gamma$	30 nM	49 nM	(Seynaeve <i>et al.</i> , 1994)
PKC- $\delta$	590 nM	330 nM	(Seynaeve <i>et al.</i> , 1994)
PKC- $\epsilon$	530 nM	160 nM	(Seynaeve <i>et al.</i> , 1994)
PKC- $\zeta$	> 30 $\mu$ M	> 30 $\mu$ M	(Seynaeve <i>et al.</i> , 1994)
PKA	42 nM	8.2 nM	(Meijer, 1995)
MAPK	910 nM	20 nM	(Meijer, 1995; Tamaoki, 1991)
Chk1	8-10 nM	4 nM	(Busby <i>et al.</i> , 2000; Luo <i>et al.</i> , 2001)
Chk2	500 nM	3.7 nM	(Yu <i>et al.</i> , 2002)
Cdk 1	31 nM	3-9 nM	(Gadbois <i>et al.</i> , 1992; Kawakami <i>et al.</i> , 1996)
Cdk 2	30 nM	7 nM	(Gadbois <i>et al.</i> , 1992; Kawakami <i>et al.</i> , 1996)
Cdk 4	32 nM	10 nM	(Gadbois <i>et al.</i> , 1992; Kawakami <i>et al.</i> , 1996)
p60 <sup>V-SRC</sup> tyrosine kinase	45 nM	6.4 nM	(Meijer, 1995; Tamaoki, 1991)

indicate that UCN-01 is a somewhat promiscuous kinase inhibitor, with at least 23 demonstrated targets (Komander *et al.*, 2003).

The effects of UCN-01 in cultured cells fall into one of two broad categories (cell cycle arrest and apoptosis), and vary with cell type, drug concentration, and interaction with other agents. As a single agent, UCN-01 has been shown to either arrest cells in the G1 phase of the cell cycle or to drive cells into apoptosis. In concert with cytotoxic drugs or radiation, UCN-01 can abrogate S or G2 cell cycle arrest, preventing damage repair, also causing apoptosis. While the effects of UCN-01 generally fall into one of these areas, the mechanism(s) underlying these responses are not entirely clear. The studies on UCN-01 will be detailed below.

### **UCN-01 and cell cycle arrest (Table 2)**

An early study on UCN-01 demonstrated a spectrum of growth inhibition on a panel of five breast cancer cell lines (Seynaeve *et al.*, 1993). Differential sensitivity among the lines was noted, with MDA-MB468 being most resistant and MCF-7 most susceptible to growth inhibition. The IC<sub>50</sub> values for UCN-01 determined by MTT assay were as follows (all in nM): H85787 22 $\pm$  3, MCF-7 30  $\pm$  1, SK-BR-3 45  $\pm$  4, MDA-MB453 68  $\pm$  3, MDA-MB468 100  $\pm$  30. A G1 to S block (DNA histogram, no quantification available) was seen following 150nM UCN-01 treatment in MDA-MB468 cells, demonstrated by propidium iodide flow cytometry. This block was accompanied by a decrease in overall cellular protein phosphorylation. Decreased phosphorylation was demonstrated by autoradiography of whole cell lysate separated by SDS-PAGE following

Table 2: UCN-01 and Cell Cycle Arrest in Cultured Cells

Cell line(s)	Drug/Dose	Experimental data	Effect/Result	Reference
H85787 (breast tumor)	22 nM UCN-01	MTT Assay	IC <sub>50</sub>	Seynaeve <i>et al.</i> , 1993
MCF-7 (breast tumor)	30 nM UCN-01	MTT Assay	IC <sub>50</sub>	Seynaeve <i>et al.</i> , 1993
Sk-Br-3 (breast tumor)	45 nM UCN-01	MTT Assay	IC <sub>50</sub>	Seynaeve <i>et al.</i> , 1993
MDA-MB453 (breast tumor)	68 nM UCN-01	MTT Assay	IC <sub>50</sub>	Seynaeve <i>et al.</i> , 1993
MDA-MB468 (breast tumor)	100 nM UCN-01 150 nM UCN-01	MTT Assay PI flow, <sup>32</sup> P protein labeling	IC <sub>50</sub> G1 block, ↓ protein phosphorylation	Seynaeve <i>et al.</i> , 1993
A431 (epidermoid carcinoma)	50 nM UCN-01	PI flow	G1 block	Akinaga <i>et al.</i> , 1993
A431 (epidermoid carcinoma)	0.26 μM UCN-01	PI flow	G1 block (50% → 70%)	Akinaga <i>et al.</i> , 1994
A431 (epidermoid carcinoma)	1.56 μM UCN-01	PI flow	G1 block (50% → 60%)	Akinaga <i>et al.</i> , 1994
A431 (epidermoid carcinoma)	5.8 nM staurosporine	PI flow	G1 block (50% → 75%)	Akinaga <i>et al.</i> , 1994
A431 (epidermoid carcinoma)	58 nM staurosporine	PI flow	G2 block (16% → 60%)	Akinaga <i>et al.</i> , 1994
Ma-31 (Rb+ lung cancer)	2.197 μM UCN-01	MTT Assay	IC <sub>50</sub> , ↓ phospho-Rb	Shimizu <i>et al.</i> , 1996
N417 (Rb- lung cancer)	737 nM UCN-01	MTT Assay	IC <sub>50</sub>	Shimizu <i>et al.</i> , 1996
H209 (Rb mut lung cancer)	181 nM UCN-01	MTT Assay	IC <sub>50</sub>	Shimizu <i>et al.</i> , 1996
Ma-31 (Rb+ lung cancer)	602 nM staurosporine	MTT Assay	IC <sub>50</sub>	Shimizu <i>et al.</i> , 1996
N417 (Rb- lung cancer)	54 nM staurosporine	MTT Assay	IC <sub>50</sub>	Shimizu <i>et al.</i> , 1996
H209 (Rb mut lung cancer)	29 nM staurosporine	MTT Assay	IC <sub>50</sub> , ↑ phospho-Rb	Shimizu <i>et al.</i> , 1996

Table 2 continued

A549 (NSCLC)	100 nM UCN-01	PI flow, anti-Rb western	G1 block, ↓ phospho-Rb	Kawakami <i>et al.</i> , 1996
A431 (epidermoid carcinoma)	260 nM UCN-01	PI flow, western, histone H1 kinase assay	G1 block (37.7% → 61.6%); ↓ phospho-Rb, cdk2 activity; ↑ p21, p27	Akiyama <i>et al.</i> , 1997
A431 (epidermoid carcinoma)	1.56 $\mu$ M UCN-01	PI flow, anti-cyclin B western	G1 block, no change in cyclin B	Akiyama <i>et al.</i> , 1999a
A431 (epidermoid carcinoma)	58 nM staurosporine	PI flow, anti-cyclin B western	G2 block, ↑ cyclin B	Akiyama <i>et al.</i> , 1999a
WiDr (Rb+ colon carcinoma)	100, 300 nM UCN-01	PI flow, western, histone H1 kinase assay	G1 block (Rb dependent), ↓ cdk2 activity, ↑ p21	Akiyama <i>et al.</i> , 1999b
HCT116 (Rb+ colon carcinoma)	100, 300 nM UCN-01	PI flow, western, histone H1 kinase assay	G1 block (Rb dependent), ↓ cdk2 activity, ↑ p21	Akiyama <i>et al.</i> , 1999b
WI-38 (Rb+ lung fibroblast)	100, 300 nM UCN-01	PI flow, western, histone H1 kinase assay	G1 block (Rb dependent), ↓ cdk2 activity, ↑ p21	Akiyama <i>et al.</i> , 1999b
Saos-2 (Rb- osteosarcoma)	100, 300 nM UCN-01	PI flow, western, histone H1 kinase assay	Apoptosis, ↓ cdk2 activity,	Akiyama <i>et al.</i> , 1999b
WI-38 VA13 (SV40 xform)	100, 300 nM UCN-01	PI flow, western, histone H1 kinase assay	Apoptosis, ↓ cdk2 activity, ↑ p21	Akiyama <i>et al.</i> , 1999b
A549 (Rb+ NSCLC)	100 nM UCN-01	PI flow, western	G1 block (73% → 86%), ↑p21, ↓ phospho-RB	Mack <i>et al.</i> , 1999
Calu1 (Rb+ NSCLC)	100 nM UCN-01	PI flow, western	G1 block (52% → 72%), ↑p21, ↓ phospho-RB	Mack <i>et al.</i> , 1999
H596 (Rb mut NSCLC)	100 nM UCN-01	PI flow, western	No G1 change, ↑p21	Mack <i>et al.</i> , 1999
5637 (Rb- bladder cancer)	100 nM UCN-01	PI flow, western	No G1 change	Mack <i>et al.</i> , 1999
RB5 (Rb+ 5637)	100 nM UCN-	PI flow,	G1 block (70%	Mack <i>et al.</i> ,

Table 2 continued

subline)	01	western	→ 90%), ↓ phospho-RB	1999
DU-145 (Rb mut prostate cancer)	100 nM UCN- 01	PI flow, western	No G1 change	Mack <i>et al.</i> , 1999
DU1.1 (Rb+ DU-145 subline)	100 nM UCN- 01	PI flow, western	G1 block (42% → 66%), ↓ phospho-RB	Mack <i>et al.</i> , 1999
76N (normal human mammary epithelium)	80 nM UCN-01	PI flow, western, HH1 kinase assay	G1 block (↑ 11%), ↓ p53, pRb, cdk4, cdk2 kinase	(Chen <i>et al.</i> , 1999)
81N (normal human mammary epithelium)	80 nM UCN-01	PI flow, western, HH1 kinase assay	G1 block (↑ 15%), ↓ p53, pRb, cdk4, cdk2 kinase	(Chen <i>et al.</i> , 1999)
76NE6 (E6 transformed 76N)	80 nM UCN-01	PI flow, western, HH1 kinase assay	Increased G1 phase (+20%), ↓ pRb, cdk4	(Chen <i>et al.</i> , 1999)
76NE7 (E7 transformed 76N)	80 nM UCN-01	PI flow, western, HH1 kinase assay	Increased S phase (+10%), no protein Δ	(Chen <i>et al.</i> , 1999)
SBC-3 (small cell lung cancer)	200 nM UCN- 01	PI flow, western, kinase assay (HH1 and Rb)	G1 block (36% → 56%), ↓ pRb, cdk2, cdk2 kinase, ↑ p21 bound cdk2, IRF-I	(Usuda <i>et al.</i> , 2000)
SBC-3/UCN (UCN-01 resistant SBC-3 subline)	200 nM UCN- 01	PI flow, western, kinase assay (HH1 and Rb)	No G1 block, no Δ in cell cycle proteins or IRF-I	(Usuda <i>et al.</i> , 2000)
HaCaT (HNSCC)	100 nM UCN- 01	PI flow, western, kinase assay (HH1 and Rb)	G1 block (35% → 52%), ↑ p21 & p27, ↓ cdk4, ↓ cdk2 & cdk4 kinase activity	(Patel <i>et al.</i> , 2002)
HN12 (HNSCC)	100 nM UCN- 01	PI flow, western, kinase assay (HH1 and Rb)	G1 block (35% → 52%), ↑ p21 & p27, ↓ cdk4, ↓ cdk2 & cdk4 kinase activity	(Patel <i>et al.</i> , 2002)
HN30 (HNSCC p53 mut)	100 nM UCN- 01	PI flow, western, kinase assay (HH1 and	G1 block (35% → 52%), ↑ p21 & p27, ↓ cdk4,	(Patel <i>et al.</i> , 2002)



Table 2 continued

		Rb)	↓ cdk2 & cdk4 kinase activity	
HCT116 (colon carcinoma)	100 nM UCN-01	PI flow, kinase assay, western	G1 block, ↑ p21,	(Facchinetti <i>et al.</i> , 2004)
HCCT p53-/-	100 nM UCN-01	PI flow, kinase assay, western	↑ p21	(Facchinetti <i>et al.</i> , 2004)
HCCT p21 -/-	100 nM UCN-01	PI flow, kinase assay, western	No G1 effect	(Facchinetti <i>et al.</i> , 2004)
HaCaT	100 nM UCN-01	PI flow, kinase assay	G1 block, ↑ ERK protein, kinase activity	(Facchinetti <i>et al.</i> , 2004)
HSC-3 (oral squamous cell carcinoma)	300 nM UCN-01	PI & Annexin V flow, western	G1 block (53% → 64%), ↑ p21, ↓ cdk2	(Otsubo <i>et al.</i> , 2007)
LMF4 (oral squamous cell carcinoma)	300 nM UCN-01	PI & Annexin V flow, western	G1 block (27% → 63%), ↑ p53, p21, ↓ cdk2, ppRb	(Otsubo <i>et al.</i> , 2007)
PrEC (normal prostate epithelium)	20 – 400 nM UCN-01	MTT assay, western	Growth arrest, ↑ p21, ↓ cyc D	(Blagosklonny <i>et al.</i> , 2001)
DU145 (prostate cancer)	20 – 400 nM UCN-01	MTT assay, western	Growth arrest, ↑ p21, ↓ cyc D	(Blagosklonny <i>et al.</i> , 2001)
PC3/M (prostate cancer)	20 – 400 nM UCN-01	PI flow, western	G1 arrest, ↑ p21, ↓ cyc D	(Blagosklonny <i>et al.</i> , 2001)
SK-GT5 (gastric cancer)	1 μM UCN-01	Western	↓ E2F1 ↑ p21, p27	(Hsueh <i>et al.</i> , 2001)
CHO (Chinese hamster ovary)	50 nM UCN-01	Western	↑ Rb, ↓ ppRb, ↑ Sp1	(Penuelas <i>et al.</i> , 2003)
K562 (myelogenous leukaemia)	50 nM UCN-01	PI flow, western	G1 block (32% → 65%), ↑ Rb, ↓ ppRb, ↑ Sp1	(Penuelas <i>et al.</i> , 2003)

<sup>32</sup>P-orthophosphate labeling for 90 minutes. Treatment of A431 human epidermoid carcinoma cells with 0.05  $\mu$ M UCN-01 also caused a G1 arrest as shown by propidium iodide flow cytometry (DNA histogram, no quantification available) (Akinaga *et al.*, 1993). Further work with these cells showed that UCN-01 and staurosporine have different effects on cell cycle distribution, depending on concentration (Akinaga *et al.*, 1994). At both 50% (0.26  $\mu$ M) and 80% (1.56  $\mu$ M) inhibitory levels, UCN-01 consistently caused a G1 accumulation. Propidium iodide flow cytometric analysis demonstrated an increase in the G1 fraction (from 50%) to 70% at 0.26  $\mu$ M UCN-01, and to 60% at 1.56  $\mu$ M. Staurosporine treatment resulted in a G1 arrest (75%) at the lower effective dose (0.0058  $\mu$ M), but shifted to a G2/M (G2 increased from 18% to 60%) accumulation at the 80% inhibitory level (0.058  $\mu$ M). It was also noted that UCN-01 did not alter the rate of DNA synthesis in these cells or the progression through mitosis; only the G1 to S phase transition was delayed. The different effects of UCN-01 and staurosporine may be due to a divergence of their effects on the retinoblastoma (Rb) protein (Shimizu *et al.*, 1996). A panel of lung cancer cell lines (Ma-31 with wild-type Rb, N417 with null Rb, and H209 with mutant Rb) was treated with both agents and IC<sub>50</sub> values for each drug on each cell line were determined by MTT assay: values for UCN-01 for Ma-31, N417 and H209 are 2197, 737 and 181 nM respectively. For staurosporine, the IC<sub>50</sub> values for Ma-31, N417 and H209 are 602, 54 and 29 nM, respectively. Treatment with each drug at IC<sub>50</sub> levels showed a decrease in the levels of Rb for Ma-31 and H209 cells. However, in the wild-type Rb line (Ma-31), staurosporine increased the ratio of hyper- to hypophosphorylated Rb, while UCN-01 decreased this ratio. Hypophosphorylated Rb can bind to E2F transcription factors, sequestering it away

from genes required for cell growth and division. A similar effect was seen in another lung cancer cell line, A549 (Courage *et al.*, 1996; Kawakami *et al.*, 1996). Cyclin dependent kinases cdk2, cdk4 and cdk6 were immunopurified from the cells and incubated *in vitro* with UCN-01; subsequent kinase assays on purified Rb demonstrated dose-dependent inhibition of Rb phosphorylation. In growing A549 cells, 100 nM UCN-01 caused a G1 arrest (DNA histogram, no quantification cited) and a decrease in hyperphosphorylated Rb. A G1 arrest induced in A431 cells also showed an increase in dephosphorylated Rb (Akiyama *et al.*, 1997). In addition, the levels of cyclin A and cyclin D1 were reduced, as was the activity of cdk2 and the levels of its active, threonine 160-phosphorylated form. The cell cycle inhibitors p21 and p27 were also increased in UCN-01 treated cells. A431 cells synchronized at M phase with nocodazole and then treated with either UCN-01 or staurosporine showed a G1 or G2/M block, respectively (Akiyama *et al.*, 1999a). While staurosporine inhibited a reduction in cyclin B, UCN-01 had no effect on cyclin B levels.

The ability of UCN-01 to produce a cell cycle arrest may be determined in part by the Rb status of the cell being treated. A study comparing Rb-proficient cell lines (colon carcinoma WiDr, HCT116 and lung fibroblast WI-38) to an Rb-defective line (Saos-2 osteosarcoma) and an SV40-transformed line (WI-38 VA13) found that functional Rb led to a UCN-01-mediated G1 arrest (DNA histogram, no quantification available) at both 100 and 300 nM, whereas lack of Rb resulted in apoptosis at both doses (Akiyama *et al.*, 1999b). The G1 arrest was accompanied by a drop in the kinase activity of cdk2 and the levels of active (Thr-160 phosphorylated) cdk2 in all five cell lines. Levels of p27 were

increased all cell lines except Saos-2 (p27 null), but p21 levels were not altered in any of these lines following UCN-01 treatment. A similar finding was reported in non-small cell lung cancer (NSCLC) lines; wild-type Rb expressing lines A549 and Calu1 were arrested in G1 (increase in G1 from 73% to 86% in A549, and from 52% to 72% in H596, both at 100nM UCN-01) after UCN-01 treatment, while no arrest was observed in the Rb-null line H596 (Mack *et al.*, 1999). Unlike the previous cited work (Akiyama *et al.*, 1999b ), UCN-01 (100 nM) caused an increase in p21 in all three cell lines, regardless of Rb status. (Hypophosphorylation of Rb was also noted in the wild-type lines, in both p53 wild-type (A549) and mutant (H596) cell lines. The role of Rb in the UCN-01-induced G1 arrest was further examined using isogenic cell lines: the bladder cancer cell line 5637 (Rb-null), prostate cancer cell line DU-145 (Rb-mutant) and their Rb-expressing sublines (RB5 and DU1.1, respectively). In both pairs, Rb hypophosphorylation and G1 arrest were seen in UCN-01 treated sublines, whereas the parental lines had no arrest. The dispensability of p53 and requirement for Rb were confirmed in mammary epithelial cells as well (Chen *et al.*, 1999). Normal mammary epithelial cell lines (76N and 81N) underwent a G1 arrest at low levels of UCN-01 (increase in G1 population of 11% in 76N and 15% in 81N, both at 80nM). Two breast cancer cell lines (p53-null and Rb-inactive MDA-MB157 and p53/Rb-null MDA-MB436) did not undergo this G1 arrest following low doses (20-80 nM) of UCN-01. Two variants of the normal 76N line were also tested: 76NE6 cells, which lack p53, and 76NE7 cells, which are p53 deficient. At 20nM UCN-01, 76NE6 cells were growth-arrested and accumulated in G1, similarly to the 76N cells. The 76NE7 cells did not, suggesting the requirement of Rb for the UCN-01 mediated arrest. In the UCN-01 sensitive cells, UCN-01 induced arrest was accompanied by

decreases in cdk2 and cdk4, as well as cdk2-associated kinase activity. As in the previous studies, Rb phosphorylation decreased concomitant with arrest, as were levels of cyclin D. However, no changes were observed in the levels of p21 and p27 in these cells, unlike in the previous reports. However, the authors demonstrated that the binding of p27 was altered following the UCN-01-mediated decrease in cdk4. As cdk4 levels decreased, the freed p27 was able to bind and inhibit cdk2. Similar to the Mack *et al.* study (Mack *et al.*, 1999), the small cell lung cancer line SBC-3 and the UCN-01 resistant subline SBC-3/UCN were examined after UCN-01 treatment (Usuda *et al.*, 2000). In the responsive SBC-3 cells, 0.2  $\mu$ M UCN-01 caused a G1 accumulation (36% G1 increased to 56%), loss of phosphorylated Rb, decreased cdk2 activity, and increases in p21 and p21 binding to cdk2. The arrest resistant SBC-3/UCN cells demonstrated no arrest at up to 1  $\mu$ M UCN-01, and none of the underlying cell cycle protein changes seen in the SBC-3 cells were recapitulated. As in other reports, p53 did not appear to play a role in the cell cycle arrest due to UCN-01. Because p21 seems to be a crucial player in the growth inhibition observed, the authors looked for regulators of p21 other than p53. One possibility is interferon regulatory factor I (IRF-I), which can bind to the promoter of p21 and cause transactivation of the gene (Coccia *et al.*, 1999). The authors found that the UCN-01 responsive SBC-3 cells, IRF-I was basally expressed, and UCN-01 increased this expression in a dose-dependent manner. In the resistant SBC-3/UCN cells, IRF-I was not seen in the untreated samples, and very little was induced, even after 1 $\mu$ M UCN-01 treatment.

Three head and neck squamous cell carcinoma (HNSCC) cell lines treated with UCN-01 displayed many of the same cell cycle alterations reported above (Patel *et al.*, 2002). HaCaT, HN12, and HN30 cells were growth-arrested and accumulated in G1 following UCN-01 treatment, with an  $IC_{50}$  as low as 17nM. The inhibitors p21 and p27 increased, and cyclin D levels and cdk2- and cdk4-associated kinase activities were diminished. A subsequent study demonstrated the same G1 arrest in HaCaT cells, but with only an increase in the inhibitor p21, but not p27 (Facchinetti *et al.*, 2004). To explore this difference further, the authors utilized the colon carcinoma cell line HCT116 and two isogenic sublines, one p21<sup>-/-</sup> and the other p53<sup>-/-</sup>. UCN-01 treatment (100 nM for 12 hours) increased p21 expression regardless of p53 status, and only p21 expressing cells underwent the UCN-01 mediated G1 arrest. Promoter deletion studies demonstrated that only the Ras-activation domain was required for increased levels of p21, and that the p53 activation site was dispensable. UCN-01 modulation of PKC, PDK1 and AKT was also ruled out as affecting the p21 levels in the cells. As the Ras activation domain was required for p21 induction, the authors investigated pathways downstream of Ras. The mitogen-activated protein kinase (MAPK) pathway is a cascade of kinase/phosphorylation interactions in which activated, upstream kinases phosphorylate and activate subsequent kinases leading to activation of several transcription factors. In the canonical pathway, Ras activates Raf, the MAPK kinase kinase (MAPKKK), which then activates MEK (MAPKK), which then activates the ERK1 and ERK2 via phosphorylation (Figure 1). HCT116 cells treated with UCN-01 displayed increased ERK kinase activity at doses that induced p21 accumulation, and the activation of ERK temporally preceded the increase in p21. Inhibition of MEK (via PD98059 or UO126)

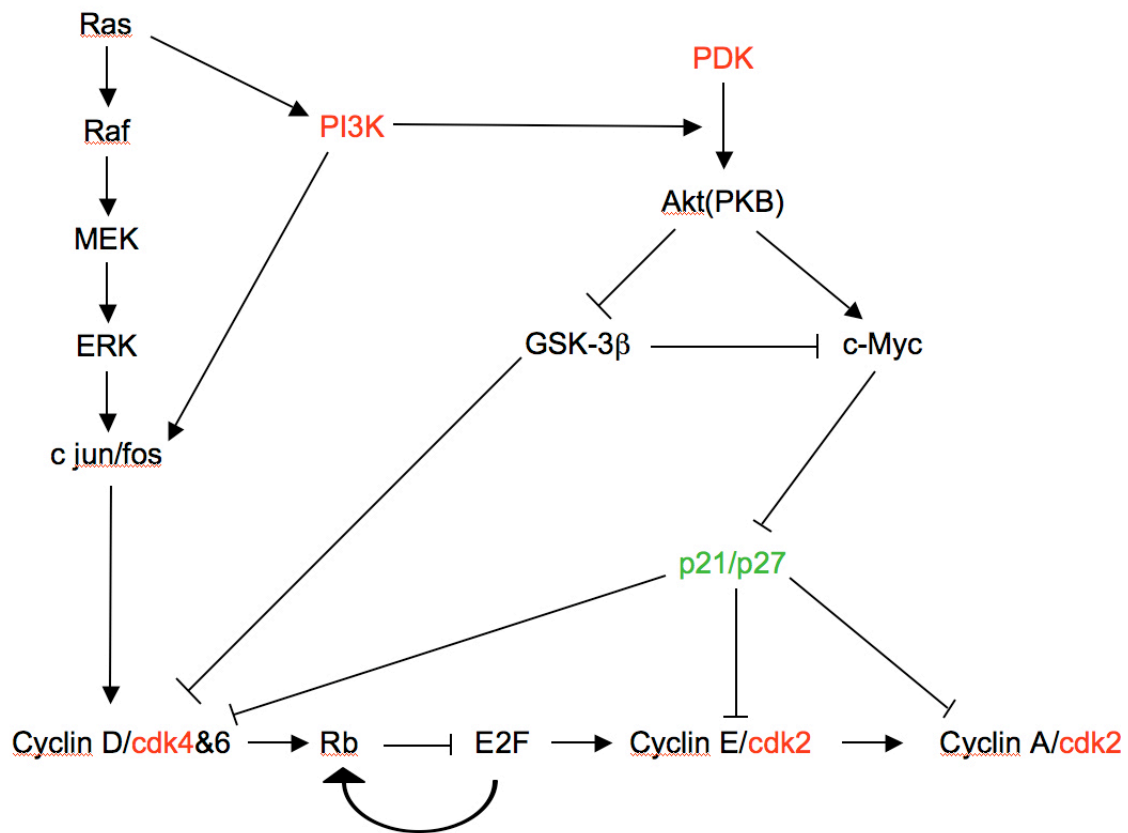


Figure 1: Proliferative pathways affected by UCN-01, resulting in cell cycle arrest. **Green** indicates activities enhanced by UCN-01, **red** designates inhibition by UCN-01.

prevented the p21 promoter activation following UCN-01 treatment, and no p21 accumulation or p21 increase was seen. Finally, p21 induced by UCN-01 was almost exclusively located in the nucleus. While the exact nature by which UCN-01, a kinase inhibitor, is able to activate a proliferative pathway such as MAPK is unknown, it is not without precedent. Other antiproliferative drugs have been shown to activate the MAPK pathway, such as cisplatin (Wang *et al.*, 2000) and paclitaxel (Bacus *et al.*, 2001). It might also be possible that UCN-01 activates a stress response which can in turn activate the MAPK pathway (Benhar *et al.*, 2002).

The inhibitor p21 has been implicated in other cell lines as well. A panel of 8 oral squamous cell carcinoma (OSCC) cell lines treated with UCN-01 demonstrated growth inhibition and G1 phase increase in both primary and metastatic cells (Otsubo *et al.*, 2007). The levels of p21 were increased, and the levels cdk2 and Rb phosphorylation were diminished. As in previous reports, levels of p27 were not affected. Induction of p21 and decreased cyclin D were also correlated with a G1 arrest in both normal prostate epithelial cells (PrEC) and prostate cancer cell lines DU145, PC3 and PC3M (Blagosklonny *et al.*, 2001). UCN-01 was unable to inhibit the growth of LNCaP cells, and was able to abrogate a G1 arrest caused by phorbol ester (a PKC activator). These disparate effects may tie in with the previous study concerning the actions of UCN-01 on the MAPK pathway (Facchinetti *et al.*, 2004). PKC can activate the MAPK pathway, which in turn can lead to increased levels of cyclin D and the inhibitor p21 (Dent *et al.*, 1998; Sherr, 1996). The balance of proliferative response to growth arrest appears to be specific for each cell type, and may shape the response to UCN-01.



While many descriptions of mechanism of UCN-01 cell cycle arrest have focused on Rb phosphorylation and the cell cycle proteins implicated in that process, it has also been reported that UCN-01 can affect E2F-mediated transcription of G1 and S phase genes by directly affecting E2F protein levels (Hsueh *et al.*, 2001). In the gastric cancer cell line SK-GT5, 1 $\mu$ M UCN-01 treatment produced a 99% drop in the levels of E2F-1. It was further shown that the decrease was due to ubiquitin/proteasome-mediated proteolysis. However, the cell cycle proteins p21, p27, and cyclin B were not diminished by the UCN-01-mediated proteolytic process responsible for degrading E2F; the levels of p21 and p27 increased after UCN-01 treatment, and cyclin B was unchanged. The authors also note that inhibition of E2F degradation (using proteasome inhibitor LnLL) was not able to prevent the UCN-01-mediated G1 arrest in these cells. E2F repression has been shown to inhibit cell cycle progression by other agents, such as retinoic acid and IFN- $\alpha$  (Iwase *et al.*, 1997; Zhu *et al.*, 1997). In bronchial epithelium, retinoic acid mediates degradation of cyclin D through the ubiquitin/proteasome pathway (Langenfeld *et al.*, 1997), similar to the results seen in A341 cells treated with UCN-01 (Akiyama *et al.*, 1997). Whether or not the drop in cyclin D is dependent upon increased degradation through the ubiquitin/proteasome pathway is still under investigation.

The ability of UCN-01 to modulate the transcription and stability of Rb has also been demonstrated in cultured cells (Penuelas *et al.*, 2003). Low levels of UCN-01 (30-50nM) were shown to cause cell cycle arrest in CHO, K562 and HeLa cells, and led to increased levels of Rb; 50 nM UCN-01 caused an increase in the G1 population from 35% to 65%

in K562 cells. This increase in Rb was attributed to both increased Rb mRNA levels and decreased degradation of Rb. The authors also noted an increase in the transcription factor Sp1 at these low concentrations of UCN-01. Sp1 has been shown to interact with Rb to enhance the transcription of Sp1, and Rb can activate transcription of p21 through Sp1 (Decesse *et al.*, 2001; Noe *et al.*, 1998). It is possible in this cell line that increased levels of Rb could both diminish the transcription of E2F-dependent genes (such as cyclins D and E) as well as increase levels of p21, leading to cell cycle arrest in G1.

UCN-01 has also been demonstrated to inhibit endothelial cell growth (Kruger *et al.*, 1998). UCN-01 prevented outgrowth from rat aortic explant cultures, and inhibited hypoxia-inducible factor (HIF-1) dependent transcription, and could possibly be used to prevent angiogenesis.

In summary, these studies have demonstrated that UCN-01 can cause growth inhibition in many cell lines, and that the arrest is due to a block in the G1 phase of the cell cycle (see Table 2). The cell cycle proteins involved in G1 and the transition to S phase are the most commonly indicated as the actors in this arrest. Rb seems to be required in most cells, and hypophosphorylated Rb is a hallmark of the arrest and could putatively be sequestering the E2F transcription factor, preventing cell cycle progression. The levels and activities of the G1 cyclin dependent kinases, and the levels of the cyclins D, E, and A, and the inhibitors p21 and p27 have all been implicated, although the effects of UCN-01 on any specific protein vary among published reports and seem to be cell type specific. It also appears that p53 is not required for this process, and that the MAPK

pathway may also be involved. However, very few studies have been done on normal cell lines, and the mutations and abnormalities necessary in tumor cells can obscure any evaluation of cell cycle processes. More importantly, none of these studies have examined the actions of UCN-01 *in vivo*, which are likely to be different than those in any immortalized cell culture line.

### **UCN-01 and apoptosis (Table 3)**

In addition to inhibiting growth, UCN-01 has also been implicated as an inducer of apoptosis in various cancer cell lines. Exposure of four T lymphoblast cell lines (Jurkat, Molt-3, Molt-4, and Hut-78) to UCN-01 for 24 hours led to decreased cell viability, G2/M phase cells, and total protein phosphorylation. The sub-G1 (apoptotic) cell population increased, beginning 3 hours after UCN-01 treatment (Wang *et al.*, 1995). Interestingly, the histone H-1 kinase activities of cdk1 and cdk2 immunoprecipitated from Jurkat cells showed a dose-dependent *increase* with UCN-01 treatment; the authors identified the lack of inhibitory phosphorylation at threonine 15 by the Wee1 kinase as the cause (Figure 2). Exposure of purified cdk1 and cdk2 to UCN-01 *in vitro* led to the expected decrease in phosphorylation of histone H1. This study highlights the possibility that a kinase inhibitor such as UCN-01 can impair the kinase ability of an upstream cell cycle inhibitor, thus potentiating downstream kinases, even if UCN-01 itself is able to inhibit the later enzymes when isolated *in vitro*. A panel of eight ovarian carcinoma cells lines, both p53-proficient (OVCAR 429, 433, 3, and 420) and p53 mutant (SKOV 3, SKOV 3 R, and OVCAR 432), exposed to UCN-01 for 24 hours displayed increased

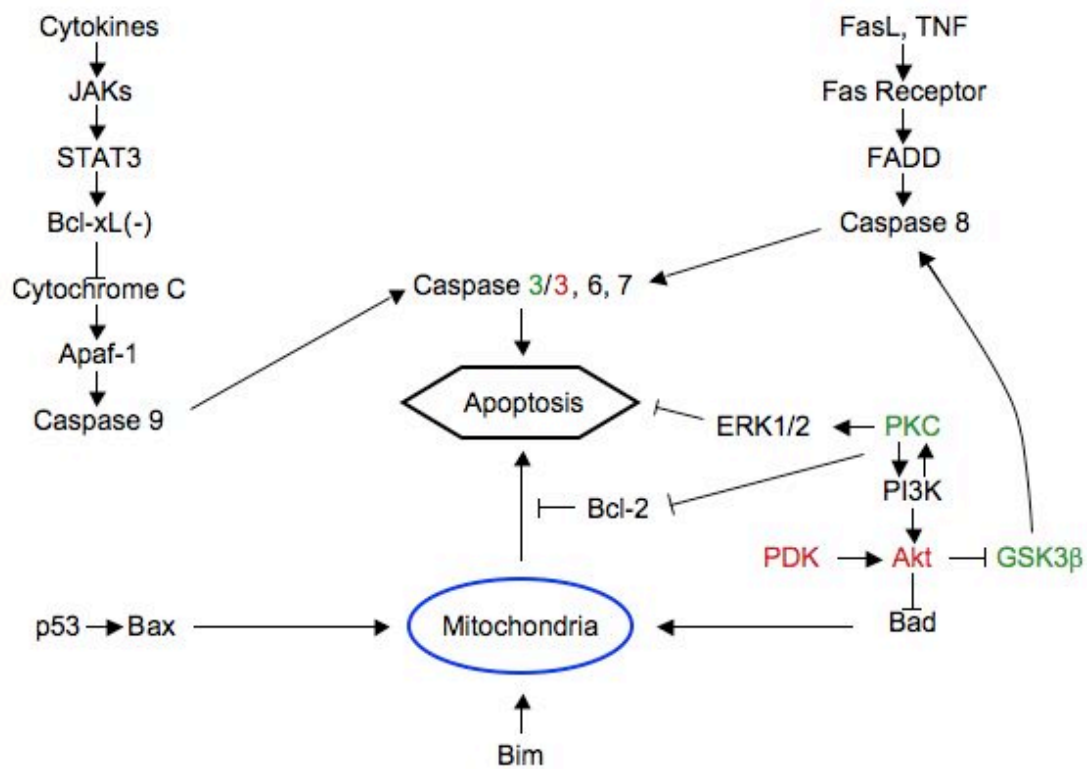


Figure 2: Apoptotic pathways affected by UCN-01. **Green** indicates activities enhanced by UCN-01, **red** designates inhibition by UCN-01.

Table 3: UCN-01 and Apoptosis in Cultured Cells

Cell line	UCN-01 dose	Experimental Data	Cellular effects	Reference
Jurkat (T-lymphoblast)	100-300 nM	MTT assay, <sup>32</sup> P labeling, PI flow, HH1 kinase assay, western	Growth inhibition, ↓ G2 (18% → 10%), apoptosis, ↑ cdk1 & cdk2 activity, ↓ Wee1 activity	(Wang <i>et al.</i> , 1995)
OVCAR 429 (ovarian cancer, p53 wt)	100 nM	MTT assay, EtBr flow	Growth inhibition (30% survival), ↑ G1 (42% → 59%), ↓ G2 (19% → 10%), apoptosis	(Husain <i>et al.</i> , 1997)
SKOV 3 (ovarian cancer, p53 null)	100 nM	MTT assay, EtBr flow	↓ G1 (50.7% → 24.1%), ↑ G2 (5.7% → 34%)	(Husain <i>et al.</i> , 1997)
SKOV SN3 (ovarian cancer, p53 trans)	100 nM	MTT assay, EtBr flow	↑ G1 (75% → 88%), apoptosis	(Husain <i>et al.</i> , 1997)
HL60 (myeloblastic leukemia)	0.1 – 10 μM  10 μM	DNA fragmentation, HH1 kinase  Western, <sup>32</sup> P labeling	↑ DNA fragmentation, apoptosis, ↓ cdk1 activity  ↑ PKCα, ↑ ppPKCα	(Shao <i>et al.</i> , 1997b)  (Shao <i>et al.</i> , 1997a)
K562 (myeloblastic leukemia)	0.1 – 10 μM	DNA fragmentation, HH1 kinase	↑ DNA fragmentation, apoptosis, ↓ cdk1 activity	(Shao <i>et al.</i> , 1997b)
HT29 (colon carcinoma)	0.1 – 10 μM	DNA fragmentation, HH1 kinase	↑ DNA fragmentation, apoptosis, ↓ cdk1 activity	(Shao <i>et al.</i> , 1997b)
A549 (NSCLC)	400 nM	PI flow, TUNEL assay, HH1 kinase, western	↑ apoptosis (60%), ↓ G1 (43% → 22%),	(Sugiyama <i>et al.</i> , 1999)

Table 3 continued

			no $\Delta$ in cdk2 activity	
A549/UCN (UCN-01 resistant A549 subline)	400 nM	PI flow, TUNEL assay, HH1 kinase, western	no $\uparrow$ apoptosis, $\uparrow$ G1 (43% $\rightarrow$ 67%), $\downarrow$ cdk2 activity, $\downarrow$ p21, $\downarrow$ p27, $\downarrow$ ppRb	(Sugiyama <i>et al.</i> , 1999)
LS513 (colon carcinoma)	100 nM – 1 $\mu$ M	Condensed nuclei, western	$\uparrow$ apoptosis (50%), $\uparrow$ PARP cleavage, $\downarrow$ bcl-xL, no NF- $\kappa$ B $\Delta$	(Bhonde <i>et al.</i> , 2005)
SW48 (colon carcinoma)	100 nM – 1 $\mu$ M	Condensed nuclei, western	$\uparrow$ apoptosis (45%), $\uparrow$ PARP cleavage, $\downarrow$ bcl-xL, no NF- $\kappa$ B $\Delta$	(Bhonde <i>et al.</i> , 2005)
WiDr (colon carcinoma)	100 nM – 1 $\mu$ M	Condensed nuclei, western	no apoptosis, no PARP cleavage, $\uparrow$ bcl-xL, $\uparrow$ NF- $\kappa$ B $\Delta$	(Bhonde <i>et al.</i> , 2005)
HT29 (colon carcinoma)	100 nM – 1 $\mu$ M	Condensed nuclei, western	no apoptosis, no PARP cleavage, $\uparrow$ bcl-xL, $\uparrow$ NF- $\kappa$ B $\Delta$	(Bhonde <i>et al.</i> , 2005)
Cos-7 (monkey kidney)	0.3 – 1 $\mu$ M	western	$\downarrow$ ppAkt	(Sato <i>et al.</i> , 2002)
HT1080 (human fibrosarcoma)	0.3 – 1 $\mu$ M	GSK-3 kinase, western, Casp-3 assay	$\downarrow$ ppAkt, $\uparrow$ caspase-3 activity, $\downarrow$ PDK1 activity	(Sato <i>et al.</i> , 2002)
NL-17 (mouse colon carcinoma)	0.3 – 1 $\mu$ M	GSK-3 kinase, western	$\downarrow$ ppAkt, $\downarrow$ PDK1 activity	(Sato <i>et al.</i> , 2002)
293T	1 $\mu$ M	GSK-3 kinase, Casp-3 assay	$\downarrow$ Akt activity, $\uparrow$ caspase-3 activity, $\downarrow$ PDK1 activity	(Sato <i>et al.</i> , 2002)
SH-EP (neuroblastoma,	50 – 500 nM	MTT assay, TUNEL,	Apoptosis, $\uparrow$ active	(Shankar <i>et al.</i> , 2004)

Table 3 continued

Bcl-2 null, p53 wt)		western, PI flow	caspase-3, ↑G1 (36% → 50%), ↓ppAkt, ↓ppGSK-3	
SH-SY5Y (neuroblastoma, Bcl-2 wt, p53 wt)	50 – 500 nM	TUNEL	Apoptosis	(Shankar <i>et al.</i> , 2004)
SK-N-MC (neuroblastoma)	50 – 500 nM	TUNEL, western	Apoptosis, ↑ active caspase-3, ↓ppAkt, ↓ppGSK-3	(Shankar <i>et al.</i> , 2004)
MSN (neuroblastoma, BCL-2 null)	50 – 500 nM	TUNEL, western	Apoptosis, ↑ active caspase-3, ↑ cleaved PARP, ↓ppAkt, ↓ppGSK-3	(Shankar <i>et al.</i> , 2004)
IMR32 (neuroblastoma, Bcl-2 wt, p53 wt)	50 – 500 nM	TUNEL	Apoptosis	(Shankar <i>et al.</i> , 2004)
SK-N-SH (neuroblastoma, Bcl-2 +/-, p53 wt)	50 – 500 nM	TUNEL	Apoptosis	(Shankar <i>et al.</i> , 2004)
HN6 (HNSCC)	100 nM	western, GSK-3 kinase	↓ppAkt, ↓Akt activity	(Amornphimoltham <i>et al.</i> , 2004)
HN12 (HNSCC)	100 nM	western	↓ppAkt	(Amornphimoltham <i>et al.</i> , 2004)
HN13 (HNSCC)	100 nM	western	↓ppAkt	(Amornphimoltham <i>et al.</i> , 2004)
HN19 (HNSCC)	100 nM	western	↓ppAkt	(Amornphimoltham <i>et al.</i> , 2004)
HN26 (HNSCC)	100 nM	western	↓ppAkt	(Amornphimoltham <i>et al.</i> , 2004)

apoptosis regardless of p53 status (Husain *et al.*, 1997). However, the cell cycle response in these cells appears to depend on p53; wild-type p53 cells demonstrated a G1 arrest, while p53-null cells accumulated in G2. Apoptosis after UCN-01 exposure was also seen in two myeloblastic leukemia cell lines (HL60 and K562) and one colon carcinoma line (HT29), all p53-null (Shao *et al.*, 1997c). The result was remarkable in that these lines have historically been resistant to apoptosis. DNA fragmentation in these cells was preceded by increased activity of cyclin B/cdk1. Inhibition of either caspases (via Z-VAD-FMK) or serine proteases (by DCI) protected these cells from apoptosis. In a subsequent study, the same group identified modulation of PKC $\alpha$  to coincide with apoptosis in the HL60 cells (Shao *et al.*, 1997a). The authors demonstrated that UCN-01 did not directly affect PKC $\alpha$ ; instead, the drug increased autophosphorylation of PKC $\alpha$ , leading to its activation, approximately 3 hours after UCN-01 treatment, at which time apoptosis also became apparent. As in the previous study, caspase inhibition with Z-VAD-FMK protected the cells from apoptosis; the activity of PKC $\alpha$  was also inhibited. The involvement of PKC $\alpha$  is further supported by an analysis of a UCN-01 resistant cell line, A549/UCN, in which levels of PKC $\alpha$  were greatly diminished (Courage *et al.*, 1997). When cultured without UCN-01 for six months, the cells regained their sensitivity to UCN-01 and also expression of PKC $\alpha$ .

Further exploration of the A549 line and UCN-01-driven apoptosis-resistant A549/UCN subline helped to uncover a mechanism which determines the cellular response to UCN-01 (Sugiyama *et al.*, 1999). After exposure to 0.4 $\mu$ M UCN-01, 62% of A549 cells were driven into apoptosis, while the resistant A549/UCN cells had no increase following



treatment; instead, 67% of these cells accumulated in G1 (compared to 22% in A549 cells). Similar to the arresting effects detailed in the previous section, the A549/UCN cells exhibited a dose dependent increase in p21 and p27, and decreases in cyclin A, phosphorylated Rb, and active cdk2. Cdk2 kinase activity was reduced as well. None of these changes were observed in the parental A549 cells. Finally, expression of the anti-apoptotic bcl-2 protein was seen in A549/UCN cells, both in UCN-01-treated cells and untreated controls. No bcl-2 expression was seen in A549 cells (Figure 2). Levels of the anti-apoptotic bcl-xL were diminished in both lines after UCN-01 treatment. Bcl-xL was also demonstrated as an actor in the apoptotic response of four colon carcinoma cell lines (Bhonde *et al.*, 2005). The cell lines LS513 and SW48, which undergo apoptosis following UCN-01 treatment also had a dose-dependent decrease in bcl-xL expression. However, the UCN-01-resistant WiDr and HT29 lines, which are resistant to apoptosis at levels of UCN-01 up to 1.0 $\mu$ M, had not such modulation; levels of bcl-xL were constant regardless of treatment. PARP cleavage mimicked the bcl-xL and apoptotic responses, with increasing cleavage in the LS513 and SW48 cells, and no cleavage seen in the resistant WiDr and HT29 lines. While the repression of bcl-xL by UCN-01 in the sensitive cells lines is a factor in the increased apoptosis observed, the authors also demonstrate that cell cycle arrest may be just as important to the survival of the resistant lines. LS513 clones transduced with a bcl-xL retrovirus were resistant to UCN-01-mediated apoptosis, unlike the mock-infected controls. The bcl-xL overexpressing clones also entered a G1 arrest following UCN-01 treatment (from 45% G1 to over 60%); the mock-infected control cells had no change in the G1 population due to UCN-01 treatment. Thus, while UCN-01 can mediate apoptotic factors such as bcl-xL and thus

possibly enhance the toxic effects of other agents, this ability may be preempted by a UCN-01-mediated cell cycle arrest. The mechanism of bcl-xL transcriptional control by UCN-01 is still under investigation.

Apoptosis caused by UCN-01 was also shown in an *ex vivo* model of leukemia. Cells harvested from chronic lymphocytic leukemia (CLL) patients treated with 0.4 $\mu$ M UCN-01 for 4 days demonstrated a 50% loss in viability, correlated with induction of apoptosis (Byrd *et al.*, 2001). No changes in the anti-apoptotic bcl-2 protein or the pro-apoptotic bax protein were observed following UCN-01 treatment. A dose dependent decrease in p53 was observed, but a subsequent study on mouse splenocytes with wild-type or null p53 showed no requirement for p53 to induce apoptosis. The mechanism by which UCN-01 is able to induce apoptosis in these cells is uncertain, but the ability to do so without p53 present holds some promise for treating CLL patients who have become resistant to other modes of therapy such as chlorambucil and fludarabine, which require p53 to cause cell death (Mentz *et al.*, 1996).

While the PDK1-Akt survival pathway (Figure 2) was previously excluded as a possible mechanism in the G1 arresting effect of UCN-01 by Komander *et al.*, it may be involved in the apoptotic response. Cos-7, HT1080 and NL-17 cells treated with 1  $\mu$ M UCN-01 exhibited a dose-dependent reduction in phosphorylated (active) Akt; the kinase activity (GSK-3 peptide substrate) of Akt was also reduced, and caspase-3 activity and PARP cleavage (markers of apoptosis) were increased (Sato *et al.*, 2002). The lack of phosphorylation was shown not to be caused by direct inhibition of PI3K or Akt, but

rather by inhibition of the upstream kinase PDK1. The inhibition of PDK1 and induction of apoptosis were also demonstrated *in vivo* using implanted NL-17 and PC-3 cells (discussed below). Alteration of the Akt pathway by UCN-01 was also demonstrated in six neuroblastoma cell lines, SH-EP, SH-SY5Y, SK-N-MC, MSN, IMR32, ANS SK-N-SH (Shankar *et al.*, 2004). Cells treated with 0.05 $\mu$ M UCN-01 were positive for apoptosis (TUNEL staining) and had active (cleaved) caspase-3 and cleaved PARP. Furthermore, UCN-01 diminished the levels of active (phosphorylated) Akt. Acting as a prosurvival protein, Akt can phosphorylate (and thus deactivate) the proapoptotic kinases GSK3 $\beta$  and Bad, and can also modulate p53 (Khwaja, 1999; Pap and Cooper, 1998). Indeed, four hours after UCN-01 exposure, when phospho-Akt was diminished, GSK3 $\beta$  phosphorylation was also reduced, allowing GSK3 $\beta$  to remain in its active, proapoptotic state. Blockade of Akt activity was also demonstrated in HNSCC cells (Amornphimoltham *et al.*, 2004). Both Akt and GSK3 $\beta$  phosphorylation were inhibited upon UCN-01 exposure in these cells, although these cells underwent growth inhibition rather than apoptosis.

Analysis of the apoptotic mechanism following UCN-01 treatment in human colon carcinoma HT-29 cells uncovered some features seen previously (Chan *et al.*, 2003). 0.1 $\mu$ M UCN-01 resulted in 50% cell death within 48 hours. Caspase-3 activity was induced, and the levels of anti-apoptotic bcl-xL were diminished. Transfection with exogenous bcl-xL was able to rescue the cells from UCN-01, as apoptosis was reduced and caspase-3 was not activated; PARP was also not cleaved in these cells. The MAPK pathway was also implicated in this study, although not the canonical growth factor

cascade shown to play a role in arrest in the study by Facchinetti *et al.* Instead, the p38 MAPK pathway was implicated. This signaling pathway responds to cellular stress and increases in inflammatory response, and leads to cytokine production and apoptosis. HT-29 cells which were treated with 0.1 $\mu$ M UCN-01 exhibited increased p38 expression; exogenous bcl-xL experiment prevented this increase, as well as apoptosis.

Several cells lines, all derived from tumors, have shown varying vulnerability to UCN-01-mediated apoptosis (see Table 3). As in the studies examining the G1 cell cycle arrest, many players have been implicated, and no clear mechanism of apoptotic induction yet exists. While the purpose of the project detailed here is to exploit the temporary arrest of normal cells following UCN-01 treatment to *prevent* apoptosis, the pathways described above are important in that they illustrate both the pluripotency of UCN-01 and may help guide the selection of tumors which would be appropriate to treat under the protection protocol. The fate of a particular cell type following UCN-01 treatment seems to depend on the balance of various cell control pathways, and it appears that the difference between cell death and cell arrest could hinge on PKC, the original target for which UCN-01 was developed. In a tumor cell, UCN-01 is able to activate PKC, likely due to constitutively active receptor tyrosine kinase signaling. The activation of PKC can then trigger apoptosis both through bcl-2 inhibition and lack of GSK3 $\beta$  repression (Figure 2). In normal cells, UCN-01 can inhibit PKC, leading to decreased NF- $\kappa$ B signaling and cell cycle arrest. Cancers with mutated stress responses and lacking pro-apoptotic machinery may be resistant to growth inhibition, which would leave them

susceptible to other cytotoxic agents after UCN-01 exposure, while normal cells would be protected in a state of temporary cell cycle arrest.

#### **UCN-01 and G2/M checkpoint abrogation (Table 4A-4D)**

While UCN-01 can clearly trigger G1 checkpoint stimulation (causing a G1 arrest) or drive some cells into apoptosis, the compound has also been exploited for its ability to prevent the G2/M phase cell cycle checkpoint from arresting cells and allowing for DNA damage repair to proceed (Eastman, 2004). Following damage from either chemotherapeutic drugs or radiation, some tumor cells enter a G2 arrest. Following cytotoxic treatment with UCN-01 can abrogate this checkpoint, forcing cells with damage to enter mitosis. These crippled cells will then undergo apoptosis, thus enhancing the damage done to the tumor. As with the studies focusing on apoptosis due to UCN-01 alone, this project does not seek to take advantage of the G2 checkpoint abrogation. It is our aim to arrest normal cells in the G1 phase of the cell cycle, thus preventing damage from agents which target actively dividing cells, not to enhance toxicity to tumor cells. However, as the mechanisms and targets of UCN-01 seem both numerous and not entirely clear, it is important to be cognizant of any and all actors in these processes. Below is a summary of the current knowledge of the ability of UCN-01 to abrogate the G2/M checkpoint arresting machinery. The tables 4A – 4D summarize the different mechanisms of UCN-01 when used in combination therapy.

The major pathway thought to be affected by UCN-01 in this paradigm is that of cdk1/cyclin B complex in G2. When active, cdk1 is unphosphorylated at both Thr<sup>14</sup> and

Table 4A: UCN-01 in S/G2 arrest abrogation when used with a second agent/IR

Cell Line	Damaging Agent	Effect(s) Observed	Reference
CA46 (lymphoma)	IR	G2 arrest abrogation, ↑cdk1 activity (loss of ppThr <sup>14</sup> & ppTyr <sup>15</sup> )	(Wang <i>et al.</i> , 1996)
MCF-7 (p53 wt)	Cisplatin	Apoptosis resistance	(Wang <i>et al.</i> , 1996)
MCF-7/E6 (p53-)	Cisplatin	Apoptosis, G2 arrest abrogation	(Wang <i>et al.</i> , 1996)
CHO (hamster ovary, p21 & p53 null)	Cisplatin	PCNA→DNA, S arrest abrogation, apoptosis	(Bunch and Eastman, 1997)
HT29 (colon carcinoma, p53 mut)	Camptothecin	↓cyclin A levels & cdk2 kinase activity, S arrest abrogation, ↑ cdk1 activity, apoptosis	(Shao <i>et al.</i> , 1997b)
HCT116/E6 (colon carcinoma, p53 null)	Camptothecin	Apoptosis	(Shao <i>et al.</i> , 1997b)
HCT116 (p53 wt)	Camptothecin	Apoptosis resistance	(Shao <i>et al.</i> , 1997b)
MCF-7/ADR (breast cancer, p53 null)	Camptothecin	Apoptosis	(Shao <i>et al.</i> , 1997b)
MCF-7 (breast cancer, p53 wt)	Camptothecin	Apoptosis resistance	(Shao <i>et al.</i> , 1997b)
A431 (human epithelial carcinoma, p53 mut)	Mitomycin C	G2 arrest abrogation, apoptosis	(Sugiyama <i>et al.</i> , 2000)
PSN-1 (human pancreatic adenocarcinoma, p53 mut)	Mitomycin C	G2 arrest abrogation, apoptosis	(Sugiyama <i>et al.</i> , 2000)
HCT-116 (p53 wt)	Mitomycin C	Apoptosis resistance	(Sugiyama <i>et al.</i> , 2000)
MCF-7 (p53 wt)	Mitomycin C	Apoptosis resistance	(Sugiyama <i>et al.</i> , 2000)
WiDr (colon carcinoma, p53 null)	Mitomycin C	Apoptosis	(Sugiyama <i>et al.</i> , 2000)
WiDr/BM (colon carcinoma, p53 +)	Mitomycin C	Apoptosis resistance	(Sugiyama <i>et al.</i> , 2000)
MDA-MB231 (breast cancer, p53 mut)	SN38	S/G2 arrest abrogation, apoptosis	(Kohn <i>et al.</i> , 2002)

Table 4A continued

MCF-10a (breast epithelium, p53 wt)	SN38	Apoptosis resistance, ↓ cyclins A & B	(Kohn <i>et al.</i> , 2002)
HCT116 (p53 wt)	IR	G2 arrest abrogation, Chk2 inhibition	(Yu <i>et al.</i> , 2002)
HCT116 (p53 null subline)	IR	G2 arrest abrogation, Chk2 inhibition	(Yu <i>et al.</i> , 2002)
HCT116 (p53 wt)	SN38	G2 arrest abrogation, ↓p21, ↑cyclin B	(Levesque <i>et al.</i> , 2008)
MCF-7 (p53 wt)	SN38	G2 arrest abrogation, ↓p21, ↑cyclin B	(Levesque <i>et al.</i> , 2008)
CAKI-1 (renal carcinoma, p53 wt)	SN38	UCN-01 unable to block G2 arrest	(Levesque <i>et al.</i> , 2008)
U87MG (glioma, p53 wt)	SN38	UCN-01 unable to block G2 arrest	(Levesque <i>et al.</i> , 2008)
SUM102 (breast cancer, p53 wt)	SN38	UCN-01 unable to block G2 arrest	(Levesque <i>et al.</i> , 2008)
A549 (lung carcinoma, p53 wt)	IR	No UCN-01-enhanced toxicity	(Xiao <i>et al.</i> , 2002)
A549/E6 (p53 null)	IR	G2 arrest abrogation, apoptosis	(Xiao <i>et al.</i> , 2002)
LXSN (lung carcinoma, p53 wt)	IR	No UCN-01-enhanced toxicity	(Xiao <i>et al.</i> , 2002)
A549 (p53 wt)	IR	G2 block abrogation, no increased toxicity	(Mack <i>et al.</i> , 2004)
Calu (lung carcinoma, p53 wt)	IR	G2 arrest abrogation, apoptosis	(Mack <i>et al.</i> , 2004)
HT29 (colon carcinoma, p53 mut)	IR	G2 arrest abrogation, apoptosis	(Playle <i>et al.</i> , 2002)
SW480 (colon carcinoma, p53 mut)	IR	G2 arrest abrogation, apoptosis	(Playle <i>et al.</i> , 2002)
SW260 (colon carcinoma, p53 mut)	IR	G2 arrest abrogation, no increased toxicity	(Playle <i>et al.</i> , 2002)
S/KS (rectal carcinoma, p53 mut)	IR	G2 arrest abrogation, no	(Playle <i>et al.</i> , 2002)

Table 4A continued

		increased toxicity	
S/KS (rectal carcinoma, p53 mut)	IR	G2 arrest abrogation, no increased toxicity	(Playle <i>et al.</i> , 2002)
CHO	Cisplatin	G2 arrest abrogation	(Bunch and Eastman, 1996)
HT29	Camptothecin	S arrest abrogation	(Shao <i>et al.</i> , 1997a)
MDA-MB231, T47D (breast cancer)	Cisplatin	S/G2 arrest abrogation	(Lee <i>et al.</i> , 1999)
MDA-MB231, GI 101A	Camptothecin	Apoptosis, S/G2 arrest abrogation	(Jones <i>et al.</i> , 2000)
A341, PSN-1, HCT116, MCF-7	Mitomycin C	Apoptosis, S/G2 arrest abrogation	(Sugiyama <i>et al.</i> , 2000)
U87MG	Temozolomide	G2 arrest abrogation, Chk1 inhibition	(Hirose <i>et al.</i> , 2001)
184B5, 184B5/E6	Adriamycin	G2 arrest abrogation	(Luo <i>et al.</i> , 2001)
HCT116	SN-38	S/G2 arrest abrogation	(Tse and Schwartz, 2004)
A549, PC-3	Perifosine	S arrest abrogation	(Dasmahapatra <i>et al.</i> , 2004)
MCF10a	SN38	S arrest abrogation, ↓p21	(Levesque <i>et al.</i> , 2005)
HT29	Ara-C	Apoptosis, ↑cdk1, chk1 inhibition, G2 arrest abrogation	(Shao <i>et al.</i> , 2004)



Table 4B: UCN-01 and apoptosis in concert with a second agent

Cell Line(s)	Damaging Agent	Effect(s) Observed	Reference
SKOV-3, OVCAR-3, -420, -429, -432	CDDP	Apoptosis (p53 dependent)	(Husain <i>et al.</i> , 1997)
SK-GT5	5-FU	Apoptosis, TS suppression	(Hsueh <i>et al.</i> , 1998)
MCF-7, T47D, HS578T, BT549, MDA-N, MDA-MB231, MDA435	Camptothecin	Apoptosis, growth inhibition (p53 independent), inverse correlation with bcl-2, bcl-xL	(Nieves-Neira and Pommier, 1999)
U937	Ara-C	Apoptosis, caspase activation, mitochondrial damage	(Tang <i>et al.</i> , 2000)
NCI-H322M, MDA-MB435, NCI-H23, HT29, MCF-7	Mitomycin C, cisplatin, 5-FU, topotecan, fludarabine	Apoptosis (p53 dependent), growth inhibition	(Monks <i>et al.</i> , 2000)
MCF-7, MCF-7/ADR	Danazol, mifepristone	Apoptosis (ER/PR dependent)	(Yokoyama <i>et al.</i> , 2000)
U937, HL-60	Fludarabine	Apoptosis (sequence dependent)	(Harvey <i>et al.</i> , 2001)
ML-1	Gemcitabine	Apoptosis, no cell cycle progression	(Shi <i>et al.</i> , 2001)
MDA-MD231, MCF-7, T47D, DU145, LNCaP	PD98059	Apoptosis, MAPK inhibition, ↑Bax	(McKinstry <i>et al.</i> , 2002)
U937	17-AAG	Apoptosis, ↓Akt, ↓MAPK	(Jia <i>et al.</i> , 2003)
Lymphocytes (normal and CLL)	UV light, 4-HC	Apoptosis, DNA repair inhibition	(Yamauchi <i>et al.</i> , 2002)
A431	FdUrd	Apoptosis, inhibition of TS and DNA repair	(Grem <i>et al.</i> , 2002)
K562, LAMA84	UO126, PD184352	Apoptosis, ↓Mcl-1, ↓ cyclin D, ↓Bcr/Abl, Jnk activation	(Yu <i>et al.</i> , 2002)
ML-1	Fludarabine	Apoptosis, cdk2 and cdc25a reactivation	(Sampath <i>et al.</i> , 2002)
RPMI8226, NCI-H929, U266 MM	PD184352	Apoptosis, inhibition of UCN-01 MEK activation	(Dai <i>et al.</i> , 2002)

Table 4B continued

A549, Calu1, H596	Cisplatin	Apoptosis, ↓cyclin A and cyclin B	(Mack <i>et al.</i> , 2003)
U937, HL-60	Ara-C	Apoptosis, ↓Bcl-2	(Wang <i>et al.</i> , 2003)
U266, MM.1S, MM.1R	Bay 11-7082	Apoptosis, IκB, NFκB disruption	(Dai <i>et al.</i> , 2004)
HMEC, HMEC/E6, MDA-MB231	Topotecan	Apoptosis, normal/tumor differential, p53 dependence	(Redkar <i>et al.</i> , 2004)
HT29	Ara-C	Apoptosis, ↑cdk1, chk1 inhibition, G2 arrest abrogation	(Shao <i>et al.</i> , 2004)
HCT116	SN-38	Apoptosis, S/G2 arrest abrogation, p53 independence	(Tse and Schwartz, 2004)
A549, PC-3	Perifosine	Apoptosis, S arrest abrogation, Akt activation	(Dasmahapatra <i>et al.</i> , 2004)
U937, HL-60, Raji, Jurkat	L744832	Apoptosis, MEK inactivation, Jnk activation	(Dai <i>et al.</i> , 2005)
U937	Rapamycin	Apoptosis, ↓MEK/ERK, ↓Bcl-2, ↓cyclin D	(Hahn <i>et al.</i> , 2005)
MCF10A	SN38	Apoptosis, S arrest abrogation, ↓p21	(Levesque <i>et al.</i> , 2005)
CD138 <sup>+</sup>	L744832	Apoptosis, Jnk activation, Akt inactivation	(Pei <i>et al.</i> , 2005)
TE2, TE12, H322, H460, H513, H211	Valproic acid	Apoptosis, NFκB suppression	(Yeow <i>et al.</i> , 2006)
U266, RPMI8226	PD184352	Apoptosis, Bim dependence	(Pei <i>et al.</i> , 2007)
MDA-MB231, GI 101A	Camptothecin	Apoptosis, S/G2 arrest abrogation	(Jones <i>et al.</i> , 2000)
A341, PSN-1, HCT116, MCF-7	Mitomycin C	Apoptosis, S/G2 arrest abrogation, p53 dependence	(Sugiyama <i>et al.</i> , 2000)
HCT116	Camptothecin	Apoptosis, DNA ds breaks, ↑γH2AX, ↓p21	(Furuta <i>et al.</i> , 2006)

Table 4C: Cell lines demonstrating growth arrest when treated with UCN-01 and a second agent

Cell Line(s)	Secondary Agent	Effect(s) Observed	Reference
A431	Mitomycin C	G1/S arrest	(Akinaga <i>et al.</i> , 1993)
A-172, T-98G	BCNU and cisplatin	n/a	(Pollack <i>et al.</i> , 1996)
MCF-7, T47D, HS578T, BT549, MDA-N, MDA-MB231, MDA-MB435	Camptothecin	p53 independence, inverse correlation to bcl-2, bcl-xL	(Nieves-Neira and Pommier, 1999)
HMEC, HE6, MDA-MB231	Camptothecin	DNA ds breaks, p53 dependence	(Jones <i>et al.</i> , 2000)
NCI-H322M, MDA-MB435, NCI-H23, HT29, MCF-7	Mitomycin C, cisplatin, 5-FU, topotecan, fludarabine	p53 dependence	(Monks <i>et al.</i> , 2000)
MCF-7	Tamoxifen	↓Rb phosphorylation	(Koh <i>et al.</i> , 2003)
MDA-MB231, MCF-7, HCT116, HEPG2	PD184352, AZD6244, FTI277, R115777	Bax/Bak dependence, ERK activity	(Hamed <i>et al.</i> , 2008)

Table 4D: Studies demonstrating p53 dependence/independence for actions of UCN-01 and a second agent

Cell Line(s)	Secondary Agent	Effect(s) Observed	Reference
HMEC, HE6, MDA-MB231	Camptothecin	DNA ds breaks, p53 <i>dependence</i>	(Jones <i>et al.</i> , 2000)
NCI-H322M, MDA-MB435, NCI-H23, HT29, MCF-7	Mitomycin C, cisplatin, 5-FU, topotecan, fludarabine	p53 <i>dependence</i>	(Monks <i>et al.</i> , 2000)
SKOV-3, OVCAR-3, -420, -429, -432	CDDP	Apoptosis (p53 <i>dependent</i> )	(Husain <i>et al.</i> , 1997)
A341, PSN-1, HCT116, MCF-7	Mitomycin C	Apoptosis, S/G2 arrest abrogation, p53 <i>dependence</i>	(Sugiyama <i>et al.</i> , 2000)
HMEC, HMEC/E6, MDA-MB231	Topotecan	Apoptosis, normal/tumor differential, p53 <i>dependence</i>	(Redkar <i>et al.</i> , 2004)
MCF-7, T47D, HS578T, BT549, MDA-N, MDA-MB231, MDA435	Camptothecin	Apoptosis, growth inhibition (p53 <i>independent</i> ), inverse correlation with bcl-2, bcl-xL	(Nieves-Neira and Pommier, 1999)
HCT116	SN-38	Apoptosis, S/G2 arrest abrogation, p53 <i>independence</i>	(Tse and Schwartz, 2004)

Tyr<sup>15</sup> (Ohi and Gould, 1999). However, upon DNA damage, cdk1 is phosphorylated at both these sites and is inactivated. The phosphorylation status of cdk1 is determined by the interplay of the Wee1 kinase and the Cdc25C phosphatase. The ATM kinase, activated by DNA damage, can phosphorylate and activate the checkpoint kinases Chk1 and Chk2 (Weinert, 1997). These kinases are able to phosphorylate Cdc25C, allowing binding to 14-3-3 proteins and sequestering it in the cytoplasm. The expulsion of Cdc25C from the nucleus prevents removal of the inhibitory phosphates on cdk1, leaving it inactive and the cell arrested in G2. By inhibition of ATM, Chk1, Chk2 and other signaling molecules, UCN-01 is able to blunt this arrest. The specific actions of UCN-01 in the G2/M transition will be reviewed here (Figure 3).

Most of the studies reviewed in this section first require induction of the G2 checkpoint prior to evaluating the ability of UCN-01 to then allow the cells to pass it. The focus will be on studies which examine the mechanism of UCN-01 action; other studies which concentrate on the enhanced ability to kill cells via this abrogation will be mentioned as appropriate.

The initial study on UCN-01 in this context was done using human lymphoma CA46 cells (Wang *et al.*, 1996). Following  $\gamma$  irradiation (6.3 Gy), the cells were arrested at the G2/M phase of the cell cycle. UCN-01 was able to inhibit the resultant G2 arrest in a dose- dependant manner. 30 nM of UCN-01 had little effect, but 100 nM allowed the progression of some cells into G1, and 300 nM completely abolished the G2 arrest (DNA histogram, no number cited). UCN-01 was able to activate the cyclin B/cdk1 complex

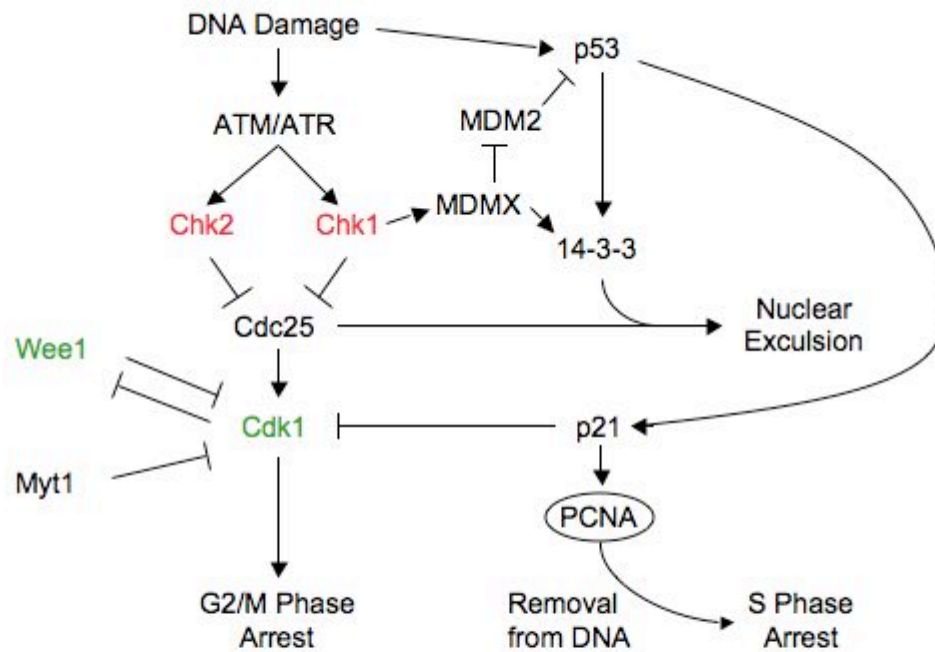


Figure 3: Pathways implicated in the abrogation of S/G2 phase arrest by UCN-01. **Green** indicates activities enhanced by UCN-01, **red** indicates inhibition by UCN-01.

3.5-fold in irradiated cells over the level seen with radiation alone; this activation of the cyclin B/cdk1 kinase complex was shown to be due to the absence of the inhibitory phosphorylations on cdk1 at Thr<sup>14</sup> and Tyr<sup>15</sup> (Figure 3). In the same study, it was also discovered that p53 may play a role in the ability of UCN-01 to abrogate the G2 arrest. MCF-7 cells with functional p53 and treated with cisplatin (2.5-15  $\mu$ M) followed by 100 nM UCN-01 were much more resistant to cell death than MCF-7/E6 cells with defective p53 subjected to the same treatment. At 10 nM cisplatin, control MCF-7 cells had a 10% survival rate, while the MCF-7/E6 survived at less than 0.01%.

An alternate mechanism was demonstrated in Chinese hamster ovary (CHO) cells (Bunch and Eastman, 1997). Cisplatin treatment induces an S phase arrest in these cells; UCN-01 speeds the cells through S into G2 and then into apoptosis. The S phase arrest was caused by sequestration of proliferating cell nuclear antigen (PCNA) away from the DNA (Figure 3). PCNA is required for DNA replication, so its removal can effectively block S phase progression. This process usually proceeds by the binding of PCNA to p21, which in turn has been induced by p53 (Figure 3). In this setting another mechanism must be responsible, as both p53 and p21 are absent in CHO cells. Nevertheless, UCN-01 treatment after cisplatin was able to return PCNA to the DNA fraction of these cells, and the S phase arrest was circumvented. However, the mechanism by which PCNA is sequestered away from the DNA and then returned via UCN-01 is unclear.

Potentiation of UCN-01 cell killing in the absence of p53 was also demonstrated following camptothecin treatment (Shao *et al.*, 1997b). HT29 colon carcinoma cells (p53

mutant) entered into an S phase arrest after camptothecin treatment. This alteration was marked by both increased levels of cyclin A and cyclin A/cdk2 kinase activity. UCN-01 prevented both these increases, and also increased cdk1 kinase activity. In the same study, UCN-01 potentiated the cell killing ability of camptothecin in HT29 cells, reducing the amount needed to kill 50% of the cells by over 6-fold. UCN-01 also potentiated the toxicity of camptothecin in HCT116/E6 and MCF-7/ADR cells, both of which are defective for p53 function (Shao *et al.*, 1997b). This enhancement was greatly diminished in the p53 wild-type HCT116 and MCF-7 cells. A similar finding was reported when using UCN-01 to nullify the G2 arrest and therefore increase the cytotoxicity of mitomycin c (MMC) (Sugiyama *et al.*, 2000). UCN-01 significantly potentiated MMC in the p53 mutant cell lines A431 (human epithelial carcinoma) and PSN-1 (human pancreatic adenocarcinoma), but showed no such effect in p53 wild-type HCT116 or MCF-7 cells. The same differential effect was observed when using p53-defective WiDr cells and a wild-type p53-transfected derivative line, WiDr/BM (Sugiyama *et al.*, 2000). The effect of p53 on UCN-01 checkpoint abrogation was also demonstrated using two breast epithelial cell lines, the p53 mutant tumor cell line MDA-MB231 and p53 wild-type MCF10a line (Kohn *et al.*, 2002). Treatment with the topoisomerase inhibitor SN38 generated a G2 arrest in both lines; subsequent UCN-01 treatment was able to block the arrest in the p53 mutant MDA-MB231 line, but not in the MCF10A human mammary epithelial cell line (see Figure 3). The resistance of MCF10A cells correlated with diminished expression of both cyclins A and B.



Not all studies have shown that UCN-01 acts primarily by inhibiting Chk1, or that p53 is important in this response. Exposure of HCT116 cells and a p53 null subline to ionizing radiation (IR) lead to a G2 arrest; secondary UCN-01 was able to blunt this arrest, regardless of p53 status (Yu *et al.*, 2002). IR induced p53 upregulation and stabilization as well as increased activity of Chk2; Chk1 activity was not altered (Figure 3). UCN-01 was able to prevent this increase in p53 levels in the wild-type cells, and also blocked phosphorylation of the stabilizing serine-20 site, a target of Chk2 (Dumaz *et al.*, 2001). This report seems to be in conflict with the previous body of work, indicating that the p53 pathway may have differing sensitivity to UCN-01 in terms of cell lines and concentrations. Also in conflict was the finding that UCN-01 can inhibit Chk2 *in vitro*. The vulnerability of p53 wild-type cells to this mechanism was demonstrated again, not only in the HCT116 cells, but also in MCF-7 cells (Levesque *et al.*, 2008). After SN38 treatment, these cells went into a G2 arrest, concomitant with repression of cyclin B and enhancement of p21 expression. UCN-01 was able to block these responses, and the cells entered mitosis and apoptosed. However, three other p53 wild-type lines, CAKI-1, U87MG, and SUM102 demonstrated the same response to SN38, and UCN-01 was ineffective in reversing this response (Levesque *et al.*, 2008). One possible factor in the p53-related UCN-01 sensitivity/resistance may be the MDM2 assistant protein, MDMX (Jin *et al.*, 2006). MDMX is a recruiting factor for MDM2, the E3 ubiquitin ligase responsible for p53 degradation. Active Chk1 phosphorylates MDMX, which enhances binding to the 14-3-3 proteins and sequesters it away from the nucleus. 293T cells stimulated to activate the DNA repair pathway via UV treatment demonstrated exactly this response, and subsequent UCN-01 exposure was able to repress all these effects.

One issue with many of these studies is that the expression and activity of the proteins noted is often correlated with the arrest and UCN-01-mediated release, but are not shown to be necessary or sufficient. In fact, a recent study using short hairpin RNA (shRNA) to block Chk1, Chk2 or both in MDA-MB231 cells seems to indicate that *neither* is required for the G2 arrest after SN38 treatment, pointing to the possibility that an alternate kinase is instead acting to produce the arrest (Zhang *et al.*, 2008). Modulation of Cdc25A was seen in the absence of both kinases, and the alternate checkpoint kinase MAPKAPK2 (MK2) was ruled out as the effector as well in MDA-MB231 cells. To date, no clear mechanism for the DNA-damage arrest and its abrogation via UCN-01 exists.

Further uncertainty about the involvement and importance of p53 in UCN-01 potentiation of cell killing comes from studies utilizing UCN-01 to enhance cell death following ionizing radiation (Xiao *et al.*, 2002). The human lung carcinoma cell lines A549 and LXSX are p53 wild-type. Upon irradiation, these cells accumulated in both G1 and G2 phases of the cell cycle. However, a p53-disrupted E6 A549 subline exhibited only a G2 arrest following the same treatment. Application of UCN-01 six hours later resulted in a significant reduction in survival of the E6 cells; the p53-competent A549 and LXSX cells were not similarly sensitized, indicating that functional p53 may protect cells from the UCN-01 enhanced mortality. However, a subsequent study on A549 and the p53 wild-type Calu1 cell lines blurs this distinction (Mack *et al.*, 2004). Ionizing radiation treatment resulted in the cell cycle arrest seen previously, and in both cell lines UCN-01 was able to abrogate the G2 arrest. As before, A549 cells were resistant to UCN-01 enhanced decrease in cell survival when given following irradiation. However, Calu1

cells were sensitive to this treatment protocol, despite expressing functional p53. The enigmatic reaction to irradiation plus UCN-01 treatment was likewise observed in a panel of five colorectal tumor cell lines with mutant p53 (Playle *et al.*, 2002). Exposure to 5 Gy of radiation resulted in a G2 arrest in all five lines (HT29, SW480, SW260, S/KS, and S/RG/C2); successive UCN-01 was able to blunt this response in all cell types. However, analysis of cell survival following this treatment demonstrated a significant decrease in survival in only the HT29 and SW480 lines when treated with UCN-01 compared to radiation alone. An *in vivo* study of p53 wild-type RIF-1 tumors in mice demonstrated a significant reduction in tumor growth when UCN-01 was given prior to 20 Gy of radiation compared to either treatment alone (Khan *et al.*, 2009). These studies indicate that p53 may partially modulate the activity of UCN-01, but the drug may have distinct actions which do not involve p53.

The ability of UCN-01 to move cells through the G2 phase of the cell cycle seems to lie at least in part upon the activation or maintenance of active cdk1. Murine FT210 cells, which have a temperature sensitive cdk1, were placed into G2 arrest using  $\gamma$  irradiation (Yu *et al.*, 1998). Successive treatment with 0.3 $\mu$ M UCN-01 was able to abrogate the G2 arrest at the permissive temperature. However, at the non-permissive temperature for cdk1 activity in these cells, UCN-01 could no longer abrogate G2 arrest. UCN-01 was still able to abrogate the G2 arrest in the parental cell line (FM3A), ruling out temperature as a complicating factor. UCN-01 treatment also resulted in the inactivation of the Wee1 kinase in FM3A cells, thus preventing it from adding inhibitory phosphate groups onto cdk1. The inactivation of Wee1 does not appear to be due to direct inhibition by UCN-01

(*in vitro* incubations showed Wee1 to be quite resistant to UCN-01 inhibition) but rather via a feedback loop. Cdk1/cyclin B can phosphorylate Wee1, thus targeting it for ubiquitination by cdc34 and proteasomal degradation (Michael and Newport, 1998). The increased activity of cdk1 could thus result in decreased Wee1. Finally, UCN-01 also prevented the phosphorylation/deactivation of the Cdc25C phosphatase (Yu *et al.*, 1998). These two activities are likely to increase the activity of cdk1 and thus push cells into mitosis. One possible upstream regulator of Cdc25C is the human checkpoint kinase, either Chk1 or Chk2. *In vitro* studies have shown direct inhibition of Chk1 by UCN-01, with an IC<sub>50</sub> of 11 nM (Busby *et al.*, 2000). K562 erythroid leukemia cells enter a G2 arrest following  $\gamma$  irradiation; subsequent UCN-01 treatment reduced the phosphorylation of Cdc25C, and completely relieved the G2 block. However, Chk2 was shown to be highly resistant to UCN-01, suggesting to action of UCN-01 is most likely through Chk1 inhibition. More evidence for the modulation of Cdc25C via Chk1 was obtained from HeLa cells arrested in G2 following  $\gamma$  irradiation (Graves *et al.*, 2000). In the absence of UCN-01, the prevailing status of Cdc25C was serine-216 phosphorylated and 14-3-3 bound (Figure 3). Addition of UCN-01 reduced the phosphorylation at serine-216 and caused Cdc25C to detach from 14-3-3; cdk1 activation and mitotic entry soon followed. One other item noted in this study was the inability of UCN-01 to induce freed Cdc25C (released from 14-3-3) to reenter the nucleus; the majority of the now serine-216 dephosphorylated, monomeric Cdc25C was still cytoplasmic. How this cytosolic phosphatase could activate the nuclear cdk1 is unclear. The role of Cdc25C is unclear in the breast tumor line MDA-MB231 as well (Kohn *et al.*, 2002). While UCN-01 can block a G2 arrest in these cells, the levels of active Cdc25C seem to depend on the

dose of UCN-01 used. While a high concentration of UCN-01 (500 nM) rapidly increased the levels of active Cdc25C, low UCN-01 (15 nM) produced very little active Cdc25C, even though this dose was sufficient to drive the arrested (p53 mutant) cells into mitosis.

While the reports concerning the ability of UCN-01 to cause a cell cycle arrest implicate many pathways and protein effects, the abrogation of a G2/M arrest following a damage response seems to be less complicated. Most of the experimental evidence indicates an increase in cdk1 kinase activity concomitant with cell cycle progression through mitosis. This increase can be due to inhibition of chk1 and/or chk2, leading to cdc25 phosphatase activity to remove the inhibitory phosphorylations on cdk1. In addition, UCN-01 can diminish p53, leading to decreased levels of 14-3-3 proteins (thus keeping cdc25 in the nucleus and able to activate cdk1) and also lower levels of p21, in turn also increasing cdk1 activity. While some of the pathways leading to G1 arrest may also be activated by UCN-01, the prior DNA-damaging stimulus may make those pathways unimportant. Damaged cells arrested in G2 and then forced through mitosis will most likely die, so activation of a G1 checkpoint may be of little consequence. In addition, the loss or mutation of p53 in many of the cell lines examined may further prevent cdk1 inhibition, thus abrogating the G2 arrest. The literature concerning UCN-01 synergism with or potentiation of secondary agents is quite extensive, but also outside the focus of this project. While many studies have been discussed here to gauge the various possible mechanisms of UCN-01 actions, other reports focus mainly upon its effects (usually inhibition of proliferation or enhanced apoptosis). Summarized in Tables 4A-D are

studies concerning UCN-01 in combination with either IR or other agents, grouped into four categories of effects and mechanisms: S/G2 arrest abrogation, growth inhibition, apoptosis, and p53 dependence/independence.

### **UCN-01 *in vivo* (Table 5)**

While the volume of work examining UCN-01 in cell culture systems is quite extensive, the *in vivo* effects and mechanisms of UCN-01 action are poorly understood, as few *in vivo* studies have been done using UCN-01. As with the *in vitro* work, UCN-01 was originally used to prevent or retard the growth of implanted tumors in mice. The first such study demonstrated a functional difference between UCN-01 and staurosporine. Using three human tumor lines (A431, HT1080 and HL-60) and two murine tumor lines (K-BAL and M-MSV-BALB), it was found that while UCN-01 was much less potent at inhibiting growth in culture than staurosporine (IC<sub>50</sub> for 72 hours of UCN-01 treatment was 9.2 – 87.4 fold less potent than staurosporine), it was effective at slowing the growth of all five lines when implanted into mice, while staurosporine had no effect (Akinaga *et al.*, 1991). The tumors were implanted into the flanks of nude mice (human tumors) or antigen-matched syngeneic mice (murine tumors), and were treated daily for 5 days with UCN-01 or staurosporine. UCN-01 prevented tumor growth at doses between 5 and 7.5 mg/kg; equivalent doses of staurosporine had no effect on these tumors. The combination of MMC and UCN-01 was synergistic in killing implanted A431 cells, and this was confirmed as a viable treatment option in two other solid tumor models (Co-3 and murine sarcoma 180) as well as the P388 murine leukemia model (Akinaga *et al.*, 1993). A constant infusion of UCN-01 of 1 mg/kg/day for one week was also effective in

Table 5: *In vivo* studies using UCN-01 in tumor-bearing animals

<b>Tumor</b>	<b>Drug Regimen</b>	<b>Tumor Effect</b>	<b>Mechanism</b>	<b>Reference</b>
A431	5 mg/kg (ip) /day X 5	60% growth inhibition	n/a	(Akinaga <i>et al.</i> , 1991)
HT1080	7 mg/kg (ip)/ day X 5	83% growth inhibition	n/a	(Akinaga <i>et al.</i> , 1991)
HL-60	7 mg/kg (ip)/day X 5	39% growth inhibition	n/a	(Akinaga <i>et al.</i> , 1991)
K-BALB	7.5 mg/kg (ip)/day X 5	73% growth inhibition	n/a	(Akinaga <i>et al.</i> , 1991)
M-MSV-BALB	7.5 mg/kg (ip)/day X 5	79% growth inhibition	n/a	(Akinaga <i>et al.</i> , 1991)
A431	4 mg/kg mitomycin c + 14.5 mg/kg UCN-01 (iv)	83% growth inhibition	n/a	(Akinaga <i>et al.</i> , 1993)
Co-3	4 mg/kg mitomycin c + 14.5 mg/kg UCN-01 (iv)	80% growth inhibition	n/a	(Akinaga <i>et al.</i> , 1993)
Murine sarcoma 180	6 mg/kg mitomycin c + 14.5 mg/kg UCN-01 (iv)	89% growth inhibition	n/a	(Akinaga <i>et al.</i> , 1993)
P388	4 mg/kg mitomycin c + 14.5 mg/kg UCN-01 (iv)	Lifespan increased 105%	n/a	(Akinaga <i>et al.</i> , 1993)
U-87	1 mg/kg/day UCN-01 X 7 days (ip)	50% decreased tumor volume, 57% survival at 60 days (vs. 0.7% control)	n/a	(Pollack <i>et al.</i> , 1996)
PAN-3-JCK	5 mg/kg/day UCN-01 X 5 days (ip)  10 mg/kg/day UCN-01 X 5 days (ip)	Tumor weight T/C = 36.3%  Tumor weight T/C = 16.8%	G1 arrest (37%→61%), ↑p21, ↓cdk2 activity  G1 arrest (67%), ↑p21, ↓cdk2 activity	(Abe <i>et al.</i> , 2001)
CRL 1420	5 mg/kg/day UCN-01 X 5 days (ip)	Tumor weight T/C = 32.3%	G1 arrest (43%→61%), ↑p21, ↓cdk2 activity	(Abe <i>et al.</i> , 2001)

Table 5 continued

	10 mg/kg/day UCN-01 X 5 days (ip)	Tumor weight T/C = 16.2%	G1 arrest (52%), ↑p21, ↓cdk2 activity	
MX-1	5 mg/kg/day UCN-01 X 5 days (ip)  10 mg/kg/day UCN-01 X 5 days (ip)	Tumor weight T/C = 89.9%  Tumor weight T/C = 66.1%	↓cdk2 activity, No Δ in p21 or cell cycle ↓cdk2 activity, ↑p21, no Δ in cell cycle	(Abe <i>et al.</i> , 2001)
Br-10	7.5 mg/kg/day UCN-01 X 5 days/week X 2 weeks (ip)	Tumor weight T/C = 27.0%	↑p21, pRb de- phosphorylation	(Koh <i>et al.</i> , 2002)
MCF-7	7.5 mg/kg/day UCN-01 X 5 days/week X 2 weeks (ip)	Tumor weight T/C = 25.0%	↑p21, pRb de- phosphorylation	(Koh <i>et al.</i> , 2002)
MX-1	7.5 mg/kg/day UCN-01 X 5 days/week X 2 weeks (ip)	Tumor weight T/C = 65.9%	↑p21, no Δ in pRb phosphorylation	(Koh <i>et al.</i> , 2002)
HN12	7.5 mg/kg/day UCN-01 X 5 days (ip)	Tumor weight T/C = 0.3%	Apoptosis (TUNEL), ↑p27, ↓cyclin D	(Patel <i>et al.</i> , 2002)
MDA-MB231	0.2 mg/kg UCN-01 X 3 + 25 mg/kg PD184352 X 3	Tumor weight T/C = 32%	Apoptosis, ↓ angiogenesis	(Hamed <i>et al.</i> , 2008; Hawkins <i>et al.</i> , 2005)
MCF-7	0.1 mg/kg UCN-01 X 3 + 25 mg/kg PD184352 X 3	Tumor weight T/C = 34%	Apoptosis, ↓ angiogenesis	(Hamed <i>et al.</i> , 2008; Hawkins <i>et al.</i> , 2005)
MDA-MB231	0.2 mg/kg/day UCN-01 X 2 days + 100 mg/kg/day R115,777 X2  0.2 mg/kg/day UCN-01 X 2 days + 25 mg/kg/day PD184352 X2	3-fold decrease in tumor volume vs. controls  4-fold decrease in tumor volume vs. controls	↓Ki-67 levels, decreased <i>ex</i> <i>vivo</i> plating efficiency of excised tumors	(Hamed <i>et al.</i> , 2008)



Table 5 continued

NL-17	5 & 10 mg/kg UCN-01 (ip)	No tumor effect noted	↓PDK1 activity	(Sato <i>et al.</i> , 2002)
PC-3	6, 9, 13 mg/kg UCN-01 (ip)	No tumor effect noted	↓PDK1 activity	(Sato <i>et al.</i> , 2002)

reducing the tumor volume of implanted (subcutaneous) U-87 malignant glioma tumors (Pollack *et al.*, 1996). 28 days after the UCN-01 treatment, no mice had evidence of tumor re-growth, and postmortem analysis was unable to identify any tumor cells. In the same study, intracranial gliomas were treated with 2 mg/kg/day for one week. By day 60, only one of fourteen control mice had survived, whereas four out of seven UCN-01-treated mice survived until day 90.

The *in vivo* mechanism by which UCN-01 can inhibit tumor growth was examined using two implanted pancreatic cancer lines (PAN-3-JCK and CRL 1420) and the breast cancer line MX-1 (Abe *et al.*, 2001). The two pancreatic lines were potently inhibited by 5 mg/kg UCN-01, while MX-1 was unaffected. The pancreatic lines had increased levels of p21 and decreased cdk2 activities. The cells were arrested in G1, and an increase in apoptosis was noted as well. The levels of p27 were not affected by UCN-01.

Interestingly, the resistant MX-1 line was demonstrated to have a baseline cdk2 activity more than 6 fold higher than the two responsive lines, leading to the conclusion that the balance between kinases and their activator/inhibitors plays a key role in determining response to UCN-01. A later study examining implanted MX-1 cells as well as two other breast carcinomas (MCF-7 and Br-10) had similar findings (Koh *et al.*, 2002). 7.5 mg/mkg UCN-01 was effective in inhibiting the *in vivo* growth of the Br-10 and MCF-7 lines, but MX-1 was again resistant. At this dose, p21 was induced in all three tumors, but only the responsive ones exhibited decreased Rb phosphorylation; MX-1 showed little change in Rb. UCN-01 also demonstrated antitumor activity against HN12 (HNSCC) implanted in mice (Patel *et al.*, 2002). 7.5 mg/kg/day for five days in these xenografts

models abolished tumor growth. Analysis of tumor tissue following UCN-01 demonstrated increased apoptosis versus vehicle-treated tumors as measured by TUNEL assay. In addition, p27 levels were elevated and cyclin D levels diminished in the UCN-01 treated tumors. Unlike the *in vitro* studies on HNSCC lines, no changes in p21 were observed after UCN-01 injection.

A different study demonstrated the efficacy of the combination of UCN-01 and a second inhibitor, PD184352 (and inhibitor of MEK1 and MEK2), in implanted MDA-MB231 and MCF-7 tumors (Hawkins *et al.*, 2005). Treatment with either agent alone for two days had minimal effect on the implanted tumors, but the combination of 25 mg/kg PD184352 and 0.2 mg/kg UCN-01 greatly reduced the growth of MDA-MB231 tumors and completely eradicated MFC- tumor growth. Reduced growth potential correlated with an increase in apoptosis at both 5 and 30 days post-treatment. This study is in agreement with a similar report using PD184352 with UCN-01 to treat both implanted MDA-MB231 and MCF-7 tumors (Hamed *et al.*, 2008). The combination treatment significantly retarded tumor growth compared to either agent alone. In addition, Ki-67 immunoreactivity was completely abolished and CD31 reduced, indicating growth arrest and reduced angiogenesis. Further experimentation with radiation and the drug combination revealed that while radiation during the drug treatment course encompassed no increase in cytotoxicity, irradiating the tumors 24 hours after the cessation of drug treat significantly increased cell death within the tumors, indicating a sequence-dependent radiosensitization effect.

The Akt-PDK1 survival pathway, which has been previously implicated in some cell lines as a possible modulator of UCN-01 activity, has also been shown to be affected by UCN-01 *in vivo* (Sato *et al.*, 2002). Mice transplanted with either the murine colon carcinoma line NL-17 or the human prostate PC-3 line were treated with 6-13.5 mg/kg UCN-01 *i.p.* for one or four hours. After tumor harvest, the authors found both decreased levels of PDK1 and PDK1 kinase activity. However, conflicting reports about the potential effects of UCN-01 on this pathway make the importance of this finding questionable. The ultimate effects of UCN-01 on tumors were not further explored, and the factor(s) that determine whether tumors apoptose, undergo growth arrest or remain unaffected is not currently understood. The studies here are summarized below in Table 5.

#### **UCN-01 in the clinic (Table 6)**

UCN-01 has been utilized in clinical trials, initially as a single agent to attempt cause apoptosis in refractory tumors and/or arrest tumor growth. Much more frequently, UCN-01 has been used in combination with cytotoxic drugs, either simultaneously or subsequently, to abrogate the G2 checkpoint response in damaged cells and force them into mitotic catastrophe or apoptosis. The trials using UCN-01 alone to suppress tumors and/or cause tumor-specific apoptosis were an attempt to translate previous studies (see above) into meaningful clinical outcomes. The Phase I trials using UCN-01 as a single agent will be discussed first; Phase I trials combining UCN-01 with other agents will be detailed next, followed by the Phase II trials.

Table 6: Clinical Trials of UCN-01

Study Reference	Study Design	Dosing Schedule	Status (enrolled)
(Sausville <i>et al.</i> , 2001)	Multiple dose, phase I trial in cancer patients	Single 72 hour infusion of 5.4 – 53 mg/M <sup>2</sup>	Completed (n=47)
(Dees <i>et al.</i> , 2005)	Multiple dose, phase I trial in cancer patients	1-5 cycles of 1-3 hour infusion of 3 – 95 mg/M <sup>2</sup> given every 28 days	Completed (n=24)
(Kortmansky <i>et al.</i> , 2005)	Multiple dose combination phase I trial in cancer patients	5-FU: weekly 24 hour infusion, 250 – 2600 mg/M <sup>2</sup>  UCN-01: 72/36 hour infusion of 135/67.5 mg/M <sup>2</sup> every 28 days	Completed (n=35)
(Lara <i>et al.</i> , 2005)	Multiple dose combination phase I trial in cancer patients	Cisplatin: 1 hour infusion 20 – 75 mg/M <sup>2</sup>  UCN-01: 72 hour infusion of 45 mg/M <sup>2</sup> /day	Early Closure (n=10)
(Perez <i>et al.</i> , 2006)	Multiple dose combination phase I trial in cancer patients	Cisplatin: 20-30 mg/M <sup>2</sup> 22 hours prior to  UCN-01: 34-45 mg/M <sup>2</sup> /day over 72 hours	Completed (n=7)
(Edelman <i>et al.</i> , 2007)	Multiple dose combination phase I trial in cancer patients	Carboplatin: 2-5 AUC for 1 hour prior to  UCN-01: 50/25 – 90/45 mg/M <sup>2</sup> /day over 72 hours	Completed (n=23)
(Hotte <i>et al.</i> , 2006)	Multiple dose combination phase I trial in cancer patients	Topotecan: 0.75 – 1 mg/M <sup>2</sup> /day X 5 days  UCN-01: 70/35 – 90/45 mg/M <sup>2</sup> over 3	Completed (n=33)

Table 6 continued

		hour infusion every 21 days	
(Jimeno <i>et al.</i> , 2008)	Multiple dose combination phase I trial in cancer patients	Irinotecan: 60 – 90 mg/M <sup>2</sup> on days 1&8  UCN-01: 50/25 – 90/45 mg/M <sup>2</sup> for 3 hour infusion every 21 days	Completed (n=16)
(Kummar <i>et al.</i> , 2009)	Multiple dose combination phase I trial in cancer patients	Prednisone: 60 mg/M <sup>2</sup> /day X 5 days  UCN-01: 17 – 34 mg/M <sup>2</sup> /day for 72 hours on days 3-5	Completed (n=15)
(Sampath <i>et al.</i> , 2006)	Multiple dose combination phase I trial in cancer patients	Ara-C: 1 – 1.5 g/M <sup>2</sup> /day for 4 days  UCN-01: 45 mg/M <sup>2</sup> /day for 3 days	Completed (n=13)
(Rini <i>et al.</i> , 2004)	Single dose phase II trial in renal cell carcinoma patients	90 mg/M <sup>2</sup> /day for 3 days initial; 45 mg/M <sup>2</sup> /day subsequent cycles of 21 days	Completed (n=21)
(Welch <i>et al.</i> , 2007)	Single dose combination phase II trial in ovarian cancer patients	Topotecan: 1 mg/M <sup>2</sup> /day days 1-5  UCN-01: 70/35 mg/M <sup>2</sup> /day for days 1-3, each cycle 21 days	Completed (n=29)
NCI-04-C-0173	Phase II trial in lymphoma patients	UCN-01 72 hour infusion every 28 days	Ongoing

### **Phase I trials using UCN-01 as a single agent**

In a phase I trial utilizing UCN-01 as a single agent, 47 patients with refractory tumors (10 renal cell carcinoma, 8 NSCLC, 7 non-Hodgkin's lymphoma, 4 colorectal, 4 melanoma, 3 leiomyosarcoma, 2 prostate, 2 head & neck, 2 Hodgkin's, and five unspecified) were given 1.8 – 53 mg/M<sup>2</sup>/d UCN-01 over a 72 hour period; the rationale was based on an *in vitro* study (Seynaeve et al., 1993) in which the breast cancer cell line MDA-MB-468 required exposure of 72 hours to become irreversibly growth arrested (Sausville et al., 2001). The initial treatment plan had called for the doses of UCN-01 to be re-administered every 2 weeks. However, patients receiving the three lowest doses (1.8, 3.6 and 6 mg/M<sup>2</sup>/d) exhibited extremely long drug half-lives, ranging from 447-1176 hours. This unexpected result was determined to be caused by extremely tight binding to the human serum protein  $\alpha_1$ -acidic glycoprotein (hAGP); this binding decreases both the clearance of UCN-01 and unbound fraction of UCN-01 in plasma (Sausville et al., 1998).

This complication caused the treatment schedule to be amended from every two weeks to every four weeks for the higher doses (12-53 mg M<sup>2</sup>/d). The subsequent doses were also given over a 36-hour period instead of the initial 72 hours. UCN-01 was generally well tolerated, with no dose limiting toxicity (DLT) until 34 mg/M<sup>2</sup>/d, and only one of eight patients treated at the 45 mg/M<sup>2</sup>/d dose experienced DLT. Patients receiving 53 mg/M<sup>2</sup>/d experienced both hyperglycemia and pulmonary toxicity, and this dose was not recommended for further study. All patients experienced at least transient hyperglycemia, which was attributed to peripheral tissue insulin resistance. Insulin treatment resolved most cases of hyperglycemia. It is believed that UCN-01 inhibits

glucose transport activity by inhibiting the phosphorylation of Akt at threonine 308, leading to the hyperglycemia observed in the patients (Kondapaka et al., 2004). The response to treatment was small; 25 had disease progression within 2 months of treatment, 19 had stable disease, and one melanoma patient displayed a partial response for 6 months. One interesting patient had recurrent large-cell lymphoma and was treated with UCN-01 and adenopathy following radiation treatment. The patient displayed no disease progression after 38 months of UCN-01 treatment at a dose of 24 mg/M<sup>2</sup>/d.

Another phase I trial utilizing UCN-01 as a single agent enrolled 24 patients with refractory solid tumors (9 colorectal, 4 prostate, 3 cervical, 2 kidney, 2 breast, and one each of gastric, lung, leiomyosarcoma, and unknown primary adenocarcinoma) (Dees et al., 2005). Patients were given UCN-01 as a 1-3 hour infusion from 3-95 mg/M<sup>2</sup>. Hypotension was the DLT at the 95 mg/M<sup>2</sup> dose. As in the previous study, mild to moderate hyperglycemia was seen in many patients, 14 out of 22 receiving  $\geq 12$  mg/M<sup>2</sup>. No treatment responses were seen in this study. 21 patients displayed tumor progression following 1-5 courses of UCN-01 treatment, 2 were removed from the study for toxicity concerns, and one patient had stable disease for one year.

### **Phase I trials of UCN-01 used in combination therapy**

The use of UCN-01 in combination with a cytotoxic drug appeared more frequently than the single agent trials. These studies all attempted to use UCN-01 to abrogate the G2 DNA-damage checkpoint response following an initial treatment with a cytotoxic drug. The rationale for this method is that inhibition of the arrest/repair pathways



(predominantly by inhibition of chk1) would prevent the tumor cells from undergoing cell cycle arrest in response to an initial toxic repairing damage and force damaged cells through mitosis and ultimately cell death.

A phase I trial of UCN-01 combined with fluorouracil was conducted on 35 patients, 21 of which were diagnosed with metastatic colon cancer (Kortmansky et al., 2005). The treatment plan followed called for weekly doses of fluorouracil (250 – 2600 mg/M<sup>2</sup>); UCN-01 was given once every four weeks, immediately after cessation of fluorouracil administration. UCN-01 was given at 135 mg/M<sup>2</sup> for the initial dose, and 67.5 mg/M<sup>2</sup> for subsequent doses. The treatment plan was set up to mimic the synergism seen in the *in vitro* study by Hsueh, et al., in which gastric cancer cells treated first with fluorouracil followed by UCN-01 demonstrated apoptosis in 46% of the cells, versus 4% for fluorouracil alone and 17% for UCN-01 followed by fluorouracil (Hsueh et al., 1998). The *in vivo* treatment regimen was tolerated well by most patients, with one DLT at 560 mg/M<sup>2</sup> fluorouracil, one at 845 mg/M<sup>2</sup>, and one at 1900 mg/M<sup>2</sup>. No DLT was observed at the highest fluorouracil doses, 2527 and 2600 mg/M<sup>2</sup>. Of 32 patients assessable for response to the treatment regimen, no positive response to the treatment was observed, although 8 patients had stable disease. UCN-01 did not affect the pharmacokinetics of 5-FU (completely cleared within the first hour of UCN-01 administration), and the concentration of 5-FU had no effect on the plasma concentrations of UCN-01. The authors felt that the treatment was safe, and planned a Phase II trial using 2600 mg/M<sup>2</sup> 5-FU in combination with UCN-01.

Another phase I trial combined cisplatin with UCN-01 treatment on ten patients with advanced, malignant solid tumors (2 NSCLC, 2 soft tissue sarcoma, and one each on esophageal, head & neck, pancreatic, melanoma, gastric, and unknown primary adenocarcinoma cancer patients) (Lara et al., 2005). Previous *in vitro* work examining the actions of UCN-01 plus cisplatin against glioma and NSCLC cells had indicated synergism between these two agents when UCN-01 was used secondarily (Mack *et al.*, 2003; Pollack *et al.*, 1996). The dose escalation scheme for the clinical study called for cisplatin to be administered at five dose levels from 20-75 mg/M<sup>2</sup>; cisplatin was to be given over a 2 hour infusion, followed 22 hours later by 45 mg/M<sup>2</sup> UCN-01. The first dose level (20 mg/M<sup>2</sup> cisplatin) exhibited one DLT of grade 3 hypoxia; the other five patients in this cohort had no adverse events. At the next dose (30 mg/M<sup>2</sup> cisplatin), one patient experienced grade 5 sepsis along with respiratory failure, and another presented with grade 3 atrial fibrillation. Grade 3 hypoxia, dysphagia, renal failure and hyponatremia were also observed at this dose, and the trial was ended due to toxicity. The authors were optimistic that alternative platinum agents could be used, but concluded that the UCN-01/cisplatin combination was too toxic for use in patients.

A second trial treating seven patients (5 melanoma, one bladder carcinoma, and one thyroid carcinoma) using UCN-01 with cisplatin also found this limiting toxicity; using the treatment regimen above, with the exception of a one-hour cisplatin infusion (rather than two), the first two patients receiving 20 mg/M<sup>2</sup> cisplatin followed by 45 mg/M<sup>2</sup>/d UCN-01 experienced grade 3 and 4 limiting toxicities, including subarachnoid hemorrhage, cardiac ischemia, hypoxia and hyperglycemia (Perez *et al.*, 2006).

However, it was found that decreasing the UCN-01 administration from 45 to 34 mg/M<sup>2</sup>/d allowed the remaining five patients to tolerate either 20 mg/M<sup>2</sup> or 30 mg/M<sup>2</sup> cisplatin with no DLT. An interesting aspect of this study was data collected on biopsies stained for geminin via IHC. Geminin is a protein expressed only in S and G2 phases of the cell cycle, and is believed to function as a preventer of DNA re-duplication (Tachibana *et al.*, 2005). This group had previously demonstrated *in vitro* that cells undergoing DNA damage and subsequent G2 arrest stain positive for geminin using the active metabolite of irinotecan, SN38 (Eastman *et al.*, 2002). In patient biopsies, geminin was increased following cisplatin administration, and then markedly decreased after subsequent UCN-01 treatment, indicating that UCN-01 is inhibiting the G2 damage checkpoint and allowing progression through mitosis. Of the seven patients, four only received one cycle of therapy and were not evaluated for impact on disease progression; the three remaining patients received two cycles of treatment, and all had progressive disease. The authors are currently continuing this area of study with a new trial, using a revised 3-hour infusion of UCN-01; results of this study are as of yet unavailable.

The platinum agent carboplatin has also been evaluated clinically in combination with UCN-01 (Edelman *et al.*, 2007). This Phase I trial included patients with the following cancers: NSCLC (10), small cell lung (3), bladder (2), head & neck (2), and one each on adrenocortical carcinoma, esophagus, gastric, adenoid cystic, pancreatic, and unknown primary carcinoma. Carboplatin was administered from an area under the curve (AUC, mg/mL min) of 2.5-5 over a one-hour infusion, followed by UCN-01 from 50-90 mg/M<sup>2</sup> given over three hours. Each treatment cycle was 21 days long, and up to six cycles were

allowed per patient. The second and all subsequent UCN-01 doses were 50% of the initial dose. 23 patients were enrolled in the study, and no DLT toxicity was observed; 6 patients were treated at the highest dose level (carboplatin AUC 5, UCN-01 90 mg/M<sup>2</sup>). No tumor response was observed, but seven patients did exhibit stable disease. Two of the small cell lung cancer patients, whose tumors were chemotherapy-refractory, were in this category, and the authors suggest further exploration of combination therapy for small cell lung cancer. It was also noted that the active metabolites of irinotecan were decreased upon UCN-01 administration. As these products are inhibited by the cytochrome P450 CYP3A4, it was unexpected that UCN-01 somehow presumably *inhibited* the CYP3A4 pathway. The specifics of UCN-01 and its effects on irinotecan metabolism are poorly understood.

UCN-01 was used in one phase I trial in combination with topotecan; this trial was somewhat different than the others, in that UCN-01 treatment *preceded* the administration of the cytotoxic drug (Hotte et al., 2006). Preclinical data indicated that UCN-01 and the topoisomerase inhibitor synergistically killed tumor cells, and that the order of administration of the two drugs was unimportant for this result (Monks *et al.*, 2000; Tse and Schwartz, 2004). 33 patients were enrolled with the following malignancies: 20 ovarian neoplasm, one ovarian epithelial cancer, three colorectal cancer, two peritoneal neoplasm, two salivary gland cancer, and one each of cervical carcinoma, endometrial cancer, renal pelvic cancer, cervical squamous cells carcinoma, and one unspecified solid tumor. Topotecan and UCN-01 were administered to 33 patients on a 21-day cycle: on day one, UCN-01 was given over 3 hours, followed by a 30 minute topotecan infusion.

Topotecan only was then given on days 2-5. Three dose levels were given, with no dose escalation. Dose 1 utilized 70 mg/M<sup>2</sup> UCN-01 for the first dose, 35 mg/M<sup>2</sup> for subsequent doses, and 0.75 mg/M<sup>2</sup> topotecan. Dose 2 used the same UCN-01 amounts with 1.0 mg/M<sup>2</sup> topotecan. The third dose group received a primary dose of UCN-01 of 90 mg/M<sup>2</sup> and then 45 mg/M<sup>2</sup> subsequently plus 1.0 mg/M<sup>2</sup> topotecan. Dose 2 was well tolerated, with one grade 3 neutropenia. The third dose group experienced one grade 4 febrile neutropenia, and thus the second dose group was considered the MTD for this protocol. The response in this study to the treatment regimen was more positive than that seen in previous studies, especially for ovarian cancer patients. Two out of three patients in dose 1 had stable disease, and 8 of 13 at dose two had stable disease, one with a partial response. This work led to a phase II study of ovarian cancer patients with advanced disease at the same facility (see phase II section below, Welch *et al.*, 2007).

The topoisomerase inhibitor irinotecan was also evaluated in combination with UCN-01 in a Phase I clinical trial (Jimeno *et al.*, 2008). Sixteen total patients with incurable solid tumors (four colorectal, three pancreatic, and one each of the following tumor types: biliary, duodenal, hepatocellular, tongue base, mesothelioma, thyroid, ovary, skin (Merkel), and unknown primary adenocarcinoma) were accrued in the study, fourteen of which could be evaluated for response. The treatment plan used four dose levels of irinotecan and UCN-01 (50/60, 70/60, 90/60 and 70/90 mg/M<sup>2</sup> of UCN-01/irinotecan respectively); irinotecan was administered as a one-hour infusion on day one, immediately followed by UCN-01 over three hours. Irinotecan was given again on day 8, and the cycle lasted for 21 days. Two of four patients experienced a DLT at the third

dose level, and two out of five had a DLT at the fourth dose level. One patient had progressive disease following one cycle, as did seven others when evaluated after two cycles. The other six patients had stable disease, and four were able to receive ten or more treatment cycles.

Prednisone was also evaluated in a Phase I trial in concert with UCN-01 in patients with refractory solid tumors and lymphomas (Kummar *et al.*, 2009). Three dose levels were used: level 1 used 51 mg/M<sup>2</sup> UCN-01 for the initial cycle, level 2 used 72 mg/M<sup>2</sup>, and level 3 102 mg/M<sup>2</sup>. The initial cycle was given over days 3-5. Each additional cycle used 50% of the initial UCN-01 dose, given over 36 hours. Each cycle was for 28 days, and prednisone was given orally on days 1-5 at 60 mg/M<sup>2</sup> daily. Fifteen patients were enrolled in the study, and a total of 55 treatment courses were undertaken. Two of the six patients at dose level 3 experienced DLT, including grade 3 hyperglycemia, hyponatremia, and leucopenia, and were dropped to dose level 2. No tumor response to treatment was observed. Five patients had stable disease for longer than 2 cycles, and two patients had stable disease for 8 and 18 months.

A phase I trial of UCN-01 in combination with cytarabine (ara-C) was carried out in patients with relapsed acute myelogenous leukemia (AML) following some promising results using this combination in the leukemia cell line ML-1 and primary AML blasts obtained from patients (Sampath *et al.*, 2006). It was demonstrated that ML-1 cells were able to survive ara-C treatment by undergoing an S-phase arrest, via activation of Chk1. Subsequent UCN-01 was able to abrogate this arrest, as well as prevent the activation of

Akt and its downstream survival pathways (Figure 3). Primary blasts treated with ara-C followed by UCN-01 also demonstrated reduced survival. A clinical trial was undertaken to evaluate this treatment scheme, in which patients were first given ara-C over 4 days at 1.0 mg/M<sup>2</sup>/d followed by 45 mg/M<sup>2</sup>/d starting on day 2; this was done for 11 patients. Two additional patients received 1.5 mg/M<sup>2</sup>/d ara-C, with the same UCN-01 given on day 2. Blasts were collected from patients during the course of therapy to monitor the effects on the S-phase checkpoint and the Akt/Jnk survival pathways. Unlike the cell culture samples examined previously, the pretreatment patient blasts had significant levels of phospho-Chk1 (Ser<sup>345</sup>) and also the inhibited form of cdk2 (phospho-Tyr<sup>15</sup>); as a result, few of the circulating blasts were actively cycling. Levels of both phospho-proteins were diminished upon both ara-C treatment and also after subsequent UCN-01, but in a very heterogenous manner; 2 samples showed less than 10% of initial phospho-Chk1 after UCN-01, while another sample registered no effect due to UCN-01 administration. The ratios of phospho-Akt to total Akt were similarly varied, and were unaffected by ara-C, but 7 out of 8 samples exhibited loss of phospho-Ser<sup>345</sup> due to UCN-01 treatment. The combination treatment resulted in only one complete response out of the thirteen patients receiving treatment. While this was a disappointing response rate, the presence of phospho-Akt and inhibited cdk2 in this previously treated and relapsed patient group does give hope that a naïve population would better respond to this treatment regimen.

### **Phase II trials utilizing UCN-01**

A phase II trial of UCN-01 as a single agent was initiated in a population of renal cell carcinoma (RCC) patients (Rini et al., 2004). Most clear cell renal carcinoma tumors have mutated von Hippel-Lindau (VHL) genes; the inactive VHL gene is unable to suppress the expression of the tumor promoter VEGF (vascular endothelial growth factor), presumably through lack of suppression of PKC (Gnarra et al., 1994; Herman et al., 1994; Nishizuka, 2001; Pal et al., 1997). As a potent PKC inhibitor, it was hoped that UCN-01 would help inhibit this process. 21 patients were enrolled in this study. UCN-01 was given at an initial dose of 90 mg/M<sup>2</sup>, and then subsequently 45 mg/M<sup>2</sup> every 21 days. Treatment was well tolerated, with hyperglycemia the only grade 3 toxicity observed. All cases of hyperglycemia were successfully managed. The trial was halted after four months (6 treatment cycles), as only 7 of the 21 patients exhibited stable disease. No response was seen, and the authors concluded that this treatment regimen was not effective in RCC.

Using previous Phase I data (Hotte *et al.*, 2006), a Phase II trial for recurrent ovarian cancer combining UCN-01 with topotecan was undertaken. Patients were treated with the dose 2 regimen (1 mg/M<sup>2</sup>/day topotecan for five days, with 70 mg/M<sup>2</sup> UCN-01 on day 1 for the first cycle; UCN-01 was cut to 35 mg/M<sup>2</sup> in subsequent cycles) from the phase I trial (Welch et al., 2007). The expected toxicities of hyperglycemia and leucopenia were observed, but none precluded treatment continuation. However, the results were not encouraging. Of the 19 patients treated in the first stage of the protocol, only one responder was observed. As the expected response for topotecan as a single agent in ovarian cancer is 10-15%, the study was halted. While it may be possible that



the co-administration of the two drugs (rather than topotecan *followed* by UCN-01) may interfere with the actions of topotecan, the authors did not feel that this combination would be appropriate for further study in the ovarian cancer setting.

A current Phase II study on UCN-01 in lymphoma patients is in progress (NCI-04-C-0173).

### **Summary of UCN-01 in clinical trials**

With the exception of the initial ovarian cancer study, the clinical data to date utilizing UCN-01 as a chemosensitizer and/or tumor suppressor has been disappointing. Although the patient populations used are not ideal (patients with no prior exposure to chemotherapeutics and presumably harboring less resistant tumors might have better responses), it was to be expected that a better response would have been observed in some of the trials. The trials reported are summarized in Table 6 below. For Phase I trials using UCN-01 alone, 71 patients were treated, leading to 20 cases of stable disease and 2 partial responders. For Phase I trials using combination therapy, 152 total patients led to only 46 cases of stable disease (some for as little as 6 weeks) and 3 responders. 40 patients enrolled in the reported Phase II trials had 1 responder and 7 patients with stable disease. The six responders across these studies do not share any obvious commonalities; no overlap in disease types or dosing (UCN-01 levels vary as well across the responsive patients) exist among them. It may be possible that the course of therapy received *prior* to UCN-01 treatment may be similar, but this information is not included in the reported data. It is also possible the specific malignant alterations in these tumors

are similar, thus potentiating the ability of UCN-01 to invoke a response. The lack of molecular characterization of the tumors in most of the clinical work makes this theory difficult to pursue as well. If the nature of the cell cycle defect(s) in specific tumors were known prior to treatment, it would likely improve the success of therapy using UCN-01. Tumors with at least a partial impairment of the DNA damage response would likely be unable to survive a combination treatment (DNA-damaging agent followed by UCN-01), while tumors with complete or partial G1 checkpoint integrity would be more likely to respond to UCN-01 as a single agent.

### **UCN-01 and Normal Cells**

One aspect of the UCN-01 has received little attention, specifically that of its effects on normal cells. Only one published report focuses on the effects of UCN-01 on the normal tissues of the mouse, specifically the hyperproliferative bone marrow and gut epithelium (Redkar *et al.*, 2001). C57BL/6 mice were injected with 0-10 mg/kg UCN-01 for either 3 or 24 hours; 20 mg/kg was lethal in these mice. Analysis of BrdU incorporation in small intestinal epithelial cells demonstrated a significant inhibition of proliferation at both 3 and 24 hours following the 5 mg/kg UCN-01 dose in all three small bowel tissues, duodenum, jejunum and ileum; colon was not affected. The 10 mg/kg dose was not able to inhibit cell proliferation, possibly indicating a pleiotropic, dose-dependent effect of UCN-01. Flow cytometric analysis of harvested bone marrow cells from these mice showed a G1 arrest at the 5 mg/kg dose; as before the 10 mg/kg dose did not induce the same effect. Further work on bone marrow cells recovered from naïve mice also noted an interesting feature of UCN-01. Simultaneous treatment of these cells with UCN-01 and

the topoisomerase I inhibitor topotecan led to a less-than-additive growth inhibition compared to either agent used alone. This antagonism between a cytotoxic drug and UCN-01 is an indicator that UCN-01 may be used *in vivo* to protect normal dividing cells from toxicity.

Another *in vivo* study which examined the effects of UCN-01 in concert with chemotherapy or fractionated radiation also lends credence to the treatment protocol proposed below. Implanted murine fibrosarcoma (FSa-II) tumors treated with UCN-01 and  $\gamma$  irradiation were significantly growth-retarded compared to radiation treatment alone (Tsuchida and Urano, 1997). However, the combination of UCN-01 and cisplatin was not any more effective than cisplatin alone. Addition of UCN-01 to fluorouracil 5-FU) was also had no effect on tumor growth compared to 5-FU alone. Survival analysis of the FSa-II cells grown in culture also showed no synerism of UCN-01 and cisplatin, and 5-FU plus UCN-01 had an effect that was less than additive, suggesting a protective action of UCN-01 in these cells.

Little else is currently known concerning the actions of UCN-01 on the normal tissues of any organism, save for the toxicities explored in the clinical trials (see below) and a few reports which have sought to explore the pharmacokinetics of UCN-01 and the influences of its binding to AGP. The maximum tolerated dose (MTD) of UCN-01 in mice is 20 mg/kg via intravenous delivery and 10 mg/kg when injected subcutaneously (Hill *et al.*, 1994). The terminal exponential phase of elimination ( $t_{1/2\beta}$ ) following intravenous 10 mg/kg UCN-01 is 85 minutes, and the area under the plasma concentration-time curve

(AUC) is 117  $\mu\text{g}/\text{minutes}/\text{ml}$ ; the values for subcutaneous delivery are 130 minutes and 113  $\mu\text{g}$  minutes/ml respectively, indicating that the two routes may have substantially the same pharmacokinetics. This study also demonstrated that UCN-01 is stable in mouse serum. A second report sought to examine the altered pharmacokinetics of UCN-01 reported in human trials and attributed to strong binding of the serum protein AGP (Hedaya and Daoud, 2001). Rats were injected (i.v.) with either UCN-01 or UCN-01 plus 30 mg/kg human AGP, and plasma and tissue concentrations of UCN-01 were determined from 30 minutes post-injection to 24 hours later. As expected, the presence of AGP increased the plasma concentrations of UCN-01 by 5- to 7-fold, and reduced the ratio of drug/tissue for all organs examined (brain, skeletal muscle, heart, liver, kidney, spleen and lungs). The AGP binding of UCN-01 will be further explored in the Discussion below. Pertinent to the project discussed in this work, the authors also evaluated these parameters following intramuscular (i.m.) injection. While the elimination and distribution kinetics were essentially the same as seen in the intravenous study, this is the only publication that has detailed them following the i.m. route. The authors found that UCN-01 delivered intramuscularly had approximately the same initial plasma concentration as the i.v. delivery (240 ng/ml), and that UCN-01 was not detectable in plasma by 14 hours post-injection.

### **Gap in Knowledge; UCN-01 as a protector of normal cells**

The clinical studies discussed previously focused primarily on the use of UCN-10 to enhance the toxicity of chemotherapeutic agents to eradicate tumors. In fact, as UCN-01 has been used in *all* of the reported clinical cases to either damage or suppress tumors,

these studies do not exclude the possibility that UCN-01 could act as a protective agent for normal dividing cells. The effects of UCN-01 seem to be highly dependent upon both the dose administered and the cell cycle status of a particular cell. The clinical trials use very high doses of UCN-01 (up to 135 mg/M<sup>2</sup>), whereas the levels of UCN-01 used as a protective agent would be much lower. The mouse protection study proposed in this thesis utilizes a much lower dose range (0.63-5.0 mg/kg, approximately equivalent to 1.26-10 mg/M<sup>2</sup>). This low dose of UCN-01 would presumably target only normal proliferating cells. Another concern is the binding of UCN-01 to hAGP and the altered pharmacokinetics that ensue. While this is not expected to complicate the mouse study, any clinical translation will have to account for this phenomenon to keep the unbound fraction of UCN-01 within the effective range for a reversible G1 arrest. One possible solution would be the use of liposomes to deliver the drug to the target cell populations. Recent reports indicate some success using these vehicles to prevent hAGP binding in the bloodstream and to control the release rate of UCN-01 (Yamauchi et al., 2005; Yamauchi et al., 2008). The plasma protein binding of UCN-01 and the clinical implications of this property will be further explicated in the discussion section below.

The work described in this thesis explores the use of UCN-01 in protecting normal dividing cells of the mouse from the toxicity of chemotherapy. The rationale for this approach is based on the *in vitro* and *in vivo* work previously mentioned. It is known that UCN-01 is able to temporarily arrest the normal dividing tissues (intestinal epithelia and hematopoietic tissue) of the mouse in G1 (Redkar *et al.*, 2001) and that no adverse effects accompany this effect. It has also been shown that non-tumorigenic cells in culture

(wild-type Rb) can be arrested in G1 with UCN-01, and that the cells can return to a proliferative state once the drug has been removed (Chen *et al.*, 1999). This state of temporary arrest is protective from drugs (in this case camptothecin) which target actively dividing cells (Chen *et al.*, 2000). Tumor cells, which are not affected by this dose of UCN-01, are not similarly protected. The ability of UCN-01-arrested normal cells to evade the toxicity of chemotherapeutic agents will be evaluated *in vivo* in a mouse model system.

The other aspect of UCN-01 which will be examined is the molecular changes in the normal dividing tissues of the mouse following treatment. UCN-01 is a very promiscuous compound, and the literature discussed above indicates many targets and effects due to its use. However, the predominant setting for these studies has been in the tumor environment, and as a result, there has been quite a variety of molecular changes and cellular fates described. The focus here will be on normal dividing cells in the mouse, and to better understand how UCN-01 affects these cells and causes an arrest in the cell cycle.

## RESULTS Chapter I. Arrest and Recovery of Normal Cells by UCN-01

**Introduction:** Several studies discussed in the introduction which examined the actions of UCN-01 in both cell culture and in mice indicate that the drug can arrest proliferating cells, usually in G0/G1. This project attempts to exploit the arrest of normal cells to protect them from chemotherapeutics which target dividing cells in an *in vivo* system (Chen *et al.*, 2000). In order to demonstrate the ability of UCN-01 to arrest normally dividing cells in the mouse, we have chosen to examine the epithelium of the small intestine of nude mice. This is a rapidly dividing tissue, in which cells are continually replicating in the crypt and to replace the cells at the villus tip as they die and are shed into the lumen. We have chosen to use the nude mouse in order to facilitate future studies in which human xenograft tumor-bearing mice are treated with the UCN-01 protection protocol. The hypothesis to be evaluated in this section is: **The normal dividing cells of the mouse small bowel can be reversibly arrested by UCN-01 administration.** In order to be able to exploit a cell cycle arrest to protect normally dividing tissues, we must be able to show that UCN-01-mediated arrest is temporary, and specifically when the cells enter into arrest and when they recover.

The cell cycle kinetics in the mouse small bowel were analyzed by flow cytometry to identify changes due to UCN-01 treatment. Cell cycle arrest of the dividing epithelial cells was demonstrated beginning 24 hours after UCN-01 administration, and this arrest was shown to reverse two weeks after treatment. Additionally, an antagonistic effect of the UCN-01 carrier DMSO was observed in the small intestine epithelial cells.

However, this effect did not prevent the arrest and reversal of UCN-01 mediated cell cycle arrest.

**Material and Methods:** Mice: Male and female nude mice from 8-12 weeks of age (approximately 24-30 grams) were obtained from the Experimental Radiation Oncology colony at M.D. Anderson Cancer Center. Mice are maintained in the specific pathogen free barrier facility on sterilized normal chow and water with no restrictions. UCN-01/mock treatment: Mice were injected with UCN-01 or carrier (dimethyl sulfoxide, DMSO, Sigma Aldrich, St. Louis MO) intramuscularly (*i.m.*) into the right hindlimb. UCN-01 was obtained from the NCI Chemotherapeutic Agents Repository, and is resuspended in DMSO at 7.5 mg/ml. Prior to injection, the UCN-01 solution is diluted 2:1 with sterile normal saline for a final concentration of 5 mg/ml. DMSO given as vehicle control was diluted in the same fashion, and was given as a volume equivalent dose. To obtain the normal mouse values for flow cytometry, mice either received no treatment or were given volume equivalent PBS in the right hindlimb.

Bromodeoxyuridine (BrdU) labeling: Mice were sacrificed at one of five timepoints following UCN-01/mock injection: 24 hours, 48 hours, and 7, 14 or 28 days. On the day of sacrifice, mice were injected *i.p.* with 60 mg/kg BrdU (Sigma Aldrich, St. Louis MO) six hours prior to sacrifice. Mice were staggered in injection and sacrifice times such that each mouse had exactly six hours of BrdU exposure. Upon sacrifice, the jejunum was dissected out and flushed with ice-cold ethanol (60% in PBS, both Fisher Scientific, Pittsburgh, PA). A small piece was fixed in formalin (10%, Fisher Scientific), and the



remainder fixed overnight in the 60% ethanol/PBS buffer. To prepare the tissues for flow cytometry, the jejunums were opened longitudinally and placed on a glass microscope slide. A second slide was dragged across the epithelial surface to dislodge the cells; care was taken not to apply excess pressure and disrupt the basement membrane. The isolated cells were placed in a 50 ml glass flask and resuspended in 5 ml of 0.04% pepsin (Fluka chemical, obtained from Sigma Aldrich) and placed in a shaking water bath at 37°C and 90 Hz for one hour. The cells were filtered through 35 µm mesh and centrifuged at 1200 RPM for 5 minutes in a swinging bucket centrifuge (Beckman Coulter, Brea CA). Cells were resuspended in 1.5 ml of 2N HCl (Fisher Scientific) for 20 minutes in a 37°C incubator. The acid was neutralized with 3 ml 0.1M sodium borate (Sigma Aldrich) and the cells were again centrifuged at 1200 RPM for 5 minutes. The cells were washed with 5 ml of PBTB (phosphate-buffered saline plus 0.5% Tween-20 (Sigma Aldrich) and 0.5% bovine serum albumin (Fisher Scientific)) and centrifuged at 1200 RPM for 5 minutes. Samples were resuspended in primary anti-BrdU antibody (IU-4, Caltag, Burlingame CA) diluted 1:100 in PBT (phosphate-buffered saline plus 0.5% Tween-20) for 60 minutes. Samples were washed in 5 ml of PBTB and centrifuged at 1200 RPM for 5 minutes. Samples were resuspended in 0.2 ml of secondary antibody (goat anti-mouse fluorescein isothiocyanate (GAM-FITC), Beckman Coulter, Brea CA) diluted 1:100 in PBTG (PBT with 2% normal goat serum) for 60 minutes, then washed in PBTB and centrifuged at 1200 RPM for 5 minutes. Samples were then suspended in propidium iodide solution (1 mg/ml PI (Roche, Branford CT) in 95% ethanol diluted 1:100 in PBT) and stored at 4°C overnight.

Flow Cytometry: Intestinal digests were analyzed using a Beckman Coulter flow cytometer. An example of the output of the bivariate analysis is shown in Figure 4. DNA content (PI, x-axis) and BrdU-positive nuclei (log BrdU, y-axis) are both counted and exported to the ModFit LT program (Verity software, Topsham ME). Labeling index is calculated by dividing the number of BrdU-positive nuclei by the total number of nuclei analyzed. The fraction of labeled divided cells ( $f^{ld}$ ) is the number of BrdU-positive nuclei which are in G1 phase divided by the total number of nuclei counted (upper left box, Figure 4). The fraction of labeled undivided cells ( $f^{lu}$ ) is the number of BrdU-positive nuclei which correspond to the S and G2/M phases of the cell cycle divided by the total number of cells analyzed. A complete explication of the flow analysis parameters and other values which may be calculated can be found in a recent methods article (Terry and White, 2006)

Immunohistochemistry: Jenunum sections were embedded in paraffin and 5  $\mu$ M sections were cut onto superfrost/plus slides (Fisher Scientific). To visualize BrdU in the sections, slides were processed as for IHC. Slides were hydrated in 3 washes of xylene (Fisher Scientific) for five minutes each, and then 3 minutes each of 100%, 90% and 70% ethanol. Slides were washed for five minutes in water, and then digested in 0.1% protease (Sigma Aldrich) for one hour. Slides were washed twice for five minutes in PBS and placed into 2 normal hydrochloric acid for fifty minutes. The acid was neutralized in 0.1 M sodium borate. Slides were washed twice in PBST (PBS plus 0.5% Tween 20, Sigma Aldrich) for five minutes and then blocked in normal horse serum (Vector Labs, 3 drops in 10 ml PBST) at 37° for thirty minutes in a humidified chamber.

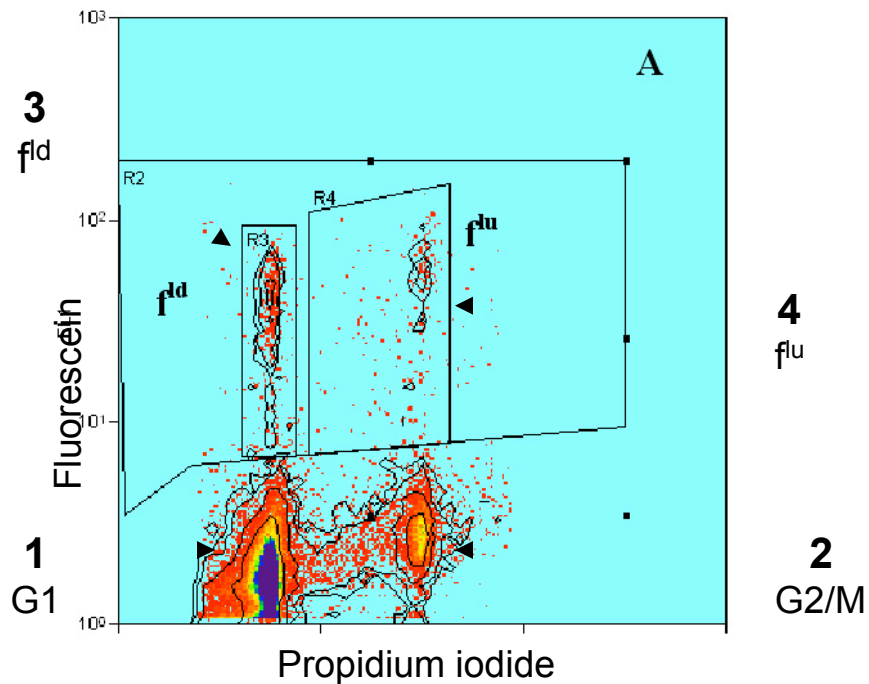


Figure 4. Typical output for bivariate analysis of mouse jejunum after 6 hours of BrdU labeling. The large upper box gates all cells positive BrdU (y-axis). The x-axis represents propidium iodide (PI), and cells are sorted by DNA content; the first large population (1) is G1/G0 cells, the second large population is G2 (2). The cells in between the two are in S phase. The small box on the upper left (3) delineates the fraction of labeled, divided cells ( $f^{ld}$ ), which are BrdU positive cells which have gone through mitosis. The upper left box (4) represents the BrdU positive cells which have yet to divide (fraction of labeled, undivided cells,  $f^{lu}$ ).

The slides were incubated with primary IU-4 antibody (1:100 in PBST) for one hour in a humidified chamber at 37°C. After two five-minute washes in PBST, the slides were incubated with secondary GAM-FITC (1:100 in PBST plus 1% normal goat serum) for one hour at 37°C in a dark humidified chamber. After two washes of five minutes each in PBST, the nuclei were stained with 0.1 µg/ml Propidium iodide (Sigma Aldrich) for fifteen minutes. Slides were mounted in antifade medium (Vectasheild, Vector Labs, Burlingame CA) and sealed with a glass coverslip.

Microscopy: BrdU was visualized on stained jejunum sections using a Leica DM400B (Wetzlar, Germany) fluorescent microscope. Images were taken using a Spot digital camera and Spot Advanced software (Spot Imaging Solutions, Sterling Heights MI).

Statistics: Pairwise comparison of means was performed using Student's t-test; a confidence level of 95% was considered to be statistically significant in these studies. All calculations were performed using the Prism software package (GraphPad Software, Inc.).

## ***Results:***

### **Initial dose range study for UCN-01 in mouse jejunum:**

The results from the study by Redkar et. al. (Redkar *et al.*, 2001) demonstrated that the proliferating tissues of the mouse (intestinal epithelium and bone marrow) could be arrested by UCN-01 at doses of 5 and 10 mg/kg. In order to establish the efficacy of this arrest in our mouse model system, an initial pilot study was performed (Figure 5). Nude

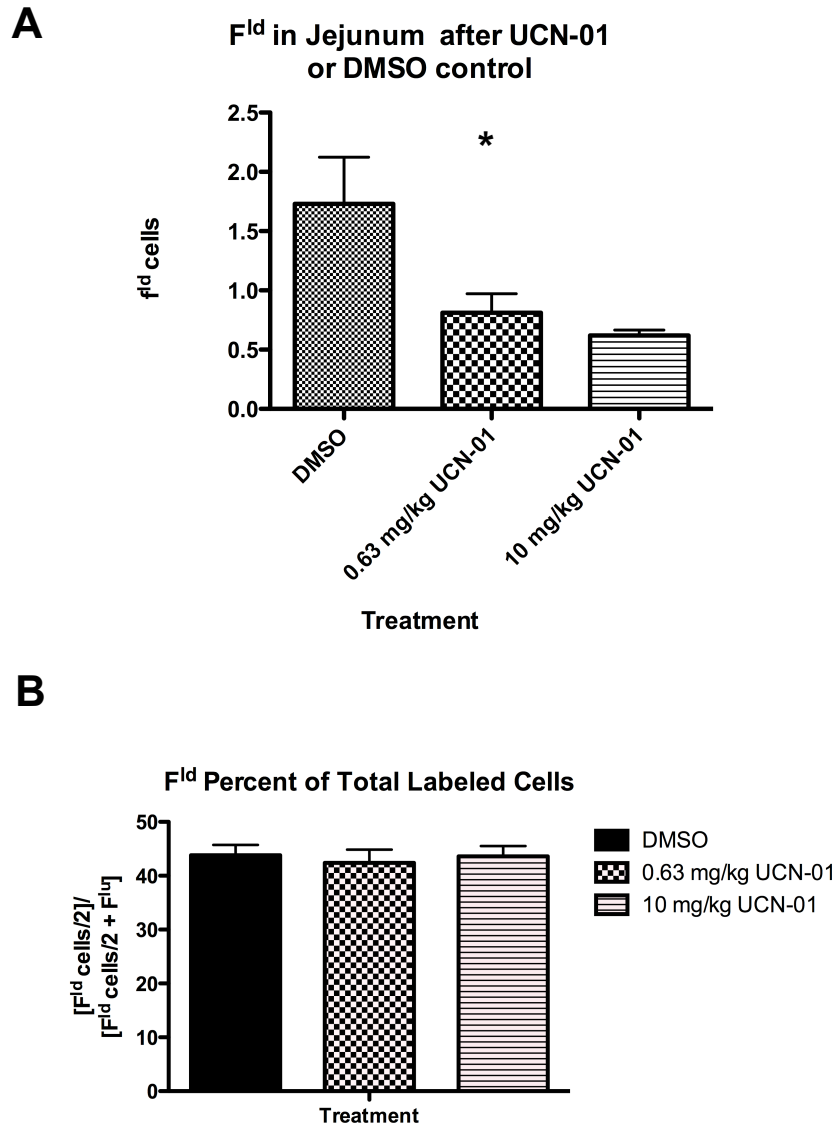


Figure 5. Flow cytometric analysis of mouse jejunums harvested 48 hours after treatment with 10 mg/kg UCN-01 (n=6), 0.63 mg/kg UCN-01 (n=5) or DMSO control (n=5). (A) Fraction of labeled divided cells ( $F^{ld}$ ) was significantly decreased in the 10 mg/kg UCN-01 group compared to vehicle (\*,  $p < 0.05$ ). The 0.63 mg/kg UCN-01 group was not significantly lower than DMSO control ( $p = 0.0516$ ). (B) Percentage of all BrdU-labeled cells which have divided. No change is evident after treatment with UCN-01, suggesting the decrease in  $F^{ld}$  in (A) is not due to a block in G2/M phase, but rather a decrease in cells entering S phase. [Calculation:  $(F^{ld}/2)/(F^{lu} + F^{ld}/2)$ ]

mice were injected with DMSO control (n=5), 0.63 mg/kg UCN-01 (n=5), or 10 mg/kg UCN-01 *im*. 48 hours after treatment, the mice were injected with BrdU and sacrificed six hours later. Jejunum was harvested and fixed overnight for flow cytometric analysis. The six-hour BrdU labeling of the mice allows time for some proliferating cells which incorporate label in S phase and pass the label through G2 phase and mitosis. This population of cells is termed the fraction of labeled, divided cells ( $f^{ld}$ ). The visual representation of this population is shown in Figure 4 by arrow 3. A complete description of the parameters measured by the flow analysis is described in the Materials and Methods section above. A decrease in  $f^{ld}$  cells is indicative of a decrease in cells progressing through the cell cycle. As shown in Figure 5, the 10 mg/kg UCN-01 treated mice had a significantly lower  $f^{ld}$  value than the DMSO vehicle control group. The 0.63 mg/kg UCN-01 mice also had a lower  $f^{ld}$  compared to controls, but the difference was not statistically significant (p=0.0516). Our results are in agreement with the previous report (Redkar *et al.*, 2001), and it appears that UCN-01 at either concentration used in this experiment is able to arrest the proliferating cells of the nude mouse small intestine.

#### **Baseline $f^{ld}$ for untreated mice:**

While it is clear from the study in Figure 5 that DMSO is not causing the decrease in cell proliferation seen in the jejunum of UCN-01 treated mice, we felt it was important to establish a baseline  $f^{ld}$  value for untreated mice. To this end, mice were either injected *im* with PBS (n=7) or left untreated (n=9). 48 hours later, BrdU was injected and mice sacrificed six hours later. Flow cytometric analysis (Figure 6) demonstrated no significant difference between the two groups. However, the combined values for the

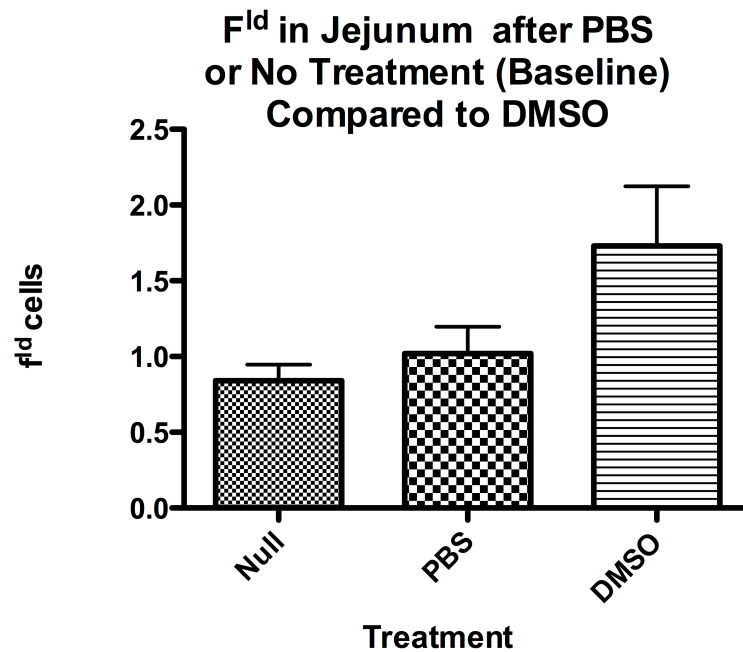


Figure 6. Flow cytometric analysis of mouse jejunums 48 hours after *im* injection of PBS (volume equivalent to 5 mg/kg UCN-01 treatment, n=7) or null (no treatment, n=9). The two groups were not significantly different (p=0.378), and the mean f<sup>ld</sup> for all control mice is 0.99%. The pooled values of f<sup>ld</sup> for the null and PBS treated mice are significantly different from the DMSO treated mice (p=.0073)

“untreated” mice in this experiment are significantly different from the value of the DMSO mice (Figure 5), which is also included in Figure 6 for comparative purposes. The mean fld value for all mice in this experiment was 0.99%. This will be used as the baseline untreated value for the rest of the studies in this section. It is also important to note that DMSO appears to stimulate proliferation in the mouse intestinal epithelium. However, the combined values for the “untreated” mice in this experiment are significantly different from the value of the DMSO mice (Figure 5), which is also included in Figure 6 for comparative purposes. The  $f^{ld}$  value in the previous experiment (Figure 5) for the DMSO control group is 1.729%, a significant increase over the untreated value of 0.99% obtained in this group of “untreated” mice. The antagonism between the effects of UCN-01 and its carrier is not particularly a desirable feature, and will be addressed in future studies. However, as the DMSO values may skew future analyses of UCN-01 activity in the mouse epithelial cells, we will use the control value for normal mice from Figure 6.

#### **UCN-01 arrest and time to recovery:**

While our work to this point and the previous study by Redkar et. al. demonstrated that UCN-01 can arrest the proliferating cells in the mouse small bowel, the time course of this effect is not known (Redkar *et al.*, 2001). In order to take advantage of any arrest to prevent chemotherapy-induced toxicity, it is crucial to know when the UCN-01-mediated arrest commences and also how long it takes for cells to return to normal levels of proliferation. To this end, we conducted a time course study in the UCN-01 treated mice to examine the reversibility of arrest following treatment. A mouse study was designed



to analyze the time course of UCN-01 effect. Nude mice were treated with 5 mg/kg UCN-01 or DMSO control, 30 mice per group. 10 mice from each group were BrdU-labeled and sacrificed each at one, two and four weeks post-treatment. Shown in Figure 7a (experiment A), the  $f^{dd}$  values for the UCN-01 treated mice are lower than the baseline level (blue bar, results of experiment in Figure 6) at one week post-treatment, suggesting that UCN-01 treatment has inhibited proliferation of the jejunum epithelial cells. By the two-week time point, the proliferation of the gut epithelial cells increases to approximately the baseline value established in Figure 5 (0.99%, indicated by the blue bar). At four weeks post-UCN-01, the mouse jejunum has a slightly higher than normal proliferative level. It is likely that this response is a reaction to the lack of proliferation caused earlier by UCN-01, in which greater cell proliferation is intended to repopulate the villi; this is similar to the response seen when mice are treated with  $\gamma$ -irradiation (Farrell *et al.*, 1998). Figure 7b displays the  $f^{dd}$  values obtained by mice treated with DMSO for one, two and four weeks. As seen previously in Figure 5, DMSO treatment appears to stimulate cell proliferation in the jejunum, as  $f^{dd}$  levels are elevated above baseline (0.99%, blue bar) at one week. By two weeks, the intestinal epithelial cells have returned to normal levels of proliferation, and the four-week samples remain at this level. This experiment provides us with the time course for UCN-01 effects on the small bowel proliferating cells; it also corroborates the previous data (Figure 5) which shows an antagonistic effect of the carrier DMSO. This information is crucial to planning future protection experiments using UCN-01 prior to a chemotherapeutic agent. Additionally, these results show that the antagonistic action of DMSO (i.e the stimulation of cell

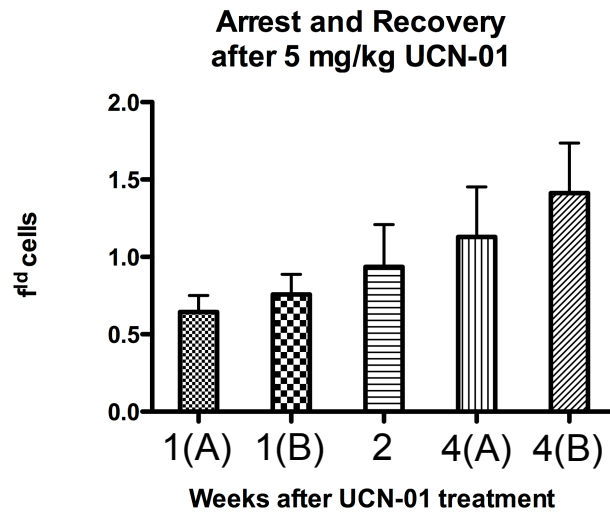


Figure 7a. Flow cytometric analysis of mouse jejunums at one, two, and four weeks after 5 mg/kg UCN-01 (n=10 for each group). Cell cycle arrest persists through one week, recovers to approximately normal levels (figure 202, 0.99% indicated by blue line) by week 2, and gives way to a slight increase in proliferation by week 4. The second set of mice was evaluated at 1 and 4 weeks post-UCN-01 (B), confirming the results of the first experiment.

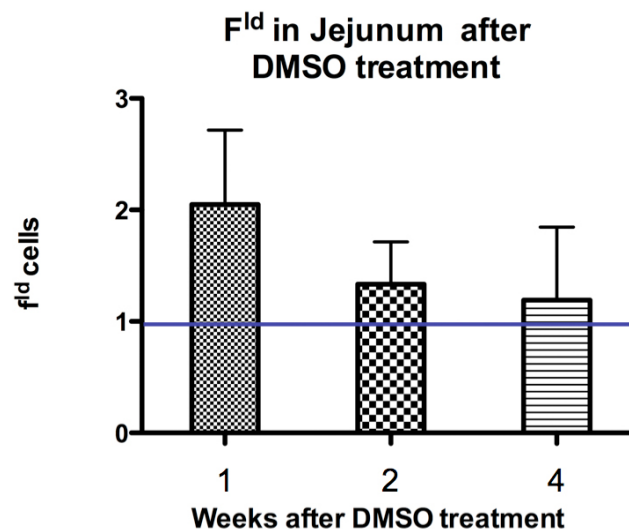


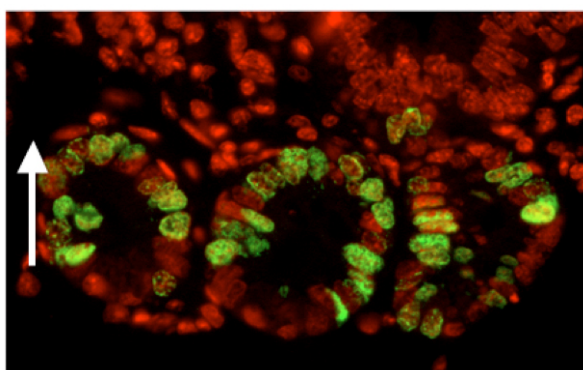
Figure 7b. Flow cytometric analysis of mouse jejunums at one, two, and four weeks after DMSO treatment (n=10 for each group). DMSO causes increased cell proliferation at one week, and this effect diminishes to normal levels by week 2. This indicates an antagonism between UCN-01 and DMSO.

proliferation) on the gut epithelium does not inhibit the UCN-01 mediated inhibition cellular proliferation or the subsequent recovery from this arrest.

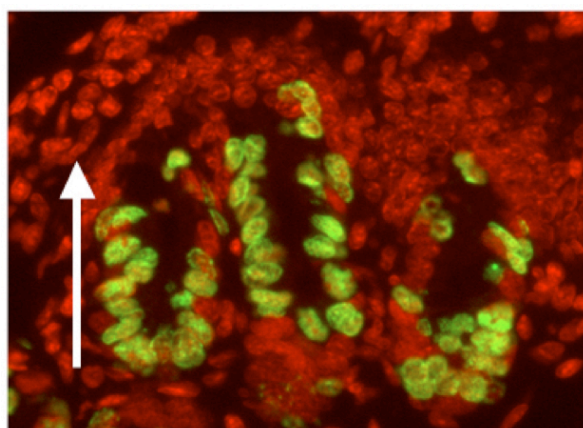
A section of jejunum for each mouse from this experiment was also fixed in formalin and embedded in paraffin for histological analysis. Sections from each time point were probed by anti-BrdU antibodies and visualized by fluorescent microscopy. In this analysis, BrdU positive cells are labeled with fluorescein and appear as green signals. A green cell indicates that BrdU was successfully incorporated into the cell, which is an indicator of active cell proliferation. In addition, the nuclei have been stained with Propidium iodide, and appear as red signals. In Figure 8, the sample from the one week time point has fewer BrdU positive cells compared to the two and four week time point samples. This indicates that gut epithelial cells are in a less proliferative state than the two and four week samples, as less BrdU has been incorporated during S phase. This staining provides visual evidence confirming the flow data shown in Figure 7.

#### **Repeat analysis of UCN-01 time course:**

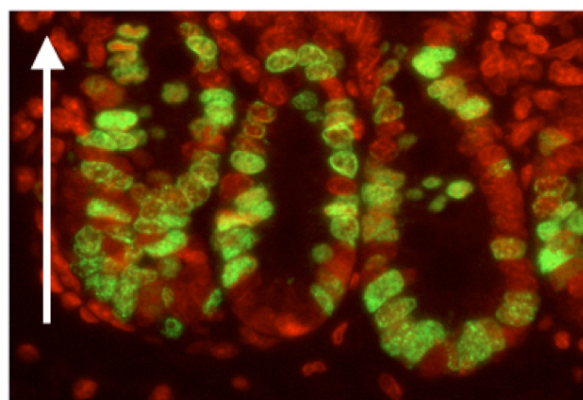
To examine the reproducibility of UCN-01 mediated arrest and subsequent reversibility of this arrest over time, a new experiment repeating the one and four week time points for UCN-01 at 5 mg/kg was planned to both validate the results in Figure 7 and to verify that a new batch of UCN-01 (from a different source) was similarly effective in affecting the small bowel epithelial cells. For this experiment, 20 mice were injected with 5 mg/kg of the new batch of UCN-01 10 mice were BrdU-labeled and sacrificed one week after UCN-01 treatment, and the remaining 10 mice labeled and sacrificed at week four. Similar to the results shown in Figure 7, the one-week mice had a lowered  $f^{dd}$  value,



**1 week**



**2 weeks**



**4 weeks**

Figure 8. Anti-BrdU immunohistochemistry of mouse jejunums harvested at one, two and four weeks after treatment with 5 mg/kg UCN-01. Mice were sacrificed six hours after BrdU injection. The qualitative levels of BrdU incorporation appear lowest in the one week sample, and increase as UCN-01 inhibition recedes over two and four weeks. White arrows indicate crypt to villus orientation. Green signal indicates BrdU incorporation, and nuclei are stained in red with pseudocolor. Quantitative analysis of BrdU IHC is shown in Figure 9.

indicative of cell cycle arrest in the repeat experiment (Figure 7, experiment B). This value increased to a slightly higher than normal value at week four, also in agreement with our previous results. This experiment demonstrates both that our previous results are reproducible, and that the new batch of UCN-01 is effective in causing a cell cycle arrest in the proliferating tissues of the mouse. Both experiments clearly show that not only is UCN-01 able to inhibit cell proliferation in the epithelial tissue of the jejunum, but that the arrested cells can resume normal proliferative activity within two weeks of UCN-01 treatment. Hence, UCN-01 causes a reversible inhibition of cell proliferation *in vivo*.

#### **Solving the solvent problem – reducing the effect of DMSO:**

UCN-01 is able to arrest the proliferating cells of the mouse small bowel, and does this despite an apparent stimulatory effect of its solvent DMSO. The results in Figures 5 and 7b indicate that DMSO causes an undesirable increase in cell cycle proliferation in the jejunum, in opposition to the arresting effect of UCN-01. To mitigate this conflict, an alternative solvent for UCN-01 was sought. UCN-01 poorly soluble in most buffers, but some previous studies have used sodium citrate as a solvent (3% w/v, pH 3.5) both *in vitro* (Hamed *et al.*, 2008) and *in vivo* (Patel *et al.*, 2002). An experiment to evaluate both UCN-01 in the citrate buffer as well as a higher concentration UCN-01 solution was planned (10 mg/ml UCN-01 versus 4.8 mg/ml in all previous studies; the higher concentration reduces the volume of DMSO injected by more than 50%). 10 mice each would be injected with (a) 5 mg/kg UCN-01 in sodium citrate, (b) sodium citrate control, (c) 5 mg/kg UCN-01 (at 10 mg/ml in DMSO), or (d) DMSO control (volume equivalent to the 10 mg/ml UCN-01 solution). 24 hours later, the mice were injected with BrdU and

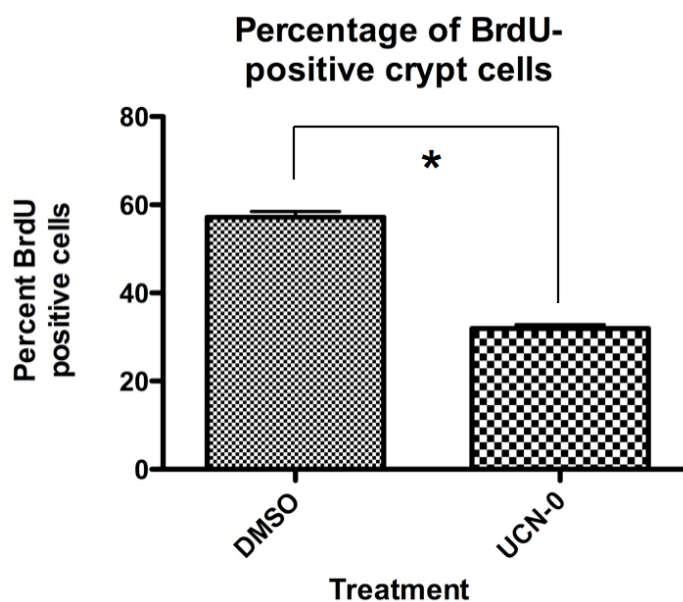


Figure 9. Quantitative analysis of anti-BrdU IHC on jejunum sections of mice treated for 48 hours with 5 mg/kg UCN-01 or DMSO control. The results mirror the analysis by flow, demonstrating a drop in DNA synthesis due to UCN-01 treatment, suggesting a block before S phase. An image of this analysis is shown in Figure 48.

sacrificed, and the jejunum processed for flow cytometry. In Figure 10a, it can be seen that both methods attempting to reduce the solvent effect of DMSO were ineffective. UCN-01 dissolved in the citrate buffer was unable to produce any cell cycle arrest, with a  $f^{ld}$  value above the baseline (blue bar). The higher concentration UCN-01 in DMSO has a significant arrest (mean  $f^{ld}$  0.615%), but the volume equivalent DMSO control group had elevated levels of cellular proliferation. The  $f^{ld}$  value for DMSO in this study (2.269%) is very close to the 2.048% value obtained previously using the more dilute 4.8 mg/ml UCN-01 solution (Figure 7b). However, neither the approach of a higher concentration of UCN-01 in DMSO nor the switch to sodium citrate as a solvent for UCN-01 were effective methods to minimize the unwanted solvent effects of DMSO.

Another attempt to minimize the DMSO effect used an even higher concentration of UCN-01 in DMSO, this time 60 mg/ml (versus 10 mg/ml used in Figure 10a). At this concentration, a 30 gram mouse would only receive 2.5  $\mu$ l of DMSO, compared to 15  $\mu$ l at the 10 mg/ml concentration. However, this volume is too small to be reliably injected, and the UCN-01 solution was brought up to 15  $\mu$ l total for each mouse immediately prior to injection with warm (37°C) saline. 10 mice were injected with the high concentration UCN-01/saline mixture, and 10 mice received the volume equivalent of DMSO/saline. However, this method also failed to alleviate the DMSO effect. Seen in Figure 10b, the DMSO group had an observed  $f^{ld}$  of 2.154%, similar to the elevated values for DMSO in both 10a and 7b. Additionally, the UCN-01-treated mice did not undergo an arrest of the small bowel epithelial cells. It is possible that the mixing of UCN-01/DMSO with saline prior to injection caused a significant amount of drug to come out of suspension; this may

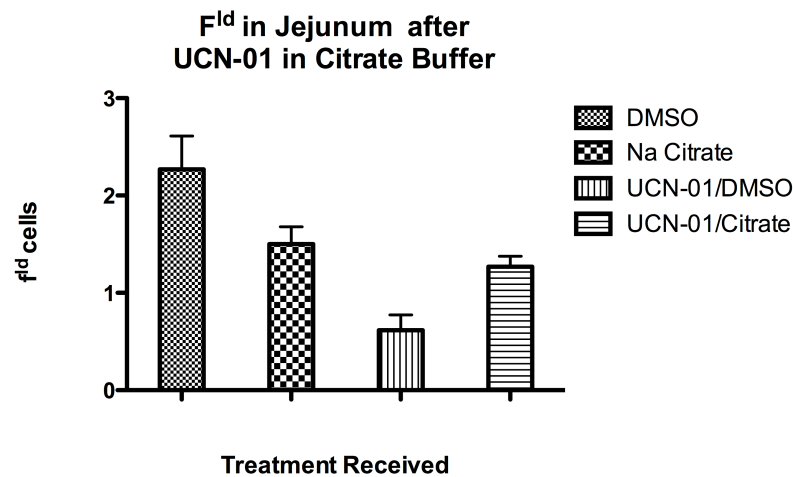


Figure 10a. Flow cytometric analysis of mice 24 hours after treatment with 5 mg/kg UCN-01 dissolved in 3% sodium citrate, pH 3.5 or higher concentration UCN-01 in DMSO (10 mg/ml versus 4.8 mg/ml in figures 7 and 8) and vehicle controls, injected *im* (n=10 for each group). No arresting effect was observed in the mice receiving citrate/UCN-01, and the diminished DMSO still caused an increase in f<sup>d</sup>.

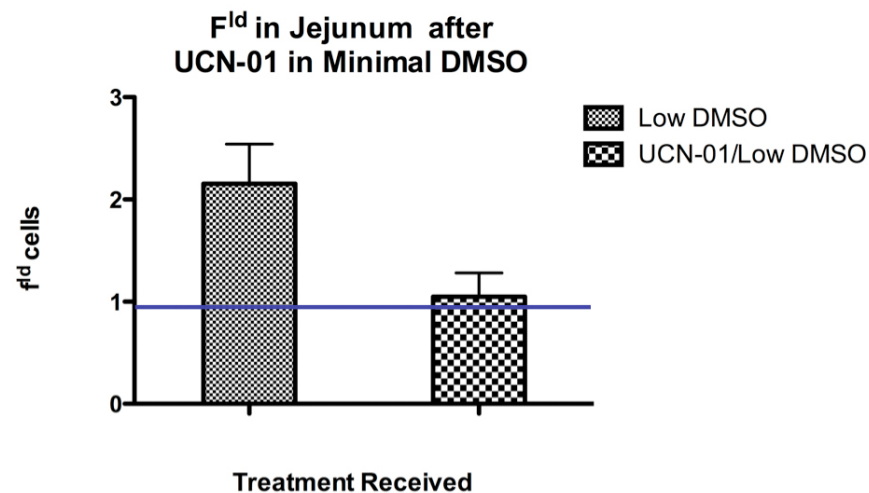


Figure10b. Flow cytometric analysis of mice 24 hours after treatment with 5 mg/kg UCN-01 dissolved at a higher concentration in DMSO (60 mg/ml versus 10 mg/ml in figure 10a). DMSO stimulation of cell proliferation was still present, but the UCN-01 at this concentration was unable to effect a cell cycle arrest.



in turn have prevented proper absorption of UCN-01 and resulted in the ineffectiveness of this treatment.

None of the attempts made to minimize the cellular proliferation stimulated by DMSO (i.e. UCN-01 antagonism) were successful. This solvent antagonism is an undesirable feature of our treatment plan, it does not appear to have any effect of the UCN-01 mediated arrest of cell proliferation and release from arrest over time. All future experiments in this study will use DMSO and the solvent for UCN-01.

#### **Effect of dosing schedule on effectiveness of UCN-01-mediated arrest:**

While UCN-01 treatment can significantly arrest the normal proliferating cells of the small bowel (Figures 5, 7a, and 9), it was questioned whether a single treatment with UCN-01 was the most effective way to bring about this arrest. Figure 11 shows anti-BrdU staining of jejunum sections of mice treated with either 5 mg/kg UCN-01 or PBS for 24 hours. The bright green signals indicate incorporation of BrdU, a marker of cellular proliferation. While the degree of BrdU incorporation (bright green signals, marked with white arrows) is much lower in the UCN-01 treated samples (indicative of reduced cellular proliferation) compared to the PBS controls, there is still a significant number of cells in the UCN-01 mice which are continuing to cycle and incorporate the BrdU label. As the half-life of UCN-01 in mice is approximately 4 hours, we questioned whether a different treatment plan would capture more cells in an arrested state.

Specifically, if we were to administer UCN-01 in two half doses separated by 12 hours, it might be possible to affect cells with the second dose which were not in the correct phase for UCN-01's action during the first dose. To test this hypothesis, 10 mice were treated

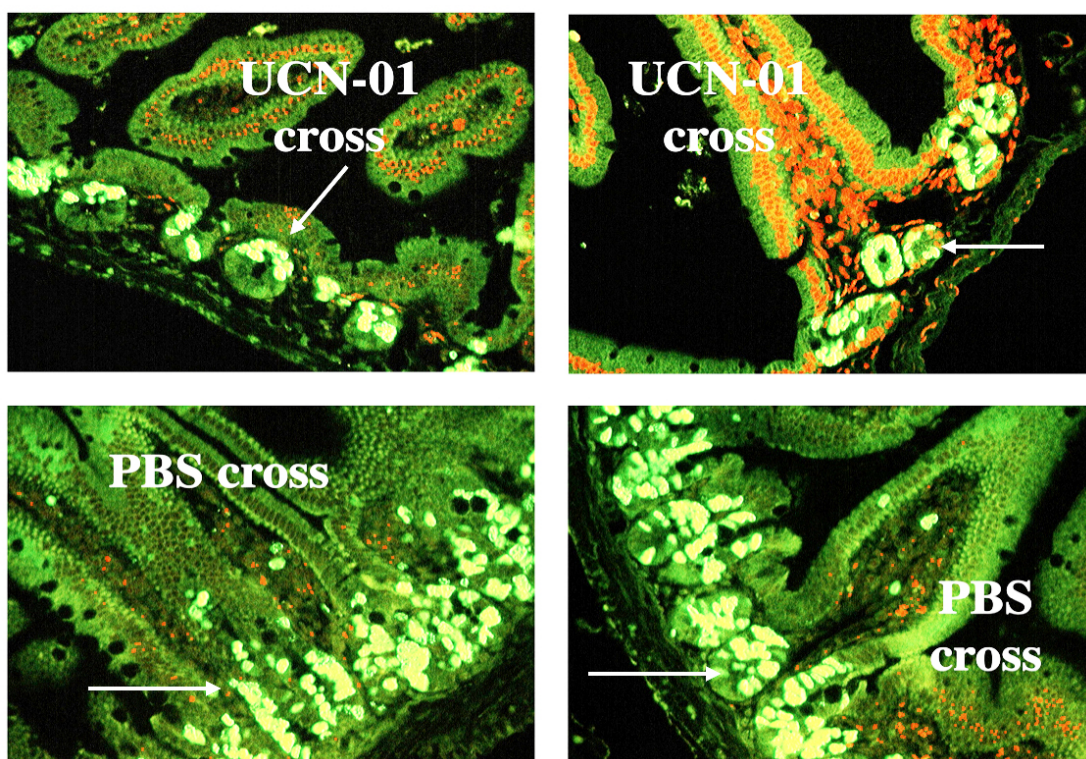


Figure 11. Anti-BrdU immunohistochemical analysis of jejunum sections of mice treated with either 5 mg/kg UCN-01 or PBS *im* for 48 hours. The UCN-01 treated mice have qualitatively lower levels of incorporated BrdU compared to PBS (this has been confirmed by flow analysis, Figure 7) controls, but some cells are still actively cycling even after UCN-01 treatment.

with a single 5 mg/kg dose of UCN-01, and then injected with BrdU 24 hours later and sacrificed. Another 10 mice were injected with 2.5 mg/kg at the same time, and then again with an additional 2.5 mg/kg UCN-01 12 hours later. These mice were also labeled with BrdU 24 hours following the initial injection and sacrificed for flow cytometric analysis. Shown in Figure 12, the two half-dose treatment group had lower levels of BrdU incorporation than the single full dose of UCN-01. However, the difference was not statistically significant ( $p=0.0944$ ). While this experiment did not show a significant improvement in cell cycle arrest when UCN-01 was administered over a greater time frame, it is possible that a treatment schedule that is even more spread out could result in greater cell cycle arrest.

### ***Discussion:***

The main purpose of the studies in this section was to demonstrate that UCN-01 could cause a reversible cell cycle arrest in our model system, the small bowel of the nude mouse. Our results indicate that 5 mg/kg UCN-01 can cause a significant arrest of the gut epithelial cells as early as 24 hours after treatment. This arrest persists through day 7 post-UCN-01 treatment, and the intestinal epithelia return to the normal level of proliferation by two weeks post-UCN-01 treatment. This information is critical in planning the experiments for protection against chemotherapeutics for normal cells, which is the goal of the next chapter. In order to take advantage of cell cycle arrest to evade the toxicity of agents targeting dividing cells, we will need to time the exposure of the cytotoxic agents to occur during the period of cell cycle arrest. As some chemotherapeutic agents are only able to target dividing cells, protection will only be

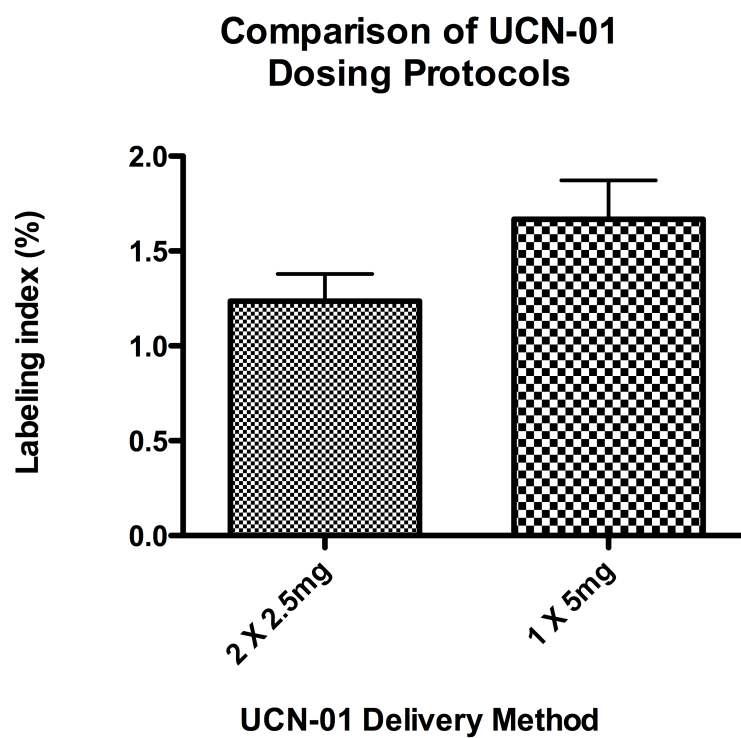


Figure 12. Comparison of the arresting effects of a single dose of 5 mg/kg UCN-01 versus two 2.5 mg/kg doses injected 12 hours apart. The level of BrdU positive nuclei is lower in the two-dose method, but the difference is not significant ( $p=.0944$ ).

afforded to the normal dividing cells if the cytotoxic agent is administered while they are in an arrested state. The exact timing of this treatment scheme will be examined in the next chapter.

The antagonism of UCN-01 by its solvent DMSO was also demonstrated. Neither alternative solvents nor minimal use of DMSO (via high concentration UCN-01) were able to alleviate this effect. While the DMSO mediated antagonism is not desirable, the use of DMSO as a solvent does not affect the inhibition of cellular proliferation by UCN-01 or this subsequent release from arrest. In our experiments, DMSO is the most effective solvent for delivering UCN-01 *in vivo*. As such, DMSO will be used for all subsequent experiments in this thesis.

The idea of separating UCN-01 doses over a 12 hour period to induce a greater level of cell cycle arrest was also found to be not statistically significant. However, the two-dose treatment plan did result in a somewhat lower level of BrdU incorporation. It may be possible that a continuous infusion of 5-10 mg/kg of UCN-01 over a 24 hour period could more effectively capture a greater percentage of dividing cells into a state of arrest. This method might also allow for an alternative solvent to be used, alleviating the DMSO complication. However, the effects of UCN-01 are dose dependent. A 5 mg/kg dose spread over time may never reach a concentration sufficient to cause a significant level of cell cycle arrest. Alternatively, a constant exposure to UCN-01 could also lead to induction of other unwanted effects of UCN-01 (see Introduction), especially those leading to apoptosis or prevention of DNA damage repair. The possible complications of this treatment plan render it beyond the scope of this investigation.

## II. Improved Tolerance of Fluorouracil following UCN-01 Administration

**Introduction:** The study by Chen et al. demonstrated that UCN-01 is able to specifically arrest normal cells in culture, while tumor cell lines are unaffected and continue to proliferate (Chen *et al.*, 1999). In another study examining the effects of the UCN-01 parent analog staurosporine, normal mammary epithelial cell lines 70N and 81N and Rb wild-type 76NE6 cells entered into a G0/G1 arrest after 48 hours of treatment with 0.5 nM of staurosporine; the tumor cell lines MDA-MB157 and MDA-MB436 as well as the Rb-deleted 76NE7 were resistant to this arrest (Chen *et al.*, 2000). Subsequent treatment with doxorubicin or camptothecin was tolerated in the arrested lines, while the tumor cell lines were susceptible apoptosis induced by the chemotherapeutic drugs. The temporary arrest increased the MTD for the normal cell lines by two orders of magnitude for camptothecin.

In the previous chapter, UCN-01 was demonstrated to cause a significant cell cycle arrest in the small bowel epithelium of the nude mouse as early as 24 hours following a single administration at 5 mg/kg *im*. This arrest persisted through day 7, and the cells returned to normal proliferative levels by day 14. These results indicate that the first requirement for the protection strategy (UCN-01-mediated arrest of normal cells in the mouse) has been met. The next part of this *in vivo* strategy is to demonstrate a protective arrest persists in the mouse while undergoing treatment with chemotherapeutic agents. In order to evaluate any potential protective effect of this arrest, mice pretreated with either UCN-01 or DMSO control will be subsequently treated with fluorouracil (5-FU). 5-FU was chosen as an agent which targets dividing cells and has been shown to

cause significant toxicity to the gut epithelium system, especially when administered in a bolus fashion (Sobrero *et al.*, 1997). 5-FU is able to kill cells in at least three ways, by thymidylate synthase inhibition (when metabolized into FdUMP), misincorporation into DNA (when metabolized into FdUTP), and prevention of rRNA maturation (Longley *et al.*, 2003). Cell death following 5-FU treatment is concomitant with an increased bax/bcl-2 ratio (Inomata *et al.*, 2002) or induction of apoptosis or permanent quiescence through the p53/p21 pathway (Pritchard *et al.*, 1998), although the exact cause of cell death is still under investigation. In patients treated with 5-FU (370-400 mg/M<sup>2</sup>), both oral and gastrointestinal mucositis can be limiting side effects, along with neutropenia and myelosuppression (Schwab *et al.*, 2008). The ability of the mice to tolerate 5-FU following UCN-01 will be evaluated by examining alterations in weight, blood markers and survival. The hypothesis for this section is that **the temporary arrest of the normal dividing tissues of the nude mouse by UCN-01 pretreatment will improve tolerance of the toxicity caused by 5-FU administration.**

Mice were treated with UCN-01 to cause a cell cycle arrest (as demonstrated chapter 1), followed by administration of the chemotherapeutic agent fluorouracil (5-FU). 5-FU was injected at time points from one to seven days post-UCN-01, and the tolerance of this treatment was evaluated by measuring weight, blood markers and survival. We show here that UCN-01 pretreated mice had significant improvements in all these facets after 5-FU treatment when compared to DMSO pretreated control mice. However, this improvement is only observed when 5-FU is administered during a window of efficacy, approximately three to five days post-UCN-01 treatment.

**Materials and Methods:** Mice: Female nude mice from 8-12 weeks of age (approximately 24-30 grams) were obtained from the Experimental Radiation Oncology colony at M.D. Anderson Cancer Center. Mice are maintained in the specific pathogen free barrier facility on sterilized normal chow and water with no restrictions. UCN-01 treatment: Mice were injected with 5 mg/kg UCN-01 (or volume equivalent DMSO for controls) *im* in the right hindlimb via a 0.5 ml insulin syringe with a 32 gauge needle. Fluorouracil treatment: Mice were given 5-FU (50 mg/ml, Abraxis Pharmaceuticals, Schaumburg IL) *ip* via a 0.5 ml insulin syringe with a 32 gauge needle. Mice were treated with either a single bolus dose or 5 daily injections, depending on the experimental protocol (see below). For doses below 80 mg/kg, normal saline was added to 5-FU to increase volumes to 50  $\mu$ l. Mice were weighed using a Scout Pro balance (Ohaus, Pine Brook NJ).

Blood collection: Mice were anesthetized by inhalation of isoflurane (Baxter Healthcare, Deerfield IL). Once sedated, the mice were bled via retro-orbital puncture of the sinus with a sterile capillary tube. For liver chemistry (aspartate aminotransferase (AST), alanine aminotransferase (ALT), and alkaline phosphatase) 50 $\mu$ l of blood was sampled and placed into a microtainer with a clotting activator (Becton Dickinson, Franklin Lakes NJ) and centrifuged at 1100 X g. Serum supernatant was collected and stored at -80° until analyzed. Enzyme levels were detected using a Roche Integra 400 Plus analyzer with liver panel cassettes (both from Roche Diagnostics, Branchburg NJ). For complete blood counts (CBC), 200 $\mu$ l of blood was collected using heparinized capillary tubes (Fisher Scientific) and placed into EDTA-coated microtainer (Becton Dickinson); these samples



were rotated at 8 RPM on a Labquake tube rotator (Barnstead, from Fisher Scientific) to prevent clotting prior to analysis. Blood counts were determined using an Advia 120 hematology analyzer (Siemens Diagnostic, Deerfield IL); results were confirmed by microscope analysis of blood smear. All samples were analyzed by the Hematology Core in the Department of Veterinary Medicine at M.D. Anderson Cancer Center.

Tissue collection: Mice were sacrificed by cervical dislocation. Sternum were harvested and preserved in 10% formalin prior to embedding in paraffin. Small bowel sections (jejunum) were dissected from the abdomen, flushed with PBS and then preserved in 10% formalin.

Hematoxylin and eosin (H&E) staining: Sternum sections were hydrated by placing slides into Histoclear (National Diagnostics, Atlanta GA) three times for five minutes each. This was followed by 100% ethanol (twice for three minutes), 95% ethanol (twice for three minutes) and 70% ethanol for three minutes. Slides were rinsed in distilled water for five minutes. Slides were stained in Gill's hematoxylin (Vector Labs) for 6 minutes and then rinsed in running tap water for 20 minutes. Slides were decolorized for two seconds in acid alcohol (1% hydrochloric acid in 70% ethanol) and rinsed in water for five minutes. Slides were next immersed in ammonia water (0.1 ammonia in distilled water) five times and were rinsed in water for five minutes. Counterstaining in eosin was done for fifteen seconds, and the slides were washed in water for five minutes.

Dehydration was accomplished by immersion in 95% ethanol twice for five minutes followed by 100% ethanol twice for five minutes. Slides were washed twice in

Histoclear for five minutes each, and samples were mounted behind a coverslip using Permount (Sigma Aldrich).

Microscopy: Mouse sternum H&E sections were visualized using a Leica DM400B (Wetzlar, Germany) microscope. Images were taken using a Spot digital camera and Spot Advanced software (Spot Imaging Solutions, Sterling Heights MI). The total area of the blood precursor cells was determined using the histogram analysis function in Photoshop (Adobe Systems, San Jose CA). This area was normalized to the total stained area of each section analyzed. Five sections were analyzed per mouse, and five mice per treatment group (UCN-01 or DMSO pretreated mice) were examined.

Statistics: Pairwise comparison of means was performed using Student's t-test; a confidence level of 95% was considered to be statistically significant in these studies. Survival analysis was interpreted using the Kaplan-Meier method and significance for comparing treatment outcomes was performed using the Mantel-Cox Log Rank test. All calculations were performed using the Prism software package (GraphPad Software, Inc.).

## ***Results:***

### **Serial injection of 5-FU beginning day 7 post-UCN-01/DMSO:**

The BrdU incorporation results presented in chapter 1 indicate that the arresting effect of UCN-01 in the small bowel was present through seven days, and that the proliferative

rate of these cells had returned to normal levels by two weeks. These results pose the question as to whether UCN-01 can be used to protect normally proliferating tissues against the toxic effects of 5-FU during this period of arrest. The ability of UCN-01 to protect mice against the toxic effects of 5-FU during this period was examined in an experiment using six groups of mice, five mice per group; the treatment protocol is shown in Figure 13. The groups were as follows:

- 1: 5 mg/kg UCN-01, followed in 7 days with 5 X daily PBS *ip*
- 2: 5 mg/kg UCN-01, followed in 7 days with 5 X daily 25 mg/kg 5-FU *ip*
- 3: 5 mg/kg UCN-01, followed in 7 days with 5 X daily 35 mg/kg 5-FU *ip*
- 4: DMSO, followed in 7 days with 5 X daily 25 mg/kg 5-FU *ip*
- 5: DMSO, followed in 7 days with 5 X daily 35 mg/kg 5-FU *ip*
- 6: DMSO, followed in 7 days with 5 X daily PBS *ip*

The levels of 5-FU administered in this experiment were chosen for their ability to induce sub-lethal enzymatic and structural damage in the mouse small bowel (Kaufmann *et al.*, 1967). The hypothesis for this experiment is that the temporary arrest of the proliferating cells of the mouse will allow better tolerance of subsequent 5-FU treatment. It was expected that the UCN-01-treated groups would have less weight loss following 5-FU compared to DMSO controls, an indication of improved gastrointestinal health. The mice were weighed daily and sacrificed one day following the final 5-FU/PBS treatment. The percent change in weight is shown in Figure 14. The weights of mice pretreated with UCN-01 and then injected with 25 mg/kg/day 5-FU were almost identical to those of

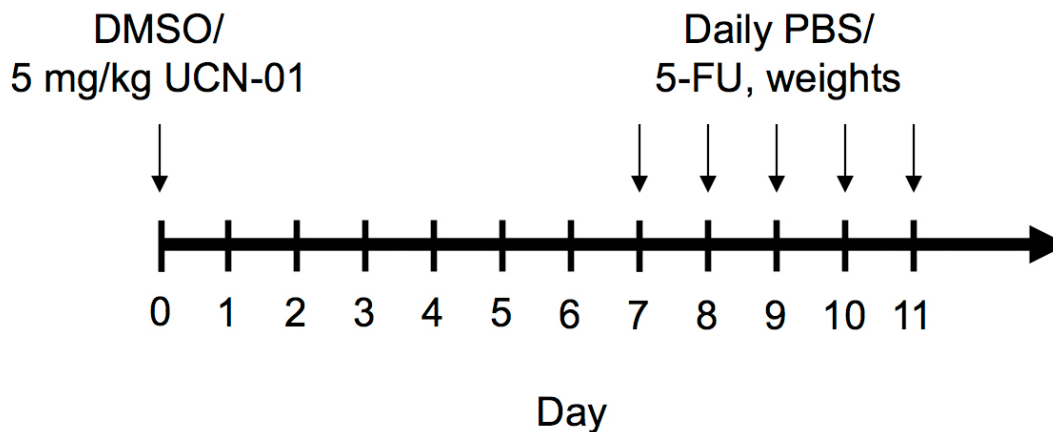


Figure 13. Treatment protocol for first mouse protection experiment. 5 mg/kg UCN-01 or DMSO injected on Day 0 (15 mice each), and then 5 mice per group injected daily with 25 or 35 mg/kg/day or PBS daily for days 7 through 11. Weight was measured daily during 5-FU treatment.

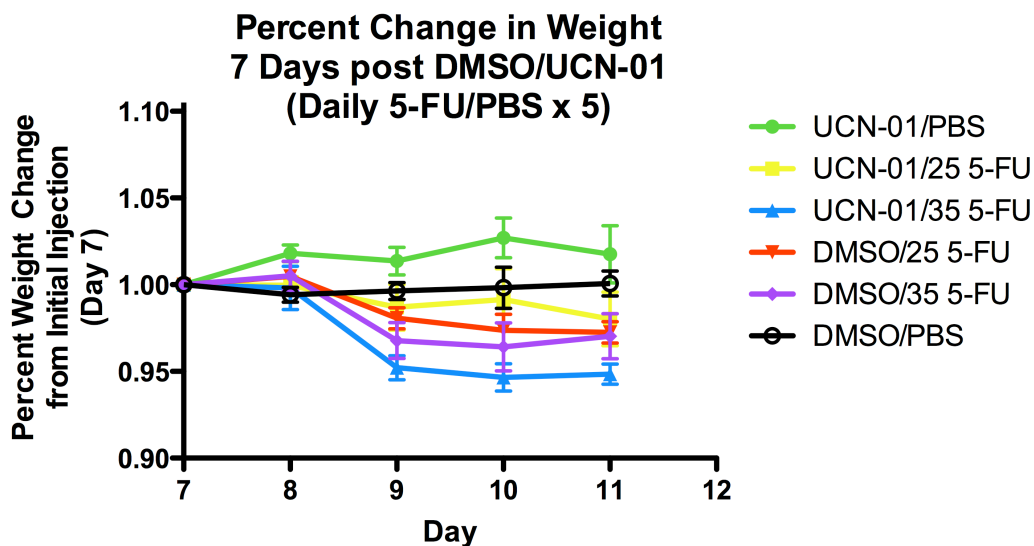


Figure 14. Percent change in daily weights for mice treated with 5-FU or PBS daily for days 7 through 11 (treatment protocol in shown in figure 13).

mice pretreated with vehicle (DMSO) and prior to 25 mg/kg/day 5-FU. Mice injected with 35 mg/kg/day 5-FU had slightly improved weight status if pretreated with vehicle as opposed to UCN-01, although this difference is not significant ( $p=0.435$ , Student's t-test). As such, the hypothesis for the concentrations and timing of 5-FU administered was tested and found to be incorrect. It is possible that the seven-day gap between UCN-01 treatment and 5-FU treatment is too long for optimal protection, especially with a daily injection of chemotherapy (the last injection would be on day 12, very close to the time at which normal proliferation returns). The arrested cells of the mouse will be resuming cell cycle activities at this point, and may be susceptible to 5-FU toxicity. While this protocol failed to demonstrate any protective effect of UCN-01, perhaps a different treatment schedule would be more successful. It was also noted that the doses of 5-FU (25 mg/kg/day and 35 mg/kg/day) were very well tolerated in the mice (greatest weight loss was just over 5%, Figure 14); further experiments will use the 35 mg/kg/day as a starting dose.

### **Serial injections of 5-FU beginning day 3 post-UCN-01/DMSO:**

The previous experiment failed to demonstrate an improvement in the tolerance to 5-FU toxicity in mice pretreated with UCN-01. These results raised the question as to whether a shorter interval between the two drugs would better exploit the arresting effect caused by UCN-01. The hypothesis for this new protocol is that earlier 5-FU administration would be better tolerated in UCN-01 pretreated mice compared to vehicle control. In order to evaluate this idea, the timing of 5-FU administration was moved from seven days post-UCN-01 to 3 days following UCN-01. The ability of UCN-01 to protect mice

against the toxic effects of 5-FU using this altered timing scheme was examined in an experiment using four groups of mice, five mice per group (Figure 15). The groups were as follows:

- 1: 5 mg/kg UCN-01, followed in 3 days with 5 X daily PBS *ip*
- 2: 5 mg/kg UCN-01, followed in 3 days with 5 X daily 35 mg/kg 5-FU *ip*
- 3: DMSO *i.m.* followed in 3 days with 5 X daily 35 mg/kg 5-FU *ip*
- 4: DMSO *i.m.*, followed in 3 days with 5 X daily PBS *ip*

As before, it was expected that the UCN-01 pretreated mice would have improved weight status compared to control mice after subsequent exposure to 5-FU. The mice were weighed daily and sacrificed one day following the final 5-FU/PBS treatment. To evaluate hepatotoxic effects of this treatment and the status of the hematopoietic system, blood was collected upon sacrifice for both complete blood counts (CBC) and liver enzyme analysis. The percent change in daily weight is shown in Figure 16. Unlike the previous experiment, pretreatment with UCN-01 was able to improve the weight status of the mice receiving 35 mg/kg/day 5-FU when administered 3 days post-UCN-01 (Figure 16). The difference was significant at day 6 ( $p = 0.0131$ ). The liver enzymes measured in the blood (AST, ALT and alkaline phosphatase) were not significantly elevated by the treatments, and no difference between UCN-0/ 5-FU and DMSO/5-FU were observed (Figure 17 a-c). 5-FU is primarily metabolized in the liver, while UCN-01 is mostly excreted. As such, it was possible that the two groups receiving 5-FU would have elevated liver enzymes in the blood. However, as can be seen in Figures 17a and 17b,

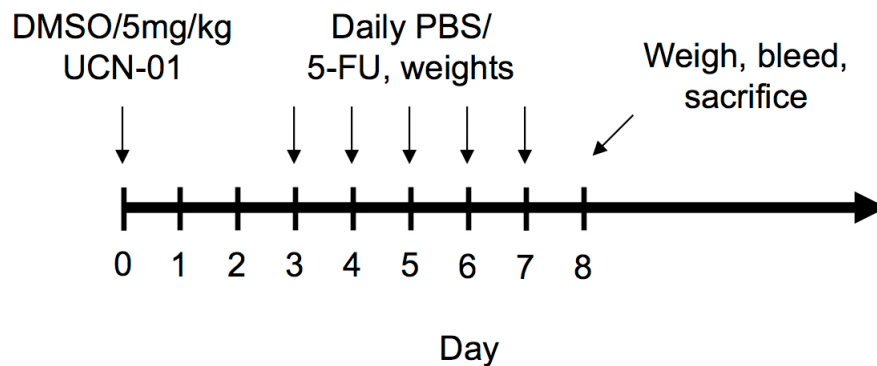


Figure 15. Treatment protocol for the second mouse protection experiment. 5 mg/kg UCN-01 or DMSO injected on Day 0 (10 mice each), and then 5 mice per group injected daily with 35 mg/kg/day or PBS daily for days 3 through 7. Weight was measured daily during 5-FU treatment. Mice were bled and sacrificed on day 8.

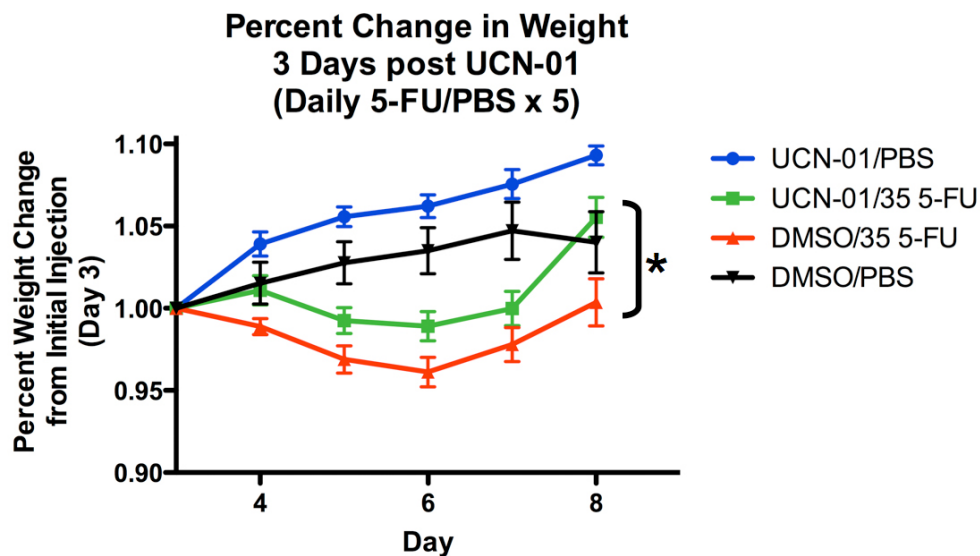


Figure 16. Percent change in daily weights for mice treated with 5-FU or PBS daily for days 3 through 7 (treatment protocol in shown in figure 15). The difference in weights between the DMSO/5-FU mice and the UCN-01/5-FU mice was significant on day 8 ( $p < 0.05$ ).

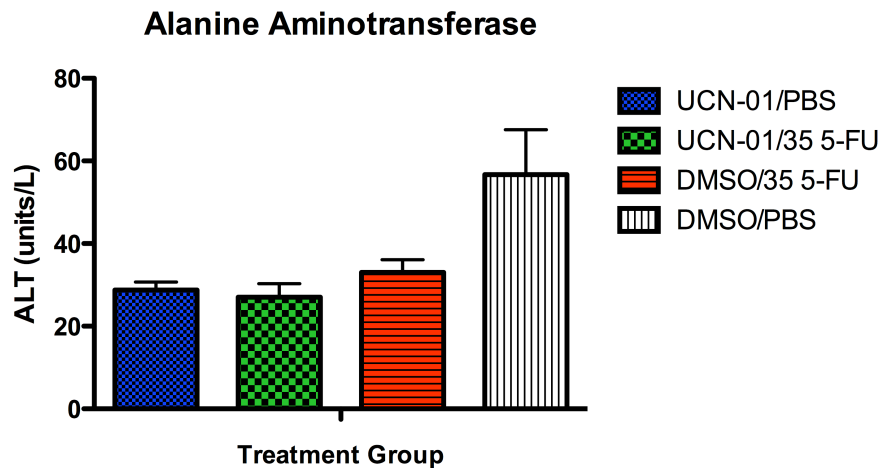


Figure 17a. ALT levels in serum for mice treated with protocol shown in figure 15. No elevation consistent with hepatic damage was seen in the mice treated with either UCN-01 or 5-FU.

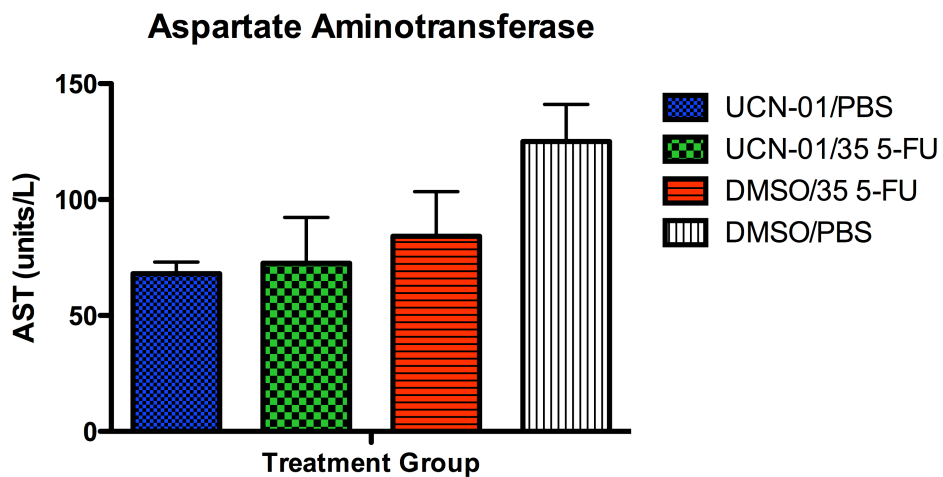


Figure 17b. AST levels in serum for mice treated with protocol shown in figure 15. No elevation consistent with hepatic damage was seen in the mice treated with either UCN-01 or 5-FU.



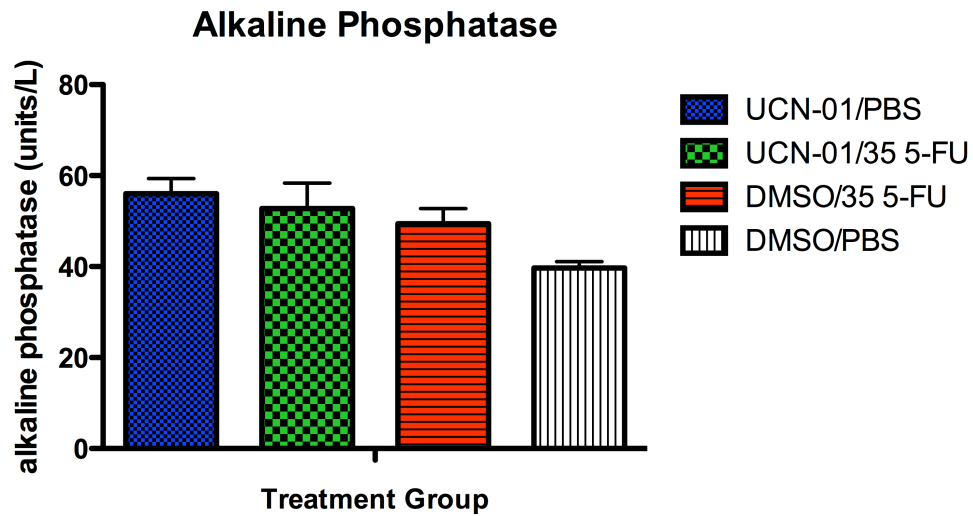


Figure 17c. Alkaline phosphatase levels in serum for mice treated with protocol shown in figure 15. Some elevation consistent with hepatic damage was seen in the mice treated with either UCN-01 or 5-FU.

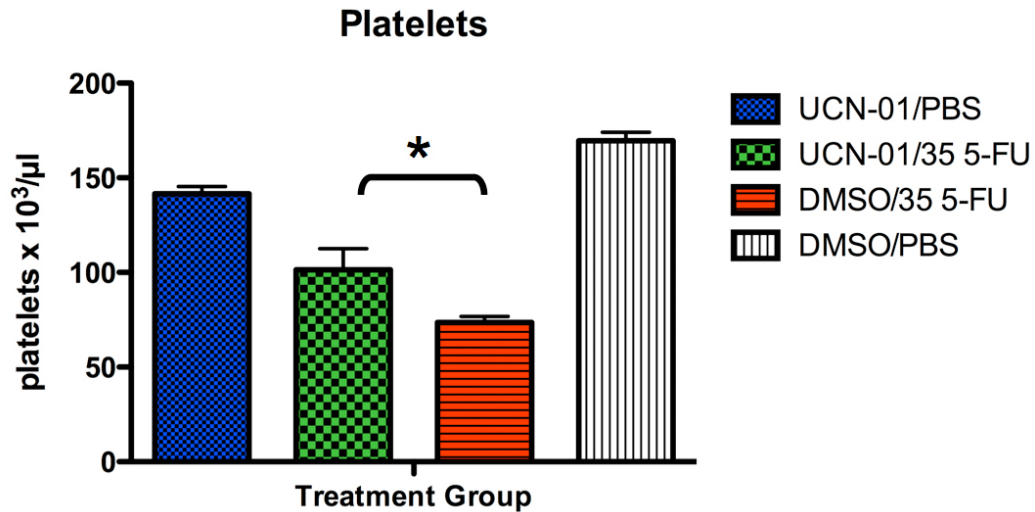


Figure 17d. Platelet counts in whole blood for mice treated with the protocol in figure 15. The difference in platelets between the UCN-01 pretreated mice receiving 5-FU and the DMSO pretreated mice receiving 5-FU was significant at day 8 (\*,  $p < 0.05$ )

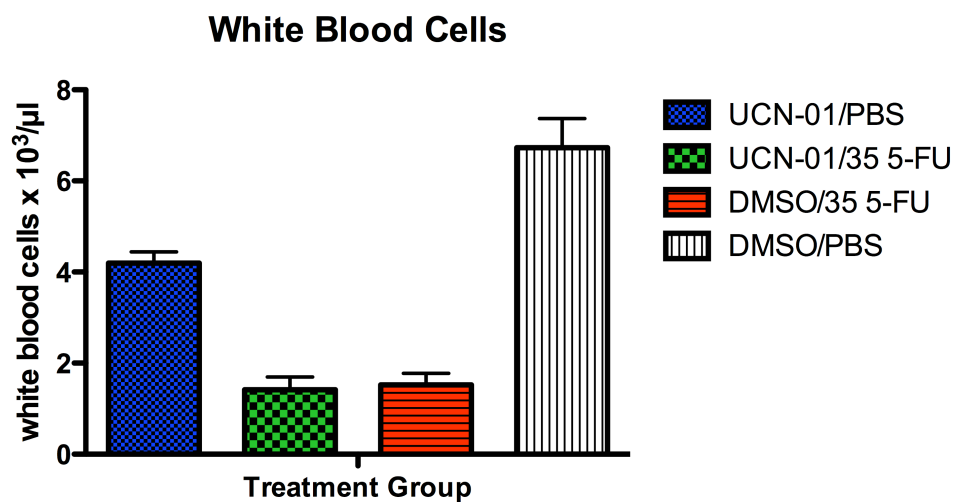


Figure 17e. White blood cell counts in whole blood for mice treated with the protocol in figure 15. No significant difference between the 5-FU mice pretreated with either DMSO or UCN-01 was seen at day 8.

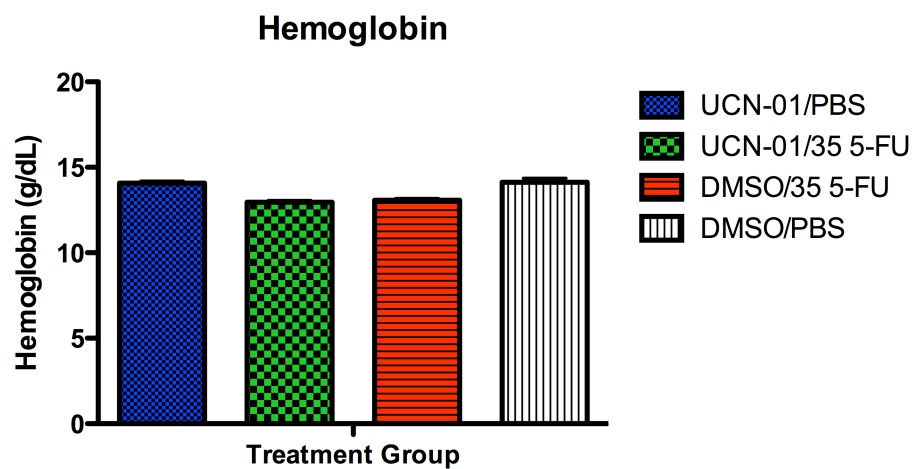


Figure 17f. Hemoglobin counts in whole blood for mice treated with the protocol in figure 15. No significant difference between the 5-FU mice pretreated with either DMSO or UCN-01 was seen at day 8.

ALT and AST levels were actually reduced in all treated groups compared to PBS control. Alkaline phosphatase levels were higher in all treated groups (Figure 17c), but overall no evidence for either UCN-01 or 5-FU related liver toxicity seems to be present at these doses. Whole blood counts demonstrated a significant improvement in platelets (Figure 17d) for the UCN-01 pretreated 5-FU group in comparison to the 5-FU/DMSO group ( $p = 0.043$ ). Hemoglobin and white blood cells were not significantly different between the UCN-01/5-FU and DMSO/5-FU (Figures 17e and 17f), although a later time point would be more appropriate to measure these parameters. This will be addressed in a later experiment (see below). In summary, this experiment did show tangible improvements in weight status (a marker for intestinal health) and platelets, which indicates an improvement in the hematopoietic system. The cause for this improvement, in comparison to the initial study, is likely the shortened time frame between UCN-01 and 5-FU treatments. The arrested status of the dividing tissues in the UCN-01 pretreated mice throughout the five-day 5-FU treatment can afford protection to these cells, and may explain the improvements observed.

#### **High dose 5-FU administered 24 hours after UCN-01/DMSO:**

The results thus far suggest that cytotoxic treatment is better tolerated in the UCN-01 pretreated mice when 5-FU is administered when the UCN-01-mediated arrest is at a high level (days 3-7 post-UCN-01); the improvement in tolerance is not observed if 5-FU is administered later in the post-UCN-01 recovery period (days 7-11 post UCN-01). These results raised the question as to the best timing of 5-FU treatment relative to UCN-01 administration. To determine the optimal dosing schedule for UCN-01 and 5-FU, it was

decided to evaluate the protective effect of UCN-01 at 24 hours post-administration, the time of the greatest measured cell cycle arrest (see chapter 1). The hypothesis for this experiment is that UCN-01 pretreated mice would best tolerate 5-FU during the period of greatest UCN-01-mediated arrest (24 hours following UCN-01 treatment). For this experiment, two groups of 15 mice were analyzed, one treated with two doses of UCN-01 separated by 12 hours, and the other naïve (treatment and bleeding schedule shown in Figure 18). The two UCN-01 doses separated by 12 hours were shown to decrease the fraction of labeled, divided cells compared to a single dose treatment (chapter 1). To clarify the effect of timing, a single bolus dose of 5-FU was given, rather than a 5-day serial injection; the effects of UCN-01 in the gut epithelium may undergo daily changes as the cells move towards recovery from arrest. A single dose administration of 5-FU would limit the effects of this process from affecting our results. 24 hours after the second administration of UCN-01, all mice were given a single *ip* dose of 450 mg/kg 5-FU. Blood was collected weekly, including a pretreatment measurement, and weight was recorded daily. Unlike the experiment with a 3 day separation of UCN-01 and 5-FU, the bolus dose of 5-FU given 24 hours after UCN-01 was more detrimental than in the mice pretreated with vehicle control in terms of weight status, survival and blood markers. As seen in Figure 19, weight loss is significantly greater in the UCN-01 pretreated group, both in the initial weight loss period (through day 8) and also in the second period, from day 11 until day 15 (\* indicates  $p < 0.05$ ). The numbers in days 8-15 are somewhat skewed, due to the diminishing survival of the UCN-01 pretreated mice. Shown in Figure 20, survival of UCN-01 pretreated mice is diminished (23% versus 60% for the untreated mice) compared to DMSO pretreated mice, although the difference was not

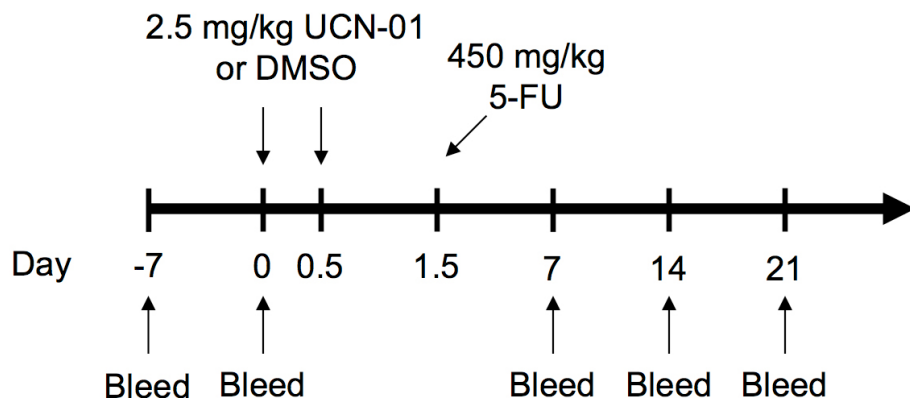


Figure 18. Treatment plan for the third mouse experiment. 15 mice each were treated with either 2.5 mg/kg UCN-01 or DMSO on Day 0 and then again 12 hours later. 450 mg/kg 5-FU was given to both groups 24 hours after the last UCN-01/DMSO treatment. Mice were bled one week prior to treatment, and then weekly beginning on Day 0.

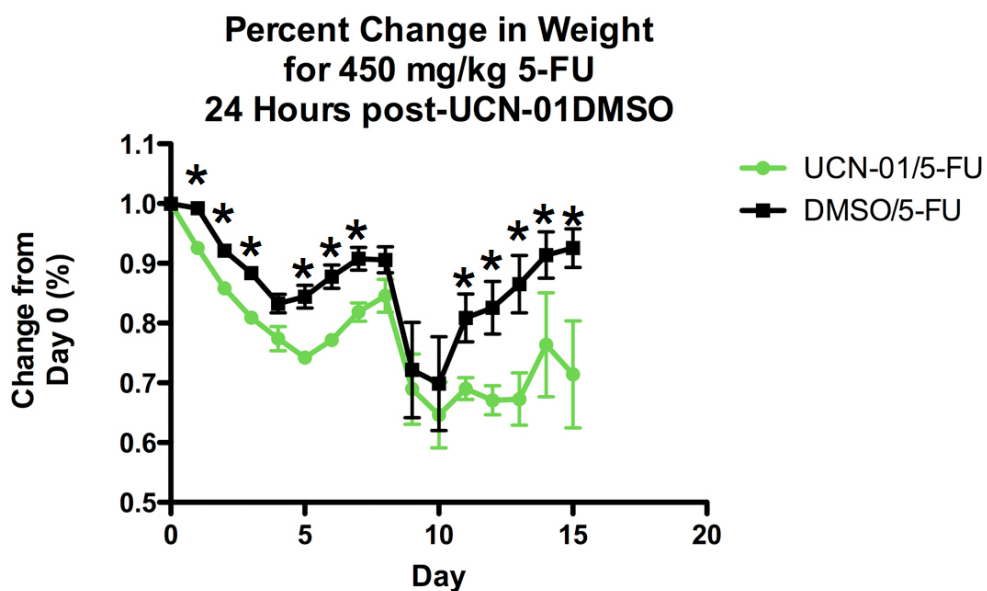


Figure 19. Percent change in weight from Day 0 for mice after 450 mg/kg 5-FU. The weight change was significantly worse in the UCN-01 pretreated mice on days marked with \* ( $p < 0.05$ ).

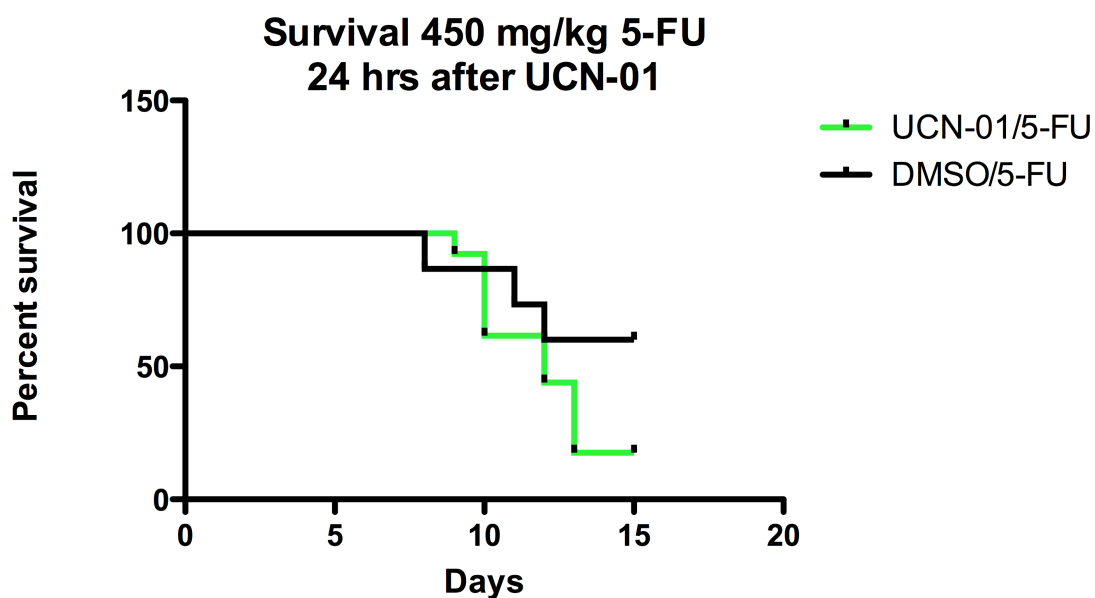


Figure 20. Survival of mice receiving 450 mg/kg 5-FU 24 hours after pretreatment with either 2 X 2.5 mg/kg UCN-01 or DMSO (15 mice per group), as shown in figure 18. Mice pretreated with UCN-01 had diminished survival compared to DMSO control mice.

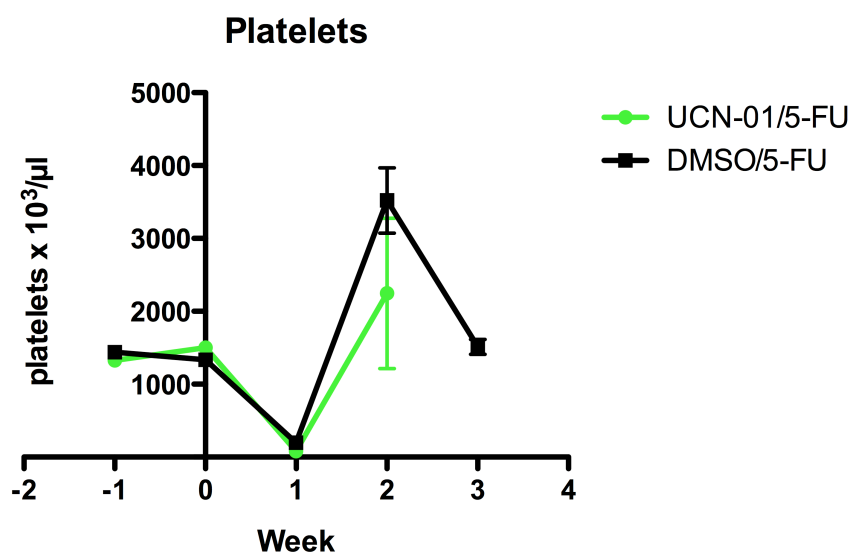


Figure 21a. Weekly platelet counts for mice before and after 450 mg/kg 5-FU (protocol in figure 18). No significant differences were observed in mice pretreated with UCN-01 versus DMSO. Poor survival of UCN-01 mice prevented collection of blood at the 3 week time point.

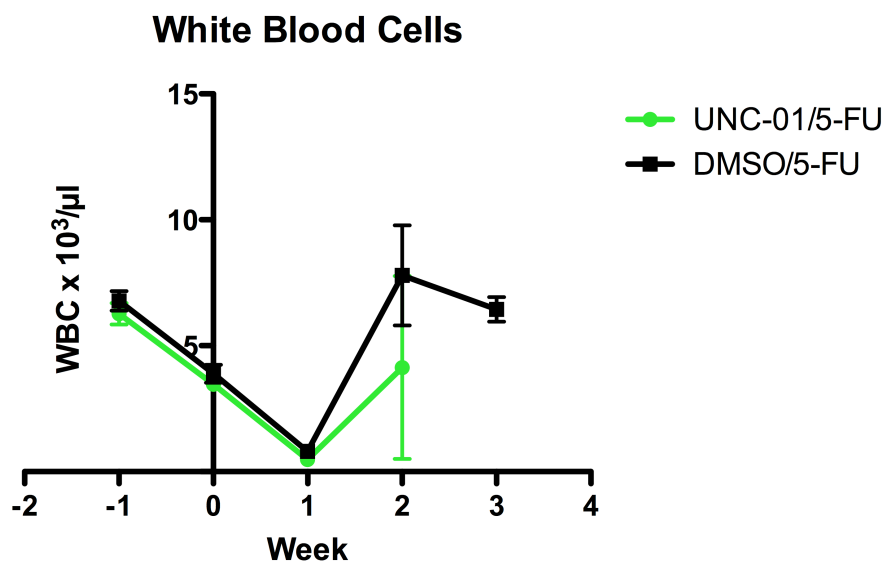


Figure 21b. Weekly white blood cell counts for mice before and after 450 mg/kg 5-FU (protocol in figure 18). No significant differences were observed in mice pretreated with UCN-01 versus DMSO. Poor survival of UCN-01 mice prevented collection of blood at the 3 week time point.

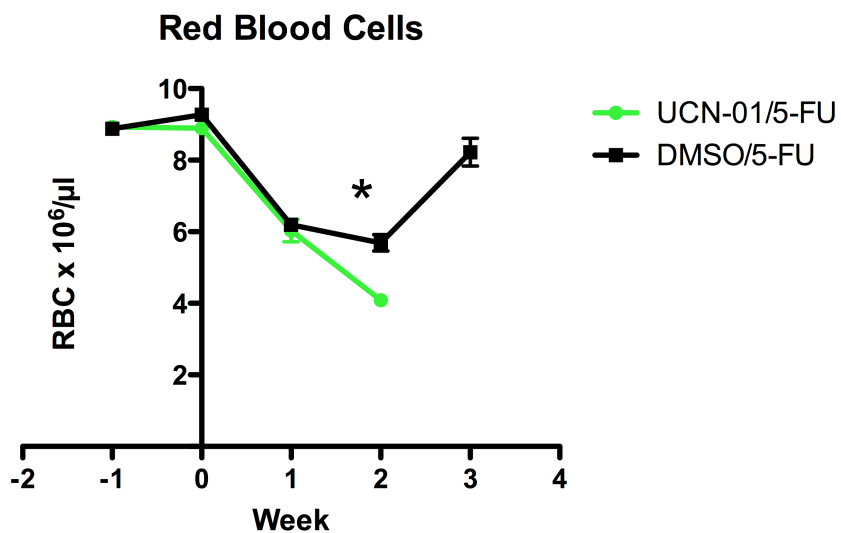


Figure 21c. Weekly red blood cell counts for mice before and after 450 mg/kg 5-FU (protocol in figure 18). Counts were significantly diminished at 2 weeks in the UCN-01 pretreated mice (\*,  $p < 0.05$ ). Poor survival of UCN-01 mice prevented collection of blood at the 3 week time point.

significant ( $p=0.0714$ ). Platelets, white blood cells and red blood cells were also lower in the UCN-01 pretreated group two weeks following 5-FU administration, although not significantly so (Figure 21a-c). Insufficient UCN-01 mice survived to obtain CBC values for the three week time period, so any comparison at this time point is not possible. A possibility raised by this data is that the decreased survival of the UCN-01 pretreated mice is due to the early administration of 5-FU; perhaps a time closer to the recovery of the normal dividing cells would be more appropriate. Mice treated with serial 5-FU treatment from days 3 until 7 post-UCN-01 (previous experiment, Figure 15) seem to obtain some benefit due to cell cycle arrest. However, when given only 24 hours after UCN-01, 5-FU seems to be more toxic than 5-FU in mice pretreated with vehicle control. These results strongly suggest that the timing of 5-FU administration after UCN-01 is a critical parameter in providing protection for the normal dividing tissues of the mouse, which requires further refinement. It may be most beneficial if the cytotoxic treatment occurs during the period of UCN-01 arrest (thus protecting some dividing cells), but very close to the recovery time from that arrest, such that the protected cells are quickly able to resume proliferation and repopulate the gastrointestinal and hematopoietic tissues after the toxic agent has been eliminated.

#### **High dose 5-FU administered on day 5 post-UCN-01/DMSO:**

The results of the different treatment strategies thus far place the optimal protective window for UCN-01 protection against 5-FU somewhere between three and seven days following UCN-01 administration. A new experiment was designed to more closely investigate this effect, using a bolus dose of 5-FU in the center of this window (day 5



post-UCN-01). As shown in the treatment scheme in Figure 22, mice were injected with either UCN-01 (7 mice) or DMSO (5 mice), both groups *im* as before. Five days following treatment, 400 mg/kg 5-FU was injected, and the mice were weighed daily, and blood was drawn for CBCs once a week. The lower 5-FU bolus dose (400 mg/kg vs. 450 mg/kg in the previous experiment) was chosen to increase the survival of both groups, in hopes of having sufficient blood samples for each group for comparative purposes. In contrast to the previous experiment (24 hour separation between UCN-01/DMSO and 5-FU), the UCN-01 pretreated mice in this treatment protocol had improved weight status and survival compared to the DMSO/5-FU control mice. Shown in Figure 23, the UCN-01 pretreated mice had significantly improved weight status on days 13 and 14 ( $p < 0.05$ ), although the diminished survival of the DMSO group prevented any meaningful analysis beyond that time. As seen in Figure 24, no DMSO mouse survived beyond 14 days post-5-FU, while 43% of the UCN-01 pretreated mice survived until day 28; at this point the surviving mice were bled and sacrificed. Blood was collected for comparative CBC analysis, but the poor survival once again prevented any meaningful differences to be measured, as no DMSO pretreated mice survived beyond two weeks. For the earlier time points, no significant differences in any blood markers were noted, although these were likely collected too soon following 5-FU to reflect the damage done to the hematopoietic system. The results from the surviving UCN-01 mice seem to indicate that the platelets decrease within about one week following 5-FU administration and then recover by two weeks (Figure 25c) while the red and white blood cells decrease at two weeks post-5-FU and then recover at 3 weeks (Figures 25a & 25b). While the protocol for this experiment (5-FU at 5 days post-UCN-01) seemed to demonstrate a protective effect of UCN-01, the

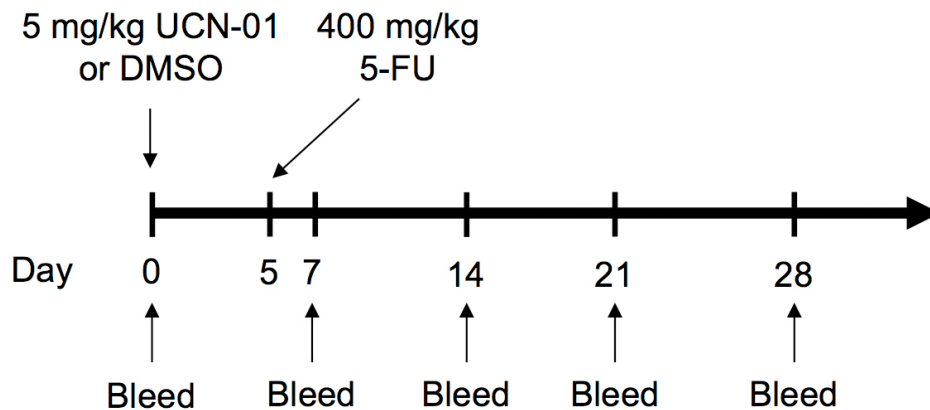


Figure 22. Treatment plan for the fourth mouse experiment. Mice were treated with either 5 mg/kg UCN-01 (n=7) or DMSO (n=5) on Day 0. 400 mg/kg was administered to both groups on Day 5. Mice were weighed daily following 5-FU treatment, and bled weekly.

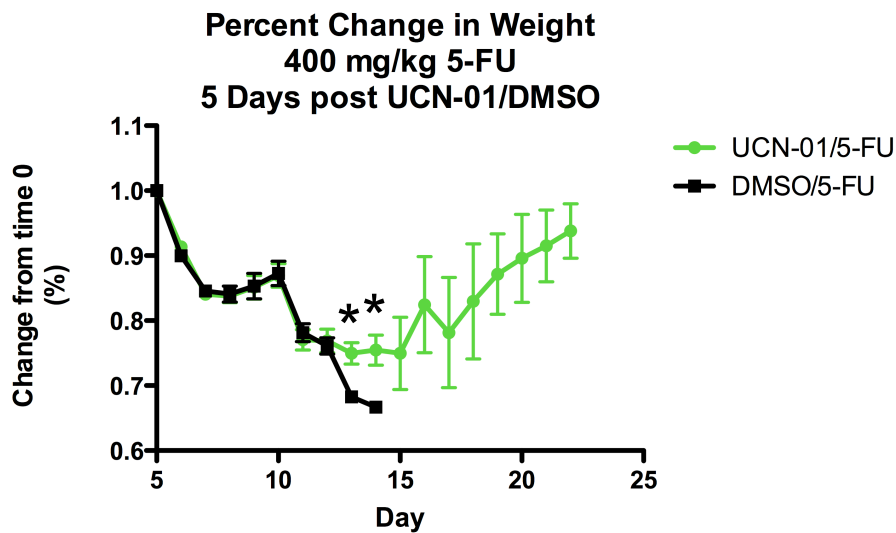


Figure 23. Daily weight changes for mice treated with 400 mg/kg 5-FU five days after 5 mg/kg UCN-01 (n=7) or DMSO (n=5) treatment. Weight loss was significantly greater in the DMSO mice on days 13 and 14 (\*,  $p < 0.05$ ), and no DMSO mice survived beyond day 14.

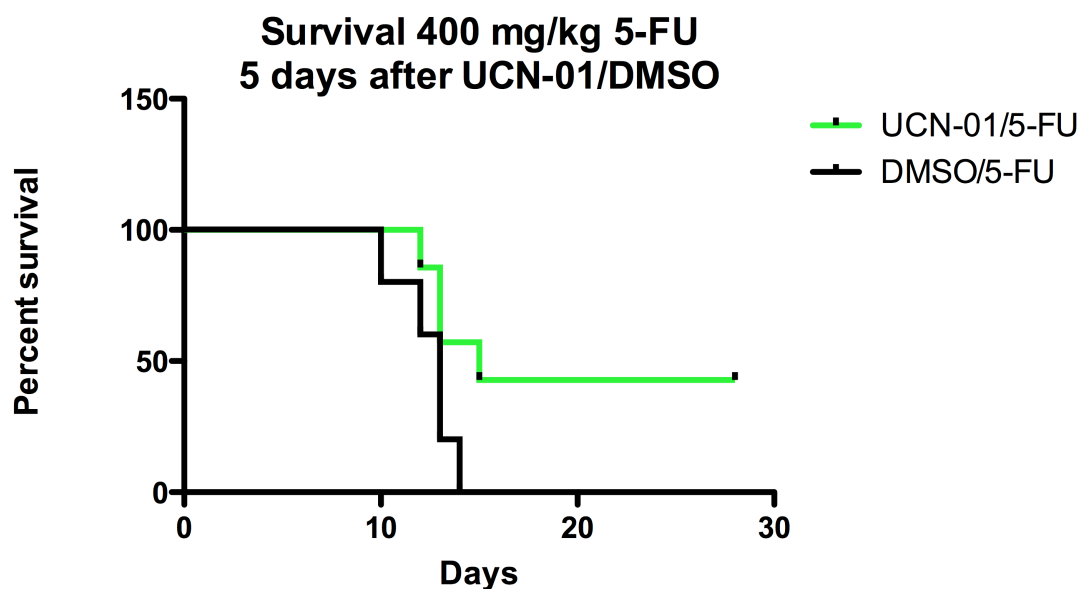


Figure 24. Survival of mice treated with 400 mg/kg 5-FU five days after administration of either 5 mg/kg UCN-01 (n=7) or DMSO (n=5).

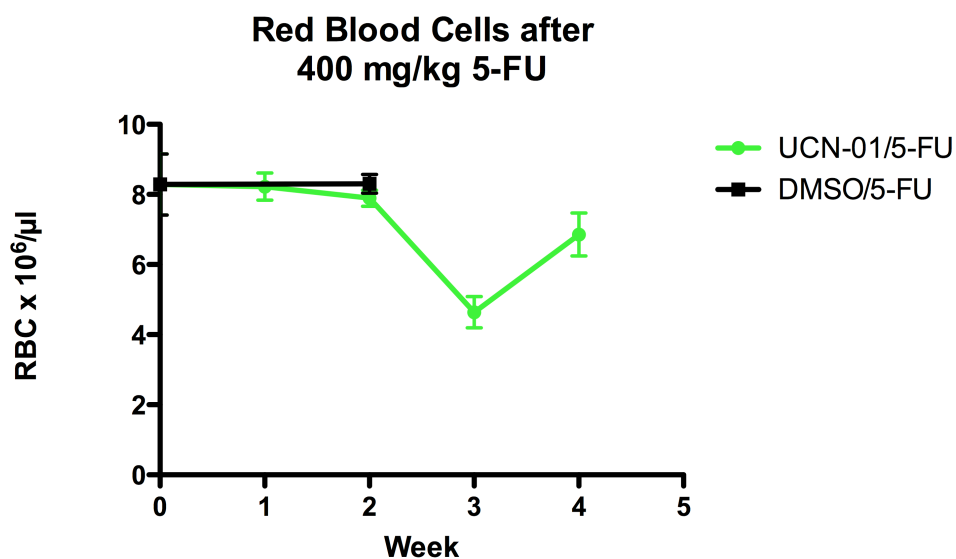


Figure 25a. Weekly red blood cell counts in mice treated with 400 mg/kg 5-FU five days after 5 mg/kg UCN-01 (n=7) or DMSO (n=5). Lack of surviving DMSO mice prevented collection of data for weeks 3 and 4.

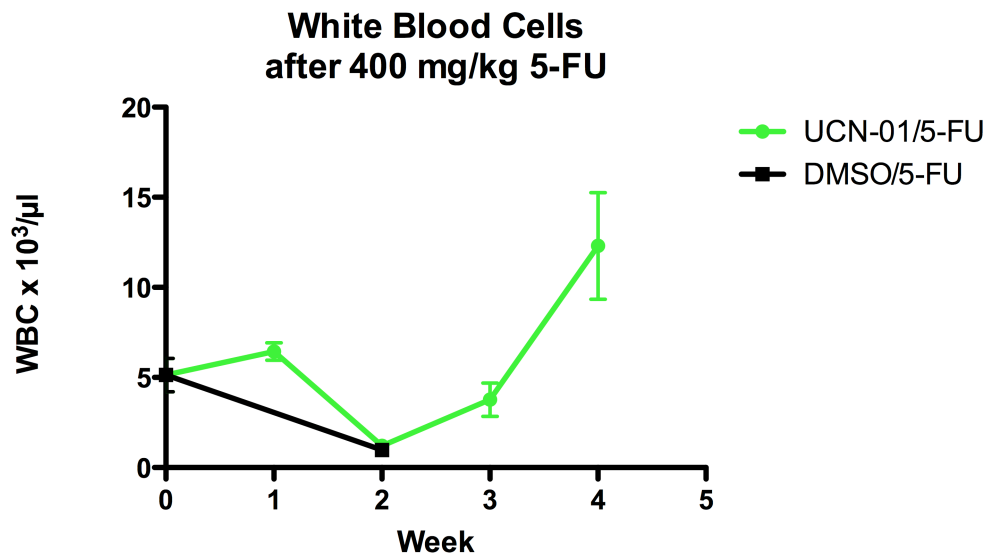


Figure 25b. Weekly white blood cell counts in mice treated with 400 mg/kg 5-FU five days after 5 mg/kg UCN-01 (n=7) or DMSO (n=5). Lack of surviving DMSO mice prevented collection of data for weeks 3 and 4.

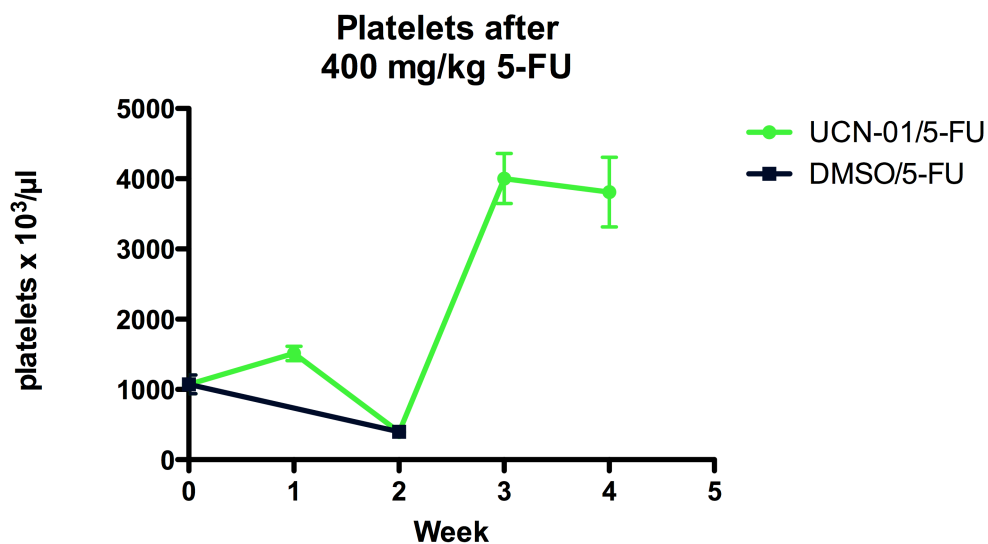


Figure 25c. Weekly platelet counts in mice treated with 400 mg/kg 5-FU five days after 5 mg/kg UCN-01 (n=7) or DMSO (n=5). Lack of surviving DMSO mice prevented collection of data for weeks 3 and 4.

low numbers of mice in both groups and the lack of control mice surviving for comparison of blood markers prevented a statistical interpretation of the results. Even though the dose of 5-FU was decreased in this experimental protocol (400 mg/kg instead of 450 mg/kg), the poor survival of the control mice is problematic and will be addressed in future experiments to ensure sufficient numbers of mice for comparison of blood markers. It is likely that weekly bleeds for CBCs are too harsh for mice which are already suffering 5-FU-induced damage to the hematopoietic system.

**Repeat high dose 5-FU on day 5 post-UCN-01/DMSO (no CBCs):**

The diminished survival of control (DMSO) mice given a bolus dose of 5-FU in the previous experiment prevented a meaningful analysis of changes in weight status (Figures 23 and 24) and blood markers (Figure 25). It is possible that the pre-bleed and weekly bleeds are too deleterious to the mice when being treated with high levels of 5-FU, so the protocol was altered in hopes of improving the survival of the control mice; no blood was collected in this experiment. To evaluate the tolerance of mice receiving a bolus dose of 5-FU, two groups of fifteen mice each were treated with either 5/mg/kg UCN-01 or volume equivalent DMSO (see Figure 26). As in the last experiment (Figure 22), five days post-UCN-01 treatment both groups were injected with 400 mg/kg 5-FU. Weight was measured daily (Figure 27). The weight status of the UCN-01-pretreated mice was significantly improved compared to DMSO control from days thirteen until twenty-two, with the exception of day twenty-one ( $p < 0.05$ , day 21  $p=0.16$ ). One UCN-01 mouse died at day 13, and two DMSO mice died at day 10, but there were no statistical differences in survival. While this level of 5-FU (400 mg/kg) does lead to

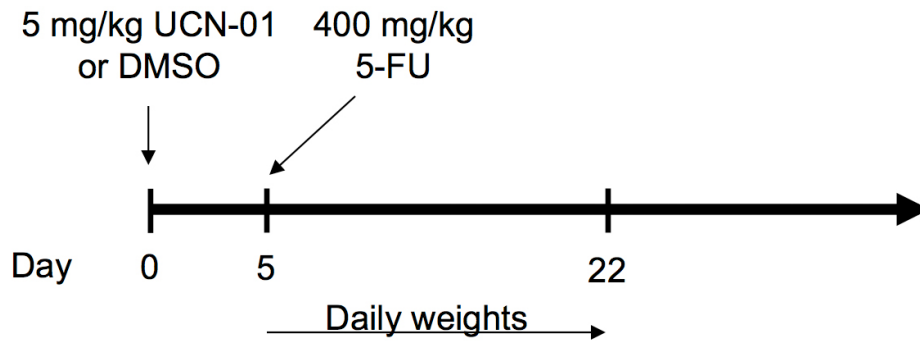


Figure 26. Treatment plan for the fifth mouse experiment. Mice were treated with either 5 mg/kg UCN-01 or DMSO on Day 0 (n=15 for each). 400 mg/kg was administered to both groups on Day 5. Mice were weighed daily following 5-FU treatment.

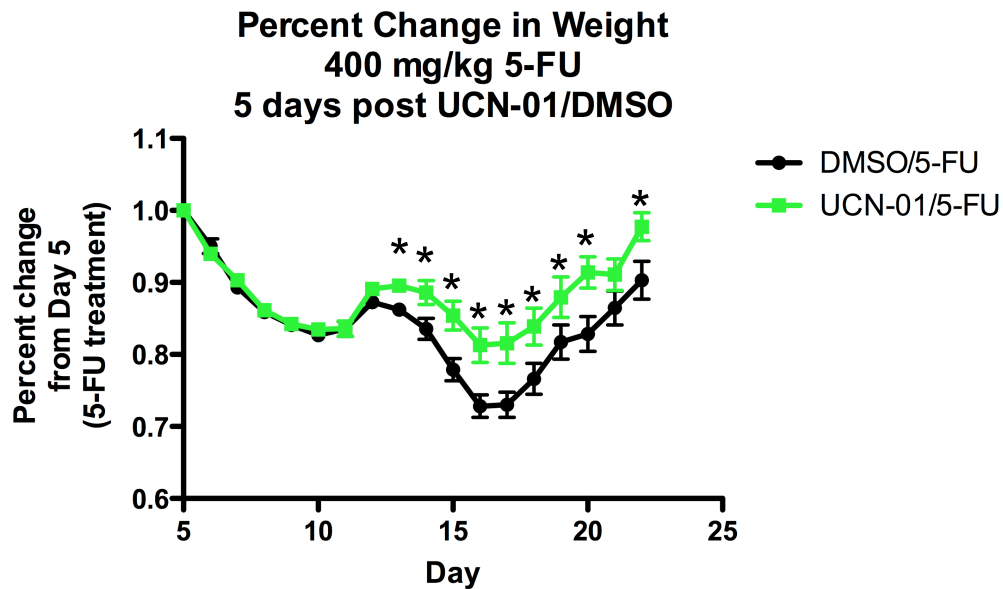


Figure 27. Daily change in weight for mice following 400 mg/kg 5-FU given 5 days post-UCN-01 or DMSO (n=15 for each group). Weight loss was significantly greater for the DMSO groups on days marked with an asterisk (p<0.05).

some significant loss of weight, the dose will have to be increased slightly to obtain any possibly differences in the survival rates of mice protected by UCN-01 pretreatment versus controls.

### **Serial injections of 5-FU beginning on day 3 post-UCN-01/DMSO:**

The results of the previous two studies (Figure 23, 24 and 27) reveal that the ability of UCN-01 to protect mice from the toxicity of a bolus dose of 5-FU appears to be effective at five days post-UCN-01 administration. Weight loss and survival are both improved in the mice pretreated with UCN-01 using this treatment scheme. The initial experiments with serial dosing demonstrate that UCN-01 given three days prior to 5-FU is protective (Figure 16) and that waiting until seven days post-UCN-01 treatment before commencing serial 5-FU administration can nullify this protective effect (Figure 14). The previous results (Figure 17d) also demonstrated that platelets are significantly elevated one week after 5-FU injection in mice pretreated with UCN-01 in comparison to DMSO pretreated mice. However, the doses used (25 and 35 mg/kg/day for five days) were not very toxic in either the UCN-01 or DMSO pretreated groups. The ability of UCN-01 to protect mice from a higher dose of serial injections of 5-FU was evaluated, to determine if a more potent dose would increase the separation in the tolerance of the UCN-01 versus DMSO pretreated mice. This experiment (serial 5-FU beginning day 3 post-UCN-01/DMSO) was repeated with a greater number of mice per group (ten versus five) and a slightly higher serial dose of 5-FU (40 mg/kg/day versus 35 mg/kg/day, see Figure 28). The higher dose was chosen to better demonstrate the ability of UCN-01 to protect against increased levels of a toxic agent. Mice were weighed daily and blood was

collected prior to 5-FU and weekly for three weeks to evaluate the effects on the hematopoietic system (Figure 28). Similar to the previous experiments in which 5-FU was given three days after UCN-01 (Figure 15), the weight status of the mice pretreated with UCN-01 was improved significantly ( $p < 0.05$ ) from day 2 until the end of the experiment compared to the DMSO pretreated mice (Figure 29). The platelet counts of the UCN-01 pretreated mice were significantly ( $p < 0.05$ ) improved at 2 weeks (Figure 30a). Red blood cell counts were similarly improved at the three week time point for the UCN-01 group, but were lower than the DMSO mice at weeks one and two (Figure 30b). This may be due to the temporary arrest caused by UCN-01. The white blood cells counts were significantly lower in the UCN-01 pretreated group compared to DMSO at week one (Figure 30c), likely due to the same cause. While arrested hematopoietic cells may indeed evade 5-FU mediated toxicity, the cell cycle arrest caused by UCN-01 can also prevent those cells from dividing and contributing to maturing blood cell counts, at least initially. Even though the red and white cell counts do not unequivocally demonstrate a protective effect of UCN-01, his experiment both corroborates the previous (35 mg/kg/day X 5 days 5-FU, Figures 16 and 17) experimental results and gives a more complete picture of the changes in the hematopoietic system in the mice after 5-FU administration, both with UCN-01 pretreatment and without. The lack of surviving control mice in the previous experiment prevented the collection of this data (Figures 24 and 25). Future experiments will also examine bone marrow to provide a visual analysis of the health of the blood-forming tissues of the mice after 5-FU treatment. As the CBC numbers indicate improved platelets and red blood cells in the UCN-01 pretreated mice,



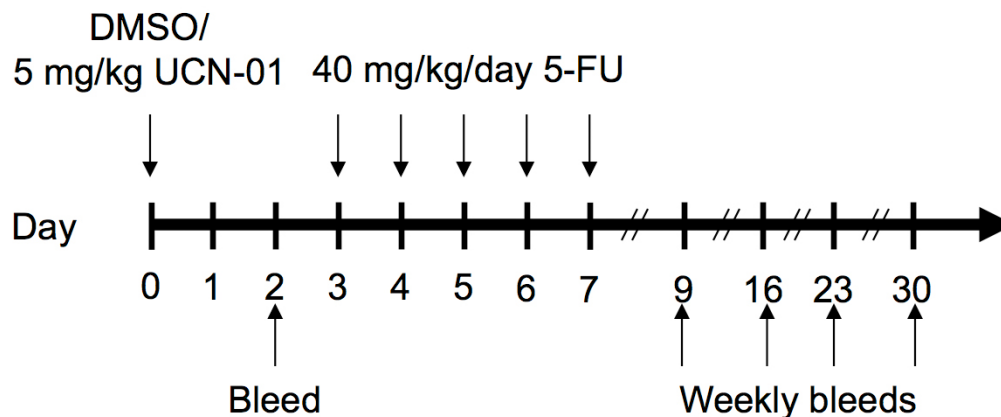


Figure 28. Treatment plan for the sixth mouse experiment. Mice were treated with either 5 mg/kg UCN-01 or DMSO on Day 0 (n=10 pre group). 40 mg/kg/day was administered to both groups daily on days 3-7. Mice were weighed daily following 5-FU treatment. Mice were bled on day 2 (prior to 5-FU) and then every seven days for a total of five bleeds.

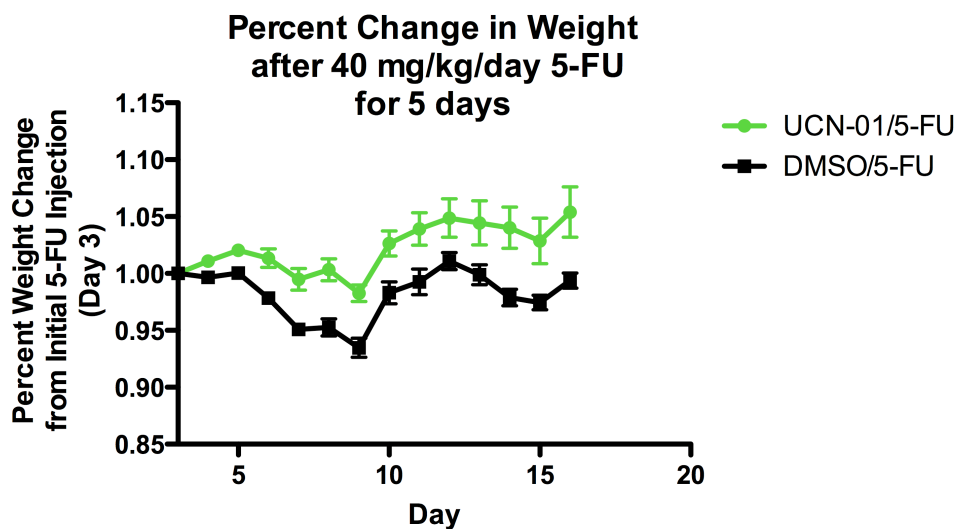


Figure 29. Percent change in weight following 40 mg/kg/day 5-FU for 5 days begun 3 days post UCN-01/DMSO (protocol in figure 28). Weight loss for the DMSO group was significantly greater than the UCN-01 group for all days marked with an asterisk (\*,  $p < 0.05$ ).

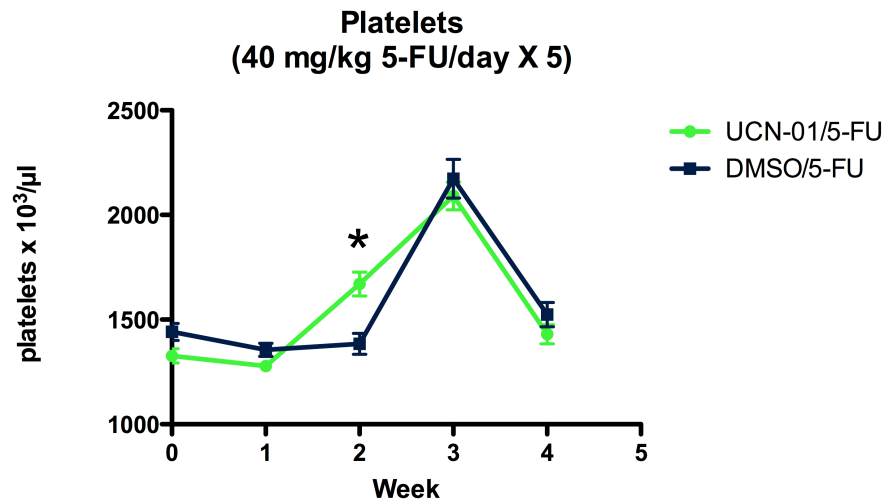


Figure 30a. Weekly platelet counts in mice treated with five daily doses of 40 mg/kg/day 5-FU beginning on day 3 post UCN-01 or DMSO (n=10 for each group). Counts were significantly higher in the UCN-01 pretreated group at week 2 (\*,  $p < 0.05$ ); however, when using the adjusted p-value for multiple comparisons ( $\alpha = 0.0125$ ) the difference is not significant.

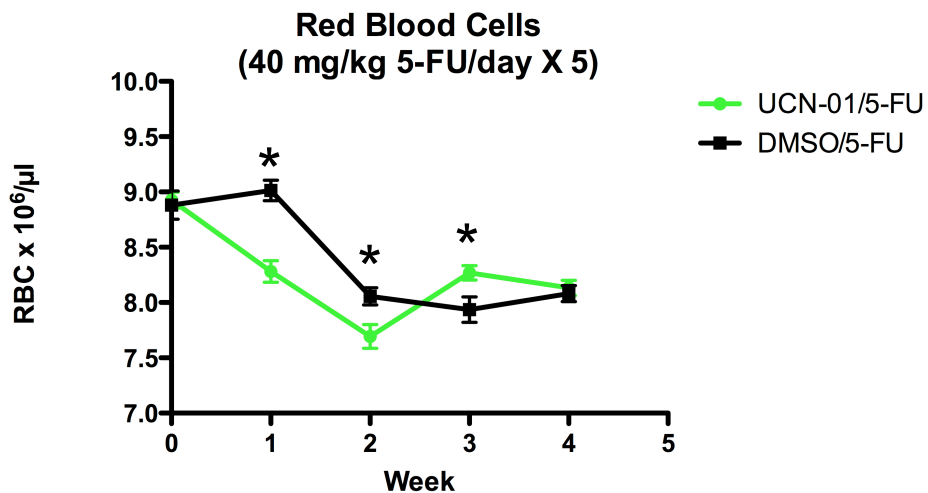


Figure 30b. Weekly red blood cell counts in mice treated with five daily doses of 40 mg/kg/day 5-FU beginning on day 3 post UCN-01 or DMSO (n=10 for each group). Counts were significantly higher in the UCN-01 pretreated group at week 3, and significantly lower at weeks 1 and 2 (\*,  $p < 0.05$ ); however, when using the adjusted p-value for multiple comparisons ( $\alpha = 0.0125$ ) the difference is not significant.

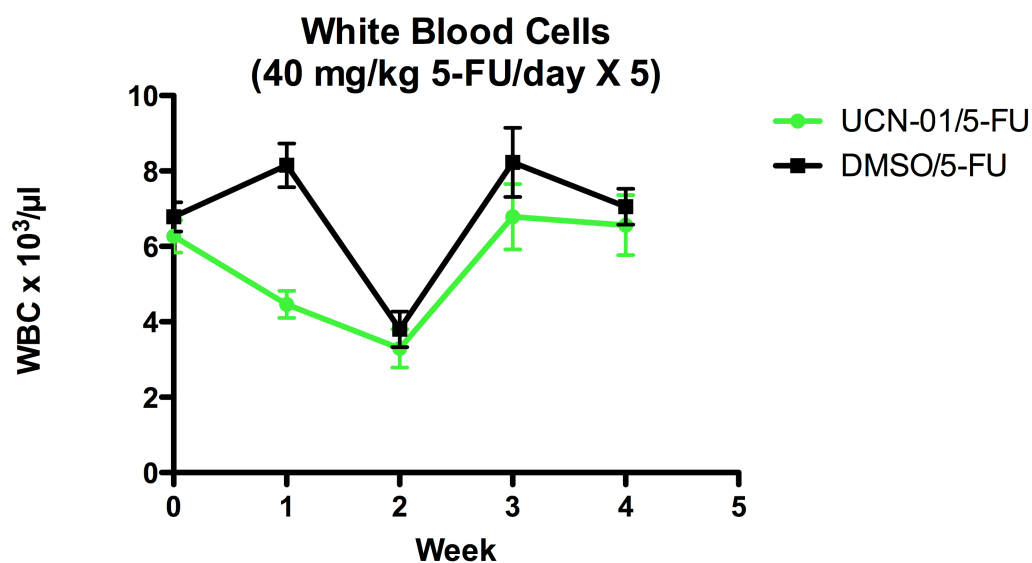


Figure 30c. Weekly white blood cell counts in mice treated with five daily doses of 40 mg/kg/day 5-FU beginning on day 3 post UCN-01 or DMSO (n=10 for each group). Counts were significantly lower in the UCN-01 pretreated group at week 1 (\*,  $p < 0.05$ ); however, when using the adjusted p-value for multiple comparisons ( $\alpha = 0.0125$ ) the difference is not significant.

the hematopoietic tissues of these mice (i.e. bone marrow) should have increased numbers of blood precursors compared to the control mice after 5-FU treatment.

**High dose bolus 5-FU administered on day 5-post UCN-01/DMSO (survival study):**

The ability of UCN-01 to improve the blood counts and weight status of mice exposed to 5-FU has been shown both in bolus (Figures 22, 23, and 27) and daily serial injections (Figures 16, 17, 29, and 30) of 5-FU. These studies clearly show that we can achieve the goal of protection of the normal proliferating cells of the mouse against high levels of 5-FU. The next study was designed to obtain robust numbers examining survival of mice given high dose 5-FU (Figure 31). Two treatment groups of twenty-two mice each were pretreated with either two doses of 5 mg/kg UCN-01 or volume equivalent DMSO (carrier control) separated by 12 hours. Five days after the second injection, mice were injected with 450 mg/kg 5-FU. Mice were monitored for survival and weighed daily. As in the last bolus 5-FU experiment, no blood was collected in order to prevent deaths due to exsanguination. Mice were also given moistened food in the bottom of cages if needed (upon signs of dehydration or the inability to feed from suspended pellets). As can be seen in Figure 32, the weight status of the UCN-01 pretreated mice was significantly improved from days eleven through twenty-one, with the exception of day fourteen. Also significantly improved was the survival of the UCN-01 pretreated group (Figure 33). Mice pretreated with UCN-01 had a survival rate of 91%, while the DMSO pretreated group had a survival rate of only 50%. This is similar to the rate seen in the 24 hour UCN-01 treatment experiment for “unprotected” mice (Figure 20). Sternums were also harvested from surviving mice at day 21 and paraffin embedded sections visualized via

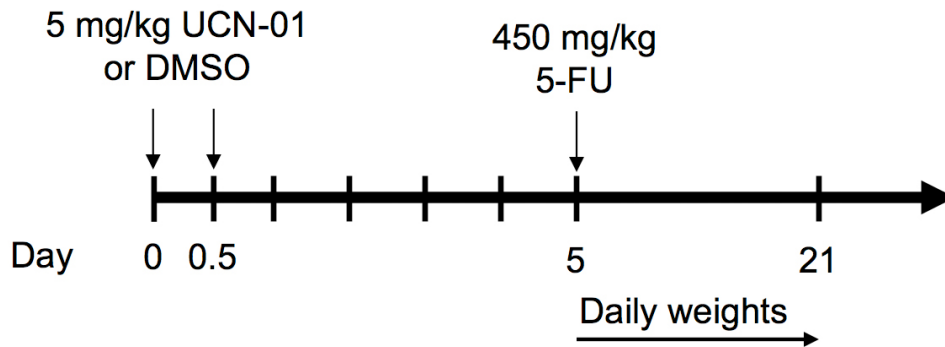


Figure 31. Treatment protocol for the seventh mouse experiment. Mice were treated with 5 mg/kg UCN-01 (n=22) or DMSO (n=22) on day 0 and then again 12 hours later. On day 5, all mice were injected with 450 mg/kg 5-FU. Weights were recorded daily, and all surviving mice were sacrificed on day 21.

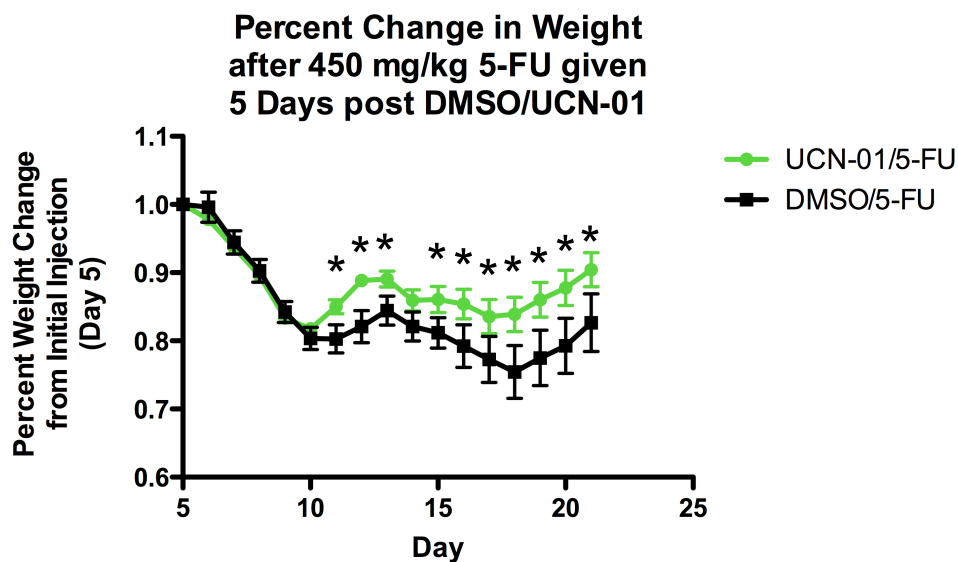


Figure 32. Percent change in weight after 450 mg/kg 5-FU, given 5 days after UCN-01 or DMSO (n=22 for each group). UCN-01 pretreated mice had significantly lower weight loss for days 11 through 21, with the exception of day fourteen (\*, p<0.05).

### Survival of Mice after 450 mg/kg 5-FU

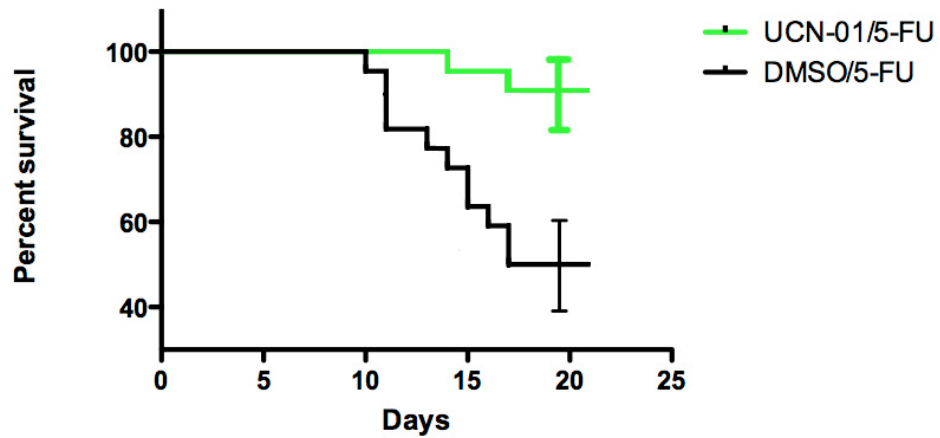
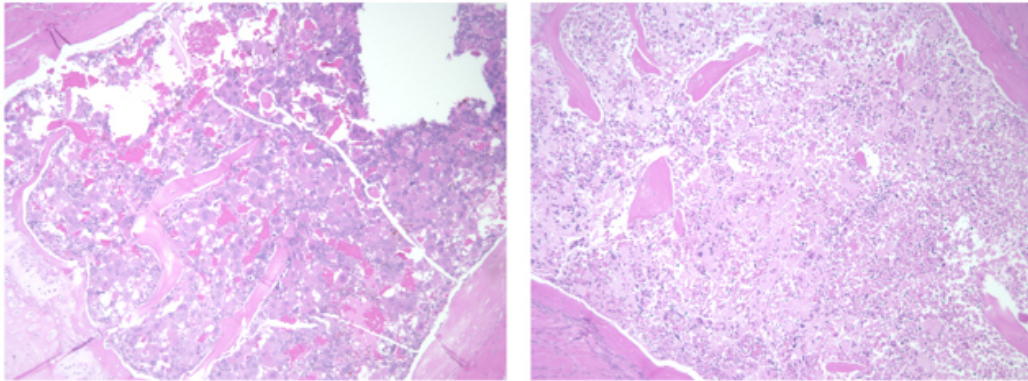


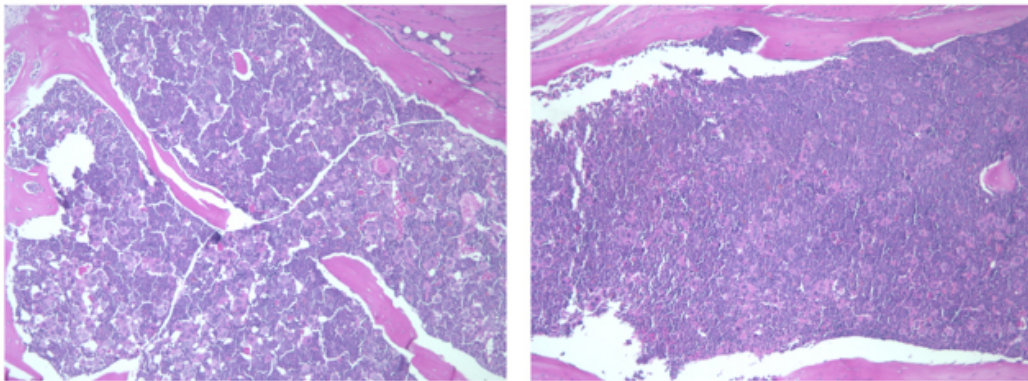
Figure 33. Kaplan-Meier survival analysis of mice treated with a bolus dose of 450 mg/kg 5-FU on day 5 following UCN-01 or DMSO pretreatment (n=22 for each group). Survival for the UCN-01 pretreated group was significantly higher ( $p=0.0025$ ). Error bars are 95% confidence intervals.

H&E staining. Shown in Figure 34, the blood precursors (small purple cells) in the UCN-01 pretreated mice are more abundant than in the DMSO pretreated mice. The area of blood precursors in the sections was quantified as a ratio of the total stained area, and the UCN-01 pretreated mice had significantly more blood precursors than the DMSO mice (Figure 35).

**Discussion:** The ability of UCN-01 to improve the tolerance of 5-FU in the mouse appears to depend critically on the dosing schedule of the two compounds. The arrest of the small bowel epithelium occurs within 24 hours of UCN-01 administration and this suppression is in effect for at least seven days (the peak is at 24 hours and decreases with time). In order for the normal proliferating tissues to take advantage of this arrest, 5-FU must be administered during this time period. However, as the major toxicity due to bolus 5-FU treatment is observed in the gut, and is also due in part to permanent suppression of cell cycling via p53 and p21 (Pritchard 1998), it is likely that 5-FU given *too early* is even more toxic than 5-FU alone. The cells arrested by UCN-01 will take better than seven days to recover, and the cells which evade UCN-01 arrest continue to cycle are then susceptible to 5-FU toxicity. As seen in the experiment dosing UCN-01 and 5-FU separated by 24 hours (Figure 18), this combination *increases* mortality; the gut cannot replenish the required enterocytes (and presumably the bone marrow cannot form sufficient blood cells) while still under arrest; unarrested cells can be killed by 5-FU, and the mouse succumbs to this combined pressure. However, when 5-FU is given closer to the time of recovery (3-5 days post-UCN-01, Figures 22, 26, 28 and 31), the mouse can evade the damage to the temporarily arrested cells, and those cells can begin cycling



DMSO



UCN-01

Figure 34. Sternum H&E samples of mice given 450 mg/kg 5-FU on day five post DMSO (top row) or UCN-01 (bottom row). Mice were sacrificed on day 21. The UCN-01 mice appear to have more abundant levels of blood precursors compared to the DMSO mice. This is quantified in figure 35.



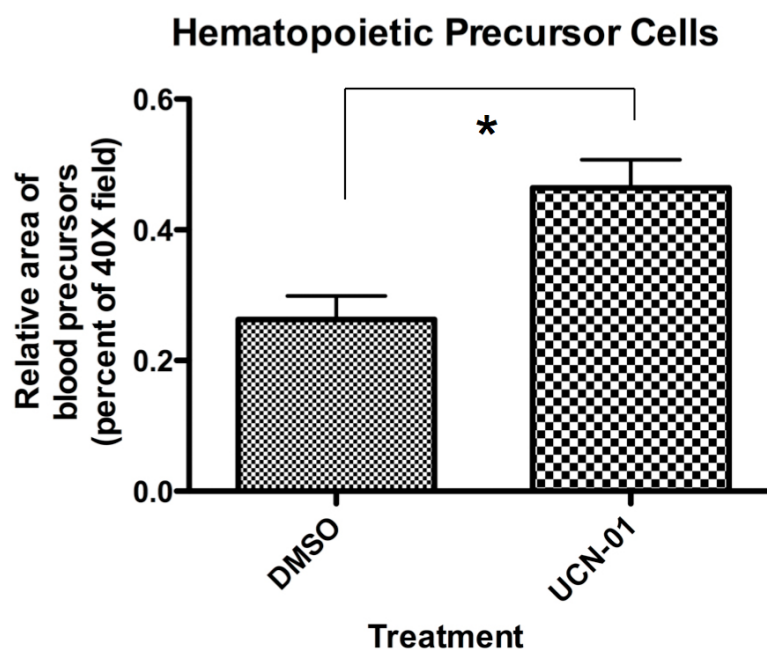


Figure 35. Quantification of blood precursors cell in mouse sternums after treatment with 450 mg/kg 5-FU. The area of blood precursor cells was normalized to the total stained area of a 40X section. Five fields were quantified per mouse, and five mice for each group were evaluated. The UCN-01 pretreated mice have significantly greater levels of blood precursors than the DMSO pretreated mice (\*,  $p < 0.05$ ).

anew within 2-3 days after 5-FU treatment ceases. This likely explains the improved tolerance and survival seen in the final two experimental protocols. Given the sum of the results of all seven mouse studies, it appears that the optimal time for protection from the toxicity of a bolus dose of 5-FU is five days post-UCN-01. For a series of 5 daily injections, beginning 5-FU administration on day 3 post-UCN-01 appears to be the optimal schedule. This treatment protocol allows the last dose to be given while some of the arresting effect of UCN-01 still persists, but also very close to the time of recovery from arrest. Based on the results of all the mouse studies, the best chance for protection against toxicity during treatment to kill tumors is the scheme shown in Figure 31.

### III. Mechanism of UCN-01 Cell Cycle Arrest in Mouse Small Bowel

**Introduction:** The analysis of BrdU incorporation into the cells in the jejunum of mice treated with UCN-01 demonstrates a slowdown in the proliferation of gut epithelium as early as 24 hours following treatment; this arrest persists through day seven post-UCN-01, and is eliminated by two weeks (Figures 5 and 7). While UCN-01 has many targets, both direct and indirect (see Introduction), the exact mechanism by which it arrests the crypt cells of the small bowel is unknown. It is the aim of this portion of the project to determine what changes in proteins governing the cell cycle are affected by UCN-01 and can contribute to the arrest seen. Previous work in our laboratory has indicated that the UCN-01 analog staurosporine causes a G1 arrest in cultured epithelial cells by downregulating the kinase cdk4 and causing subsequent hypophosphorylation of Rb (McGahren-Murray *et al.*, 2006). The hypothesis for this section of the project is: **UCN-01 causes a decrease in cdk4 levels in the jejunum of the mouse, leading to the cell cycle arrest demonstrated in chapter 1.** Our analysis of mouse small bowel epithelium treated with UCN-01 revealed modulation of some key cell cycle proteins, including cdk4 and p27. However, unlike the *in vitro* studies, we have shown that level of cdk4 are increased following UCN-01 administration. In addition, the inhibitor p27 was increased by UCN-01. No changes in the activities of G1 phase cyclin dependent kinases (cdk2 and cdk4) were observed, and the levels of cdk2, cyclin E and active cdk2 were unaltered as well. UCN-01 had no effect on the levels of Rb or p53. Interestingly, the levels of phospho-Rb were increased in the UCN-01 treated mice. However, analysis of BrdU incorporation demonstrates that the UCN-01 treated mice have reduced cellular

proliferation, so the increase in phospho-Rb is unexpected. It is thought that UCN-01 is preventing the arrested cells from traversing the restriction point, but may not be inhibiting the early G1 phase phosphorylation of Rb by cdk4.

**Materials and Methods:** Mice: Nude mice (see Chapter 1) were injected with 5 mg/ml UCN-01 in the right hindlimb muscle. 24 hours later, the mice were sacrificed by cervical dislocation. For studies using whole epithelial tissue, the jejunum was dissected from the abdomen and flushed with 10 ml of ice-cold PBS. A small section (~1 cm) was removed and fixed in 10% formalin for histology. The tissue was then opened longitudinally and placed on a glass microscope slide. A second glass slide was dragged across the surface of the tissue to dislodge the epithelium. The cells were suspended in ice-cold PBS and spun down at 1100RPM for 5 minutes at 4°C. The cells were then resuspended in a minimum (40-50 µl) of protease/phosphatase inhibition (PPI) buffer: 25µg/ml leupeptin, 25µg/ml aprotinin, 10µg/ml pepstatin, 1 mM benzamidine, 10µg/ml soybean trypsin inhibitor, 0.5mM PMSF (Phenyl methyl sulfonyl fluoride), 50mM sodium fluoride, 0.5 mM sodium orthovanadate. Cells are lysed by 2 rounds of sonication (one round = 3 minutes sonication, 1 minute rest, 3 minutes sonication) and are vortexed between rounds. Sonication is performed in a ice/water bath by a Sonicator XL (Misonix, Inc., Farmingdale, NY). The protein suspension is then separated by centrifugation at 125000 x g for 45 minutes at 4°. The protein suspension is stored at -80°C. In order to minimize the background of nondividing villus cells, serial fractionation to enrich for crypt cells was performed. For the serial fractionation of the gut epithelium, the jejunum is dissected out of the abdomen and flushed with 10 ml ice-

cold PBS, followed by 10 ml ice-cold PBS plus 1 mM dithiothreitol (DTT). The tissue is then tied closed on one end with 3-0 silk suture (Ethicon/Johnson & Johnson, Warsaw IN) and then everted. The everted tissue is filled with ice-cold PBS to distension and then tied closed. The tissue is incubated in a citrate buffer (96 mM NaCl, 1.5 mM KCl, 27 mM Na citrate, 8 mM KH<sub>2</sub>PO<sub>4</sub>, and 5.6 mM Na<sub>2</sub>HPO<sub>4</sub>, pH 7.3) for 15 minutes at 37°C. The tissue was then placed in a 50 ml glass flask in 15 ml of a PBS buffer with 1.5 mM EDTA, 0.5 mM DTT and 1 mg/ml bovine serum albumin (BSA). The flask is placed in a 37°C water bath shaking at 90Hz for 25 minutes. The buffer with dislodged cells is collected and spun down at 1100 RPM for 5 minutes at 4°C; the cell pellet is washed with 10 ml ice-cold PBS, spun down again, and resuspended in PPI and processed as above. This is designated as fraction 1. The tissue is placed in a new flask and shaken at 37°C for an additional 35 minutes; the cells are processed as before and comprise fraction 2. A third incubation for 60 minutes is collected and processed as fraction 3. All fractions are processed using the sonication/centrifugation procedure shown above.

Western analysis: Samples are separated on either a 10% or 7% (for Rb blots) SDS-PAGE vertical denaturing gel. Concentration matched extracts are boiled in denaturing sample buffer: 1.4M β-mercaptoethanol (Samples are run at 150 volts for 90-120 minutes, depending on the location of the proteins of interest. After running, the gels are transferred to polyvinylidene fluoride (PVDF) membranes (Immobilon-P, Millipore, Billerica, MA) using a BioRad (Hercules, CA) transfer cell. Transfer buffer is: 57.6g glycine, 12g Tris base, 800ml methanol; bring up to 4l with H<sub>2</sub>O. Transfer in overnight

at 35 volts or for 90 minutes at 85 volts (quick transfer requires ice block in the transfer cell). Following transfer, membranes are blocked at 4° overnight in TBS/Tween Blotto: 20mM Tris base, 500mM sodium chloride, 0.05% Tween 20 with 5% nonfat dry milk. Blots are incubated in primary antibody for one hour, are washed for 6 x 10 minutes in TBS/Tween, and are placed in secondary antibody (Immunopure HRP, diluted 1:25,000 in Blotto) for one hour. Membranes are again washed 6 x 10 minutes in TBS/Tween. Membranes are developed with “Western Lightning” chemiluminescence reagent (PerkinElmer, Wellesley, MA) and exposed on Blue x-ray film (Phenix, Hayward, CA). The primary antibodies used in this aim are: anti-cyclin E (0.3 µg/ml), anti-CDK2 (1.0 µg/ml) – both from SantaCruz. Anti-p21 is 1.0 µg/ml from Calbiochem. Anti-p27 (1.0 µg/ml) is from BD TransLab. Anti-Rb is from Millipore.

Immunoprecipitation assays: Protein samples are collected as above. For immunoprecipitation, protein g sepharose beads (GE HealthCare, ? ) are washed in a lysis/protease/phosphatase buffer (0.5M tris, pH 7.5, 2.5M sodium chloride, 1% NP-40 (Igepal), 25µg/ml leupeptin, 25µg/ml aprotinin, 10µg/ml pepstatin, 1 mM benzamidine, 10µg/ml soybean trypsin inhibitor, 0.5mM PMSF (Phenyl methyl sulfonyl fluoride), 50mM sodium fluoride, 0.5 mM sodium orthovanadate. The buffer is added to the beads at a 2:1 ratio, mixed, and then centrifuged at 4° for 5 minutes at 1000 x g. This wash is carried out 3 times. After the wash buffer is removed, the beads (30 µl/sample) are added to a 10mM DTT/lysis buffer (36 µl/sample). Anti-FLAG antibody (1 µl/sample) is added to the mixture, and the beads plus antibody are left to rotate slowly at 4° overnight. The following day, 150 µg of protein sample is added to each mixture, and allowed to mix at

4° for one hour. The beads are then washed in 250 µl of the lysis/protease/phosphatase buffer 4 times. For a Western analysis of the immunoprecipitated samples, 3 further washes are carried out, and then the beads are centrifuged for 5 minutes at 1200 x g.

Kinase assays: Immunoprecipitation for kinase assays was carried out as above.

Following the final wash, four additional washes in H1 buffer (10mM MgCl<sub>2</sub>, 1mM DTT, 0.1 mg/ml BSA, 25mM Tris HCL pH 7.5, 125mM NaCl) are done. Following the washes, the wash solution is removed as for the IP Western. Beads are then resuspended in the kinase reaction buffer: 10mM magnesium chloride, 1mM dithiothreitol, 0.1 mg/ml bovine serum album, 25mM Tris hydrochloride pH 7.5, 125mM sodium chloride, along with 60mM ATP, 5µCi of  $\gamma$ -<sup>32</sup>P ATP and 5µg of histone H1 substrate (for cdk2 kinase assay, Roche Diagnostics) or GST-Rb substrate (for cyclin D kinase assay, Santa Cruz Biotechnology). The reaction proceeds for 30 minutes at 37°C, and is then inactivated by addition of 15µl of sample buffer. The samples are separated on a 13% SDS-PAGE gel. The gel is stained in Brilliant Blue (Sigma, St. Louis, MO) overnight. The following day, the gel is destained and dried onto Whatman filter paper. The dried gel is exposed to a phosphorimager screen for one hour and analyzed for quantitation by a Typhoon scanner (Molecular Dynamics).

Immunohistochemistry: Sections of jejunum were embedded in paraffin, sectioned onto slides and processed for immunohistochemical analysis. Deparaffination was done with three washes in HistoClear for five minutes each. Samples were rehydrated by washing in 100%, 90% and 70% ethanol for five minutes each, and then washed in PBS for five

minutes. Antigen retrieval was performed in antigen unmasking solution (Vector Labs) heated in a steam chamber for 20 minutes. Slides were allowed to cool for 20 minutes in the unmasking buffer, and were washed twice in distilled water and twice with PBS for three minutes each. Endogenous peroxidase was blocked by incubation in 90 % ethanol/3% hydrogen peroxide for ten minutes. After three washes in PBS for five minutes each, excess buffer was removed around the samples and 50-100 µl of blocking buffer (5% BSA/0.5% Tween-20 in PBS) was applied to the tissue sections. Blocking was accomplished by overnight incubation in a humidified chamber at room temperature for one hour. Blocking solution was drained from the slides, and 50-100 µl of primary antibody (diluted blocking buffer) was applied to the sections. Primary antibody was incubated overnight in a humidified chamber at 4°C. After incubation, slides were washed three times for ten minutes each in PBS. Secondary antibody (diluted in blocking buffer) was applied to the sections and incubated for one hour in a humidified chamber at room temperature. Slides were washed in PBS (three times for ten minutes) and then dried to remove excess solution around samples. Avidin-biotin complex (ABC, Vector Labs) was applied to the sections and incubated for 30 minutes at room temperature. Slides were washed in PBS for five minutes. Staining with daiminobenzidine (DAB peroxidase substrate kit, Vector Labs) was performed for two to ten seconds under a microscope; slides were washed in water once desired levels of staining were attained. Counterstaining in hematoxylin (DAKO) for 10 seconds was followed by two washes in tap water for 5 minutes. Slides were dehydrated in 70, 90 and 100% ethanol for five minutes each. Slides were washed with Histoclear twice for five minutes, and then mounted behind a glass coverslip using Permout. Primary antibodies used for IHC:



anti-phospho T160 cdk2, Cell Signaling, used at 1:100. Anti-phospho S807/811 Rb, from Cell Signaling, was used at 1:500. Both of these rabbit primary antibodies were used with the secondary anti-rabbit ABC elite kit from Vector for development. For the BrdU staining, the primary antibody (rat anti-BrdU) from GeneTex was used at a 1:500 dilution, and the secondary anti-rat biotin antibody (Vector) was used at a 1:200 dilution. For quantification of IHC results, ten crypts of complete integrity (both sides of the crypt visibly transitioning to villi) were counted for both positive cells and total crypt cells; results were reported as a percentage of positive crypt cells.

Densitometry: Films produced in the western analyses above were scanned using a Microtek 9800TM scanner and saved in the TIFF format. Signals were quantified using IP Lab Gel H software (Signal Analytics, Vienna, VA).

Statistics: Pairwise comparison of means was performed using Student's t-test; a confidence level of 95% was considered to be statistically significant in these studies. All calculations were performed using the Prism software package (GraphPad Software, Inc.).

### ***Results:***

This chapter focuses on identifying the molecular changes which accompany the UCN-01-mediated arrest in the dividing small bowel epithelial cells. One complication in this endeavor is the makeup of the crypt/villus architecture in the gut. The area of interest is the small proliferating region of the crypt, approximately cell positions 4-8 upward from

the crypt base. However, the majority of the epithelial cells in the small bowel are differentiated enterocytes, which exist in a quiescent state. This is a very large background of nondividing cells, against which changes in the small region of proliferation will likely be dwarfed. To help alleviate this problem, we have adapted a method of isolating cells along the crypt-villus axis in fractions. This method, detailed in the Material and Methods above, was first described by Weiser (Weiser, 1973) for use in rats, and was further refined for use in the mouse small bowel (Ferraris *et al.*, 1992). This method uses heat and shaking of everted intestinal sections to detach “fractions” of gut epithelial cells into a buffered PBS solution over a 2-hour period. The early fractions contain cells near the villus tip, while the late fractions are enriched for cells from the crypt region. This separation method has been validated by immunohistochemistry and gene array analysis (Mariadason *et al.*, 2005; Smartt *et al.*, 2007). Protein isolated using the fractionation method was first evaluated for efficacy of this process. 10 mice were injected with either 5 mg/kg UCN-01 or DMSO. 24 hours later, the mice were sacrificed and the jejunum harvested and serially digested. The fractions from the villus to the crypt (1 -> 3) were analyzed for PCNA via Western blotting. As seen in Figure 36, the levels of PCNA were lowest in the outermost villus tip fraction (#1), and highest in the proliferating crypt (fraction 3). Analysis by densitometry indicates a 2-fold increase in PCNA levels from fraction 1 to fraction 2, and a 2.5 fold increase to fraction 3. In addition, H&E sections taken after each incubation are shown in Figure 37, demonstrating visually the digestive process in the tissue from the villus tip inward. As proliferation in the jejunum occurs exclusively in the crypt region, all subsequent analysis will focus on fraction 3 of the mouse gut samples.

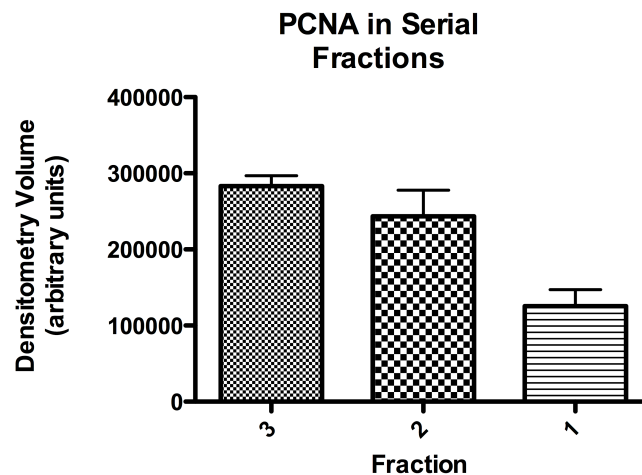
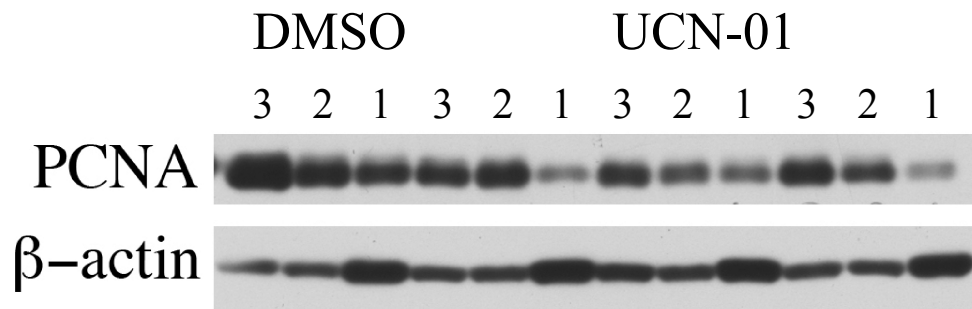


Figure 36. Serial fractions of jejunum epithelium separated using the Weiser method (see Material and Methods). The image represents protein from four mice, each divided into three fractions. The three mice on the right side were treated with UCN-01; the mouse on the left side is a DMSO control. The first fraction, taken after 24 minutes of incubation, is low in PCNA (a proliferative marker) and high in the structural  $\beta$ -actin. The second fraction (taken after an additional 36 minute incubation) has increased levels of PCNA, and the third fraction (final 60 minute incubation) contains the highest levels of PCNA, indicative of the proliferating cells found in the crypt. The control DMSO mouse, which should have a greater level of proliferation than the UCN-01 mice, has a greater amount of PCNA at all three fractions; this indicates that the UCN-01 treatment was effective in causing a cell cycle arrest. Densitometry of UCN-01 fractions indicates increased levels of PCNA in the crypt fraction (3).

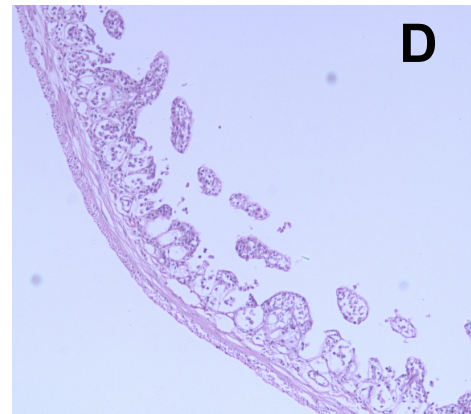
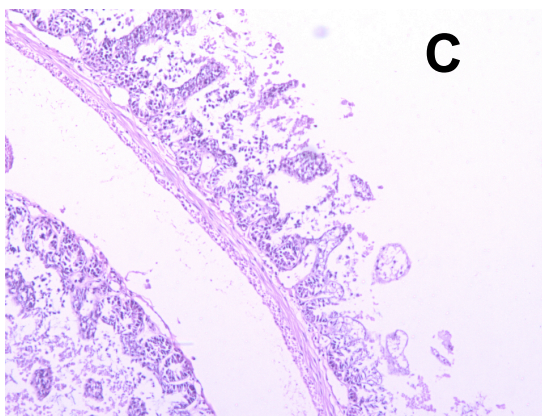
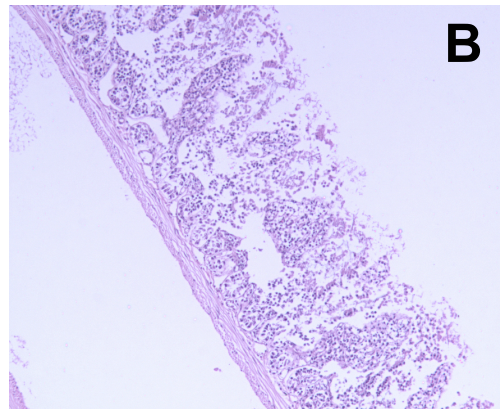
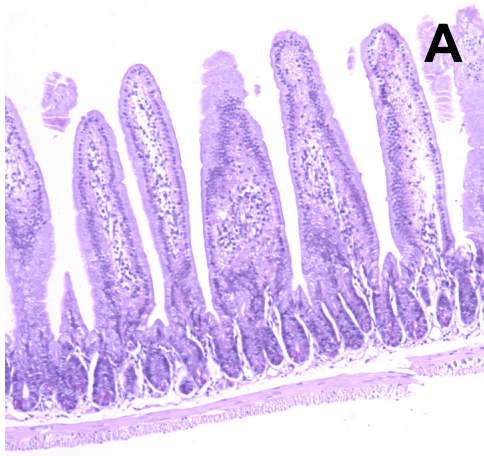


Figure 37. H&E stained sections of everted small bowel at the 4 stages of the serial fractionation procedure. Samples were processed to display the tissue at time zero (A), and after incubation times of 24 minutes (fraction 1 cells removed), (B) 60 minutes (fraction 2 cells removed) and (C) 120 minutes (fraction 3 cells removed). The images demonstrate the continual digestion of the epithelial cells from the villus tip downwards into the crypt.

### **Examination of early G1 cell cycle proteins:**

The work with cultured cells arrested by the UCN-01 analog staurosporine (McGahren-Murray *et al.*, 2006) demonstrated that cell cycle arrest was dependent on wild-type Rb and that staurosporine treatment caused a decrease in cdk4 levels and its kinase activity. To determine if UCN-01 will have a similar effect on proliferation *in vivo*, fraction 3 samples from UCN-01 treated mice and DMSO controls were analyzed by western blotting for cdk4 expression. For each biochemical analysis performed (western blot, immunoprecipitation, and kinase assays), we used the fraction 3 material from five different mice per treatment group, loaded into five different lanes. Densitometry was performed on each lane, and values for each treatment group averaged. This method was chosen to reduce the variability naturally seen among mice. As shown in Figure 38a, the levels of cdk4 in the UCN-01 treated mice are *higher* than the levels in the DMSO mice. Densitometric analysis (Figure 38b) confirms that the levels of cdk4 are significantly higher in the UCN-01 treated mice compared to the DMSO control mice.

As UCN-01 treatment causes an increase in the levels of cdk4, the mechanism of UCN-01-induced arrest likely differs from that of staurosporine. This led us to examine the other proteins controlling the early events of the G1 phase. The first candidate was the cyclin binding partner for cdk4, cyclin D. In Figure 39a, the western analysis for cyclin D shows a higher level in the UCN-01 treated mice compared to DMSO control, although the difference is not statistically significant when the results of all five mice are averaged (densitometry in Figure 39b). Also analyzed were the levels of the cyclin dependent

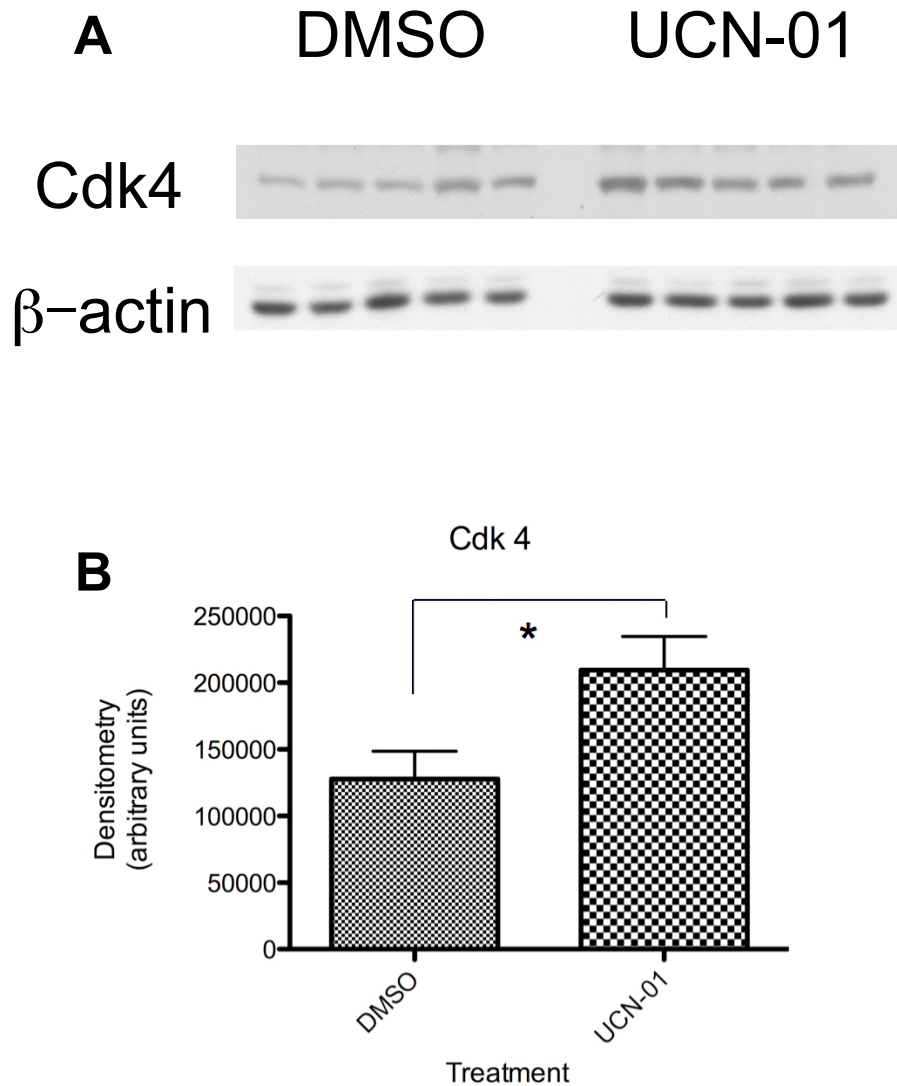


Figure 38. (A) Western analysis of mouse jejunum crypt fractions for levels of cdk4.  $\beta$ -actin is used as a loading control. (B) Densitometry of western shown in (A). Levels of cdk4 are significantly elevated in the UCN-01 treated mice in comparison to DMSO controls (\*,  $p < 0.05$ ).

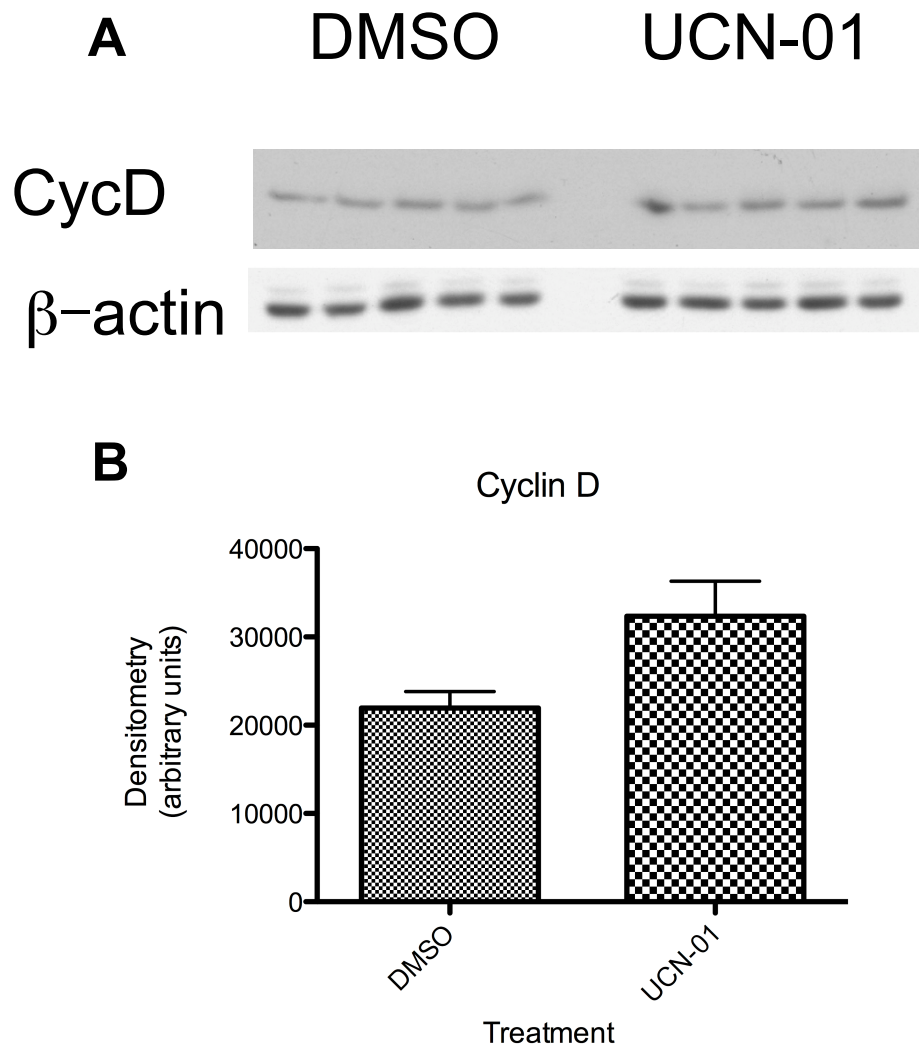


Figure 39. (A) Western analysis of mouse jejunum crypt fractions for levels of cyclin D.  $\beta$ -actin is used as a loading control. (B) Densitometry of western shown in (A). Levels of cyclin D are not significantly altered in the UCN-01 treated mice compared to DMSO control mice.

kinase inhibitors p21 and p27. The levels of p21, shown in Figure 40, did not differ between the mice treated with UCN-01 and the DMSO control mice. Levels of p27, however, were altered by UCN-01 treatment. Shown in Figure 41, p27 was significantly higher in the UCN-01 treated mice compared to the DMSO control mice. These results both agree and conflict with the data from A549 cells (which were analyzed *ini vitro*), in which UCN-01 treatment significantly increased both p21 and p27 levels (Akiyama *et al.*, 1999).

To assess any change in the kinase activity due to UCN-01 treatment, cyclin D was immunoprecipitated from both sets of lysates (from UCN-01 and DMSO treated mice). The immunoprecipitated complexes were incubated with  $^{32}\text{P}$  (gamma) and the substrate GST-Rb to determine the cyclin D associated kinase activity of both groups of samples. Figure 42a is the phosphor screen image of the kinase reactions. Lysate incubated with beads only (no cyclin D antibody) was used as a negative control, and MCF-7 cell lysate was the positive control. The cyclin D associated kinase activity of the UCN-01 treated group samples appears to be slightly higher than the activity of samples from the DMSO control mice; however, the difference is not significant (densitometry in Figure 42b). The results of this experiment can be reconciled with the previous data demonstrating the altered levels of cyclin D and p27 in the UCN-01 treated group. It is possible that any increase in cdk4 activity that could result from an abundance of cyclin D is being blunted by the increased levels of the kinase inhibitor p27.

#### **Examination of late G1 cell cycle proteins:**



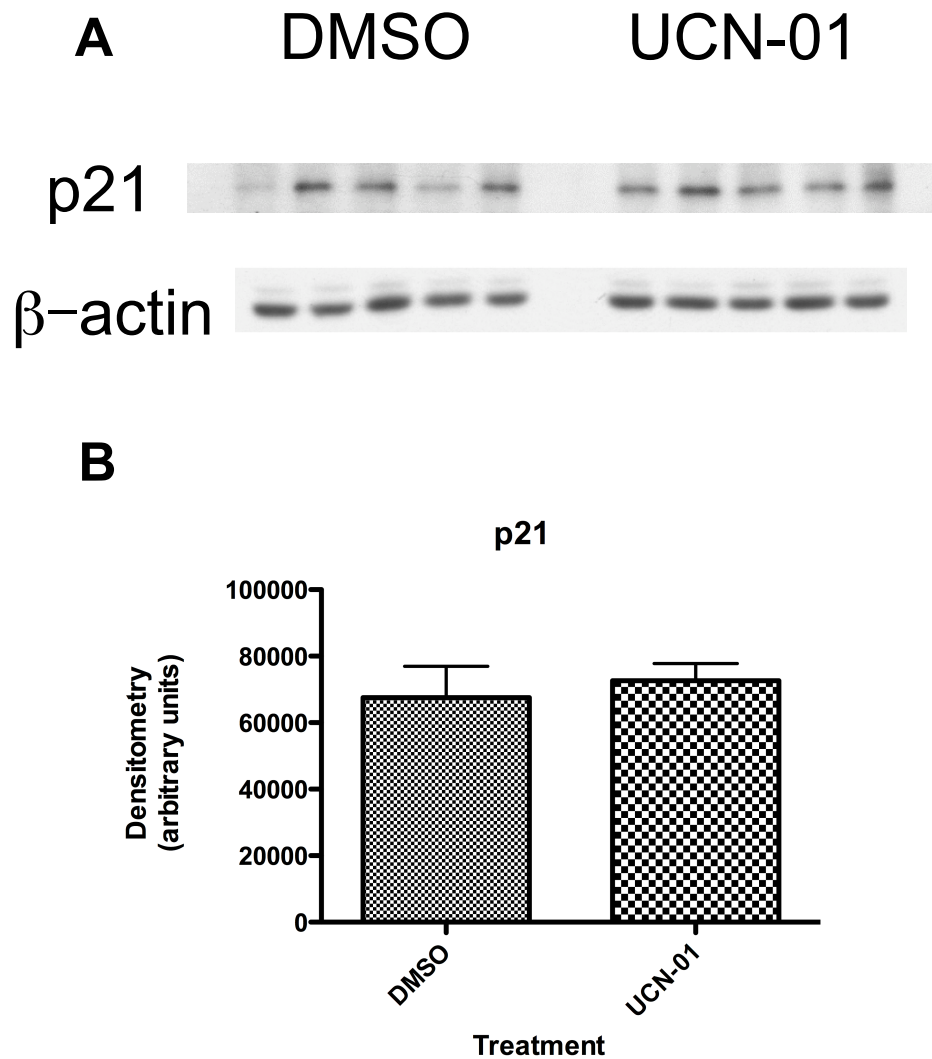


Figure 40. (A) Western analysis of mouse jejenum crypt fractions for levels of p21.  $\beta$ -actin is used as a loading control. (B) Densitometry of western shown in (A). Levels of p21 are not significantly altered in the UCN-01 treated mice compared to DMSO control mice.

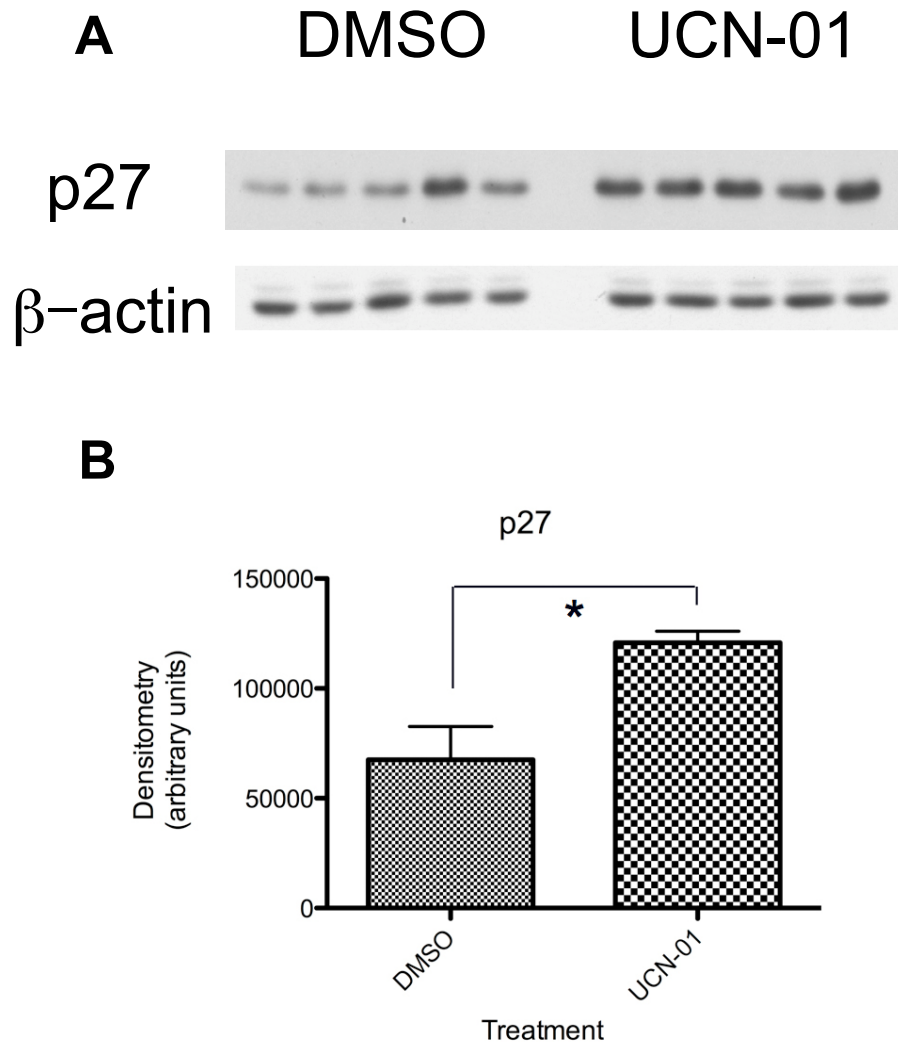


Figure 41. (A) Western analysis of mouse jejunum crypt fractions for levels of p27.  $\beta$ -actin is used as a loading control. (B) Densitometry of western shown in (A). Levels of p27 are significantly higher in the UCN-01 treated mice compared to DMSO control mice (\*,  $p < 0.05$ ).

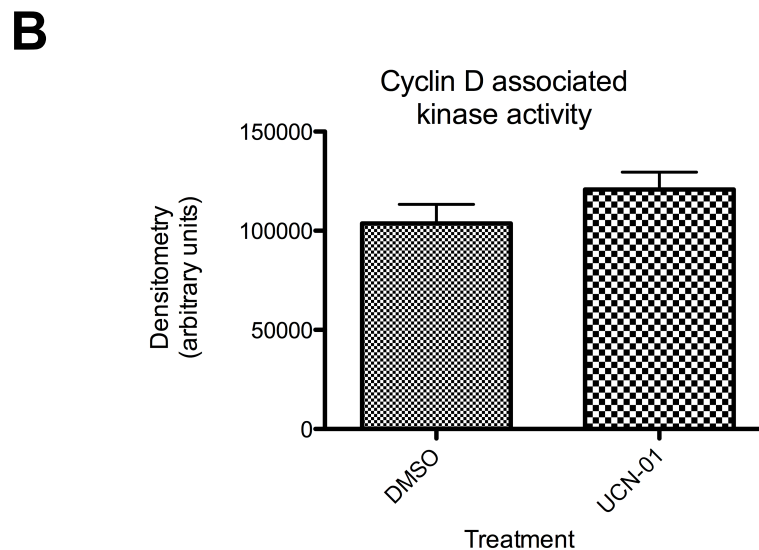
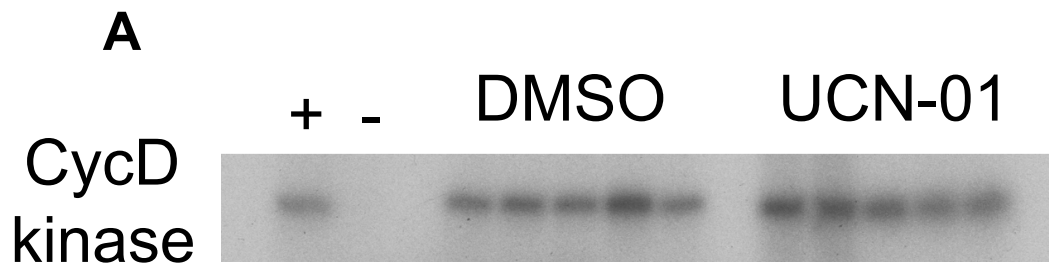


Figure 42. (A) Kinase assay of cyclin D immunoprecipitated complexes from the jejunums of mice treated with 5 mg/kg UCN-01 or DMSO control. GST-Rb peptide is used as the substrate. Positive control is lysate from MCF-7 cells. (B) Densitometry of the results shown in (A). The cyclin D associated kinase activity does not differ significantly between the UCN-01 treated mice and the DMSO control mice.

The results of the analysis of early G1 cell cycle proteins are both in agreement and in conflict with previous reports; the increased level of p27 after UCN-01 treatment had been demonstrated by Akiyama et al, but the same report showed a decrease in cdk4 levels and kinase activity, which is differs from our results here (Akiyama *et al.*, 1997). This unique response to UCN-01 in the mouse gut epithelial cells persuaded us to look elsewhere for other possible molecular changes, since it is likely that proliferating tumor cells in culture respond differently to UCN-01 than normal proliferative mouse epithelium. The next logical step was to examine the late G1 cell cycle protein cyclin E and its kinase binding partner cdk2. Western analysis for both proteins is shown in Figure 43; UCN-01 did not alter the levels of either protein. Although the levels of both cdk2 and cyclin E were unaffected by UCN-01, it is possible that the increased levels of the inhibitor p27 (Figure 41) have an effect on the kinase activity of cdk2. To examine this possibility, cdk2 was immunoprecipitated from jejunum lysates from both UCN-01 treated mice and DMSO treated controls and incubated with <sup>32</sup>P (gamma) and the substrate histone H1. Jejunum lysate incubated with naked beads (no antibody) was used as a negative control, and MCF-7 cell lysate was used as a positive control. The phosphor screen image of the kinase assay is shown in Figure 44a. Similar to the results of the cyclin D associated kinase assay (Figure 42a), treatment with UCN-01 did not significantly alter the kinase activity of cdk2 in comparison to DMSO control treatment (densitometry in Figure 44b). This lack of change in cdk2 kinase activity following UCN-01 differs from other reports in which UCN-01-mediated cell cycle arrest is accompanied by a decrease in cdk2 activity and subsequent lack of Rb phosphorylation,

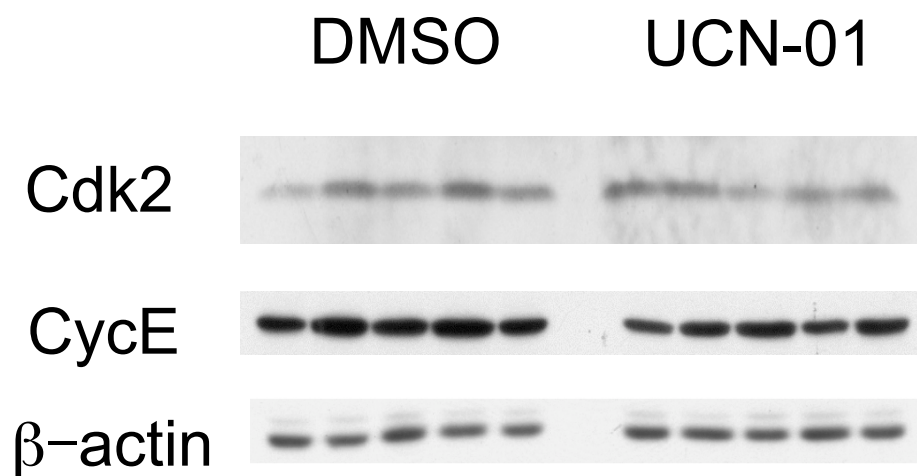


Figure 43. Western analysis of mouse jejunum crypt fractions for levels of cdk2 and cyclin E.  $\beta$ -actin is used as a loading control. Levels of each protein were not significantly different in the UCN-01 samples compared to the DMSO samples.



**B**

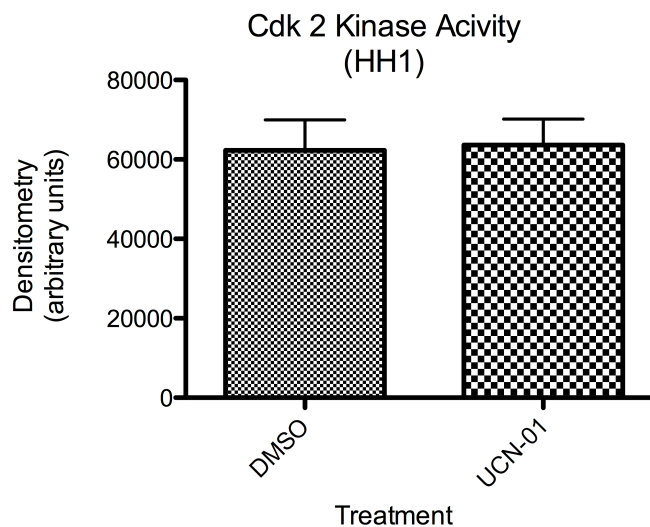


Figure 44. (A) Kinase assay of cdk2 immunoprecipitated complexes from the jejunums of mice treated with 5 mg/kg UCN-01 or DMSO control. Histone H1 used as the substrate. Positive control is lysate from MCF-7 cells. (B) Densitometry of the results shown in (A). The cdk2 kinase activity does not differ significantly between the UCN-01 treated mice and the DMSO control mice.

although these studies were all done on cells in culture rather than in an animal model system (Akiyama *et al.*, 1999b; Chen *et al.*, 1999; Facchinetti *et al.*, 2004).

### **UCN-01 and the phosphoproteins p53 and pRb:**

The reported data on the necessity vs. dispensability of p53 for cellular response to UCN-01 was a feature of many UCN-01 studies presented in the Introduction. Some studies indicated that active, wild-type p53 was required for UCN-01-mediated cell cycle arrest (Byrd *et al.*, 2001; Facchinetti *et al.*, 2004; Husain *et al.*, 1997), while others demonstrated that the absence or presence of p53 did not modulate the cellular response to UCN-01 (Chen *et al.*, 1999; Shao *et al.*, 1997c; Wang *et al.*, 1996). The hypophosphorylation of Rb accompanying UCN-01-mediated cell cycle arrest was also shown in previous work (Chen *et al.*, 1999; Courage *et al.*, 1996; Kawakami *et al.*, 1996). Even though the kinase assays for this study did not demonstrate any change in cdk2 (Figure 44) or cyclin D-associated (Figure 42) kinase activities following UCN-01 treatment in the mice, it was possible that modulation of either p53 or Rb was occurring in the mouse gut epithelium. Western analysis of the crypt fractions (Figure 45), however, showed no significant alterations in the levels of Rb or p53 in the mice treated with UCN-01 compared to the DMSO controls. While total Rb levels did vary somewhat within each treatment group, no consistent pattern of change is present when the results of five mice were averaged. Also of note is the fact that no shift due to phosphorylation is present in the Rb western analysis. As hypophosphorylation has been shown in some studies to accompany UCN-01-mediated arrest, this result provided little insight into this mechanism. The samples were also probed with anti-phospho Rb antibodies (S780,

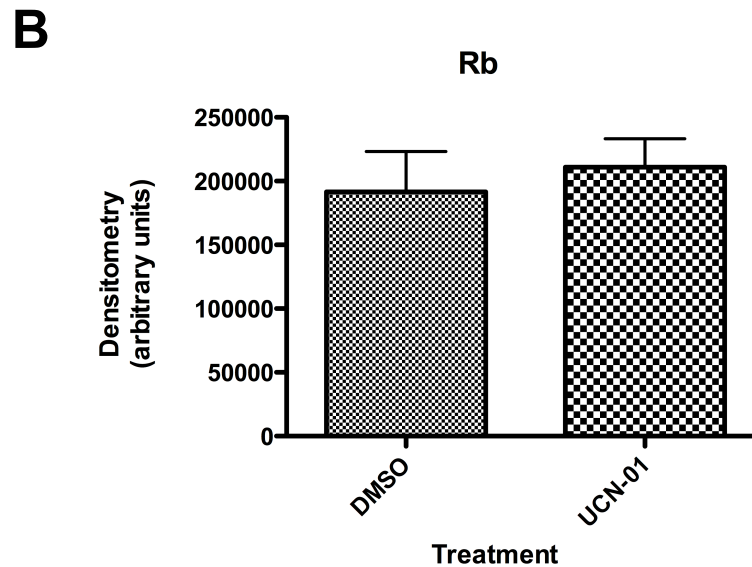
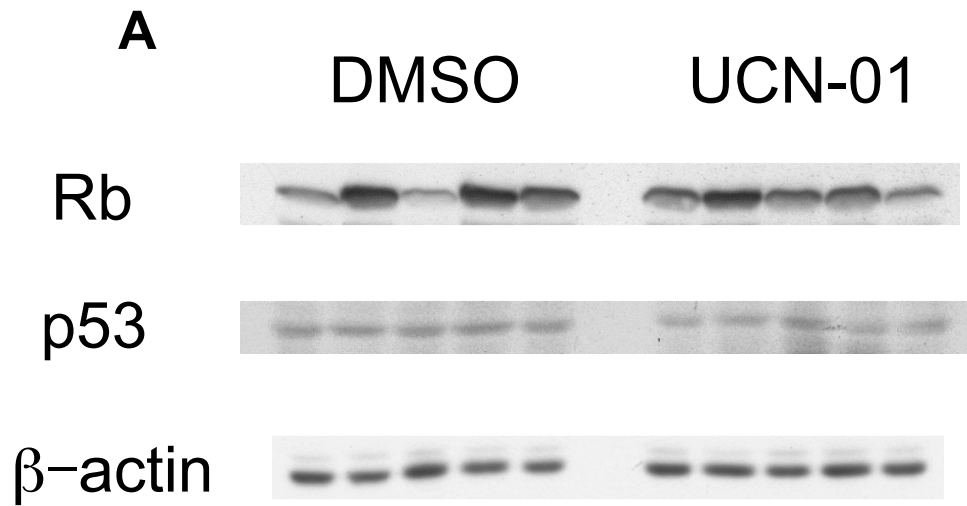


Figure 45. (A) Western analysis of mouse jejunum crypt fractions for levels of Rb and p53.  $\beta$ -actin is used as a loading control. No shifts in Rb migration due to phosphorylation are evident. (B) Densitometry of Rb levels shown in (A). Levels of Rb do not differ significantly between UCN-01 treated mice and DMSO control mice.



S795, and S807/811) but unfortunately no signal was observed in these analyses (data not shown).

The data collected to this point do not give a clear indication of how UCN-01 is able to arrest the proliferating cells in the mouse small bowel. One concern with the serial fractionation method is that the long incubation (up to 2 hours) in heated (37°C) buffer may negatively affect the proteins harvested. While no sample degradation was observed in the western analyses shown in this study, it may be possible that the activities of certain proteins are affected by the separation process. To address this concern, we decided to directly assess kinase activity via immunohistochemistry. For these analyses, the jejunum samples taken for IHC are harvested immediately after sacrifice, flushed and placed into formalin. The remainder of the tissue is then processed for serial fractions. As such, the proteins in the fixed tissue should be unaltered. We decided to assess the levels of active cdk2 in the crypts of the mice by IHC. The levels of cdk2 kinase activity measured in the UCN-01 treated mice were similar to the levels seen in the DMSO control mice. If the process of fractionation does not affect the integrity of cdk2 activity, it should then be true that levels of active (phospho Thr 160) cdk2 are similar in the two groups when the tissue sections (which do not undergo fractionation) are analyzed. IHC using anti-phospho-Thr 160 cdk2 is shown in Figure 46a (UCN-01) and 46b (DMSO). Positive cells were specific to the crypt region, and no difference was observed in the levels of active cdk2 in the UCN-01 mice versus the DMSO control mice. This result is in agreement with the cdk2 kinase activity levels shown in Figure 44, and indicates that cdk2 has not been altered by the serial fractionation process. It should also be noted that

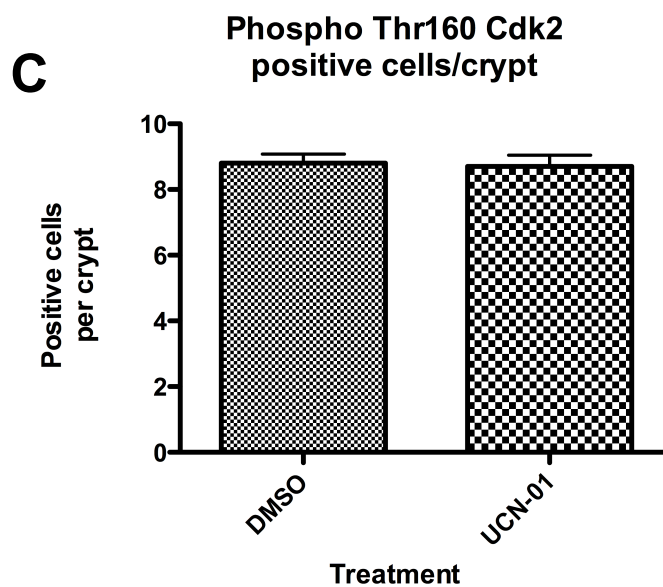
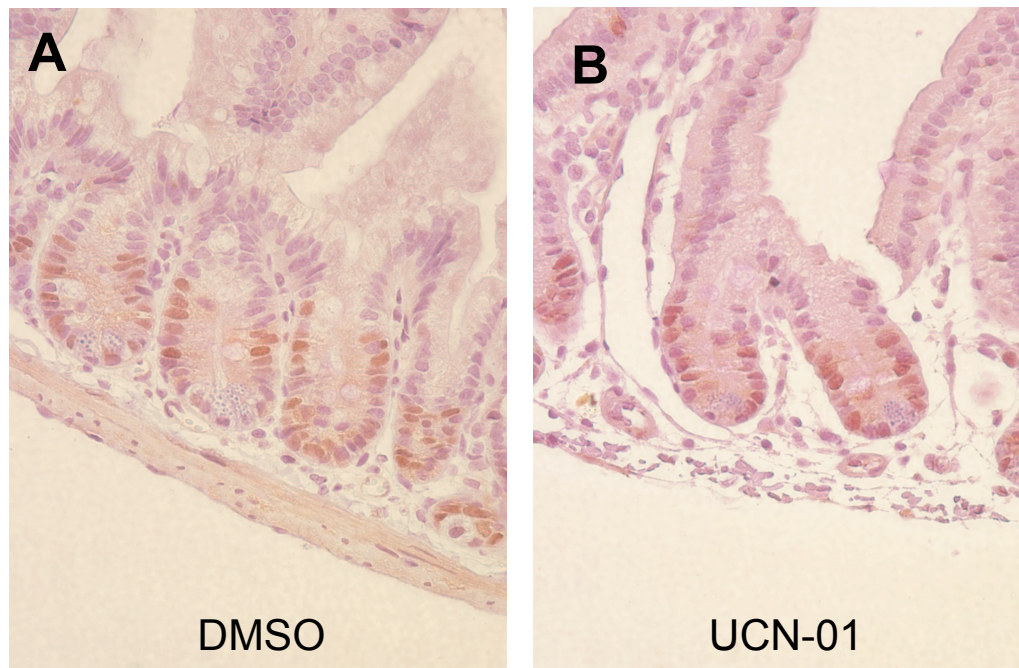


Figure 46: IHC analysis of active (phospho-Thr160) cdk2 in jejunum of mice treated with DMSO (A) or 5 mg/kg UCN-01 (B) for 24 hours. 10 crypts per mouse were analyzed, with 5 mice per treatment group. Results of the quantification of positive cells (C) indicates no difference in the levels of active cdk2 between the two treatment groups.

the serial digestion method has been successfully used to assess cdk2 kinase activity in a recent publication (Smartt *et al.*, 2007). The authors of this study were able to demonstrate an increase in cdk2 kinase activity in the crypt fraction of transgenic mice harboring defective p27 compared to cdk2 from wild-type mice. It therefore seems probable that the proteins isolated using the serial fractionation method are not altered by the process.

### **UCN-01 and Rb phosphorylation:**

While the assessment of active cdk2 by IHC (Figure 46) does indicate that our methodology for examining changes in the crypt cells of the mouse gut is sound, the results to this point do not give a clear indication of how UCN-01 is able to arrest these cells. One piece of information of great interest in this process is the phosphorylation status of Rb. Attempts utilizing phospho-specific antibodies for Rb (S708, S795 and S807/811) in western analyses were unsuccessful, even when Rb was first isolated from whole lysates via immunoprecipitation and then examined (data not shown). The positive staining of active cdk2 via IHC was encouraging, so we applied the same battery of phospho-specific anti-Rb antibodies to sections of mouse jejunum. While the phospho-S780 and phospho-S795 antibodies failed to display a specific signal, the phospho-S807/S811 antibody resulted in specific staining of cells in the crypts. Shown in Figure 47a, this staining shows that phospho-Rb is significantly increased in the UCN-01 samples compared to DMSO controls. These results were quantified, with 10 crypts per mouse analyzed, five mice per treatment group. The results indicate that UCN-01 treated mice have a significantly increased level of phospho-Rb compared to the DMSO control

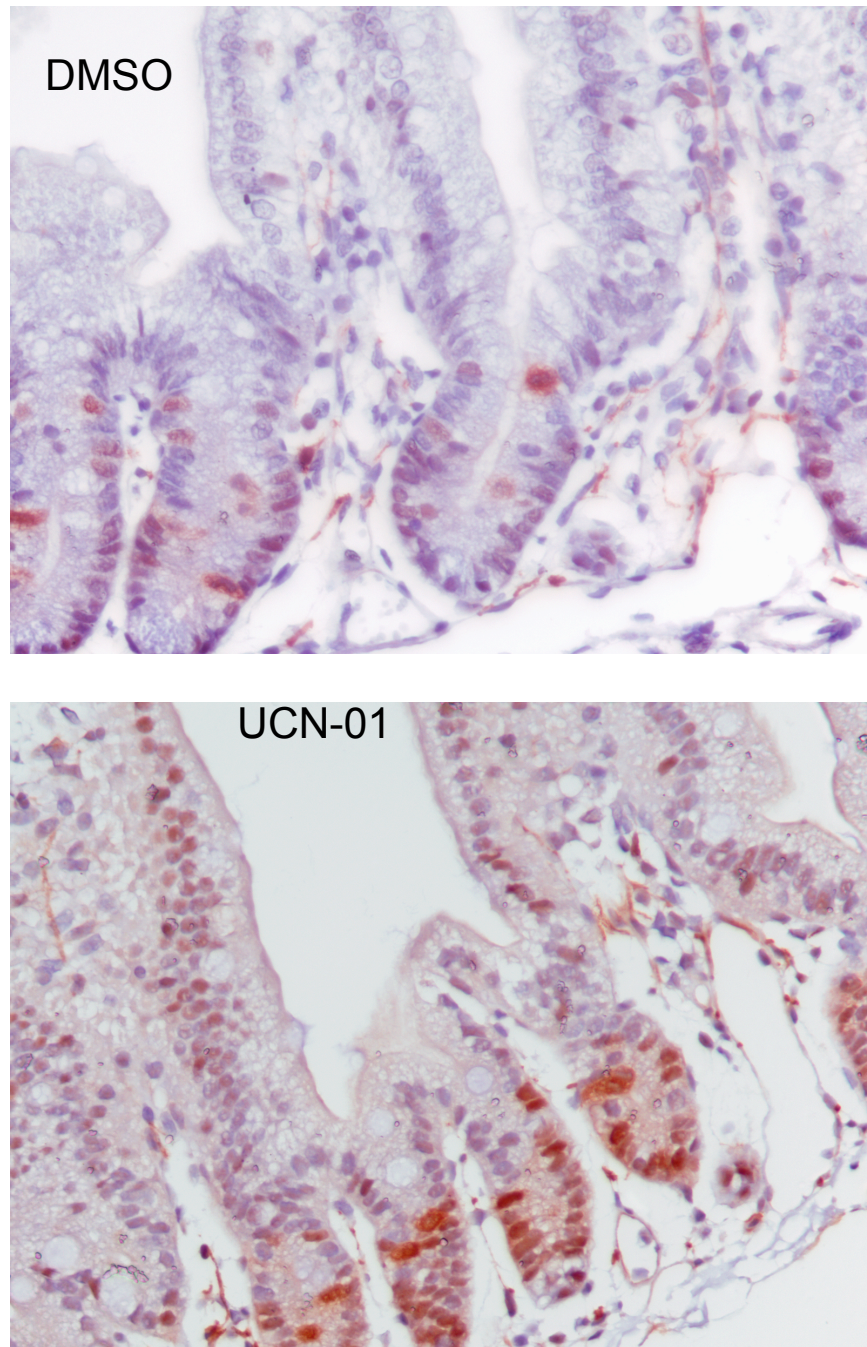


Figure 47a. IHC analysis of phospho-Ser 807/811 Rb on jejuna from mice treated with either DMSO control (top panel) or 5 mg/kg UCN-01 (bottom panel) for 24 hours.

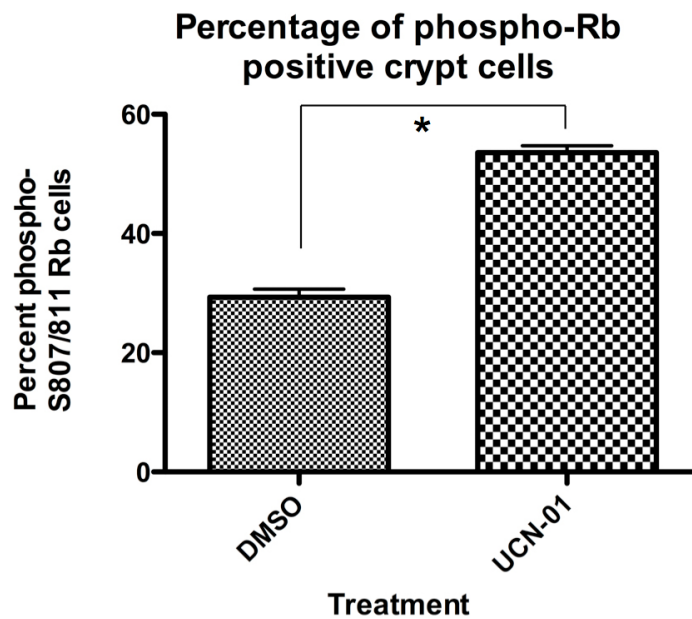


Figure 47b. Quantification of IHC analysis of phospho-Ser 807/811 Rb positive crypt cells. 10 crypts per mouse were analyzed, with 5 mice per treatment group. Statistical analysis indicates a significant increase in phospho-Rb cells in the UCN-01 treated mice in comparison to DMSO treated mice.

mice. While the results clearly show a difference in Rb phosphorylation, the *increase* in phospho-Rb was not expected, as cell culture results using UCN-01 have shown a *decrease* in Rb phosphorylation in cells arrested by UCN-01 treatment (Chen *et al.*, 1999; Courage *et al.*, 1996; Kawakami *et al.*, 1996). While the results of animal studies can often depart somewhat from findings in cultured cells, this alteration in phospho-Rb was a very intriguing result. The preponderance of phospho-Rb in cells arrested in G1 is perplexing, as Rb phosphorylation is a hallmark of progress through G1 phase and into S phase. To ensure that this result truly reflected the arresting action of UCN-01 that was demonstrated in chapter 2, the proliferative status of the crypt cells in these mice were analyzed. Six hours prior to sacrifice, both the UCN-01 treated mice and the DMSO control mice had been injected with BrdU. Sections of jejunum were stained with anti-BrdU and analyzed for incorporation via IHC. In Figure 48, it can be seen that the UCN-01 treated mice had fewer BrdU positive crypt cells than the DMSO control mice. The percent of BrdU-positive crypt cells was significantly lower in the UCN-01 treated mice versus the DMSO control mice (Figure 48c), indicating a decreased level of DNA synthesis in the UCN-01 mice. The combination of low levels of DNA synthesis (indicative of cell cycle arrest) and high levels of phospho-Rb seems to indicate that the cells exposed to UCN-01 are traversing the post-mitotic portion of G1 (thus phosphorylating Rb) but are not crossing the restriction point into S phase (leading to the diminished levels of BrdU incorporation). Further investigation will be required to better understand how UCN-01 is causing this block, although the exact mechanism governing passage through the restriction point is not completely understood (Ekholm *et al.*, 2001).



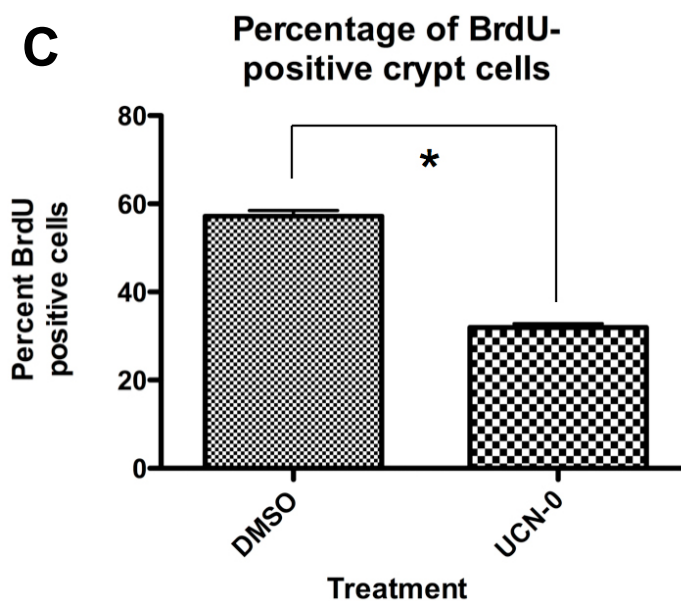
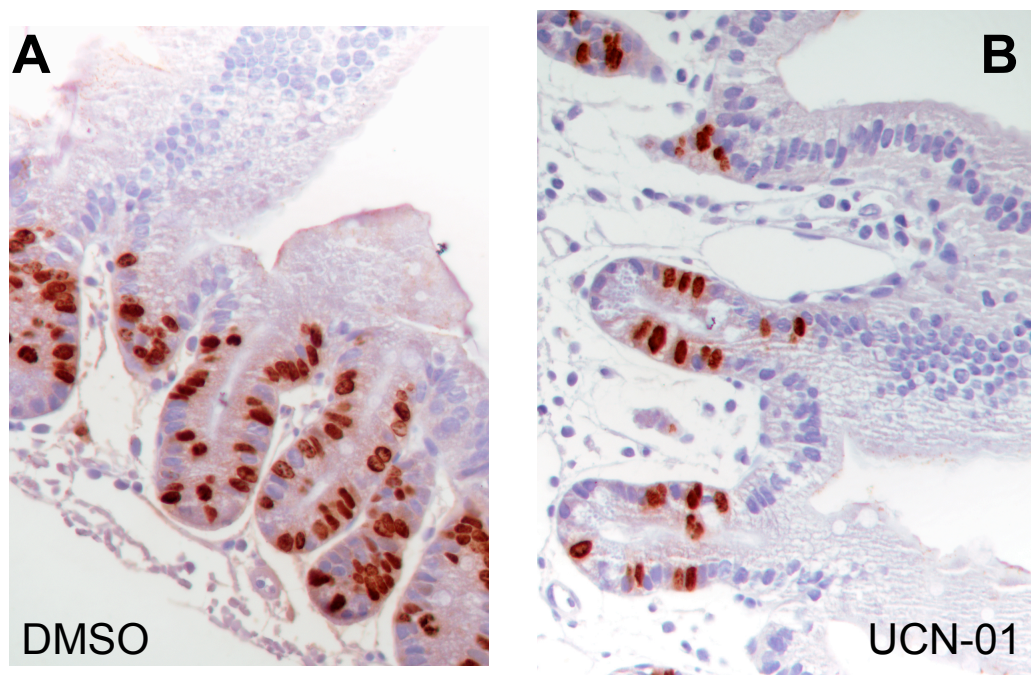


Figure 48: IHC analysis of BrdU incorporation into nuclei of the jejunum of mice treated with DMSO (A) or 5 mg/kg UCN-01 (B) for 24 hours. 10 crypts per mouse were analyzed, with 5 mice per treatment group. Results of the quantification of positive cells (C) indicates a significant decrease in the level of BrdU incorporation in the mice treated with UCN-01

## **Conclusions:**

The data presented in this chapter sought to uncover the mechanism responsible for the UCN-01-mediated cell cycle arrest in the mouse small bowel epithelium. Some of the results, such as the increased levels of p27 following UCN-01 treatment (Figure 41), are in agreement with previous reports on cultured cells treated with UCN-01. However, the increases in cdk4 (Figure 38), cyclin D (Figure 39), and phospho-Rb (Figure 47) are a departure from the effects of UCN-01 observed in cell culture. A common motif of cells arrested in G1 is lack of Rb phosphorylation, due to decreased cyclin levels (D and/or E), increased inhibitor levels (p21, p27, p16), and the concomitant suppression of E2F-governed transcription of genes required for entrance into S phase. The greatly increased levels of phospho-Rb and the increases in cdk4 and cyclin D were unexpected, but might simply be a consequence of increased numbers of cells arrested in late G1; a greater proportion of cells in late G1 phase would lead to increased levels of early G1 proteins. High levels of cyclin D and cdk4 could then increase the levels of phospho-Rb. The lack of an increase in cyclin E (Figure 43) and the drop in BrdU incorporation (Figure 48) in the UCN-01 treated mice indicate that the crypt cells are unable to cross the restriction point into S phase. It has been demonstrated that accumulation of cyclin E occurs after passage through the restriction point (Ekholm *et al.*, 2001), so it is likely that the UCN-01 treated cells are arrested at this point. The lack of increased cdk2 kinase activity in the UCN-01 treated mice (Figure 44) supports this conclusion as well.

The mechanism by which UCN-01 is able to arrest the normal proliferating cells of the mouse small intestine will require further investigation. The results reported here show



some unexpected consequences of UCN-01 treatment, especially the increased levels of phospho-Rb. An understanding of the *in vivo* mechanism of UCN-01 is important not only in the setting of normal proliferating cells, but may also be important in identifying appropriate tumor tissues for treatment with the UCN-01 protection protocol. Successful treatment would require that a tumor *not* respond to UCN-01-mediated arrest, leaving it vulnerable to chemotherapeutic treatment, while the normal dividing tissues are spared this toxicity due to temporary arrest. Possible future directions to further uncover the mechanism of UCN-01 cell cycle arrest are presented in the Discussion below.

## **Discussion:**

Our findings indicate that UCN-01 is able to reversibly arrest the normal dividing tissues of the nude mouse, and that this arrest commences 24 hours following treatment and persists for seven days. Two weeks following UCN-01 treatment, the proliferation rate returns to normal levels. This arrest can provide protection from the toxicity of 5-FU if administered during a specific window of efficacy. Mice treated with 5-FU between three and five days post-UCN-01 administration demonstrate improvements in weight status, survival and blood markers. However, if 5-FU is given either too early or too late following UCN-01, no protective effect is realized. 5-FU administered 24 hours following UCN-01 is actually more toxic than in control mice treated with 5-FU, likely due to the combined toxicity of 5-FU and the length of time until cessation of the UCN-01 mediated arrest. Mice treated with 5-FU at one week following UCN-01 administration also failed to benefit from pretreatment, perhaps due to the initiation of recovery from UCN-01 mediated arrest. The mechanism of this arrest was also examined in the mouse small bowel. Treatment with UCN-01 caused an increase in the early G1 phase cell cycle proteins cdk4 and cyclin D, as well as the inhibitor p27. However, no increase in cdk4 kinase activity was measured. Late G1 phase proteins cyclin E and cdk2 were also unaltered by UCN-01 treatment, and the level of cdk2 activity was unchanged as well. Interestingly, the levels of phosphorylated Rb in the UCN-01 treated samples were significantly higher than in control mice. While BrdU analysis demonstrates that the UCN-01 treated mice had reduced levels of proliferation in the gut epithelium, the

increase in Rb phosphorylation was unexpected. The mechanism of UCN-01 arrest in normal tissues will require further investigation.

The work presented in this thesis has been divided into three parts. The initial work was done to assess the ability of UCN-01 to arrest the dividing cells of the small bowel and the time frame for commencement and release of this arrest. While the arrest of the dividing tissues of the mouse had already been demonstrated (Redkar *et al.*, 2001), it was important to identify both the commencement and the cessation times for UCN-01-mediated cell cycle arrest in these tissues. If this cell cycle arrest is to be properly exploited to minimize damage to dividing cells, it is critical to understand when the arrest is in effect. Our results indicate that UCN-01 is able to arrest the gut epithelial cells as early as 24 hours following treatment, and that this arrest persists through day 7 post-treatment. The arrest ceases by week two, and week four samples displayed a slightly hyperproliferative state, likely the result of increased epithelial cell division to repopulate the villi after the arrest. An interesting finding was the antagonistic effect of the solvent DMSO. Attempts to mollify this effect by decreasing the volume of DMSO injected or by using an alternative solvent (sodium citrate) were unsuccessful. UCN-01 was also administered in a fractionated fashion (2 doses separated by 12 hours) in hopes of increasing the number of cells susceptible to UCN-01-mediated arrest. While it is likely that some cells which escaped the effects of the first injection of UCN-01 were affected by the second dose, the increase in arrest measured was not significant. While the DMSO antagonism is undesirable, the goal of this part of the study was to understand the time frame of UCN-01-mediated arrest, which was accomplished.

The timing of UCN-01-mediated arrest was crucial knowledge for designing experiments to evaluate the protective ability of UCN-01 in mice receiving 5-FU, the aim of the second part of this thesis. Our results demonstrate that treatment with 5-FU either too early after cell cycle arrest (24 hours, Figure 18) or too close to recovery from arrest (days 7-11, Figure 13) did not benefit from UCN-01 pretreatment. Only when cytotoxic treatment was given *during* the period of arrest but *proximal* to the time of recovery from arrest was a protective effect of UCN-01 pretreatment realized (figures 15, 22, 26, 28 and 31). Pretreatment with UCN-01 three to five days prior to high dose 5-FU led to improvements in weight status, blood cell counts (platelets and red and white blood cells) and overall survival compared to control mice. While protection from apoptosis has been shown to be responsible for the enhanced survival of arrested normal cells in culture after cytotoxic treatment (Chen *et al.*, 2000), this type of protection may only be part of the effect *in vivo*. The toxicity to gut epithelial cells following high dose 5-FU treatment is not solely apoptosis, but also conversion of proliferating cells to a permanent state of quiescence (Pritchard *et al.*, 1998). Mice treated with 400 mg/kg 5-FU displayed similar levels of apoptosis to mice treated with only 40 mg/kg at both 24 and 48 hours after treatment. The large difference observed between the two treatment groups was the induction of p21 through p53. After treatment with 400 mg/kg 5-FU, cells in the proliferating region of the crypt displayed a significant and prolonged increase in the levels of p21, leading to a permanent decrease in cellular proliferation and breakdown of the crypt-villus architecture by 96 hours. Mice null for p53 had significantly less inhibition of cell proliferation and displayed improved numbers of crypt cells and total

villus area after 5-FU treatment. The permanent arrest caused by p21 after high dose 5-FU treatment was also demonstrated in a different study (Inomata *et al.*, 2002). The fate of cells in the crypt hinged upon the comparative levels of p21 and bax after 5-FU treatment. High levels of bax led to apoptosis, while high p21 led to a permanent state of arrest. Our treatment plan may help avoid both of these fates. Arrested cells should be spared some toxicity of 5-FU if they are unable to enter S phase. In addition, the cells pretreated with UCN-01 might also evade the p53/p21 mediated permanent arrest pathway; in a fashion, activating one type of cell cycle arrest may prevent the cells from entering into the permanent p21-mediated arrest seen in these two studies. An interesting future experiment would be to examine the levels of p53 and p21 in the mouse small bowel after treatment with 5-FU following UCN-01 pretreatment. A lack of increase of these proteins in the UCN-01 pretreated mice would indicate that UCN-01 is able to prevent the p21 increase and subsequent quiescence caused by high dose 5-FU.

An alternative possibility to explain the protection afforded by UCN-01 is to think of the arrested population of cells as similar to a potential energy source. Villus structure is maintained by balancing the loss of apoptotic cells at the villus tip with proliferation of cells in the crypt. The newly divided cells differentiate into mature enterocytes and migrate upwards along the crypt-villus axis as more cells continue to be produced in the proliferative zone of the crypt. This balance is maintained by signaling through at least two zinc-finger transcription factors, Kruppel-like factors 9 (Klf9) and 5 (Klf5) (Shindo *et al.*, 2002; Simmen *et al.*, 2007). This homeostasis has also been linked to the Wnt pathway through c-Myc (Pinto *et al.*, 2003), although later work has demonstrated that

mice lacking c-Myc in the intestine were able to maintain normal epithelial turnover and maintenance (Bettess *et al.*, 2005). A lack of cellular proliferation due to UCN-01 treatment may activate one or more of these control pathways, leading to initiation of signaling to increase proliferation. If UCN-01 continues to block cells in G1, this could lead to a feedback loop in which the Klf5/9 pathway attempts to further stimulate cellular proliferation in the crypt. When the arrest caused by UCN-01 treatment recedes, the buildup of cells stimulated to proliferate could quickly repopulate the villi. If this release occurs very soon after cytotoxic treatment, this repopulation could ameliorate the effects of cell death due to treatment. This seems similar in principle to the palifermin protocol discussed in the introduction, in which stimulation of cellular proliferation is used to improve patient tolerance of chemotherapeutics. Transcriptional activation of targets of Klf5 and Klf9 would demonstrate that this hypothesis is responsible for at least some of the protection afforded by UCN-01.

A third possibility for the response to UCN-01 pretreatment may also account for the increased levels of phospho-S708/811 Rb shown in chapter three (Figure 47). One notable feature of the phospho-Rb staining is that the positive cells in the UCN-01 treated groups are not only in the proliferative region of the crypt (approximately positions 4 – 8 from the base of the crypt), but in cells above and below this range as well. These Paneth cells and maturing enterocytes are largely quiescent or are terminally differentiated and are in G0. Cell cycle arrest due to UCN-01 treatment may stimulate these cells to re-enter the G1 phase of the cell cycle to help repopulate the villus. It has been shown that inactivation (phosphorylation) of Rb can force G0 cells to enter G1 (Sage *et al.*, 2003). It

has also been shown that cyclin C can bind to cdk3 in G0 cells and phosphorylate Rb on serines 807 and 811, and that this phosphorylation is required for entry into G1 (Ren and Rollins, 2004). The increase in phospho S/870/811 Rb observed in the UCN-01 treated cells may not be due to cdk4 kinase activity, but rather a consequence of cyclin C/cdk3 activity attempting to stimulate G0 cells to re-enter the cell cycle. As with the previous “potential energy” theory, this increase in cells which can quickly repopulate the gut after cytotoxic treatment could account for the protective benefit observed with UCN-01 treatment. Future examination of cyclin C and cdk3 activity could determine whether this mechanism is responsible for the increased phospho-Rb seen in the UCN-01 treated mice.

The unexpected increases in the G1 phase proteins cdk4, cyclin D and phosphorylated Rb may also be a consequence of comparison with DMSO as the control group. As shown in the first results section, DMSO appears to increase the proliferative rate of gut epithelial cells. The increase in proliferation may cause alterations in cell cycle proteins; it is possible that some of these changes occur even when UCN-01 is administered, as DMSO is required as the solvent. Further investigation of this mechanism will require an assessment of the actions of DMSO as well as UCN-01 versus untreated mice to help distinguish the actions of these two agents.

The most common criticism of the protection protocol has been the failure of UCN-01 in clinical trials to produce improvement in patient response or survival. A second concern has been the pharmacologic problems associated with the strong binding of UCN-01 to

hAGP in the blood. This indeed is a problem, and will be discussed below. However, the initial concern (the disappointing clinical trials reports) is more a product of faulty comparison than truly a robust criticism of the concept of protection via cell cycle arrest. The UCN-01 clinical trials (see Introduction above) have either sought to prevent tumor growth/induce apoptosis (single agent trials) or to enhance the toxicity in tumors by treating patients with a primary cytotoxic agent and then a simultaneous or subsequent dose of UCN-01 to prevent a G2/M arrest and enhance cell killing. There is a fair argument that neither of these treatment protocols has been successful, and in some settings the UCN-01 treatments have performed worse than the standard of care. However, the protection of normal cells afforded by a temporary cell cycle arrest by UCN-01 pretreatment *prior* to administration of a cytotoxic agent (5-FU) has not been addressed by *any* of the clinical protocols. An important feature of this proposed treatment scheme is that UCN-01 does *not* arrest the growth of some tumor types, while causing a G1/S arrest in normal proliferating tissues (Chen *et al.*, 2000). It could be argued that any tumors which did respond to the UCN-01 single agent protocols should be excluded from evaluation of the protection protocol, as the tumor might benefit from protection due to cell cycle arrest; only tumors which can divide in the presence of UCN-01 would be appropriate for this scheme. The double agent (UCN-01 following cytotoxic agent) protocols would be less relevant to evaluating the work presented in this thesis. The protective effect of cell cycle arrest necessitates that the arresting agent (UCN-01) be administered *prior* to any cytotoxic treatment. The temporary arrest allows the normal cells to evade toxicity of a subsequent chemotherapeutic drug. However, when UCN-01 is given *after* chemotherapy, it may actually be more damaging to these tissues. Some



damaged cells which had arrested in the G2/M phase would be unable to complete DNA repair and could be forced instead into mitotic catastrophe. Other cells could be potentially arrested in G1; this arrest can last more than one week, preventing repopulation of damaged tissues and further increasing the toxicity borne by the patient. This effect can be seen in the protection experiment in which mice were treated with 5-FU only 24 hours after UCN-01 treatment. While some of the intestinal and hematopoietic cells were potentially spared from 5-FU toxicity, the combined loss of some “unprotected” cells to apoptosis plus the weeklong arrest of the “protected” cells culminated in worse survival for the UCN-01 pretreated mice than DMSO control mice after 5-FU treatment. Only when 5-FU was administered closer to the release of UCN-01-induced arrest was a protective effect demonstrated.

The second concern with UCN-01 use in humans is the strong binding of the drug to the plasma protein hAGP, which maintains UCN-01 at a high concentration in the blood while greatly diminishing the distribution volume and clearance. Initial UCN-01 studies in mice demonstrated a half-life of 3-4 hours, and greater distribution to implanted PSN-1 tumors than in plasma (Kurata *et al.*, 1999). However, initial data from Phase I clinical trials in the United States (Sausville *et al.*, 2001) and in Japan demonstrated a different behavior of UCN-01 in humans (Fuse *et al.*, 1998). The elimination half-life in patients was between 253 and 1660 hours, and the distribution volume was extremely low. This altered behavior was attributed to extremely tight, specific binding to the serum protein hAGP. Rats infused with 150 nmol/h/kg of hAGP prior to injection of UCN-01 had significantly reduced distribution volumes (1/250) and clearance (1/700) of UCN-01

compared to control rats (Fuse *et al.*, 2000). The pharmacokinetics of UCN-01 in humans is responsible for the altered dosing in clinical trials, in which subsequent doses of UCN-01 are typically half that of the initial dose (see Table 3).

This aspect of UCN-01 in humans is problematic in the context of our protection protocol. As demonstrated in chapter 3, the protective effect of UCN-01 is limited to a narrow window of efficacy, approximately 3 -5 days after UCN-01 treatment. Cytotoxic treatment (5-FU) outside this period is at best unaffected (later) and can be even more detrimental than 5-FU alone (earlier). As the half-life for UCN-01 in humans can be greater than two *months*, coordinating the administration of a chemotherapeutic agent during the period of UCN-01-mediated arrest would likely be impossible. Moreover, it is possible that constant exposure to UCN-01 alone would be detrimental to normal proliferative tissues; a semi-permanent arrest would prevent the replenishment of tissues which undergo frequent turnover.

Some effort has been made to address this concern. Liposomes (capsules of polyethylene glycol (PEG)) have been used as carriers for drugs such as cisplatin and topotecan to increase delivery to tumor sites and reduce interaction with blood components (Burke and Gao, 1994; Newman *et al.*, 1999). Initial studies using liposomes to encapsulate UCN-01 showed some efficacy in shielding the drug from hAGP when coadministered in rats (Yamauchi *et al.*, 2005). Six hours after administration, almost 18% of the UCN-01 injected was still present in the liposomes, shielded away from the coadministered hAGP. However, by 24 hours very little protected UCN-01 remained. Refinement of this

method focused on increasing the size of the liposomes, with the hope that a greater lipid shield would enhance the protection of UCN-01 from serum interaction (Yamauchi *et al.*, 2008). The results were somewhat promising, with almost 25% of the injected UCN-01 remaining encapsulated in the liposome at 24 hours when the size was increased from 112 nm to 155 nm.

The use of UCN-01 to protect normal dividing cells from the toxicity of 5-FU in this study was successful when employed during a limited window of efficacy. Weight loss, blood markers and survival were all significantly improved, proving the validity of this model of protection. The ability of UCN-01 to place normal dividing cells into a reversible state of arrest and the length of this arrest have also been determined. The exact mechanism behind this arrest remains largely unknown, and the pharmacokinetics of UCN-01 further complicate any potential use in humans. The idea of protecting normal cells from chemotherapeutic damage is an attractive one, but its implementation may require identification of other agents which mimic the differential arresting effects of UCN-01 without the complications associated with its use.

An optimal agent to protect normal cells by inhibiting proliferation would need three features. First, it must have a very specific rate of clearance, and preferably one short in duration. The results with UCN-01 pretreatment clearly indicate that protection is available only in a short time period. This time frame would be easier to evaluate for a drug which had a short, defined period of bioavailability. A prolonged clearance process would make this definition less clear, especially when taken in context of the cell cycle.

If a candidate compound took longer than 24 hours to clear from the system, it could affect more than one cycle, so having a truly uniformly affected cell population would be difficult, and again a window of efficacy difficult to predict. Unlike UCN-01, an ideal compound would also have a much shorter duration of effect. The effect(s) of UCN-01 take longer than 7 days to recede; this is a very long time for cells to be held from dividing, and is not ideal for the host. Replenishment of rapidly dividing tissues is essential for maintenance of homeostasis, and a prolonged interruption plus a second toxic insult is not an ideal situation. It would be preferred that the reduction in cell proliferation last no more than 48 hours; this would allow protection from toxic agents targeting the cell cycle, but then allow for a rapid return to cell division and maintenance of the bone marrow and intestinal epithelium. This would be preferable to the situation with UCN-01, in which proliferation is impaired for more than seven days. There are few side effects of UCN-01 at the doses used in this study, but the prolonged inhibition of cycling cells is undesirable, and any alternative compound would hopefully have a much shorter period of action.

Screening for potential protective compounds can be initially done in cultured primary cells, and any candidate drugs could subsequently be evaluated as UCN-01 has been in this dissertation. It is essential that any new potential agents cause a reversible cell cycle arrest in only normal cells, and that tumor cells derive little or no protection. If animal studies are successful, the screening in a Phase I toxicity trial would require not only assessment of dosing and side effects, but also a way to measure proliferation of normal dividing tissues. DNA labeling methods would likely not be appropriate; in this case,

profiling of blood markers (red & white blood cells and platelets) would be less invasive and still powerful method to determine the period of attenuation of normal cycling cells. Once the times of cell cycle inhibition and return to proliferation are understood, treatment with a toxic chemotherapeutic compound can be scheduled during the period of inhibition. Successful protection would be measured in terms of both intestinal health (weight, appetite, nausea, and diarrhea) and the blood markers previously mentioned. Hair loss could also be assessed, although this would be difficult to quantify and would be a qualitative indicator. Successful protection would improve most or all of these parameters compared to patients without the protective regimen.

The results of this study indicate that temporary cell cycle inhibition can be exploited to improve the survival and health of mice receiving high dose chemotherapy. While the pharmacokinetic issues of UCN-01 in humans will likely prevent this protocol from being taken into a clinical setting, the work discussed here provides a framework for developing alternative agents which could also provide this protection. It is hoped that other compounds will be identified to carry the protection protocol successfully into a clinical trial setting.

## References:

Abe S, Kubota T, Otani Y, Furukawa T, Watanabe M, Kumai K *et al* (2001). UCN-01 (7-hydroxystaurosporine) inhibits in vivo growth of human cancer cells through selective perturbation of G1 phase checkpoint machinery. *Jpn J Cancer Res* **92**: 537-45.

Akinaga S, Gomi K, Morimoto M, Tamaoki T, Okabe M (1991). Antitumor activity of UCN-01, a selective inhibitor of protein kinase C, in murine and human tumor models. *Cancer Res* **51**: 4888-92.

Akinaga S, Nomura K, Gomi K, Okabe M (1993). Enhancement of antitumor activity of mitomycin C in vitro and in vivo by UCN-01, a selective inhibitor of protein kinase C. *Cancer Chemother Pharmacol* **32**: 183-9.

Akinaga S, Nomura K, Gomi K, Okabe M (1994). Effect of UCN-01, a selective inhibitor of protein kinase C, on the cell-cycle distribution of human epidermoid carcinoma, A431 cells. *Cancer Chemother Pharmacol* **33**: 273-80.

Akiyama T, Shimizu M, Okabe M, Tamaoki T, Akinaga S (1999a). Differential effects of UCN-01, staurosporine and CGP 41 251 on cell cycle progression and CDC2/cyclin B1 regulation in A431 cells synchronized at M phase by nocodazole. *Anticancer Drugs* **10**: 67-78.

Akiyama T, Sugiyama K, Shimizu M, Tamaoki T, Akinaga S (1999b). G1-checkpoint function including a cyclin-dependent kinase 2 regulatory pathway as potential determinant of 7-hydroxystaurosporine (UCN-01)-induced apoptosis and G1-phase accumulation. *Jpn J Cancer Res* **90**: 1364-72.

Akiyama T, Yoshida T, Tsujita T, Shimizu M, Mizukami T, Okabe M *et al* (1997). G1 phase accumulation induced by UCN-01 is associated with dephosphorylation of Rb and CDK2 proteins as well as induction of CDK inhibitor p21/Cip1/WAF1/Sdi1 in p53-mutated human epidermoid carcinoma A431 cells. *Cancer Res* **57**: 1495-501.

Amornphimoltham P, Sriuranpong V, Patel V, Benavides F, Conti CJ, Sauk J *et al* (2004). Persistent activation of the Akt pathway in head and neck squamous cell carcinoma: a potential target for UCN-01. *Clin Cancer Res* **10**: 4029-37.

Bacus SS, Gudkov AV, Lowe M, Lyass L, Yung Y, Komarov AP *et al* (2001). Taxol-induced apoptosis depends on MAP kinase pathways (ERK and p38) and is independent of p53. *Oncogene* **20**: 147-55.

Ben-Ishay Z, Farber E (1975). Protective effects of an inhibitor of protein synthesis, cycloheximide, on bone marrow damage induced by cytosine arabinoside or nitrogen mustard. *Lab Invest* **33**: 278-90.

Benhar M, Engelberg D, Levitzki A (2002). ROS, stress-activated kinases and stress signaling in cancer. *EMBO Rep* **3**: 420-5.

Bertrand R, Solary E, O'Connor P, Kohn KW, Pommier Y (1994). Induction of a common pathway of apoptosis by staurosporine. *Exp Cell Res* **211**: 314-21.

Bettess MD, Dubois N, Murphy MJ, Dubey C, Roger C, Robine S *et al* (2005). c-Myc is required for the formation of intestinal crypts but dispensable for homeostasis of the adult intestinal epithelium. *Mol Cell Biol* **25**: 7868-78.

Bhonde MR, Hanski ML, Magrini R, Moorthy D, Muller A, Sausville EA *et al* (2005). The broad-range cyclin-dependent kinase inhibitor UCN-01 induces apoptosis in colon carcinoma cells through transcriptional suppression of the Bcl-x(L) protein. *Oncogene* **24**: 148-56.

Blagosklonny MV, Bishop PC, Robey R, Fojo T, Bates SE (2000a). Loss of cell cycle control allows selective microtubule-active drug-induced Bcl-2 phosphorylation and cytotoxicity in autonomous cancer cells. *Cancer Res* **60**: 3425-8.

Blagosklonny MV, Dixon SC, Robey R, Figg WD (2001). Resistance to growth inhibitory and apoptotic effects of phorbol ester and UCN-01 in aggressive cancer cell lines. *Int J Oncol* **18**: 697-704.



Blagosklonny MV, Robey R, Bates S, Fojo T (2000b). Pretreatment with DNA-damaging agents permits selective killing of checkpoint-deficient cells by microtubule-active drugs.

*J Clin Invest* **105**: 533-9.

Booth D, Haley JD, Bruskin AM, Potten CS (2000). Transforming growth factor-B3 protects murine small intestinal crypt stem cells and animal survival after irradiation, possibly by reducing stem-cell cycling. *Int J Cancer* **86**: 53-9.

Brizel DM, Murphy BA, Rosenthal DI, Pandya KJ, Gluck S, Brizel HE *et al* (2008). Phase II study of palifermin and concurrent chemoradiation in head and neck squamous cell carcinoma. *J Clin Oncol* **26**: 2489-96.

Bruno S, Ardelt B, Skierski JS, Traganos F, Darzynkiewicz Z (1992). Different effects of staurosporine, an inhibitor of protein kinases, on the cell cycle and chromatin structure of normal and leukemic lymphocytes. *Cancer Res* **52**: 470-3.

Bunch RT, Eastman A (1997). 7-Hydroxystaurosporine (UCN-01) causes redistribution of proliferating cell nuclear antigen and abrogates cisplatin-induced S-phase arrest in Chinese hamster ovary cells. *Cell Growth Differ* **8**: 779-88.

Burke TG, Gao X (1994). Stabilization of topotecan in low pH liposomes composed of distearoylphosphatidylcholine. *J Pharm Sci* **83**: 967-9.

Busby EC, Leistritz DF, Abraham RT, Karnitz LM, Sarkaria JN (2000). The radiosensitizing agent 7-hydroxystaurosporine (UCN-01) inhibits the DNA damage checkpoint kinase hChk1. *Cancer Res* **60**: 2108-12.

Byrd JC, Shinn C, Willis CR, Flinn IW, Lehman T, Sausville E *et al* (2001). UCN-01 induces cytotoxicity toward human CLL cells through a p53-independent mechanism. *Exp Hematol* **29**: 703-8.

Campisi J, Medrano EE, Morreo G, Pardee AB (1982). Restriction point control of cell growth by a labile protein: evidence for increased stability in transformed cells. *Proc Natl Acad Sci U S A* **79**: 436-40.

Castagna M, Takai Y, Kaibuchi K, Sano K, Kikkawa U, Nishizuka Y (1982). Direct activation of calcium-activated, phospholipid-dependent protein kinase by tumor-promoting phorbol esters. *J Biol Chem* **257**: 7847-51.

Castiglione F, Dalla Mola A, Porcile G (1999). Protection of normal tissues from radiation and cytotoxic therapy: the development of amifostine. *Tumori* **85**: 85-91.

Chan UP, Lee JF, Wang SH, Leung KL, Chen GG (2003). Induction of colon cancer cell death by 7-hydroxystaurosporine (UCN-01) is associated with increased p38 MAPK and decreased Bcl-xL. *Anticancer Drugs* **14**: 761-6.

Chen X, Lowe M, Herliczek T, Hall MJ, Danes C, Lawrence DA *et al* (2000). Protection of normal proliferating cells against chemotherapy by staurosporine-mediated, selective, and reversible G(1) arrest. *J Natl Cancer Inst* **92**: 1999-2008.

Chen X, Lowe M, Keyomarsi K (1999). UCN-01-mediated G1 arrest in normal but not tumor breast cells is pRb-dependent and p53-independent. *Oncogene* **18**: 5691-702.

Coccia EM, Del Russo N, Stellacci E, Orsatti R, Benedetti E, Marziali G *et al* (1999). Activation and repression of the 2-5A synthetase and p21 gene promoters by IRF-1 and IRF-2. *Oncogene* **18**: 2129-37.

Courage C, Bradder SM, Jones T, Schultze-Mosgau MH, Gescher A (1997). Characterisation of novel human lung carcinoma cell lines selected for resistance to anti-neoplastic analogues of staurosporine. *Int J Cancer* **73**: 763-8.

Courage C, Snowden R, Gescher A (1996). Differential effects of staurosporine analogues on cell cycle, growth and viability in A549 cells. *Br J Cancer* **74**: 1199-205.

Crissman HA, Gadbois DM, Tobey RA, Bradbury EM (1991). Transformed mammalian cells are deficient in kinase-mediated control of progression through the G1 phase of the cell cycle. *Proc Natl Acad Sci U S A* **88**: 7580-4.

Culy CR, Spencer CM (2001). Amifostine: an update on its clinical status as a cytoprotectant in patients with cancer receiving chemotherapy or radiotherapy and its potential therapeutic application in myelodysplastic syndrome. *Drugs* **61**: 641-84.

Daley GQ, Van Etten RA, Baltimore D (1990). Induction of chronic myelogenous leukemia in mice by the P210bcr/abl gene of the Philadelphia chromosome. *Science* **247**: 824-30.

de Klein A, van Kessel AG, Grosveld G, Bartram CR, Hagemeijer A, Bootsma D *et al* (1982). A cellular oncogene is translocated to the Philadelphia chromosome in chronic myelocytic leukaemia. *Nature* **300**: 765-7.

Decesse JT, Medjkane S, Datto MB, Cremisi CE (2001). RB regulates transcription of the p21/WAF1/CIP1 gene. *Oncogene* **20**: 962-71.

Dees EC, Baker SD, O'Reilly S, Rudek MA, Davidson SB, Aylesworth C *et al* (2005). A phase I and pharmacokinetic study of short infusions of UCN-01 in patients with refractory solid tumors. *Clin Cancer Res* **11**: 664-71.

Dent P, Jarvis WD, Birrer MJ, Fisher PB, Schmidt-Ullrich RK, Grant S (1998). The roles of signaling by the p42/p44 mitogen-activated protein (MAP) kinase pathway; a potential route to radio- and chemo-sensitization of tumor cells resulting in the induction of apoptosis and loss of clonogenicity. *Leukemia* **12**: 1843-50.

Dosik GM, Barlogie B, Johnston DA, Murphy WK, Drewinko B (1978). Lethal and cytotoxic effects of anguidine on a human colon cancer cell line. *Cancer Res* **38**: 3304-9.

Druker BJ, Guilhot F, O'Brien SG, Gathmann I, Kantarjian H, Gattermann N *et al* (2006). Five-year follow-up of patients receiving imatinib for chronic myeloid leukemia. *N Engl J Med* **355**: 2408-17.

Druker BJ, Tamura S, Buchdunger E, Ohno S, Segal GM, Fanning S *et al* (1996). Effects of a selective inhibitor of the Abl tyrosine kinase on the growth of Bcr-Abl positive cells. *Nat Med* **2**: 561-6.

Dumaz N, Milne DM, Jardine LJ, Meek DW (2001). Critical roles for the serine 20, but not the serine 15, phosphorylation site and for the polyproline domain in regulating p53 turnover. *Biochem J* **359**: 459-64.

Eastman A (2004). Cell cycle checkpoints and their impact on anticancer therapeutic strategies. *J Cell Biochem* **91**: 223-31.

Eastman A, Kohn EA, Brown MK, Rathman J, Livingstone M, Blank DH *et al* (2002). A novel indolocarbazole, ICP-1, abrogates DNA damage-induced cell cycle arrest and

enhances cytotoxicity: similarities and differences to the cell cycle checkpoint abrogator UCN-01. *Mol Cancer Ther* **1**: 1067-78.

Edelman MJ, Bauer KS, Jr., Wu S, Smith R, Bisaccia S, Dancey J (2007). Phase I and pharmacokinetic study of 7-hydroxystaurosporine and carboplatin in advanced solid tumors. *Clin Cancer Res* **13**: 2667-74.

Edelstein MB, Heilbrun LK (1988). Specificity, schedule, and proliferation dependence of infused L-histidinol after 5-fluorouracil in mice. *Cancer Res* **48**: 1470-5.

Ekholm SV, Zickert P, Reed SI, Zetterberg A (2001). Accumulation of cyclin E is not a prerequisite for passage through the restriction point. *Mol Cell Biol* **21**: 3256-65.

Facchinetti MM, De Siervi A, Toskos D, Senderowicz AM (2004). UCN-01-induced cell cycle arrest requires the transcriptional induction of p21(waf1/cip1) by activation of mitogen-activated protein/extracellular signal-regulated kinase/extracellular signal-regulated kinase pathway. *Cancer Res* **64**: 3629-37.

Farrell CL, Bready JV, Rex KL, Chen JN, DiPalma CR, Whitcomb KL *et al* (1998). Keratinocyte growth factor protects mice from chemotherapy and radiation-induced gastrointestinal injury and mortality. *Cancer Res* **58**: 933-9.

Ferraris RP, Villenas SA, Diamond J (1992). Regulation of brush-border enzyme activities and enterocyte migration rates in mouse small intestine. *Am J Physiol* **262**: G1047-59.

Frazier JL, Wang PP, Case D, Tyler BM, Pradilla G, Weingart JD *et al* (2003). Local delivery of minocycline and systemic BCNU have synergistic activity in the treatment of intracranial glioma. *J Neurooncol* **64**: 203-9.

Fujiki H, Suganuma M, Suguri H, Yoshizawa S, Hirota M, Takagi K *et al* (1989). Diversity in the chemical nature and mechanism of response to tumor promoters. *Prog Clin Biol Res* **298**: 281-91.

Fukumoto H, Tamura T, Kamiya Y, Usuda J, Suzuki T, Kanzawa F *et al* (1999). Activation-induced apoptosis of peripheral lymphocytes treated with 7-hydroxystaurosporine, UCN-01. *Invest New Drugs* **17**: 335-41.

Fuse E, Hashimoto A, Sato N, Tanii H, Kuwabara T, Kobayashi S *et al* (2000). Physiological modeling of altered pharmacokinetics of a novel anticancer drug, UCN-01 (7-hydroxystaurosporine), caused by slow dissociation of UCN-01 from human alpha1-acid glycoprotein. *Pharm Res* **17**: 553-64.

Fuse E, Tanii H, Kurata N, Kobayashi H, Shimada Y, Tamura T *et al* (1998).

Unpredicted clinical pharmacology of UCN-01 caused by specific binding to human alpha1-acid glycoprotein. *Cancer Res* **58**: 3248-53.

Garces YI, Okuno SH, Schild SE, Mandrekar SJ, Bot BM, Martens JM *et al* (2007).

Phase I North Central Cancer Treatment Group Trial-N9923 of escalating doses of twice-daily thoracic radiation therapy with amifostine and with alternating chemotherapy in limited stage small-cell lung cancer. *Int J Radiat Oncol Biol Phys* **67**: 995-1001.

Gnarra JR, Tory K, Weng Y, Schmidt L, Wei MH, Li H *et al* (1994). Mutations of the VHL tumour suppressor gene in renal carcinoma. *Nat Genet* **7**: 85-90.

Graves PR, Yu L, Schwarz JK, Gales J, Sausville EA, O'Connor PM *et al* (2000). The Chk1 protein kinase and the Cdc25C regulatory pathways are targets of the anticancer agent UCN-01. *J Biol Chem* **275**: 5600-5.

Grzegorzewski K, Ruscetti FW, Usui N, Damia G, Longo DL, Carlino JA *et al* (1994). Recombinant transforming growth factor beta 1 and beta 2 protect mice from acutely lethal doses of 5-fluorouracil and doxorubicin. *J Exp Med* **180**: 1047-57.

Hamed H, Hawkins W, Mitchell C, Gilfor D, Zhang G, Pei XY *et al* (2008). Transient exposure of carcinoma cells to RAS/MEK inhibitors and UCN-01 causes cell death in vitro and in vivo. *Mol Cancer Ther* **7**: 616-29.



Hartwell LH, Kastan MB (1994). Cell cycle control and cancer. *Science* **266**: 1821-8.

Hashimoto T, He Z, Ma WY, Schmid PC, Bode AM, Yang CS *et al* (2004). Caffeine inhibits cell proliferation by G0/G1 phase arrest in JB6 cells. *Cancer Res* **64**: 3344-9.

Hawkins W, Mitchell C, McKinstry R, Gilfor D, Starkey J, Dai Y *et al* (2005). Transient exposure of mammary tumors to PD184352 and UCN-01 causes tumor cell death in vivo and prolonged suppression of tumor regrowth. *Cancer Biol Ther* **4**: 1275-84.

Hedaya MA, Daoud SS (2001). Tissue distribution and plasma pharmacokinetics of UCN-01 at steady-state and following bolus administration in rats: influence of human alpha1-acid glycoprotein binding. *Anticancer Res* **21**: 4005-10.

Heisterkamp N, Jenster G, ten Hoeve J, Zovich D, Pattengale PK, Groffen J (1990). Acute leukaemia in bcr/abl transgenic mice. *Nature* **344**: 251-3.

Herman JG, Latif F, Weng Y, Lerman MI, Zbar B, Liu S *et al* (1994). Silencing of the VHL tumor-suppressor gene by DNA methylation in renal carcinoma. *Proc Natl Acad Sci U S A* **91**: 9700-4.

Hill DL, Tillery KF, Rose LM, Posey CF (1994). Disposition in mice of 7-hydroxystaurosporine, a protein kinase inhibitor with antitumor activity. *Cancer Chemother Pharmacol* **35**: 89-92.

Hotte SJ, Oza A, Winkist EW, Moore M, Chen EX, Brown S *et al* (2006). Phase I trial of UCN-01 in combination with topotecan in patients with advanced solid cancers: a Princess Margaret Hospital Phase II Consortium study. *Ann Oncol* **17**: 334-40.

Hromas R, Barlogie B, Swartzendruber D, Drewinko B (1983). Selective protection by anguidine of normal versus transformed cells against 1-beta-D-arabinofuranosylcytosine and Adriamycin. *Cancer Res* **43**: 1135-7.

Hsueh CT, Kelsen D, Schwartz GK (1998). UCN-01 suppresses thymidylate synthase gene expression and enhances 5-fluorouracil-induced apoptosis in a sequence-dependent manner. *Clin Cancer Res* **4**: 2201-6.

Hsueh CT, Wu YC, Schwartz GK (2001). UCN-01 suppresses E2F-1 mediated by ubiquitin-proteasome-dependent degradation. *Clin Cancer Res* **7**: 669-74.

Huang TY, Chu HC, Lin YL, Ho WH, Hou HS, Chao YC *et al* (2009). Minocycline attenuates 5-fluorouracil-induced small intestinal mucositis in mouse model. *Biochem Biophys Res Commun* **389**: 634-9.

Husain A, Yan XJ, Rosales N, Aghajanian C, Schwartz GK, Spriggs DR (1997). UCN-01 in ovary cancer cells: effective as a single agent and in combination with cis-diamminedichloroplatinum(II) independent of p53 status. *Clin Cancer Res* **3**: 2089-97.

Inomata A, Horii I, Suzuki K (2002). 5-Fluorouracil-induced intestinal toxicity: what determines the severity of damage to murine intestinal crypt epithelia? *Toxicol Lett* **133**: 231-40.

Iwase S, Furukawa Y, Kikuchi J, Nagai M, Terui Y, Nakamura M *et al* (1997). Modulation of E2F activity is linked to interferon-induced growth suppression of hematopoietic cells. *J Biol Chem* **272**: 12406-14.

Jacobson MD, Evan GI (1994). Apoptosis. Breaking the ICE. *Curr Biol* **4**: 337-40.

Jatoi A, Martenson J, Mahoney MR, Lair BS, Brindle JS, Nichols F *et al* (2004). Results of a planned interim toxicity analysis with trimodality therapy, including carboplatin AUC = 4, paclitaxel, 5-fluorouracil, amifostine, and radiation for locally advanced esophageal cancer: preliminary analyses and treatment recommendations from the North Central Cancer Treatment Group. *Int Semin Surg Oncol* **1**: 9.

Jatoi A, Martenson JA, Foster NR, McLeod HL, Lair BS, Nichols F *et al* (2007). Paclitaxel, carboplatin, 5-fluorouracil, and radiation for locally advanced esophageal cancer: phase II results of preliminary pharmacologic and molecular efforts to mitigate

toxicity and predict outcomes: North Central Cancer Treatment Group (N0044). *Am J Clin Oncol* **30**: 507-13.

Jimeno A, Rudek MA, Purcell T, Laheru DA, Messersmith WA, Dancey J *et al* (2008). Phase I and pharmacokinetic study of UCN-01 in combination with irinotecan in patients with solid tumors. *Cancer Chemother Pharmacol* **61**: 423-33.

Jin Y, Dai MS, Lu SZ, Xu Y, Luo Z, Zhao Y *et al* (2006). 14-3-3gamma binds to MDMX that is phosphorylated by UV-activated Chk1, resulting in p53 activation. *Embo J* **25**: 1207-18.

Kaufmann HJ, Spiro HM, Floch MH (1967). Intestinal epithelial enzyme abnormalities induced by 5-fluorouracil: translocation of NADPH2-dehydrogenase. *Am J Dig Dis* **12**: 598-606.

Kawakami K, Futami H, Takahara J, Yamaguchi K (1996). UCN-01, 7-hydroxyl-staurosporine, inhibits kinase activity of cyclin-dependent kinases and reduces the phosphorylation of the retinoblastoma susceptibility gene product in A549 human lung cancer cell line. *Biochem Biophys Res Commun* **219**: 778-83.

Kemp G, Rose P, Lurain J, Berman M, Manetta A, Roullet B *et al* (1996). Amifostine pretreatment for protection against cyclophosphamide-induced and cisplatin-induced

toxicities: results of a randomized control trial in patients with advanced ovarian cancer. *J Clin Oncol* **14**: 2101-12.

Khan N, Mupparaju SP, Hou H, Lariviere JP, Demidenko E, Swartz HM *et al* (2009). Radiotherapy in conjunction with 7-hydroxystaurosporine: a multimodal approach with tumor pO<sub>2</sub> as a potential marker of therapeutic response. *Radiat Res* **172**: 592-7.

Khwaja A (1999). Akt is more than just a Bad kinase. *Nature* **401**: 33-4.

Koh J, Kubota T, Migita T, Abe S, Hashimoto M, Hosoda Y *et al* (2002). UCN-01 (7-hydroxystaurosporine) inhibits the growth of human breast cancer xenografts through disruption of signal transduction. *Breast Cancer* **9**: 50-4.

Kohn EA, Ruth ND, Brown MK, Livingstone M, Eastman A (2002). Abrogation of the S phase DNA damage checkpoint results in S phase progression or premature mitosis depending on the concentration of 7-hydroxystaurosporine and the kinetics of Cdc25C activation. *J Biol Chem* **277**: 26553-64.

Komander D, Kular GS, Bain J, Elliott M, Alessi DR, Van Aalten DM (2003). Structural basis for UCN-01 (7-hydroxystaurosporine) specificity and PDK1 (3-phosphoinositide-dependent protein kinase-1) inhibition. *Biochem J* **375**: 255-62.

Kondapaka SB, Zarnowski M, Yver DR, Sausville EA, Cushman SW (2004). 7-hydroxystaurosporine (UCN-01) inhibition of Akt Thr308 but not Ser473 phosphorylation: a basis for decreased insulin-stimulated glucose transport. *Clin Cancer Res* **10**: 7192-8.

Konopka JB, Watanabe SM, Witte ON (1984). An alteration of the human c-abl protein in K562 leukemia cells unmasks associated tyrosine kinase activity. *Cell* **37**: 1035-42.

Kortmansky J, Shah MA, Kaubisch A, Weyerbacher A, Yi S, Tong W *et al* (2005). Phase I trial of the cyclin-dependent kinase inhibitor and protein kinase C inhibitor 7-hydroxystaurosporine in combination with Fluorouracil in patients with advanced solid tumors. *J Clin Oncol* **23**: 1875-84.

Kruger EA, Blagosklonny MV, Dixon SC, Figg WD (1998). UCN-01, a protein kinase C inhibitor, inhibits endothelial cell proliferation and angiogenic hypoxic response. *Invasion Metastasis* **18**: 209-18.

Kummar S, Gutierrez ME, Gardner ER, Figg WD, Melillo G, Dancey J *et al* (2009). A phase I trial of UCN-01 and prednisone in patients with refractory solid tumors and lymphomas. *Cancer Chemother Pharmacol*.

Kurata N, Kuwabara T, Tanii H, Fuse E, Akiyama T, Akinaga S *et al* (1999).

Pharmacokinetics and pharmacodynamics of a novel protein kinase inhibitor, UCN-01.

*Cancer Chemother Pharmacol* **44**: 12-8.

Langenfeld J, Kiyokawa H, Sekula D, Boyle J, Dmitrovsky E (1997). Posttranslational regulation of cyclin D1 by retinoic acid: a chemoprevention mechanism. *Proc Natl Acad Sci U S A* **94**: 12070-4.

Lara PN, Jr., Mack PC, Synold T, Frankel P, Longmate J, Gumerlock PH *et al* (2005).

The cyclin-dependent kinase inhibitor UCN-01 plus cisplatin in advanced solid tumors: a California cancer consortium phase I pharmacokinetic and molecular correlative trial.

*Clin Cancer Res* **11**: 4444-50.

Letari O, Booth C, Bonazzi A, Garofalo P, Makovec F, Rovati LC *et al* (2009). Efficacy of CR3294, a new benzamidine derivative, in the prevention of 5-fluorouracil-induced gastrointestinal mucositis and diarrhea in mice. *Cancer Chemother Pharmacol*.

Levesque AA, Fanous AA, Poh A, Eastman A (2008). Defective p53 signaling in p53 wild-type tumors attenuates p21waf1 induction and cyclin B repression rendering them sensitive to Chk1 inhibitors that abrogate DNA damage-induced S and G2 arrest. *Mol Cancer Ther* **7**: 252-62.

Liao LL, Grollman AP, Horwitz SB (1976). Mechanism of action of the 12,13-epoxytrichothecene, anguidine, an inhibitor of protein synthesis. *Biochim Biophys Acta* **454**: 273-84.

Longley DB, Harkin DP, Johnston PG (2003). 5-fluorouracil: mechanisms of action and clinical strategies. *Nat Rev Cancer* **3**: 330-8.

Lugo TG, Pendergast AM, Muller AJ, Witte ON (1990). Tyrosine kinase activity and transformation potency of bcr-abl oncogene products. *Science* **247**: 1079-82.

Mack PC, Gandara DR, Bowen C, Edelman MJ, Paglieroni T, Schnier JB *et al* (1999). RB status as a determinant of response to UCN-01 in non-small cell lung carcinoma. *Clin Cancer Res* **5**: 2596-604.

Mack PC, Gandara DR, Lau AH, Lara PN, Jr., Edelman MJ, Gumerlock PH (2003). Cell cycle-dependent potentiation of cisplatin by UCN-01 in non-small-cell lung carcinoma. *Cancer Chemother Pharmacol* **51**: 337-48.

Mack PC, Jones AA, Gustafsson MH, Gandara DR, Gumerlock PH, Goldberg Z (2004). Enhancement of radiation cytotoxicity by UCN-01 in non-small cell lung carcinoma cells. *Radiat Res* **162**: 623-34.



Mariadason JM, Nicholas C, L'Italien KE, Zhuang M, Smartt HJ, Heerdt BG *et al* (2005).

Gene expression profiling of intestinal epithelial cell maturation along the crypt-villus axis. *Gastroenterology* **128**: 1081-8.

Massague J, Cheifetz S, Imitola J, Boyd FT (1987). Multiple type-beta transforming growth factors and their receptors. *J Cell Physiol Suppl* **Suppl 5**: 43-7.

McCormack ES, Borzillo GV, Ambrosino C, Mak G, Hamablet L, Qu GY *et al* (1997). Transforming growth factor-beta3 protection of epithelial cells from cycle-selective chemotherapy in vitro. *Biochem Pharmacol* **53**: 1149-59.

McDonnell AM, Lenz KL (2007). Palifermin: role in the prevention of chemotherapy- and radiation-induced mucositis. *Ann Pharmacother* **41**: 86-94.

McGahren-Murray M, Terry NH, Keyomarsi K (2006). The differential staurosporine-mediated G1 arrest in normal versus tumor cells is dependent on the retinoblastoma protein. *Cancer Res* **66**: 9744-53.

Medrano EE, Pardee AB (1980). Prevalent deficiency in tumor cells of cycloheximide-induced cycle arrest. *Proc Natl Acad Sci U S A* **77**: 4123-6.

Meggio F, Donella Deana A, Ruzzene M, Brunati AM, Cesaro L, Guerra B *et al* (1995).

Different susceptibility of protein kinases to staurosporine inhibition. Kinetic studies and molecular bases for the resistance of protein kinase CK2. *Eur J Biochem* **234**: 317-22.

Mentz F, Mossalayi MD, Ouaz F, Baudet S, Issaly F, Ktorza S *et al* (1996).

Theophylline synergizes with chlorambucil in inducing apoptosis of B-chronic lymphocytic leukemia cells. *Blood* **88**: 2172-82.

Michael WM, Newport J (1998). Coupling of mitosis to the completion of S phase through Cdc34-mediated degradation of Wee1. *Science* **282**: 1886-9.

Monks A, Harris ED, Vaigro-Wolff A, Hose CD, Connelly JW, Sausville EA (2000).

UCN-01 enhances the in vitro toxicity of clinical agents in human tumor cell lines. *Invest New Drugs* **18**: 95-107.

Newman MS, Colbern GT, Working PK, Engbers C, Amantea MA (1999). Comparative pharmacokinetics, tissue distribution, and therapeutic effectiveness of cisplatin encapsulated in long-circulating, pegylated liposomes (SPI-077) in tumor-bearing mice. *Cancer Chemother Pharmacol* **43**: 1-7.

Nishizuka Y (2001). The protein kinase C family and lipid mediators for transmembrane signaling and cell regulation. *Alcohol Clin Exp Res* **25**: 3S-7S.

Noe V, Alemany C, Chasin LA, Ciudad CJ (1998). Retinoblastoma protein associates with SP1 and activates the hamster dihydrofolate reductase promoter. *Oncogene* **16**: 1931-8.

Obrig TG, Culp WJ, McKeehan WL, Hardesty B (1971). The mechanism by which cycloheximide and related glutarimide antibiotics inhibit peptide synthesis on reticulocyte ribosomes. *J Biol Chem* **246**: 174-81.

Ohi R, Gould KL (1999). Regulating the onset of mitosis. *Curr Opin Cell Biol* **11**: 267-73.

Omura S, Iwai Y, Hirano A, Nakagawa A, Awaya J, Tsuchya H *et al* (1977). A new alkaloid AM-2282 OF Streptomyces origin. Taxonomy, fermentation, isolation and preliminary characterization. *J Antibiot (Tokyo)* **30**: 275-82.

Otsubo A, Bhawal UK, Nomura Y, Mitani Y, Ozawa K, Kuniyasu H *et al* (2007). UCN-01 (7-hydroxystaurosporine) induces apoptosis and G1 arrest of both primary and metastatic oral cancer cell lines in vitro. *Oral Surg Oral Med Oral Pathol Oral Radiol Endod* **103**: 391-7.

Pal S, Claffey KP, Dvorak HF, Mukhopadhyay D (1997). The von Hippel-Lindau gene product inhibits vascular permeability factor/vascular endothelial growth factor

expression in renal cell carcinoma by blocking protein kinase C pathways. *J Biol Chem* **272**: 27509-12.

Pap M, Cooper GM (1998). Role of glycogen synthase kinase-3 in the phosphatidylinositol 3-Kinase/Akt cell survival pathway. *J Biol Chem* **273**: 19929-32.

Pardee AB, James LJ (1975). Selective killing of transformed baby hamster kidney (BHK) cells. *Proc Natl Acad Sci U S A* **72**: 4994-8.

Patel V, Lahusen T, Leethanakul C, Igishi T, Kremer M, Quintanilla-Martinez L *et al* (2002). Antitumor activity of UCN-01 in carcinomas of the head and neck is associated with altered expression of cyclin D3 and p27(KIP1). *Clin Cancer Res* **8**: 3549-60.

Penuelas S, Alemany C, Noe V, Ciudad CJ (2003). The expression of retinoblastoma and Sp1 is increased by low concentrations of cyclin-dependent kinase inhibitors. *Eur J Biochem* **270**: 4809-22.

Perez RP, Lewis LD, Beelen AP, Olszanski AJ, Johnston N, Rhodes CH *et al* (2006). Modulation of cell cycle progression in human tumors: a pharmacokinetic and tumor molecular pharmacodynamic study of cisplatin plus the Chk1 inhibitor UCN-01 (NSC 638850). *Clin Cancer Res* **12**: 7079-85.

Pierelli L, Scambia G, Fattorossi A, Bonanno G, Battaglia A, Perillo A *et al* (1998). In vitro effect of amifostine on haematopoietic progenitors exposed to carboplatin and non-alkylating antineoplastic drugs: haematoprotection acts as a drug-specific progenitor rescue. *Br J Cancer* **78**: 1024-9.

Pinto D, Gregorieff A, Begthel H, Clevers H (2003). Canonical Wnt signals are essential for homeostasis of the intestinal epithelium. *Genes Dev* **17**: 1709-13.

Playle LC, Hicks DJ, Qualtrough D, Paraskeva C (2002). Abrogation of the radiation-induced G2 checkpoint by the staurosporine derivative UCN-01 is associated with radiosensitisation in a subset of colorectal tumour cell lines. *Br J Cancer* **87**: 352-8.

Pollack IF, Kawecki S, Lazo JS (1996). Blocking of glioma proliferation in vitro and in vivo and potentiating the effects of BCNU and cisplatin: UCN-01, a selective protein kinase C inhibitor. *J Neurosurg* **84**: 1024-32.

Pospisil M, Hofer M, Znojil V, Vacha J, Netikova J, Hola J (1995). Synergistic effect of granulocyte colony-stimulating factor and drugs elevating extracellular adenosine on neutrophil production in mice. *Blood* **86**: 3692-7.

Pritchard DM, Potten CS, Hickman JA (1998). The relationships between p53-dependent apoptosis, inhibition of proliferation, and 5-fluorouracil-induced histopathology in murine intestinal epithelia. *Cancer Res* **58**: 5453-65.

Qi W, Qiao D, Martinez JD (2002). Caffeine induces TP53-independent G(1)-phase arrest and apoptosis in human lung tumor cells in a dose-dependent manner. *Radiat Res* **157**: 166-74.

Raffaghello L, Lee C, Safdie FM, Wei M, Madia F, Bianchi G *et al* (2008). Starvation-dependent differential stress resistance protects normal but not cancer cells against high-dose chemotherapy. *Proc Natl Acad Sci U S A* **105**: 8215-20.

Redkar AA, Meadows GG, Daoud SS (2001). UCN-01 dose-dependent inhibition of normal hyperproliferative cells in mice. *Int J Oncol* **19**: 193-9.

Ren S, Rollins BJ (2004). Cyclin C/cdk3 promotes Rb-dependent G0 exit. *Cell* **117**: 239-51.

Rini BI, Weinberg V, Shaw V, Scott J, Bok R, Park JW *et al* (2004). Time to disease progression to evaluate a novel protein kinase C inhibitor, UCN-01, in renal cell carcinoma. *Cancer* **101**: 90-5.

Roberts AB, Anzano MA, Wakefield LM, Roche NS, Stern DF, Sporn MB (1985). Type beta transforming growth factor: a bifunctional regulator of cellular growth. *Proc Natl Acad Sci U S A* **82**: 119-23.

Ruegg UT, Burgess GM (1989). Staurosporine, K-252 and UCN-01: potent but nonspecific inhibitors of protein kinases. *Trends Pharmacol Sci* **10**: 218-20.

Sage J, Miller AL, Perez-Mancera PA, Wysocki JM, Jacks T (2003). Acute mutation of retinoblastoma gene function is sufficient for cell cycle re-entry. *Nature* **424**: 223-8.

Saikali Z, Singh G (2003). Doxycycline and other tetracyclines in the treatment of bone metastasis. *Anticancer Drugs* **14**: 773-8.

Sakai T, Aoike A, Marui N, Kawai K, Nishino H, Fukushima M (1989). Protection by cycloheximide against cytotoxicity induced by vincristine, colchicine, or delta 12-prostaglandin J2 on human osteosarcoma cells. *Cancer Res* **49**: 1193-6.

Sako T, Tauber AI, Jeng AY, Yuspa SH, Blumberg PM (1988). Contrasting actions of staurosporine, a protein kinase C inhibitor, on human neutrophils and primary mouse epidermal cells. *Cancer Res* **48**: 4646-50.

Sampath D, Cortes J, Estrov Z, Du M, Shi Z, Andreeff M *et al* (2006).

Pharmacodynamics of cytarabine alone and in combination with 7-hydroxystaurosporine (UCN-01) in AML blasts in vitro and during a clinical trial. *Blood* **107**: 2517-24.

Sasse AD, Clark LG, Sasse EC, Clark OA (2006). Amifostine reduces side effects and improves complete response rate during radiotherapy: results of a meta-analysis. *Int J Radiat Oncol Biol Phys* **64**: 784-91.

Sato S, Fujita N, Tsuruo T (2002). Interference with PDK1-Akt survival signaling pathway by UCN-01 (7-hydroxystaurosporine). *Oncogene* **21**: 1727-38.

Sausville EA, Arbuck SG, Messmann R, Headlee D, Bauer KS, Lush RM *et al* (2001). Phase I trial of 72-hour continuous infusion UCN-01 in patients with refractory neoplasms. *J Clin Oncol* **19**: 2319-33.

Sausville EA, Lush RD, Headlee D, Smith AC, Figg WD, Arbuck SG *et al* (1998). Clinical pharmacology of UCN-01: initial observations and comparison to preclinical models. *Cancer Chemother Pharmacol* **42 Suppl**: S54-9.

Schwab M, Zanger UM, Marx C, Schaeffeler E, Klein K, Dippon J *et al* (2008). Role of genetic and nongenetic factors for fluorouracil treatment-related severe toxicity: a prospective clinical trial by the German 5-FU Toxicity Study Group. *J Clin Oncol* **26**: 2131-8.

Secrist JP, Sehgal I, Powis G, Abraham RT (1990). Preferential inhibition of the platelet-derived growth factor receptor tyrosine kinase by staurosporine. *J Biol Chem* **265**: 20394-400.



Seynaeve CM, Kazanietz MG, Blumberg PM, Sausville EA, Worland PJ (1994).

Differential inhibition of protein kinase C isozymes by UCN-01, a staurosporine analogue. *Mol Pharmacol* **45**: 1207-14.

Seynaeve CM, Stetler-Stevenson M, Sebers S, Kaur G, Sausville EA, Worland PJ (1993).

Cell cycle arrest and growth inhibition by the protein kinase antagonist UCN-01 in human breast carcinoma cells. *Cancer Res* **53**: 2081-6.

Shankar SL, Krupski M, Parashar B, Okwuaka C, O'Guin K, Mani S *et al* (2004). UCN-01 alters phosphorylation of Akt and GSK3beta and induces apoptosis in six independent human neuroblastoma cell lines. *J Neurochem* **90**: 702-11.

Shao RG, Cao CX, Pommier Y (1997a). Activation of PKCalpha downstream from caspases during apoptosis induced by 7-hydroxystaurosporine or the topoisomerase inhibitors, camptothecin and etoposide, in human myeloid leukemia HL60 cells. *J Biol Chem* **272**: 31321-5.

Shao RG, Cao CX, Shimizu T, O'Connor PM, Kohn KW, Pommier Y (1997b).

Abrogation of an S-phase checkpoint and potentiation of camptothecin cytotoxicity by 7-hydroxystaurosporine (UCN-01) in human cancer cell lines, possibly influenced by p53 function. *Cancer Res* **57**: 4029-35.

Shao RG, Shimizu T, Pommier Y (1997c). 7-Hydroxystaurosporine (UCN-01) induces apoptosis in human colon carcinoma and leukemia cells independently of p53. *Exp Cell Res* **234**: 388-97.

Sherr CJ (1996). Cancer cell cycles. *Science* **274**: 1672-7.

Shimizu E, Zhao MR, Nakanishi H, Yamamoto A, Yoshida S, Takada M *et al* (1996). Differing effects of staurosporine and UCN-01 on RB protein phosphorylation and expression of lung cancer cell lines. *Oncology* **53**: 494-504.

Shindo T, Manabe I, Fukushima Y, Tobe K, Aizawa K, Miyamoto S *et al* (2002). Kruppel-like zinc-finger transcription factor KLF5/BTEB2 is a target for angiotensin II signaling and an essential regulator of cardiovascular remodeling. *Nat Med* **8**: 856-63.

Sing GK, Keller JR, Ellingsworth LR, Ruscetti FW (1988). Transforming growth factor beta selectively inhibits normal and leukemic human bone marrow cell growth in vitro. *Blood* **72**: 1504-11.

Simmen FA, Xiao R, Velarde MC, Nicholson RD, Bowman MT, Fujii-Kuriyama Y *et al* (2007). Dysregulation of intestinal crypt cell proliferation and villus cell migration in mice lacking Kruppel-like factor 9. *Am J Physiol Gastrointest Liver Physiol* **292**: G1757-69.

Slapak CA, Fine RL, Richman CM (1985). Differential protection of normal and malignant human myeloid progenitors (CFU-GM) from Ara-C toxicity using cycloheximide. *Blood* **66**: 830-4.

Smartt HJ, Guilmeau S, Nasser SV, Nicholas C, Bancroft L, Simpson SA *et al* (2007). p27kip1 Regulates cdk2 activity in the proliferating zone of the mouse intestinal epithelium: potential role in neoplasia. *Gastroenterology* **133**: 232-43.

Sobrero AF, Aschele C, Bertino JR (1997). Fluorouracil in colorectal cancer--a tale of two drugs: implications for biochemical modulation. *J Clin Oncol* **15**: 368-81.

Sonis ST, Van Vugt AG, Brien JP, Muska AD, Bruskin AM, Rose A *et al* (1997). Transforming growth factor-beta 3 mediated modulation of cell cycling and attenuation of 5-fluorouracil induced oral mucositis. *Oral Oncol* **33**: 47-54.

Sparreboom A, Chen H, Acharya MR, Senderowicz AM, Messmann RA, Kuwabara T *et al* (2004). Effects of alpha1-acid glycoprotein on the clinical pharmacokinetics of 7-hydroxystaurosporine. *Clin Cancer Res* **10**: 6840-6.

Spencer A, Horvath N, Gibson J, Prince HM, Herrmann R, Bashford J *et al* (2005). Prospective randomised trial of amifostine cytoprotection in myeloma patients undergoing high-dose melphalan conditioned autologous stem cell transplantation. *Bone Marrow Transplant* **35**: 971-7.

Spielberger R, Stiff P, Bensinger W, Gentile T, Weisdorf D, Kewalramani T *et al* (2004).

Palifermin for oral mucositis after intensive therapy for hematologic cancers. *N Engl J Med* **351**: 2590-8.

Stolfi RL, Sawyer RC, Martin DS (1987). Failure of L-histidinol to improve the therapeutic efficiency of 5-fluorouracil against murine breast tumors. *Cancer Res* **47**: 16-20.

Sugiyama K, Akiyama T, Shimizu M, Tamaoki T, Courage C, Gescher A *et al* (1999). Decrease in susceptibility toward induction of apoptosis and alteration in G1 checkpoint function as determinants of resistance of human lung cancer cells against the antisenescence drug UCN-01 (7-Hydroxystaurosporine). *Cancer Res* **59**: 4406-12.

Sugiyama K, Shimizu M, Akiyama T, Tamaoki T, Yamaguchi K, Takahashi R *et al* (2000). UCN-01 selectively enhances mitomycin C cytotoxicity in p53 defective cells which is mediated through S and/or G(2) checkpoint abrogation. *Int J Cancer* **85**: 703-9.

Tachibana KE, Gonzalez MA, Guarguaglini G, Nigg EA, Laskey RA (2005). Depletion of licensing inhibitor geminin causes centrosome overduplication and mitotic defects. *EMBO Rep* **6**: 1052-7.

Takahashi A, Hirata H, Yonehara S, Imai Y, Lee KK, Moyer RW *et al* (1997). Affinity labeling displays the stepwise activation of ICE-related proteases by Fas, staurosporine, and CrmA-sensitive caspase-8. *Oncogene* **14**: 2741-52.

Takahashi I, Asano K, Kawamoto I, Tamaoki T, Nakano H (1989). UCN-01 and UCN-02, new selective inhibitors of protein kinase C. I. Screening, producing organism and fermentation. *J Antibiot (Tokyo)* **42**: 564-70.

Takahashi I, Kobayashi E, Asano K, Yoshida M, Nakano H (1987). UCN-01, a selective inhibitor of protein kinase C from Streptomyces. *J Antibiot (Tokyo)* **40**: 1782-4.

Takahashi I, Kobayashi E, Nakano H, Murakata C, Saitoh H, Suzuki K *et al* (1990). Potent selective inhibition of 7-O-methyl UCN-01 against protein kinase C. *J Pharmacol Exp Ther* **255**: 1218-21.

Takano S (1994). Staurosporine inhibits STA2-induced platelet aggregation by inhibition of myosin light-chain phosphorylation in rabbit washed platelets. *Ann N Y Acad Sci* **714**: 315-7.

Tamaoki T, Nomoto H, Takahashi I, Kato Y, Morimoto M, Tomita F (1986). Staurosporine, a potent inhibitor of phospholipid/Ca<sup>++</sup>dependent protein kinase. *Biochem Biophys Res Commun* **135**: 397-402.

Teodori L, Barlogie B, Drewinko B, Swartzendruber D, Mauro F (1981). Reduction of 1-beta-D-arabinofuranosylcytosine and adriamycin cytotoxicity following cell cycle arrest by anguidine. *Cancer Res* **41**: 1263-70.

Terry NH, White RA (2006). Flow cytometry after bromodeoxyuridine labeling to measure S and G2+M phase durations plus doubling times in vitro and in vivo. *Nat Protoc* **1**: 859-69.

Tse AN, Schwartz GK (2004). Potentiation of cytotoxicity of topoisomerase i poison by concurrent and sequential treatment with the checkpoint inhibitor UCN-01 involves disparate mechanisms resulting in either p53-independent clonogenic suppression or p53-dependent mitotic catastrophe. *Cancer Res* **64**: 6635-44.

Tsuchida E, Urano M (1997). The effect of UCN-01 (7-hydroxystaurosporine), a potent inhibitor of protein kinase C, on fractionated radiotherapy or daily chemotherapy of a murine fibrosarcoma. *Int J Radiat Oncol Biol Phys* **39**: 1153-61.

Usuda J, Saijo N, Fukuoka K, Fukumoto H, Kuh HJ, Nakamura T *et al* (2000). Molecular determinants of UCN-01-induced growth inhibition in human lung cancer cells. *Int J Cancer* **85**: 275-80.

Verbin RS, Farber E (1967). Effect of cycloheximide on the cell cycle of the crypts of the small intestine of the rat. *J Cell Biol* **35**: 649-58.

Walters RA, Gurley LR, Tobey RA (1974). Effects of caffeine on radiation-induced phenomena associated with cell-cycle traverse of mammalian cells. *Biophys J* **14**: 99-118.

Wang Q, Fan S, Eastman A, Worland PJ, Sausville EA, O'Connor PM (1996). UCN-01: a potent abrogator of G2 checkpoint function in cancer cells with disrupted p53. *J Natl Cancer Inst* **88**: 956-65.

Wang Q, Worland PJ, Clark JL, Carlson BA, Sausville EA (1995). Apoptosis in 7-hydroxystaurosporine-treated T lymphoblasts correlates with activation of cyclin-dependent kinases 1 and 2. *Cell Growth Differ* **6**: 927-36.

Wang X, Martindale JL, Holbrook NJ (2000). Requirement for ERK activation in cisplatin-induced apoptosis. *J Biol Chem* **275**: 39435-43.

Warrington RC (1978). Selective killing of oncogenic human cells cocultivated with normal human fibroblasts. *J Natl Cancer Inst* **61**: 69-73.

Warrington RC, Fang WD (1982a). L-histidinol protection against cytotoxic action of cytosine arabinoside and 5-fluorouracil in cultured mouse spleen cells. *J Natl Cancer Inst* **68**: 279-86.

Warrington RC, Fang WD (1982b). Proliferative responses to L-histidinol correlate with the phenotypic status of normal and transformed cho cells. *Cell Biol Int Rep* **6**: 309-16.

Warrington RC, Fang WD (1985). Histidinol-mediated enhancement of the specificity of two anticancer drugs in mice bearing leukemic bone marrow disease. *J Natl Cancer Inst* **74**: 1071-7.

Warrington RC, Muzyka TG (1983). Responses of mouse cell lines transformed by various means to histidinol/cytosine arabinoside treatment. *Cell Biol Int Rep* **7**: 283-92.

Warrington RC, Muzyka TG, Fang WD (1984). Histidinol-mediated improvement in the specificity of 1-beta-D-arabinofuranosylcytosine and 5-fluorouracil in L 1210 leukemia-bearing mice. *Cancer Res* **44**: 2929-35.

Warrington RC, Wratten N, Hechtman R (1977). L-Histidinol inhibits specifically and reversibly protein and ribosomal RNA synthesis in mouse L cells. *J Biol Chem* **252**: 5251-7.

Way KJ, Chou E, King GL (2000). Identification of PKC-isoform-specific biological actions using pharmacological approaches. *Trends Pharmacol Sci* **21**: 181-7.

Weinert T (1997). A DNA damage checkpoint meets the cell cycle engine. *Science* **277**: 1450-1.



Weiser MM (1973). Intestinal epithelial cell surface membrane glycoprotein synthesis. I. An indicator of cellular differentiation. *J Biol Chem* **248**: 2536-41.

Weissberg JB, Herion JC, Walker RI, Palmer JG (1978). Effect of cycloheximide on the bone marrow toxicity of nitrogen mustard. *Cancer Res* **38**: 1523-7.

Weiterova L, Hofer M, Pospisil M, Znojil V, Vacha J, Vacek A *et al* (2000). Influence of the joint treatment with granulocyte colony-stimulating factor and drugs elevating extracellular adenosine on erythropoietic recovery following 5-fluorouracil-induced haematotoxicity in mice. *Eur J Haematol* **65**: 310-6.

Welch S, Hirte HW, Carey MS, Hotte SJ, Tsao MS, Brown S *et al* (2007). UCN-01 in combination with topotecan in patients with advanced recurrent ovarian cancer: a study of the Princess Margaret Hospital Phase II consortium. *Gynecol Oncol* **106**: 305-10.

Xia S, Forman LW, Faller DV (2007). Protein kinase C delta is required for survival of cells expressing activated p21RAS. *J Biol Chem* **282**: 13199-210.

Xiao HH, Makeyev Y, Butler J, Vikram B, Franklin WA (2002). 7-Hydroxystaurosporine (UCN-01) preferentially sensitizes cells with a disrupted TP53 to gamma radiation in lung cancer cell lines. *Radiat Res* **158**: 84-93.

Yamauchi M, Kusano H, Nakakura M, Kato Y (2005). Reducing the impact of binding of UCN-01 to human alpha1-acid glycoprotein by encapsulation in liposomes. *Biol Pharm Bull* **28**: 1259-64.

Yamauchi M, Kusano H, Saito E, Abe M, Tsutsumi K, Uosaki Y *et al* (2008). Controlled release of a protein kinase inhibitor UCN-01 from liposomes influenced by the particle size. *Int J Pharm* **351**: 250-8.

Yu L, Orlandi L, Wang P, Orr MS, Senderowicz AM, Sausville EA *et al* (1998). UCN-01 abrogates G2 arrest through a Cdc2-dependent pathway that is associated with inactivation of the Wee1Hu kinase and activation of the Cdc25C phosphatase. *J Biol Chem* **273**: 33455-64.

Yu Q, La Rose J, Zhang H, Takemura H, Kohn KW, Pommier Y (2002). UCN-01 inhibits p53 up-regulation and abrogates gamma-radiation-induced G(2)-M checkpoint independently of p53 by targeting both of the checkpoint kinases, Chk2 and Chk1. *Cancer Res* **62**: 5743-8.

Zhang WH, Poh A, Fanous AA, Eastman A (2008). DNA damage-induced S phase arrest in human breast cancer depends on Chk1, but G2 arrest can occur independently of Chk1, Chk2 or MAPKAPK2. *Cell Cycle* **7**: 1668-77.

Zhou BB, Elledge SJ (2000). The DNA damage response: putting checkpoints in perspective. *Nature* **408**: 433-9.

Zhu WY, Jones CS, Kiss A, Matsukuma K, Amin S, De Luca LM (1997). Retinoic acid inhibition of cell cycle progression in MCF-7 human breast cancer cells. *Exp Cell Res* **234**: 293-9.

## **Vita**

Benjamin Barrett Mull was born in Woodland, California on December 24, 1972, the son of Joan Elise Mull and Ronald Loyd Mull. After graduating from Alexis I. DuPont High School in Greenville, Delaware, he entered Rice University in Houston, Texas. He received the degree of Bachelor of Arts with a major in Biochemistry in May 1996. For the next eight years, he worked as a research technician in the Department of Molecular of Human Genetics at Baylor College of Medicine. In 2002 he entered the University of Texas Health Science Center at Houston Graduate School of Biomedical Sciences. He received the degree of Masters of Science in May 2007.

Permanent address: 4404 Castle Court Place  
Houston, TX 77006